A University of Sussex PhD thesis

Available online via Sussex Research Online:

http://sro.sussex.ac.uk/

This thesis is protected by copyright which belongs to the author.

This thesis cannot be reproduced or quoted extensively from without first obtaining permission in writing from the Author

The content must not be changed in any way or sold commercially in any format or medium without the formal permission of the Author

When referring to this work, full bibliographic details including the author, title, awarding institution and date of the thesis must be given

Please visit Sussex Research Online for more information and further details

UNDERSTANDING THE ROLES OF THE SMC5/6 COMPLEX ON MEIOTIC RECOMBINATION

JACOB DANIEL KIRK

DPHIL BIOCHEMISTRY

UNIVERSITY OF SUSSEX

SUBMITTED SEPTEMBER 2016

UNIVERSITY OF SUSSEX

JACOB DANIEL KIRK

DPHIL BIOCHEMISTRY

UNDERSTANDING THE ROLES OF THE SMC5/6 COMPLEX ON MEIOTIC RECOMBINATION

SUMMARY

During meiotic cell division, the formation of chiasmata is required for the segregation of homologous chromosomes. This involves the formation of a programmed series of double strand breaks and repair by homologous recombination to form crossovers within the chromosomes. This process is highly regulated to ensure the timely formation of interhomolog linkages, which are normally repressed by the mitotic repair pathways. A protein complex of particular interest here is Smc5/6, which is closely related to two complexes with a fundamental role controlling chromosome structure (cohesin and condensin). In the absence of the Smc5/6 complex, cells are unable to separate their chromosomes efficiently during meiosis, resulting in a ‘cut phenotype’; this is thought to be due to major aberrations in the formation and resolution of joint molecule intermediates throughout meiotic prophase.

Here, I characterize the aberration in the formation of recombination intermediates in *smc5/6*-depleted cells in order to infer functions of the Smc5/6 complex in regulating recombination intermediates. Using the well-characterised DNA double strand break hotspot *HIS4LEU2*, I show that depletion of the Smc5/6 complex rescues joint molecule formation in a *zmm* repair pathway mutant. To understand the timing of Smc5/6 complex function during strand invasion, I analyse the genetic interactions between two recA orthologues and cohesin, all of which promote the orderly formation of recombination events between homologous chromosomes. Collectively, the findings suggest that the Smc5/6 complex stabilizes early recombination intermediates between homologous DNA substrates thereby imposing an interhomolog repair fate. I analyse the formation of repair intermediates in the absence of cohesin, and demonstrate that the role of the Smc5/6 complex in interhomolog repair bias is independent of the presence of cohesin, which is normally considered a fundamental factor in the establishment of repair bias.

Acknowledgements

I would like to thank Dr Eva Hoffmann for her guidance and support throughout my PhD. I have learned a great deal from her and am grateful for her time and patience supervising me.

I am also grateful to all members of the Hoffmann lab, past and present, for both their valuable scientific insight regarding my research project, and the emotional support they have provided when things have gone wrong.

I would like to thank Dr Jon Baxter for his impartial advice on my research project, and offering me support when I was concerned about my progress.

I would like to acknowledge the Medical Research Council for funding my 3.5 year studentship, as without this financial support, I would not have been able to undertake this programme of research and study.

I would like to thank my friends at 6th Brighton Scout Troop, with whom I spent many a weekend camping to keep me sane throughout the PhD, I am eternally thankful for having met such great supportive people, with whom I have so much in common.

I would like to thank my family for their support throughout the PhD, be it from the sage advice of my parents, and their constant care (and eternal lifts); to the good spirits and jokes that I have with my sisters, who are also great friends to me. Without the four of you, I could never have completed this project.

Finally, I would like to thank my fiancée, Sayeh, for being my rock throughout this process. I know it hasn't always been easy putting up with my grump when things have gone wrong, but you managed it, and always made me smile afterwards. Your love has kept me going, and I can't wait to continue our journey together.

Contents

Figure list

Chapter 1
Introduction

1.1 Meiosis

1.1.1 Meiosis overview

During meiosis, the reductive cell division, homologous chromosomes separate into four daughter cells, a process that generates haploid progeny from diploid parent cells. This process is thought to have been present in the last eukaryotic common ancestor (RAMESH, et al., 2005) and seems to be a necessary process for most of the organisms in this kingdom of life. This fundamental process requires the formation of programmed double strand breaks (DSBs), which are generally repaired by homologous recombination (HR) to generate chiasmata, causing linkages between homologues that allow them to be segregated to different poles of the cell at the first meiotic division. The recombination process also generates crossovers and non-crossovers, with crossovers allowing for alternative combinations of alleles within the progeny than is observed in either parent, generating genetic diversity and potentially increasing the fitness of the offspring (Figure 1.1).

The nature of meiotic division differs fundamentally from mitosis on both a biochemical and cytological level: following pre-meiotic S phase, double strand breaks (DSBs) are induced in the DNA, which enables single-end invasion (SEI) of homologous chromosomes by the resected end (KEENEY, et al., 1997),

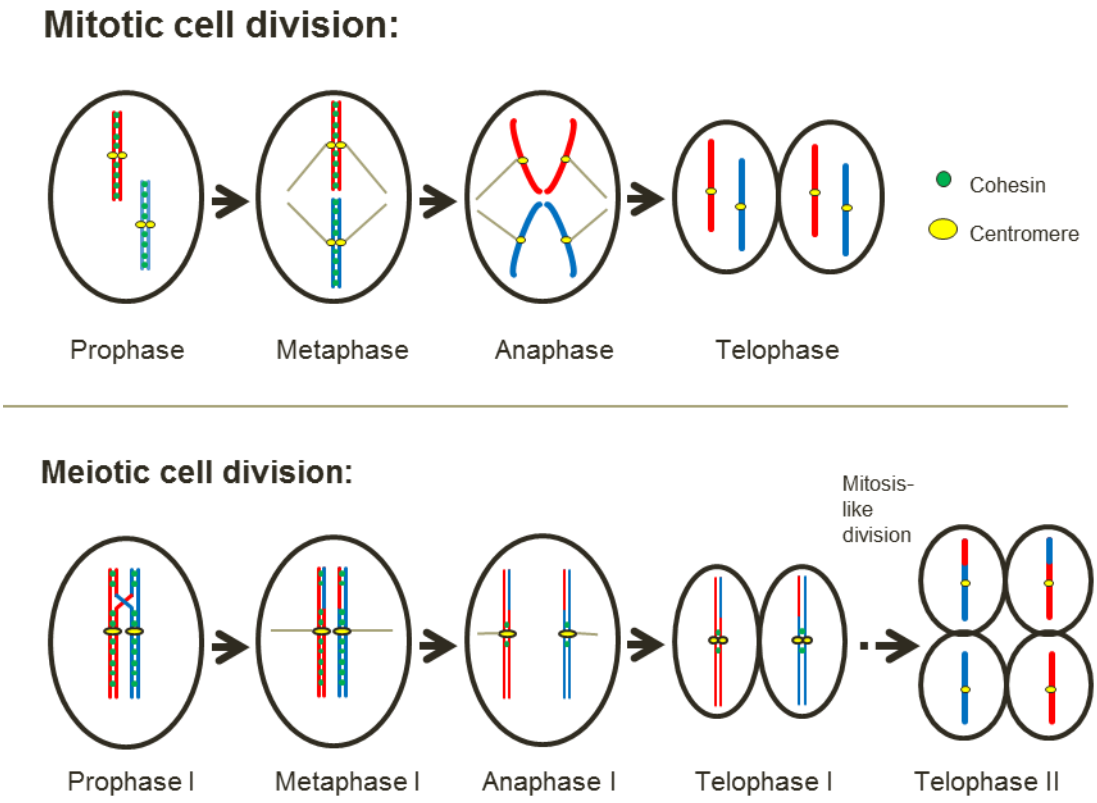

Figure 1.1 The two eukaryotic cell divisions; mitosis and meiosis.

Both cell divisions include a single round of DNA replication prior to initiating cell division, with most species initiating a G2 (gap) phase before progressing into cell division.

In mitosis, replicated sister chromatids are held together by the action of the cohesin protein complex, and chromosomes condense during prophase. During metaphase, chromosomes align on the nuclear equator, with microtubules attaching the their centromeres in a bipolar fashion. During anaphase, cohesin is cleaved to allow the separation of sister chromatids to different poles of the cell, to generate two identical daughter cells after telophase.

In meiosis, following DNA replication, chromosomes condense. During prophase I, a programmed series of DSB formation and repair leads to the pairing of homologous chromosomes, and the formation of chiasmata to generate physical linkage between chromosomes. At metaphase I, homologous chromosomes align at the nuclear equator, with the kinetochore of each homolog attached to a different pole. At anaphase I onset, arm cohesin is cleaved, allowing the separation of homologs from each other, however centromeric cohesin allows sister chromatids to remain cohesed. This is then followed by a second mitotic like division, leading to the production of 4 genetically distinct haploid progeny

whilst recombination between sister chromatids is repressed, in stark contrast to mitotic cell division (SCHWACHA & KLECKNER, 1997), in order to encourage the formation of recombination intermediates, culminating in double Holliday junctions (dHJs) (SCHWACHA & KLECKNER, 1995). These are then resolved to either a crossover (CO; where there is a reciprocal transfer of DNA between parental chromosomes) or non-crossovers, (NCO; where a transfer does not occur).

1.1.2 Meiosis in budding yeast

The budding yeast *S. cerevisiae* is used as a tool study meiosis generally, and meiotic DNA repair more specifically in this study. It is ideally suited for this task, due to the well-characterised genetic tools at our disposal in this organism, such as the *HIS4LEU2* double strand break hotspot, which can be used to probe meiotic homologous recombination outcomes (SCHWACHA & KLECKNER, 1995; SCHWACHA & KLECKNER, 1997). Furthermore, budding yeast has the ability enter meiosis with a high degree of synchronicity, allowing the repair outcomes of a population of cells to be determined via Southern analysis.

Entry into meiosis of diploid yeast is determined by nutritional signals; when the yeast cell lacks nutrients, this triggers the transcriptional regulator Ime1, a master regulator of yeast meiosis, which is required for the transcription of early meiotic genes (KASSIR, et al., 1988; SMITH, et al., 1993). Ime1 initiates a cascade of transcription factors and other factors, which enable the co-ordinated progression of meiosis. Through the activity of Ime2, pre-meiotic S-phase is promoted (DIRICK, et al., 1998). Ime2 is also required for the activation of the transcriptional regulator Ndt80, (PAK & SEGALL, 2002), which

is required for pachytene exit (XU, et al., 1995), and the activation of middle meiotic genes.

Cdc5, a polo-like kinase homologue, is required for several meiotic processes. It is required for the dissociation of a proportion of cohesin from meiotic chromosomes during prophase (prophase pathway) (YU & KOSHLAND, 2005). In addition, Cdc5 is necessary to assure mono-orientation of sister kinetochores at metaphase I, by promoting the localisation of components of the monopolin complex (CLYNE, et al., 2003). Cdc5 kinase activity is also required for the release of CDC14 from the nucleolus (VISINTIN, et al., 2003) which is in turn required for anaphase I spindle disassembly and exit from meiosis I.

Following the first meiotic division, meiosis II occurs rapidly, leading to the generation of four haploid spores. This is another benefit of utilising *S. cerevisiae* – dissection of these tetrads reveals all the products of a single meiosis, which can be used as a tool for genetic analysis of mutants and growth conditions.

1.1.3 **Cytological progression in budding yeast**

In *S. cerevisiae* meiosis, there are substantial changes in chromosome morphology as cells progress through meiosis. These can generally be distinguished through the assembly of the synaptonemal complex (SC), and the degree of compaction of meiotic DNA. Following pre-meiotic S-phase, leptotene occurs: centromeres pair in a homology independent manner (CHUONG & DAWSON, 2010), DSBs are formed, simultaneously with punctate staining of SC component Zip1 (CHUA & ROEDER, 1998). Subsequently, longer stretches of linear Zip1 are observed in zygotene, with some punctate staining remaining, before chromosomes are completely synapsed (and Zip1 is contained only in linear stretches) at pachytene. DNA is also becoming more compacted throughout this period. Upon pachytene exit, as double Holliday junctions are resolved into crossovers, and for the physical linkage chiasmata, the SC disassembles. Further chromosome compaction also occurs prior to the separation of chromosomes at anaphase I (Figure 1.2).

1.1.3.1 Synaptonemal complex

In *S. cerevisiae,* the formation of the synaptonemal complex begins with the assembly of the axial elements prior to synapsis. These are composed of meiotic cohesin, in addition to Red1 and Hop1 (KLEIN, et al., 1999; SMITH & . ROEDER, 1997). The axial element is termed the lateral element upon synapsis (Figure 1.3). The central and transverse elements of the *S. cerevisiae* synaptonemal complex are composed of Zip1 (SYM, et al., 1993; DONG & ROEDER, 2000). The progression of Zip1 filament begins at sights of future

Meiotic prophase I:

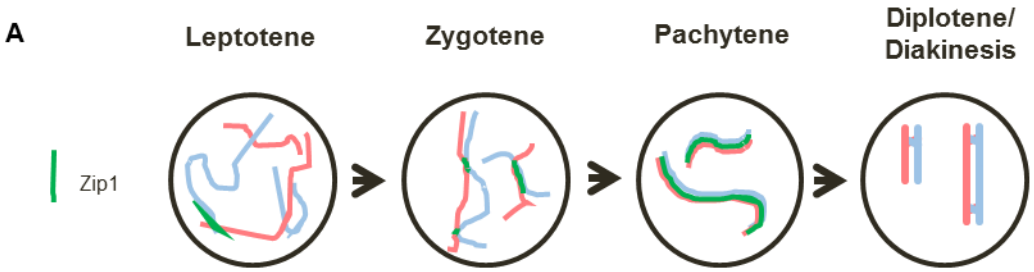

B

Zip1	Punctate staining	Punctate + Linear	Linear staining	No staining
DNA compaction	Diffuse DNA		Highly condensed	DNA condensation
DSB repair stage	DSB formation	Stable SEI	dHJ formation	CO/chiasmata

Figure 1.2 Cytological and biochemical changes occurring in prophase I of *S. cerevisiae* meiosis

(A) A diagrammatic representation of the cytological changes observed in the cell. Each red or blue line represents a pair of sister chromatids. Punctate ZIP1 staining is observed in leptotene, progressing to linear ZIP1 structures in pachytene when synapsis has completed, and with ZIP1 being removed when the cell enters the later diplotene/diakinesis stages.

(B) A summary table of the major changes during meiotic prophase I, noting the stages when different aspects of the DSB repair pathway are occurring

A

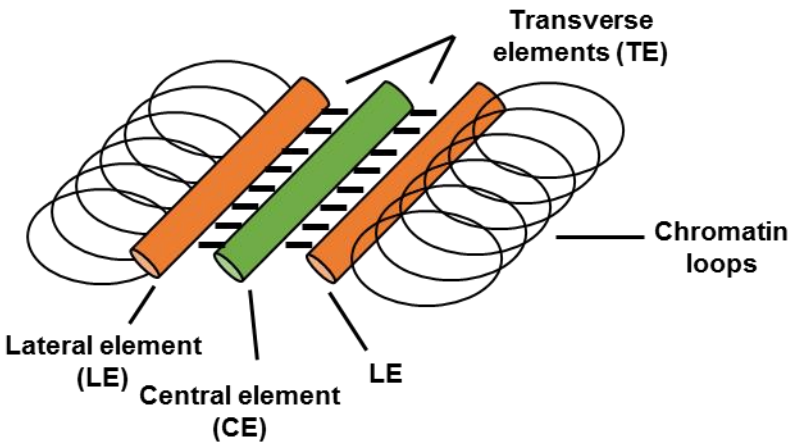
Transverse elements (TE)
Chromatin loops
Lateral element (LE)
Central element (CE)
LE

B

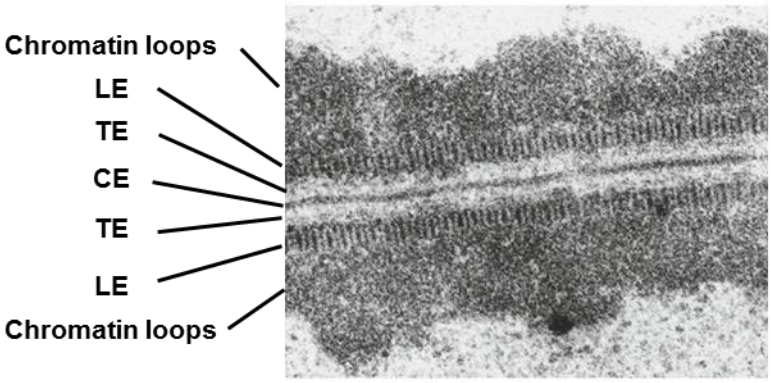
Chromatin loops
LE
TE
CE
TE
LE
Chromatin loops

C

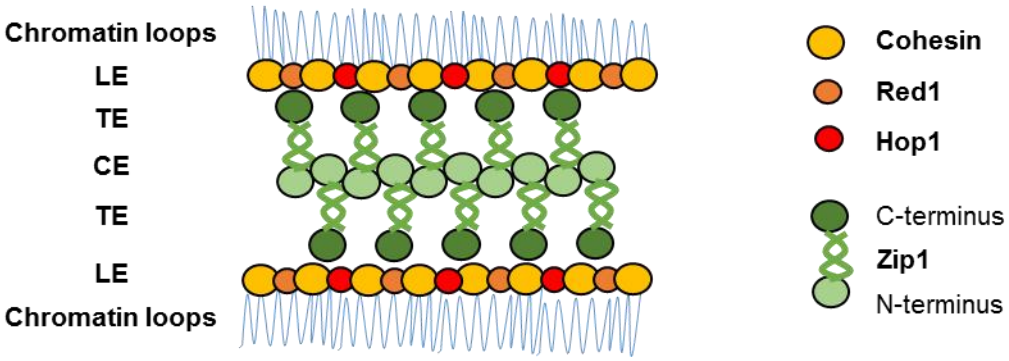
Chromatin loops
LE
TE
CE
TE
LE
Chromatin loops
Cohesin
Red1
Hop1
C-terminus
Zip1
N-terminus

Figure 1.3 Synaptonemal complex in *S. cerevisiae*

During *S. cerevisiae* meiosis, a proteinaceous structure, the synaptonemal complex, is formed between homologous chromosomes, and it is in this context that the biochemical reactions of meiotic DNA repair take place.

(A) Diagram of the elements which can be observed by microscopy

(B) Electron micrograph of the synaptonemal complex in *Neottiella* (from Strasburger's Plant Sciences, 2013, figure 39)

(C) The essential structural components of the synaptonemal complex, and their relative locations, are displayed here.

crossovers, which is dependent on the presence of Zip3 (TSUBOUCHI, et al., 2008) and at the centromeres of chromosomes, promoting homologous coupling in a Zip3 independent manner. The synapsis initiation complex proteins Zip2-4 and Spo16 are essential for the efficient formation of linear synaptonemal complexes (CHUA & ROEDER, 1998; PERRY, et al., 2005).

1.2 Progression of recombination in budding yeast

1.2.1 Pre-meiotic S-phase and DSB formation

The earliest molecular event which initiates pre-meiotic S-phase is the sustained activity of Ime2, a protein kinase which is required for the destruction of CDK inhibitor Sic1 (DIRICK, et al., 1998). Subsequently, a programmed series of DSBs are induced by the action of a topoisomerase VI like protein, Spo11 (KEENEY, et al., 1997), which forms a covalent link with the DNA strands (LIU, et al., 1995; KEENEY, et al., 1997). Cleavage of the DNA strand adjacent to the Spo11 complex is subsequently undertaken by the Mre11 endonuclease (NAIRZ & KLEIN, 1997; NEALE, et al., 2005), which enables the Exo1 exonuclease to resect the DSB in the 5' to 3' direction (TSUBOUCHI & OGAWA, 2000; ZHU, et al., 2008), to generate a 3' overhang of ssDNA (Figure 1.4). This takes place in the context of leptotene, and the formation of punctate Zip1 staining (CHUA & ROEDER, 1998).

1.2.2 Strand invasion of resected DSBs, and Synthesis Dependant Strand Exchange

The ssDNA regions are bound into nucleoprotein filaments, containing *RecA* homologues Rad51 and the meiosis specific Dmc1 (BISHOP, 1994) (SHINOHARA & SHINOHARA, 2004). The assembly of these filaments is essential for homology search by the ssDNA, and for the formation of semi-stable SEIs (Figure 1.4). Rad51 and Dmc1 have redundant roles in

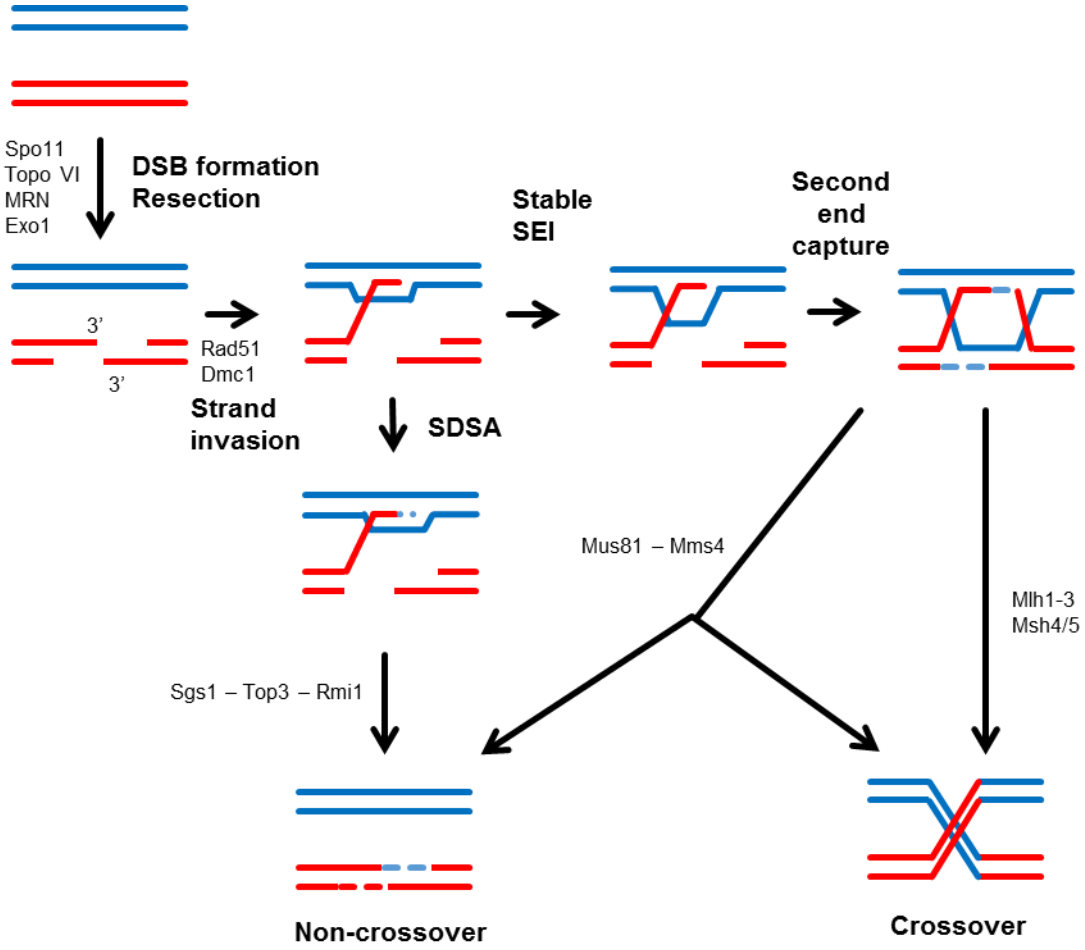
Spo11
Topo VI
MRN
Exo1
DSB formation
Resection
3'
3'
Rad51
Dmc1
Strand
invasion
Stable
SEI
Second
end
capture
SDSA
Mus81 – Mms4
Mlh1-3
Msh4/5
Sgs1 – Top3 – Rmi1
Non-crossover
Crossover

Figure 1.4 Meiotic DSB repair in *S. cerevisiae*

Meiotic DSB repair begins with the generation of induced DSBs by the action Spo11/TopoVI. These DSBs are then resected by the action of the Exo1 exonuclease to generate regions of ssDNA. *RecA* homologues Dmc1 and Rad51 form nucleoprotein filaments in association with the ssDNA, and enable strand invasions into the homologous double stranded DNA. This is followed by either, synthesis dependent strand annealing, where the nascent D-loop is destabilized by the action of Sgs1-Top3, and repair is undertaken with the other resected DSB, leading to a non-crossover. Alternatively, the nascent D-loop may be stabilized to form a stable single end invasion (SEI), and subsequently the other side of the resected DSB may be captured by the DNA loop which has been formed (second end capture). This leads to the formation of the stable branched intermediate, double Holliday junctions. These dHJs are resolved, either by the action of the meiosis specific repair by Mlh1/3 to generate crossovers, or the action on Mus81-Mms4 in a mitotic-like repair pathway, which generates an equal proportion of crossovers and non-crossovers

S. cerevisiae meiosis in certain specific contexts (TSUBOUCHI & ROEDER, 2006); however, more recent studies have demonstrated that Dmc1 is the primary actor in the formation of JM intermediates: differential mutations in the active sites of the two proteins leads to distinct phenotypes; the low affinity DNA binding site of Rad51 is not essential for spore viability, whilst total meiotic arrest occurs in Dmc1 mutants lacking this site (CLOUD, et al., 2012). The strand exchange activity of Rad51 is repressed by the activity of Hed1 in the meiotic environment (TSUBOUCHI & ROEDER, 2006). Recent data has shown that both Dmc1 and Rad51 occupy both ends of the resected DSB, in small tracts (BROWN, et al., 2015), which would indicate that both have some role in the repair of DSBs in meiosis.

At this stage, a subset of strand exchange interactions are dissolved and repaired via synthesis dependant strand annealing (SDSA) (MCMAHILL, et al., 2007; PAQUES & HABER, 1999). Repair DNA synthesis occurs, extending the invading strand passed the site of the original DSB (FORMOSA & ALBERTS, 1986). The *RecQ* family helicase Sgs1, in a complex with Top3-Rmi1, acts to displace the extended strand from the D-loop (DE MUYT, et al., 2012; KAUR, et al., 2015), thus enabling the DSB ends to re-associate via complementary base pairing, and undergo repair to generate a non-crossover product that does not contribute to chiasmata formation. This final repair stage is catalysed by the activity of Rad52, which also has a crucial role in the formation of double Holliday junctions (LAO, et al., 2008).

1.2.3 Second end capture and double Holliday junction formation

Chiasmata formation require double Holliday junction formation and resolution. In a subset of cells, the second DSB end is captured by the stable single-end invasion, and repaired to form a double Holliday junction. Both resected ends are associated with both Dmc1 and Rad51 (BROWN, et al., 2015), however in the case of the second end, the action of Rad52, the bacterial *RecO* homolog, is shown to be required for the formation of stabilised joint molecules (NIMONKAR, et al., 2009; LAO, et al., 2008). Double Holliday junctions form between adjacent chromosomes, which are then resolved into either crossovers, which generate the physical linkage chiasmata, or non-crossovers, dependent upon the resolution pathway employed.

1.2.4 Resolution pathways for joint molecules

1.2.4.1 ZMM repair pathway

In *S. cerevisiae,* there are two major pathways for the resolution of double Holliday junctions. The ZMM pathway (named for the Zip1-4, Msh4/5, Mer3) generates a majority of crossovers (ZAKHEREYVICH, et al., 2012), with mutants lacking these proteins generating approximately 85% fewer crossovers (BORNER, et al., 2004; PERRY, et al., 2005) than wild type. Non-crossover levels are unaffected in these mutants, suggesting that non-crossover levels are not affected by the ZMM pathway. Designation of the ZMM pathway processed joint molecules happens prior to dHJ formation, with Mer3 instrumental in the formation of heteroduplex DNA between the invading ssDNA and the donor

DNA (MAZINA, et al., 2004). Human Msh4/5 binds to single Holliday junctions, and acts as a sliding clamp once bound (SNOWDEN, et al., 2004), which would imply an early role in stabilising SEI interactions. Msh4/5 interacts with the endonuclease Mlh1/3 (SANTUCCI-DARMANIN, et al., 2002), which acts as the resolvase for the ZMM pathway mediated double Holliday junctions. The Mlh1/3 endonuclease appears to be a crossover specific resolvase (ZAKHEREYVICH, et al., 2012; NISHANT, et al., 2008) (Figure 1.5). In addition, positive crossover interference, the mechanism that inhibits crossovers from forming adjacent to one another, is lost in the absence of *msh4*, suggesting that only crossovers formed through the ZMM pathway are influenced by crossover interference (NOVAK, et al., 2001).

1.2.4.2 Mus81-Mms4 repair

The mitotic-like Mus81-Mms4 pathway generates an equal number of crossovers and non-crossovers, and processes fewer molecules overall than the ZMM pathway. The Mus81-Mms4 repair pathway appears to be entirely independent from the ZMM pathway (DE LOS SANTOS, et al., 2003). The exact nature of the Mus81-Mms4 pathway suggests that rather than processing formed dHJs, Mus81-Mms4 is involved in processing the D-loop generated in SEIs (discussed in HOLLINGSWORTH & BRILL, 2004). Crossovers generated by the Mus81-Mms4 pathway do not show crossover interference (DE LOS SANTOS, et al., 2003) (Figure 1.5). The Mus81-Mms4 resolvases localisation to meiotic chromosomes is dependent upon the presence of the Smc5/6 complex,

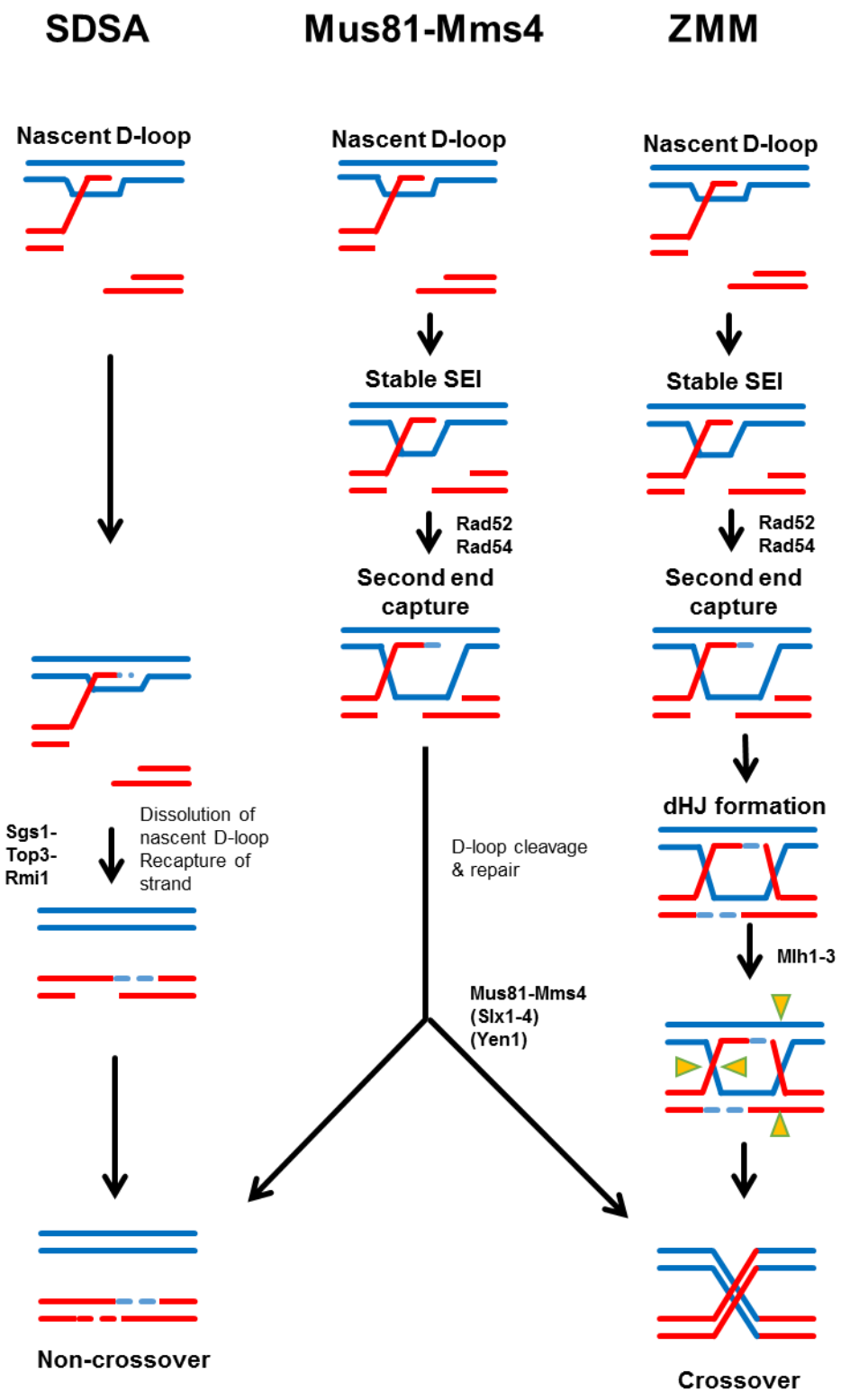
SDSA
Mus81-Mms4
ZMM
Nascent D-loop
Nascent D-loop
Nascent D-loop
Stable SEI
Stable SEI
Rad52
Rad54
Rad52
Rad54
Second end capture
Second end capture
dHJ formation
Sgs1-Top3-Rmi1
Dissolution of nascent D-loop
Recapture of strand
D-loop cleavage & repair
Mus81-Mms4 (Slx1-4) (Yen1)
Mlh1-3
Non-crossover
Crossover

Figure 1.5 Joint molecule resolution pathways in *S. cerevisiae*

The three major repair pathways in *S. cerevisiae* are displayed.
Synthesis dependent strand annealing, where the strand invasion interactions are destabilized by the action of Sgs1-Top3-Rmi1, and repair is undertaken with the other resected DSB end, leading to a non-crossover.
In the ZMM repair pathway (determined by the presence of ZMM proteins), a stable SEI is formed, and the other side of the resected DSB may be captured by the DNA loop which has been formed (second end capture). This leads to the formation of the stable branched intermediate, double Holliday junctions. These dHJs are resolved, either by the action of the meiosis specific repair by Mlh1/3 to generate crossover. The sites of cleavage in the ZMM repair pathway are indicated by the orange pointers.
In the Mus81-Mms4 repair pathway, the second end is captured, however no dHJ is formed, and the nicked D-loop structure that is present is resolved by the XPF-like endonuclease Mus81-Mms4, which generates an equal proportion of crossovers and non-crossovers.

and the Mus81-Mms4 repair pathway appears to be severely abrogated in Smc5/6 complex mutants (COPSEY, et al., 2013).

In addition to these two main pathways, a subset of cryptic endonuclease, whose activity is mainly detected when a major repair pathway is abrogated, also exist in budding yeast. Yen1 has resolvase activity that is mostly observed in the absence of the Mus81-Mms4 repair pathway, whilst Slx1-Slx4 is predominantly active in resolving joint molecules in the absence of Sgs1 (ZAKHEREYVICH, et al., 2012; DE MUYT, et al., 2012; FRICKE & BRILL, 2005; MATOS, et al., 2011).

1.2.5 ZMMs role in coupling synaptonemal complex formation and recombination pathways

Synaptonemal complex formation and recombination events appear to be temporally linked. The earliest deposition of Zip1 as punctate staining comes at a time when the earliest stages of meiotic recombination are occurring (PADMORE, et al., 1991). The two processes are intimately linked in budding yeast; mutations in Zip1 or the Synapsis initiation complex (Zip2-4, Spo16) genes lead to a reduction in the number of crossovers (BORNER, et al., 2004), and those crossovers which are formed lack crossover interference (SYM, et al., 1993). On the other hand, mutants which are impaired in the progression of recombination also suffer defects in the assembly of the SC (ALANI, et al., 1990; BISHOP, et al., 1992). In the absence of DSBs, and hence meiotic recombination, Zip1 protein is aberrantly aggregated into a polycomplex, as

opposed to forming the transverse and central elements of the SC (CHUA & ROEDER, 1998). Zip3, a member of the synapsis initiation complex, co-localises with Zip2, which is required for the initiation of synapsis, also associates with early and late meiotic recombination proteins, suggesting that the two processes are inherently linked (AGARWAL & ROEDER, 2000). Furthermore, Zip3 has been shown to associate specifically with crossover designated sites (SERRENTINO, et al., 2013). Together, these data indicate that the formation of the synaptonemal complex and the repair of meiotic DSBs are intimately linked through components of the ZMM repair pathway.

1.2.6 Repair template choice in homologous recombination

DNA repair by homologous recombination requires a donor DNA molecule to act as a template for repair. However, in different cellular contexts, the choice of repair template differs. During mitotic repair, the sister chromatid is the preferred template for repair (KADYK & HARTWELL, 1992), as sister chromatid repair is less likely to result in a loss of homozygosity between chromosomes, which might be potentially deleterious for daughter cells. The aim of meiotic homologous repair is distinct, with the aim of generating physical linkages between homologous chromosomes, and so the choice of repair template must be distinct; rather than the prevalent intersister repair observed in mitosis, a bias is generated toward interhomolog repair templates (SCHWACHA & KLECKNER, 1997).

1.2.6.1 Repression of intersister repair during meiosis

During mitotic repair, repair template choice appears to be determined by the most proximal template, which is in most situations the sister chromatid (SJOGREN & STROM, 2010), discussed in (HONG, et al., 2013), leading to an overwhelming occurrence of intersister repair. However, during meiotic recombination, this bias is reversed, and instead a bias towards interhomolog repair is observed, of approximately 4:1 (SCHWACHA & KLECKNER, 1997; BISHOP, et al., 1999; KIM, et al., 2010).

The first component that is required for the formation of bias is cohesin, which acts to hold sister chromatids together, and is a component of the axial element of the synaptonemal complex among other functions. In the absence of the kleisin subunit Rec8, the bias towards interhomolog repair is abolished (KIM, et al., 2010), suggesting that Rec8 is required for the establishment of this bias. There is another group of factors which are required to maintain this bias: interhomolog bias maintenance factors (Mek1, Red1, Hop1). In mutants lacking these factors, intersister bias is specifically promoted, as opposed to the abolition of bias as seen in Rec8 mutants. However, double mutants lacking Rec8 and the interhomolog bias maintenance factors experience a *rec8*Δ phenotype. It has hence been suggested that meiotic cohesin promotes intersister bias specifically, but that this bias is repressed by other factors (KIM, et al., 2010). It has been suggested that cohesin is required to enable interhomolog interactions to be distinguished from intersister interactions, and

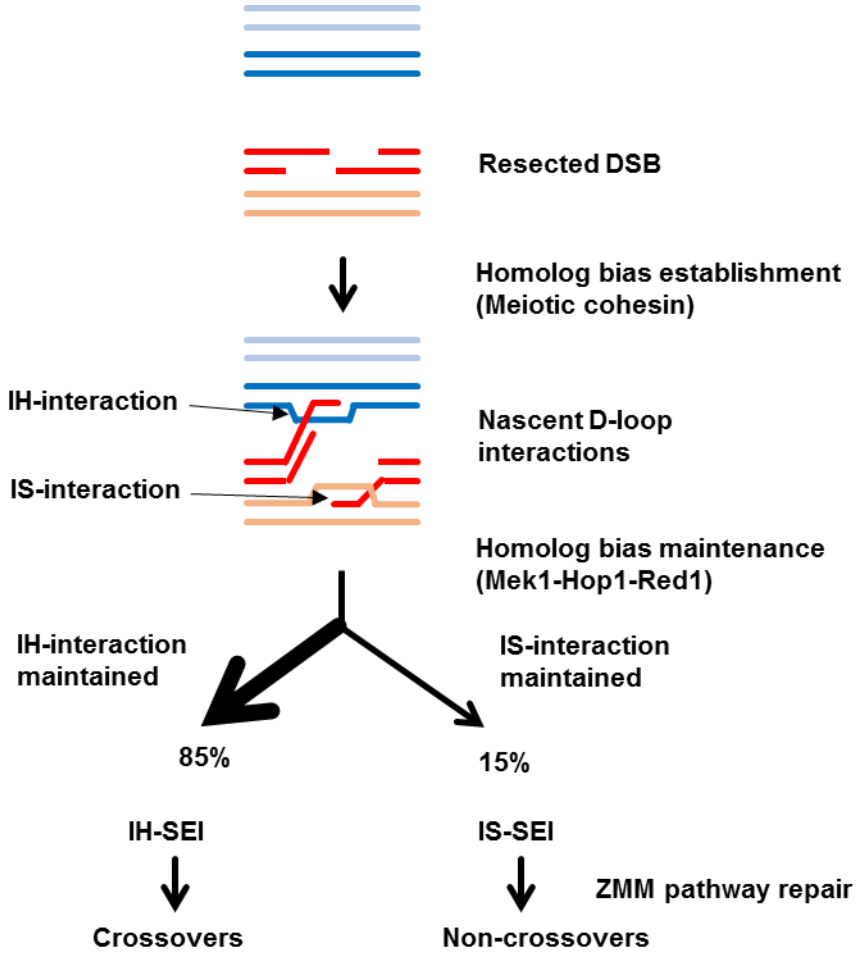

Figure 1.6 Establishment and maintenance of interhomolog bias (adapted from HONG et al. 2013)

Following the formation of programmed DSBs, and their resection to generate ssDNA, the single end interacts with the homologous DNA strand, generating an interhomolog interaction via the nascent D-loop. The other end maintains some form of interaction, possibly a nascent D-loop, with the sister chromosome. This is dependent upon the presence of meiotic cohesin. The choice of which interaction is maintained (homolog bias maintenance) and which is dissociated, is then determined by the Mek1-Hop1-Red1 kinase pathway, with interhomolog interactions being favored in wild type, which then progress to stable SEIs, and eventually resolved into crossovers.

so, in its absence, events have a 50% chance of occurring between sisters, and 50% chance of forming between homologs (HONG, et al., 2013) (Figure 1.6).

However, the establishment of bias is inherently more active. A meiosis specific protein-kinase pathway containing Hop1, Mek1 and Red1, has been shown to promote IH:IS bias – in the absence of these component, the bias of repair is reversed, so that intersister interactions are more prevalent, as in the mitotic cell cycle (CARBALLO, et al., 2008; WAN, et al., 2004). It should be noted that intersister recombination does occur during budding yeast meiosis (GOLDFARB & LICHTEN, 2010), and it has been suggested to act as a safeguard mechanism should interhomolog repair not be viable. The mode of action of this pathway appears to be via modulating the activity of Rad51. In *dmc1* mutants, meiotic prophase is blocked and DSBs accumulate; however, this is overcome when members of the Red1-Mek1-Hop1 pathway are mutated (WAN, et al., 2004; XU, et al., 1997). The joint molecule interactions in these mutant environments are between sister chromosomes, and can be explained by a model which suggests that Rad51 activity is repressed by the actions of these kinases in a meiosis specific environment (NIU, et al., 2009), leading to the catalysis of meiotic DNA repair by Dmc1. It has been shown that this activity is promoted by the action of HED1, which physically interacts with Rad51 to repress its activity in meiotic cells (TSUBOUCHI & ROEDER, 2006).

Furthermore, the intersister bias observed in Red1-Mek1-Hop1 mutants is abolished by the absence of meiotic cohesin (HONG, et al., 2013). This

suggests that cohesin mutations render the interhomolog bias pathway non-functional, implying that cohesin is fundamental for the establishment of bias in all mutant contexts.

1.3 SMC complexes

1.3.1 Overview of SMC complexes

The cohesin complex belongs to a family of three related complexes that are involved in higher order chromosome organisation and dynamics (GUACCI, et al., 1997; FREEMAN, et al., 2000; OUTWIN, et al., 2009) and which are comprised of two heterodimeric Structural Maintenance of Chromosomes (SMC) proteins: Smc1/3 in cohesin, Smc2/4 in condensin, Smc5/6 in the complex of the same name (HAERING, et al., 2002; HIRANO, et al., 1997; SERGEANT, et al., 2005) (Figure 1.7). These six proteins have a highly homologous structure (COBBE & HECK, 2004), possessing two long alpha helical domains separated by a central hinge region, which enables the protein to fold back on itself generating an antiparallel coiled coil (MELBY, et al., 1998) They also possess walker A and B motifs at the C and N terminus respectively (LOWE, et al., 2001). The two SMC proteins dimerise at the hinge domain (MELBY, et al., 1998), whilst the walker domains bind ATP. These protein complexes are conserved across a wide variety of species, and details of species specific homologues are indicated in Table 1.1.

1.3.2 Cohesin

1.3.2.1 Structure and loading of the cohesin complex

Cohesin, a multi-subunit protein complex, is required to hold sister chromosomes together from DNA replication during S-phase (MICHAELIS, et al., 1997), in addition to being an essential component of the lateral elements of the SC. The manner in which the complex associates with DNA is still a matter

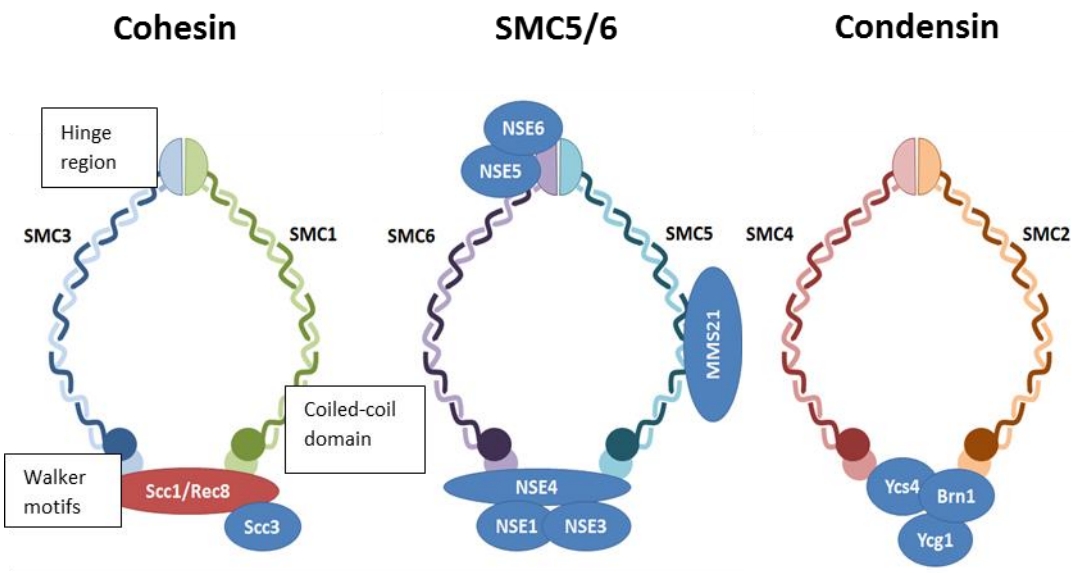

Figure 1.7 SMC family of complexes

SMC proteins have a highly conserved structure, possessing two extended alpha helical domains separated by a flexible hinge domain, allowing the protein to fold back on itself to generate a coiled-coil structure. This figure demonstrates the subunits found in *S.cerevisiae* complexes. The kleisin subunit of the cohesin subunit is variable: Scc1 during mitotic growth, Rec8 in meiosis.

The SMC complexes in different organisms

	Cohesin	Condensin	SMC5/6
S. cerevisiae	Smc1/3 Scc1/ Rec8 Scc3	Smc2/4 Ycs4 Ycg1 Brn4	Smc5/6 Nse1/3/4 Nse5/6 Mms21 (Nse2)
S. pombe	Psm1/ Psm3 Rad21 Psc3	Cut14/ Cut3 Cnd1 Cnd3 Cnd2	Spr18/Rad18 Nse1/3/ Rad62 Nse5/6 Nse2
C. elegans	HIM-1/ SMC-3 REC-8/ COH3-4/ SCC-1 SCC3	MIX-1/ SMC-4 DPY-28 CAP-G1 DPY-26	SMC-5/6 (other sub-units are uncharacterised)
H. sapiens	SMC1/ SMC3 RAD21/ REC8/ RAD21L SA1/SA2	SMC2/ SMC4 NCAPD2 NCAPG NCAPHH	SMC5/6 NSMCE1/3/4 NSMCE5/6 NSMCE2

Table 1.1 The SMC complexes in different organisms

Homologous proteins in *S. cerevisiae, S. pombe, C. elegans* and *H. sapiens* are shown for each SMC complex. It should be noted that whilst there are genes with homology for non-smc elements for Smc5/6 in *C. elegans,* these have not been characterized or named.

of debate, with some suggesting that each cohesin complex associates with a single chromosome, and those cohesin complexes then associate to hold chromosomes together (RUDRA & SKIBBENS, 2013). However, the majority of the evidence suggests that cohesion is achieved by encircling both DNA strands in a ring like structure (HAERING, et al., 2008). In cohesin, a non-SMC subunit of the cohesin complex, an alpha kleisin, binds to head domains of both Smc1 and Smc3 (HAERING, et al., 2002), closing the ring-shaped complex (GRUBER, et al., 2003). The alpha kleisin varies depending on the developmental stage of the cell cycle (Scc1 during mitotic growth, Rec8 during meiosis (WATANABE & NURSE, 1999)). The N-terminal domain of Scc1 interacts with the coiled-coil region of Smc3, some way from the ATPase domain (GLIGORIS, et al., 2014); however, hydrolysis of ATP is required in order for the complex to stably associate with DNA (ARUMUGAM, et al., 2003).

1.3.2.2 Mitotic functions in *S. cerevisiae*

The cohesin complex dynamically loads and unloads onto DNA before S phase, with cohesin being loaded onto the DNA by the action of the Scc2/4 loading complex (CIOSK, et al., 2000) entering the complex through dissociation of the hinge domain interface (GRUBER, et al., 2006). It dynamically releases DNA as a result of the action of a complex containing Wap1 (Scc3/Pds5/Rad61 in *S. cerevisiae*) which has a cohesion anti-establishment activity, and enables DNA to exit the cohesin ring via the dissociation of the Smc3/Scc1 interface (ROWLAND, et al., 2009). During interphase, the cohesin complex slides along the mitotic chromosomes as a result of transcription, and this does not require

the traditional loading/unloading mechanisms (OCAMPO-HAFALLA, et al., 2016). At S-phase, as the replication fork passes, Eco1 acetylates Smc3 at its ATPase domain (ZHANG, et al., 2008), which counteracts the activity of the Rad61 complex (ROWLAND, et al., 2009): this is the point at which sister chromatid cohesion is established (TOTH, et al., 1999). The cohesin complex then holds DNA together through G2 phase and into the beginning of mitosis. At the metaphase to anaphase transition, phosphorylation of the alpha kleisin Scc1 occurs as a result of increased activity of the Polo like kinase (Cdc5 in *S. cerevisiae*) (ALEXANDRU, et al., 2001) this makes Scc1 a target for degradation. Simultaneously, the level of Cdc20, an activator of the Anaphase Promoting Complex (APC/C), is increasing, which leads to the ubiquitination and eventual degradation of securin (Pds1 in *S. cerevisiae*) (COHEN-FIX, et al., 1996; LIM, et al., 1998), an inhibitor of the protease separase. Separase then cleaves Scc1 (UHLMANN, et al., 1999), which allows the separation of sister chromatids under the force generated by depolymerisation of microtubules at the spindle pole body (anaphase A) as well as the kinetochore (anaphase B).

In mitotic mammalian cells, it should be noted that there is a large scale removal of cohesin prior to anaphase by the prophase pathway (WAIZENEGGER, et al., 2000). This process has been demonstrated to be dependent on both Polo like kinase and Aurora B kinase activity (LOSADA, et al., 2002; SUMARA, et al., 2002). In budding yeast meiosis, there is a removal of cohesin prior to the onset of anaphase, which is dependent on the kinase activity of Cdc5, the localisation of which is dependent on the Condensin complex, bringing the kinase to the chromosome axis (YU & KOSHLAND,

2005). In addition to its role in mitosis, cohesin has a further role in the repair of DNA damage, by de novo loading of the complex at sites of DSBs (STROM, et al., 2004); this has been shown to be dependent on the related SMC5/6 complex. Cohesin also possesses non-canonical roles, such as recruitment to DNase I hypersensitive sites in a CTCF (CCCTC-binding factor) dependent manner (PARELHO, et al., 2008), which has led to the implication that cohesin has a role in gene regulation (WENDT & PETERS, 2009).

1.3.2.3 Meiotic functions in *S. cerevisiae*

During meiosis, reciprocal exchange of DNA at crossover sites leads to the meiotic cohesin complex encircling homologous chromosomes distal from centromeres, whilst proximal complexes still encircle sister chromatids at the centromere, with stable associations between homologues formed at chiasmata (Figure 1.8). Meiotic cohesin complexes are also constructed from different core subunits than those observed during mitosis, with Rec8 (in addition to homologous protein Rad21L in mammalian cells) replacing the alpha kleisin Scc1 (WATANABE & NURSE, 1999; LEE & HIRANO, 2011). It has been suggested that the differential localisation of Rad21L and Rec8 during mammalian meiosis leads to a molecular barcode that may facilitate homologous chromosomes to pair efficiently (LEE & HIRANO, 2011), although no similar mechanism has been demonstrated in yeast. The use of variant subunits is thought to enable additional levels of regulation that are not observed in mitosis, with Separase-dependant Rec8 cleavage being regulated by phosphorylation generated by Caesin Kinase 1 and Dbf4-dependant kinase

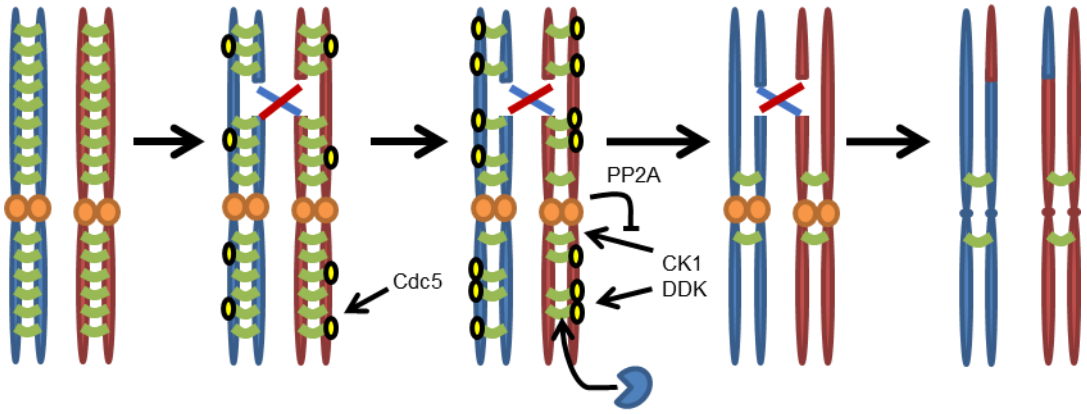

Figure 1.8 Cohesin regulation throughout the meiotic division

The majority of cohesin is loaded onto chromosomes during S phase, where it holds sister chromatids together (cohesion) until the meiotic division. During meiosis DSBs are induced by Spo11, and cohesin is initially loaded locally at these sites to facilitate homologous recombination (Not shown in this diagram). There is also evidence that cohesin is then removed from DSBs to allow processing of recombination intermediates. During prophase, polo like kinase cdc5 phosphorylates Rec8, causing a subset of chromatin bound cohesin to dissociate – the prophase pathway. At the metaphase to anaphase transition, caesin kinase and Dbf4 dependent kinase (CK1 and DDK respectively) phosphorylate Rec8. Simultaneously, the anaphase promoting complex (APC/C) targets securin, the Separase inhibitor, for degradation. Centromeric cohesion is protected by the phosphatase activity of Sgo1/PP2A, which protects centromeric cohesin' from Separase cleavage. This allows sister chromatids to remain attached during anaphase I, whilst homologous chromosomes are separated to different poles.

Cdc7 (DDK). Cdc5 also phosphorylates Rec8, but this does not seem to have an effect on cleavage by Separase (KATIS, et al., 2010), instead it has been demonstrated that this affects the dissociation of cohesin during prophase (YU & KOSHLAND, 2005). It is further worth noting that Rec8 has a complex role in the bias towards repair utilising the homologous chromosome (IH:IS bias), with an early role promoting intersister (IS) recombination, which is suppressed by other lateral element components Red1 and Hop1, but a later function in maintaining interhomolog (IH) bias (KIM, et al., 2010; HONG, et al., 2013)

Chromosome arm localised-cohesin is removed at the onset of anaphase I (BUONOMO, et al., 2000), however it is important that sister chromatids remain attached throughout meiosis I, in order to avoid the loss or gain of chromosomes through random segregation at the cell division, whilst homologous chromosomes are able to separate. This distinction is achieved via recruitment of Shugoshin (Sgo1) to yeast centromeres, where cohesin encircles only sister chromatids. Sgo1 recruits protein phosphatase 2A (PP2A) to centromeres (KITAJIMA, et al., 2006), which dephosphorylates Rec8 in nearby regions, making it a less favourable substrate for separase cleavage (KATIS, et al., 2010). Fission yeast possesses two Shugoshin variants, with both regulating meiotic chromosome segregation (RABITSCH, et al., 2004), whilst in mammalian cells, of the two homologues, SGO1 and SGO2, SGO2 has been shown to be essential for the completion of meiosis (LLANO, et al., 2008). The use of meiotic variants potentially distinguishes the roles of the Shugoshin complexes between vegetative growth and sexual cell divisions. Given that centromeric cohesin is exclusively protected via this mechanism, and cohesin

localised to chromosome arms is cleaved in a Separase dependant manner at anaphase I, homologs can thus be efficiently segregated during the first meiotic division, whilst sister chromatids remain attached. Sgo1 disappears from centromeres during anaphase I (RIEDEL, et al., 2006), hence during meiosis II, centromeric Rec8 is no longer protected from kinase activity by PP2A, which leads to its phosphorylation and cleavage, allowing sister chromatids to separate into daughter cells.

1.3.2.4 DNA repair and the cohesin complex

Cohesin subunits were first identified in DNA damage mutant screens (BIRKENBIHL & SUBRAMANI, 1992), and the complex has since been shown to have a variety of roles in DNA damage repair. Cohesin mutants have been shown to be defective in repairing damaged DNA, seen as a function of its ability to generate cohesion between sister chromatids, and thus ensure that a repair template is proximal to the break site *in vivo* (SJOGREN & NASMYTH, 2001). Cohesin has been shown to accumulate proximal to the sites of DSBs in a manner dependent upon its loader, Scc2/4. (STROM, et al., 2004). It has also been demonstrated in *S. pombe* that when the removal of cohesin is inhibited, by either inactivating Separase or utilising Separase resistant Scc1 alleles, DNA damage repair defects occur (NAGAO, et al., 2004). In addition, the cohesin complex has been demonstrated to interact with meiotic DSBs and affect meiotic DSB repair in a variety of ways. In the absence of the meiosis specific kleisin subunit Rec8, a mild DSB hyper-resection phenotype is observed (KLEIN, et al., 1999), suggesting that cohesin has a protective role with regards

to DSBs. Rec8 mutants also exhibit reduced recombinant formation, whilst appearing to maintain similar levels of DSBs to wild type cells (KLEIN, et al., 1999; BRAR, et al., 2009).

1.3.3 Condensin

The condensin complex plays a crucial role in both the compaction of chromosomes during the cell cycle, and in enabling chromosome separation at cell division. Higher eukaryotes possess two distinct condensin complexes, comprised of different subunits (condensin I and condensin II) (ONO, et al., 2003), whilst yeast possess a single condensin complex to perform all cellular functions. Prokaryotes also possess condensin complexes, enabling efficient chromosome segregation during cell division (MASCARENHAS, et al., 2002).

In *S. cerevisiae,* condensin localises to the nucleus throughout the cell cycle (FREEMAN, et al., 2000). It has been demonstrated that it is essential for the faithful segregation of repetitive ribosomal DNA regions (FREEMAN, et al., 2000), and in addition that it is necessary to allow segregation of sister chromatids at anaphase by allowing chromosome arm recoiling (RENSHAW, et al., 2010). During the meiotic cell cycle, the condensin complex localises to the meiotic chromosomes at pachytene stage, and is required for efficient axial compaction (YU & KOSHLAND, 2003). Furthermore, SC assembly, and the resolution of joint molecules is abrogated in the absence of the condensin complex – DNA bridges are observed in anaphase I in the absence of condensin. Finally, condensin contributes to the mono-orientation of sister

kinetochores at meiosis I, by interacting with the monopolin complex component, Mam1 (BRITO, et al., 2010).

1.3.4 The Smc5/6 complex

1.3.4.1. Structure and function of the Smc5/6 complex

The related Smc5/6 complex was first discovered in *S. pombe* (LEHMANN, et al., 1995). It is essential for viability in most organisms, including *S. cerevisiae* and is conserved in all eukaryotes; however, its cellular roles are less well defined than those of cohesin and condensin. The Smc5/6 complex consists of two SMC proteins, and Non-Smc Elements (NSE) 1-6 (SERGEANT, et al., 2005; DUAN, et al., 2009). Nse1, 3 and 4 form a sub complex which acts as an alpha kleisin to bridge the walker domains of the Smc5/6 heterodimer (PALECEK, et al., 2006). Nse5-6 acts as a dimer, and binds to the hinge region of the Smc5/6 complex (DUAN, et al., 2009), whilst Nse2/MMS21 is a SUMO ligase that SUMOylates Smc6 in response to DNA damage (ANDREWS, et al., 2005). Other targets of the ligase activity remain unknown. All components of the Smc5/6 complex are essential for viability in *S. cerevisiae*, and all subunits are essential for its canonical role in DNA repair. The Nse5/6 dimer is not essential in *S. pombe* (PEBERNARD, et al., 2006).

1.3.4.2. Mitotic functions of the Smc5/6 complex

The Smc5/6 complex has been shown to influence a number of processes including replication fork stability (AMPATZIDOU, et al., 2006) and the repair of

DNA damage, specifically by homologous recombination (VERKADE, et al., 1999; DE PICCOLI, et al., 2006). Smc5/6 complex components are specifically required for replication fork stability in highly transcribed and repetitive regions of the genome, such as the rDNA (TORRES-ROSELL, et al., 2005), which tend to lose copies in *smc5/6* hypomorphic strains. This is likely as a result of increased tendency for replication fork stalling and collapse in these highly-transcribed regions (MURRAY & CARR, 2008; MENOLFI, et al., 2015). In a Top2 deficient environment, the Smc5/6 complex associates with chromosome arms, and it thus assumed that it is involved in resolving sister chromatid intertwining's that occur in this background (JEPPSSON, et al., 2014).

Hypomorphic mutations in the complex are hypersensitive to DNA damaging agents, consistent with their role co-ordinating DNA damage response (VERKADE, et al., 1999; COST & COZZARELLI, 2006). Smc5/6 complex mutants experience the "cut" phenotype, whereby chromosomes fail to segregate efficiently into daughter cells, and DNA remains unencapsulated outside of spore walls (FOUSTERI & LEHMANN, 2000; AMPATZIDOU, et al., 2006; FARMER, et al., 2011). Smc5/6 complex components are synthetic lethal with Mus81-Mms4 mutants, a well characterised recombination complex which is required for stabilisation/repair of paused and collapsed replication forks, implying a similar role for the Smc5/6 complex. The role in HR also has important implications for telomere maintenance and cellular senescence, specifically through the SUMO ligase activity of Nse2/MMS21 (CHAVEZ, et al., 2010).

1.3.4.3. Meiotic functions of the Smc5/6 complex

The Smc5/6 complex has been shown to play a crucial role in meiosis. Nse1-1 hypomorphic mutations produce asci with aberrant spores, and have a significant reduction in spore viability. DNA is not segregated effectively and is divided unequally between spores (PEBERNARD, et al., 2004). This is likely to be at least partially due to a failure to adequately resolve recombination intermediates in mutant cells. This is experimentally determined utilising the *spo11Δ/spo13Δ* mutant system, which allows for a meiotic-like early cell division, but which blocks the formation of meiotic DSBs (*spo11Δ*) and allows a return to growth (*spo13Δ*), whereby a mitotic division is undertaken, as opposed to meiotic. This enables the separation of the functions of complexes involved in multiple pathways, to see whether their role in meiotic DNA repair is leading to a particular phenotype.

The *smc5-meiotic null/spo11Δ/spo13Δ* triple mutants, which exhibit a hypomorphic depletion of Smc5 at the onset of meiosis, do not induce DSBs, and undergo a mitosis like division to form dyads when incubated in sporulation media, show no difference in the levels of dyad formation compared to *spo11Δ/spo13Δ* double mutants (COPSEY, et al., 2013) whilst *smc5-meiotic null/spo11Δ* show a 50-fold increase in spore viability when compared with *smc5-meiotic null* single mutants (PEBERNARD, et al., 2004). This suggests that induced DSBs are partially responsible for the cut phenotype, and it would logically follow that there is a failure to resolve recombination intermediates in Smc5/6 complex meiotic-null cell lines. The SMC5/6 complex, through its

SUMO ligase subunit Mms21, also has an important role in removing multichromatid joint molecules (MCJMs) that persist after dHJs have been resolved (XAVER, et al., 2013), and also a role in the resolution of intersister recombination intermediates (LILIENTHAL, et al., 2013; COPSEY, et al., 2013).

The other notable feature of Smc5/6 complex mutants is that they fail to trigger checkpoints that might otherwise halt cell division, leading to cells dividing without a segregation of chromosomes. There is an abrogation of the Chk2 dependant DNA damage checkpoint in Smc5/6 complex mutants. There are two hypotheses as to how this might affect joint molecule resolution. Mutant cell lines may fail to respond appropriately to checkpoint activation that would normally sense the presence of these unresolved joint molecules and arrest the cell cycle (HARVEY, et al., 2004). Alternatively, given that Rad60 is phosphorylated in response to Chk2 activation (MIYABE, et al., 2009), and associates with the Smc5/6 complex (BODDY, et al., 2000; BODDY, et al., 2003) the recombination intermediates and collapsed replication forks generated in an *smc5/6* null environment may not be substrates that activate DNA damage response pathway. In either case, it is a failure of the checkpoint/repair pathway which ultimately leads the mitotic and meiotic catastrophe.

The Smc5/6 complex has been shown to be associated with these early recombination events in a number of studies. The Smc5/6 complex has been shown to co-localise with Rad51 foci on meiotic spreads (XAVER, et al., 2013),

and with meiotic DSB sites by ChIP analysis (COPSEY, et al., 2013) in *S. cerevisiae*. In *C. elegans*, it has been demonstrated that Smc5/6 complex component SMC-6 is enriched at meiotic chromosomes at early pachytene, when meiotic DSBs are generated (BICKEL, et al., 2010). In human spermatocytes, SMC6 foci co-localise with DMC1 foci on XY bodies (VERVER, et al., 2014). These data indicate a crucial role for the Smc5/6 complex during the earliest stages of meiotic repair, although the exact mechanism by which the complex acts at this early stage has not been fully explored. It has been suggested to specifically mediate DSB repair between sister chromatids (BICKEL, et al., 2010), which would be in stark contrast to the anti-crossover functionality observed in the BLM helicase Sgs1, with which it has many overlapping functions.

1.3.5 The interaction between Smc5/6 and cohesin

There is a strong inter-relationship between the Smc5/6 complex and cohesin. The cohesin loading complex Scc2/4 is necessary for the chromosomal association of the Smc5/6 complex, through the action of cohesin itself (JEPPSSON, et al., 2014) and the two protein complexes have a much higher correlation of localisations than would be expected from random dispersal along the chromosome (COPSEY, et al., 2013; JEPPSSON, et al., 2014) There also seems to be interplay between the two complexes, with Smc5/6 complex mutants aberrantly retaining arm cohesin long after anaphase onset (OUTWIN, et al., 2009; COPSEY, et al., 2013). Paradoxically, mutants also experience precocious loss of centromeric cohesion during meiosis, with centromeres

separating before anaphase onset (COPSEY, et al., 2013). It should be noted that there is some evidence that sister chromatid cohesion is normal in *smc5/6* meiotic mutants (LILIENTHAL, et al., 2013), although these results were achieved utilising temperature sensitive mutants in what has been shown to be a highly temperature sensitive environment. Furthermore, it is unlikely that subtle alterations observed utilising live cell imaging in (COPSEY, et al., 2013) would be detectable using the hourly time points taken in this paper (LILIENTHAL, et al., 2013). The over expression of Separase partially rescues the Smc5/6 complex mutant phenotype in mitosis (OUTWIN, et al., 2009). These results seem to suggest a fundamental role for the Smc5/6 complex in the regulation of cohesin; either directly by the catalytic activity of subunits of the Smc5/6 complex, or indirectly by altering the higher order structure of the chromosome, making cohesin more accessible to regulatory factors. The exact nature by which these complexes interact has yet to be fully determined.

Chapter 2

Materials and Methods

2.1. Materials

2.1.1 Growth Media

2.1.1.1. Bacterial Media

Bacteria were grown in Luria Broth (1% w/v bacto-tryptone, 0.5% w/v yeast extract, 0.5% w/v NaCl, pH 7.0) at 37°C. For solid media, 2% w/v agar was added before autoclaving. In order to ensure that plasmids were retained, specific antibiotics were added at concentrations listed in **2.1.4.**

2.1.1.2. Yeast media

Media	Purpose	Composition
YEPEG	Selection against petite colonies	Yeast extract 1.0% Bacto-peptone 2.0% Glycerol 2.0% Succinate 1.0% Adenine 0.5 mM Ethanol 2.0% (added post-autoclave) pH 5.5
YPD	Vegetative growth	Yeast extract 1.0% Bacto-peptone 2.0% D-glucose 2.0% Adenine 0.5 mM Antibiotics if required (see **2.1.4.**) pH 6.5
Drop-out media	Auxotrophic selection	YNB without αα and NH_4SO_4 0.17% D-glucose 2.0% Ammonium sulphate 0.5% Amino acid supplement (see table 2.2) pH 7.25
SPS	Pre-sporulation media	Yeast extract 0.5% Bacto-peptone 1.0% YNB without αα and NH_4SO_4 0.17% Potassium Acetate 1.0% Ammonium sulphate 0.5% Potassium hydrogen phthalate 0.05 M pH 5.5

Table 2.1 (continued overleaf)

Media	Purpose	Composition
Supplemented 1% KAc (liquid)	Sporulation media (time courses)	Potassium Acetate 1.0% Raffinose 0.02% Amino acid supplement (see table 2.2) pH 7.0
1% KAc (plates)	Sporulation media (where stated)	Potassium Acetate 1.0% Raffinose 0.02% pH 7.0
KAc – COM (plates)	Sporulation media (where stated)	Potassium Acetate 2.0% Yeast extract 0.22% D-glucose 0.05% Amino acid supplement (see table 2.2) pH 7.0

Table 2.1 (continued from overleaf). For plate media, 2% w/v agar was added before autoclaving was undertaken. For Potassium Acetate based media, separate recipes were liquid media and for plate media – both are given above. SPS and KAc-COM liquid also have 20µl antifoam added to them prior to use.

Amino acid	**Sigma-Aldrich product numbers**	**Amount (mg)**	**Final conc. (% w/v)**
Adenine (hemisulfate salt)	A9126	800	0.003
L-arginine (HCL)	A5006	800	0.003
L-aspartic acid	A9256	4000	0.016
L-histidine	H8000	800	0.003
L-leucine	L8000	800	0.003
L-lysine (mono-HCl)	L5626	1200	0.005
L-methionine	M9625	800	0.003
L-phenylalanine	P2126	2000	0.007
L-threonine	T8625	8000	0.032
L-tryptophan	T0254	800	0.003
L-tyrosine	T3754	1200	0.005
Uracil	U0750	800	0.003

Table 2.2. Amino acids (obtained as powders from sigma) used to make complete and drop-out supplements for media.

2.1.2. Buffers

Buffer	Composition
TAE	40 mM Tris (hydroxymethyl) methylamine 20 mM Acetic Acid 1 mM EDTA
TBE	89 mM Tris (hydroxymethyl) methylamine 89 mM Boric acid 2 mM EDTA
10× TNE	100 mM Tris (hydroxymethyl) methylamine 2 M NaCl 10 mM EDTA
PBS	137 mM NaCl 2.7 mM KCl 10 mM Na_2HPO_4 1.8 mM KH_2PO_4
Hybridisation buffer	250 mM Na-phosphate, pH 7.2 250 mM NaCl 1 mM EDTA 7% SDS 5% Dextran Sulphate
Sodium phosphate wash buffer	50 mM Na-phosphate, pH 7.2

Table 2.3 continued overleaf

Low stringency wash buffer	0.1% SDS 300 mM NaCl 30 mM Na-citrate
High stringency wash buffer	0.1% SDS 15 mM NaCl 1.5 mM Na-citrate
10/1 TE	10 mM Tris HCl 1 mM EDTA
50/50 TE	50 mM Tris HCl 50 mM EDTA
Spheroblasting buffer	1 M Sorbitol 50 mM K-phosphate, pH 7.0 10 mM EDTA
Dissection buffer	1 M Sorbitol 10 mM Na-phosphate, pH 7.2 10 mM EDTA

Table 2.3

2.1.3. Enzymes

Enzyme	**Supplier**
DreamTaq™ DNA polymerase	ThermoFisher Scientific
T4 DNA ligase	New England Biolabs
Restriction Enzymes	New England Biolabs
Zymolyase (100T and 20T)	Seikagaku Corporations
RNase A from bovine pancreas	Sigma Aldrich
Proteinase K from *Tritirachium album*	Sigma Aldrich

Table 2.4

2.1.4. Antibiotics

Antibiotic	**Supplier**	**Concentration used**
Ampicillin	Sigma-Aldrich	100µg/ml
Geneticin-418	Invitrogen	200µg/ml or 400µg/ml
Hygromycin B	Invitrogen	300µg/ml
Nourseothricin	Werner Biotech	100µg/ml

Table 2.5

2.1.5. Antibodies

Antibody number	Description	Working dilution	Supplier	Catalogue number
AB5	Texas Red ® conjugated Anti-rabbit IgG (Donkey IgG)	1:100	Jackson immunoResearch	711-586-152
AB10	Fluorescein (FITC) conjugated Anti-rat IgG (Donkey IgG)	1:100	Jackson immunoResearch	712-095-153
AB19	Anti-tubulin (rat IgG) - YOL1/34W	1:400	Novus biologicals	NB100-1639
AB23	Anti-ZIP1 (rabbit IgG) – produced by Alice Copsey	1:200	Eurogentec	N/A

Table 2.6

2.1.6. Oligonucleotides

Oligo number	Oligo name	Sequence	Application
O605	NDT80_A	GTGACTTTACATTGTTACTTCCGC	Forward primer anneals 290-314 bp upstream to the NDT80 start codon
O606	NDT80_B	TCTCTCACTAATTCAAATGGAGGTC	Reverse primer anneals 197-221 bp downstream of the NDT80 start codon
O630	NDT80_MX.F	TAAAAAGCGCTTAAAATGGATGTCCACGAGGTCTCTATTGCATGTCAAGGCAGCCC*CG*TACGCTGCAGGTCGAC	MX forward cassette primer, anneals upstream of NDT80 start codon
O631	NDT80_MX.R	AAATCATTAGTTTATTTACGGTGTCGGTCTCGTAGGCTCAGCATCAAGCACATTAATCGATGAATTCGAGCTCG	MX reverse cassette primer, anneals downstream of NDT80 stop codon
O233	SMC5_A	GATTAACCTTTACAGAACCGCTACA	Forward primer anneals 375-351 bp upstream to the SMC5 start codon
O234	SMC5_B	GTAACATTTGGTGAATTTTTCAAGG	Reverse primer anneals 344-368 bp downstream of the SMC5 start codon
O237	NSE4_A	CAACATTTACTATCATCTTGTGCCA	Forward primer anneals 275-299 bp upstream to the NSE4 start codon

O238	NSE4_B	ATTTCACTTTCCAGGTCCCTATATC	Reverse primer anneals 158-182 bp downstream of the NSE4 start codon
O933	Msh5_MX.F	ATACTGCCACCAAATGGAATCGTACGCTGCAGGTC	MX forward cassette primer, anneals upstream of MSH5 start codon
O934	Msh5_MX.R	TTTTATTCTTTGATATATTAATCGATGAATTCGAG	MX reverse cassette primer, anneals downstream of MSH5 stop codon
O2146	MSH5_A	AACAAAGGAAAAAGGATTCATTACC	Forward primer anneals 226-250bp upstream to the MSH5 start codon
O2147	MSH5_B	AGCAGTACTGTCATTGTATTCACCA	Reverse primer anneals 627-651 bp downstream of the MSH5 start codon
O2111	RAD51_A	CCAATCTAGTTTAGCTATCCTGCAA	Forward primer anneals 308-332 bp upstream to the RAD51 start codon
O2112	RAD51_B	AAAGTGTGACATAGCTGGGACTTAC	Reverse primer anneals 569-593 bp downstream of the RAD51 start codon
O887	DMC1_A	CTGAAGATACTTGGGACTTCAAAAA	Forward primer anneals 391 bp upstream from DMC1 start codon
O888	DMC1_B	TGTATATCCCACCAGACTTCAATTT	Reverse primer anneals 124 bp downstream from DMC1 start codon

O927	REC8_A	ACGTGTTCTTTTTGTCTCGTTTTAG	Forward primer anneals 228 bp upstream from REC8 start codon
O928	REC8_B	AGGTGATTTAGGTCATTCAACACAT	Reverse primer anneals 320 bp downstream from REC8 start codon

Table 2.7

2.1.7. Bacterial Plasmids

Plasmid number	**Alternative name**	**Description**	**Application**
pEH91	pRED460	Longtine plasmid containing HPHMX cassette	Gene knockout by selectable drug marker (LONGTINE, et al., 1998)
pEH172	pRED231	pFA6a-containing KANMX4 cassettes	Gene knockout by selectable drug marker

Table 2.8

2.1.8. Yeast strains

2.1.8.1. Base yeast strains

Strain number	Other names	Strain background	Ploidy	Genotype
Y957		SK1	1n	*MAT α, his3::hisG, leu2::hisG, trp1::hisG, lys2, ura3, ho::LYS2*
Y958		SK1	1n	*MAT **a**, his3::hisG, leu2::hisG, trp1::hisG, lys2, ura3, ho::LYS2*
Y3007		SK1	1n	*MAT α, HIS4::LEU2-(BamHI;+ori), leu2::hisG, ura3Δ(sma-pst), ho::hisG*
Y3008		SK1	1n	*MAT **a**, his4-X::LEU2-(NgoMIV;+ori)--URA3, leu2::hisG, ura3Δ(sma-pst), ho::hisG*
Y97	EY76	Y55	1n	*MAT α, his4:ATC, LEU2, ade1-1, trp5-1, cyhR, MET, lys2-c, CAN S, ura3-1, FUS::HYG, RRP7::NAT*
Y128	EY30	Y55	1n	*MAT **a**, HIS4-HhaI, leu2-r, ADE1, TRP, CYH, met13-2, lys2-d, CANS, ura3-1, BIK1-939 (or BIK1-PvuII)*
Y198		Y55	1n	*MAT **a**, HIS4, leu2-r, ADE1, TRP, CYH, met13-2, lys2-d, CANS, ura3-1, BIK1-939 (or BIK1-PvuII)*

Y5534	PD74	XJ24-24a	1n	*MAT **a**, his4-ATC, leu2, ade6, TRP1, ARG4, TYR7, ura3, mal2, ho*
Y5535	AS4	XJ24-24a	1n	*MAT α, HIS4, LEU2, ADE6, trp1, arg4, tyr7, ura3, MAL2, ho*

Table 2.9

2.1.8.2. Experimental yeast strains

Strain number	**Other names**	**Strain background**	**Ploidy**	**Genotype**
Y3912	JKD1	SK1	2n	*MAT α, HIS4::LEU2-(BamHI;+ori) , leu2::hisG, ura3Δ(sma-pst), ho::hisG* *MAT **a** his4-X::LEU2-(NgoMIV;+ori)--URA3 leu2::hisG ura3Δ(sma-pst) ho::hisG*
Y5725	JKD200	SK1	2n	*MAT α, HIS4::LEU2-(BamHI;+ori) , leu2::hisG, ura3Δ(sma-pst), ho::hisG* *MAT **a** his4-X::LEU2-(NgoMIV;+ori)--URA3 leu2::hisG ura3Δ(sma-pst) ho::hisG*
Y5726	JKD174	SK1	2n	*MAT α, HIS4::LEU2-(BamHI;+ori) , leu2::hisG, ura3Δ(sma-pst), ho::hisG* *MAT **a** his4-X::LEU2-(NgoMIV;+ori)--URA3 leu2::hisG ura3Δ(sma-pst) ho::hisG* *ndt80Δ::KANMX6* *ndt80Δ::KANMX6*
Y5727	JKD175	SK1	2n	*MAT α, HIS4::LEU2-(BamHI;+ori) , leu2::hisG, ura3Δ(sma-pst), ho::hisG* *MAT **a** his4-X::LEU2-(NgoMIV;+ori)--URA3 leu2::hisG ura3Δ(sma-pst) ho::hisG* *ndt80Δ::KANMX6* *ndt80Δ::KANMX6*

Y5728	JKD176	SK1	2n	*MAT α, HIS4::LEU2-(BamHI;+ori) , leu2::hisG, ura3Δ(sma-pst), ho::hisG* *MAT **a** his4-X::LEU2-(NgoMIV;+ori)--URA3 leu2::hisG ura3Δ(sma-pst) ho::hisG* *rec8Δ::HphMX4* *rec8Δ::HphMX4*
Y5729	JKD177	SK1	2n	*MAT α, HIS4::LEU2-(BamHI;+ori) , leu2::hisG, ura3Δ(sma-pst), ho::hisG* *MAT **a** his4-X::LEU2-(NgoMIV;+ori)--URA3 leu2::hisG ura3Δ(sma-pst) ho::hisG* *rec8Δ::HphMX4* *rec8Δ::HphMX4*
Y5732	JKD110	SK1	2n	*MAT α, HIS4::LEU2-(BamHI;+ori) , leu2::hisG, ura3Δ(sma-pst), ho::hisG* *MAT **a** his4-X::LEU2-(NgoMIV;+ori)--URA3 leu2::hisG ura3Δ(sma-pst) ho::hisG* *rec8Δ::HphMX4, ndt80Δ::KANMX6* *rec8Δ::HphMX4 ndt80Δ::KANMX6*
Y5733	JKD201	SK1	2n	*MAT α, HIS4::LEU2-(BamHI;+ori) , leu2::hisG, ura3Δ(sma-pst), ho::hisG* *MAT **a** his4-X::LEU2-(NgoMIV;+ori)--URA3 leu2::hisG ura3Δ(sma-pst) ho::hisG* *rec8Δ::HphMX4, ndt80Δ::KANMX6* *rec8Δ::HphMX4 ndt80Δ::KANMX6*
Y5736	JKD111	SK1	2n	*MAT α, HIS4::LEU2-(BamHI;+ori) , leu2::hisG, ura3Δ(sma-pst), ho::hisG* *MAT **a** his4-X::LEU2-(NgoMIV;+ori)--URA3 leu2::hisG ura3Δ(sma-pst) ho::hisG* *rec8Δ::HphMX4, ndt80Δ::KANMX6, KANMX6-pCLB2-3HA-NSE4* *rec8Δ::HphMX4 ndt80Δ::KANMX6 KANMX6-pCLB2-3HA-NSE4*

Y5737	JKD180	SK1	2n	*MAT α, HIS4::LEU2-(BamHI;+ori) , leu2::hisG, ura3Δ(sma-pst), ho::hisG* *MAT **a** his4-X::LEU2-(NgoMIV;+ori)--URA3 leu2::hisG ura3Δ(sma-pst) ho::hisG* *rec8Δ::HphMX4, ndt80Δ::KANMX6, KANMX6-pCLB2-3HA-NSE4* *rec8Δ::HphMX4 ndt80Δ::KANMX6 KANMX6-pCLB2-3HA-NSE4*
Y5740	JKD112	SK1	2n	*MAT α, HIS4::LEU2-(BamHI;+ori) , leu2::hisG, ura3Δ(sma-pst), ho::hisG* *MAT **a** his4-X::LEU2-(NgoMIV;+ori)--URA3 leu2::hisG ura3Δ(sma-pst) ho::hisG* *rec8Δ::HphMX4, KANMX6-pCLB2-3HA-SMC5* *rec8Δ::HphMX4 KANMX6-pCLB2-3HA-SMC5*
Y5741	JKD182	SK1	2n	*MAT α, HIS4::LEU2-(BamHI;+ori) , leu2::hisG, ura3Δ(sma-pst), ho::hisG* *MAT **a** his4-X::LEU2-(NgoMIV;+ori)--URA3 leu2::hisG ura3Δ(sma-pst) ho::hisG* *rec8Δ::HphMX4, KANMX6-pCLB2-3HA-SMC5* *rec8Δ::HphMX4 KANMX6-pCLB2-3HA-SMC5*
Y5744	JKD113	SK1	2n	*MAT α, HIS4::LEU2-(BamHI;+ori) , leu2::hisG, ura3Δ(sma-pst), ho::hisG* *MAT **a** his4-X::LEU2-(NgoMIV;+ori)--URA3 leu2::hisG ura3Δ(sma-pst) ho::hisG* *rec8Δ::HphMX4, KANMX6-pCLB2-3HA-NSE4* *rec8Δ::HphMX4 KANMX6-pCLB2-3HA-NSE4*
Y5755	JKD178	SK1	2n	*MAT α, HIS4::LEU2-(BamHI;+ori) , leu2::hisG, ura3Δ(sma-pst), ho::hisG* *MAT **a** his4-X::LEU2-(NgoMIV;+ori)--URA3 leu2::hisG ura3Δ(sma-pst) ho::hisG* *rec8Δ::HphMX4, KANMX6-pCLB2-3HA-NSE4* *rec8Δ::HphMX4 KANMX6-pCLB2-3HA-NSE4*

Y5597		SK1	2n	*MAT α, HIS4::LEU2-(BamHI;+ori) , leu2::hisG, ura3Δ(sma-pst), ho::hisG* *MAT **a** his4-X::LEU2-(NgoMIV;+ori)--URA3 leu2::hisG ura3Δ(sma-pst) ho::hisG* *dmc1Δ::KANMX6,* *dmc1Δ::KANMX6*
Y5746	JKD184	SK1	2n	*MAT α, HIS4::LEU2-(BamHI;+ori) , leu2::hisG, ura3Δ(sma-pst), ho::hisG* *MAT **a** his4-X::LEU2-(NgoMIV;+ori)--URA3 leu2::hisG ura3Δ(sma-pst) ho::hisG* *dmc1Δ::KANMX6,* *dmc1Δ::KANMX6*
Y5601		SK1	2n	*MAT α, HIS4::LEU2-(BamHI;+ori) , leu2::hisG, ura3Δ(sma-pst), ho::hisG* *MAT **a** his4-X::LEU2-(NgoMIV;+ori)--URA3 leu2::hisG ura3Δ(sma-pst) ho::hisG* *dmc1Δ::KANMX6, KANMX6-pCLB2-3HA-NSE4* *dmc1Δ::KANMX6 KANMX6-pCLB2-3HA-NSE4*
Y5747	JKD192	SK1	2n	*MAT α, HIS4::LEU2-(BamHI;+ori) , leu2::hisG, ura3Δ(sma-pst), ho::hisG* *MAT **a** his4-X::LEU2-(NgoMIV;+ori)--URA3 leu2::hisG ura3Δ(sma-pst) ho::hisG* *dmc1Δ::KANMX6, KANMX6-pCLB2-3HA-NSE4* *dmc1Δ::KANMX6 KANMX6-pCLB2-3HA-NSE4*
Y5748	JKD196	SK1	2n	*MAT α, HIS4::LEU2-(BamHI;+ori) , leu2::hisG, ura3Δ(sma-pst), ho::hisG* *MAT **a** his4-X::LEU2-(NgoMIV;+ori)--URA3 leu2::hisG ura3Δ(sma-pst) ho::hisG* *KANMX6-pCLB2-3HA-SMC5* *KANMX6-pCLB2-3HA-SMC5*

Y5749	JKD197	SK1	2n	*MAT α, HIS4::LEU2-(BamHI;+ori) , leu2::hisG, ura3Δ(sma-pst), ho::hisG* *MAT **a** his4-X::LEU2-(NgoMIV;+ori)--URA3 leu2::hisG ura3Δ(sma-pst) ho::hisG* *KANMX6-pCLB2-3HA-SMC5* *KANMX6-pCLB2-3HA-SMC5*
Y5750	JKD198	SK1	2n	*MAT α, HIS4::LEU2-(BamHI;+ori) , leu2::hisG, ura3Δ(sma-pst), ho::hisG* *MAT **a** his4-X::LEU2-(NgoMIV;+ori)--URA3 leu2::hisG ura3Δ(sma-pst) ho::hisG* *KANMX6-pCLB2-3HA-NSE4* *KANMX6-pCLB2-3HA-NSE4*
Y5751	JKD199	SK1	2n	*MAT α, HIS4::LEU2-(BamHI;+ori) , leu2::hisG, ura3Δ(sma-pst), ho::hisG* *MAT **a** his4-X::LEU2-(NgoMIV;+ori)--URA3 leu2::hisG ura3Δ(sma-pst) ho::hisG* *KANMX6-pCLB2-3HA-NSE4* *KANMX6-pCLB2-3HA-NSE4*
Y5705		SK1	2n	*MAT α, HIS4::LEU2-(BamHI;+ori) , leu2::hisG, ura3Δ(sma-pst), ho::hisG* *MAT **a** his4-X::LEU2-(NgoMIV;+ori)--URA3 leu2::hisG ura3Δ(sma-pst) ho::hisG* *rad51Δ, KANMX6-pCLB2-3HA-SMC5* *rad51Δ KANMX6-pCLB2-3HA-SMC5*
Y5706		SK1	2n	*MAT α, HIS4::LEU2-(BamHI;+ori) , leu2::hisG, ura3Δ(sma-pst), ho::hisG* *MAT **a** his4-X::LEU2-(NgoMIV;+ori)--URA3 leu2::hisG ura3Δ(sma-pst) ho::hisG* *rad51Δ, KANMX6-pCLB2-3HA-SMC5* *rad51Δ KANMX6-pCLB2-3HA-SMC5*

Y5707		SK1	2n	*MAT α, HIS4::LEU2-(BamHI;+ori) , leu2::hisG, ura3Δ(sma-pst), ho::hisG* *MAT **a** his4-X::LEU2-(NgoMIV;+ori)--URA3 leu2::hisG ura3Δ(sma-pst) ho::hisG* *rad51Δ, KANMX6-pCLB2-3HA-NSE4* *rad51Δ KANMX6-pCLB2-3HA-NSE4*
Y5708		SK1	2n	*MAT α, HIS4::LEU2-(BamHI;+ori) , leu2::hisG, ura3Δ(sma-pst), ho::hisG* *MAT **a** his4-X::LEU2-(NgoMIV;+ori)--URA3 leu2::hisG ura3Δ(sma-pst) ho::hisG* *rad51Δ, KANMX6-pCLB2-3HA-NSE4* *rad51Δ KANMX6-pCLB2-3HA-NSE4*
Y5709		SK1	2n	*MAT α, HIS4::LEU2-(BamHI;+ori) , leu2::hisG, ura3Δ(sma-pst), ho::hisG* *MAT **a** his4-X::LEU2-(NgoMIV;+ori)--URA3 leu2::hisG ura3Δ(sma-pst) ho::hisG* *dmc1Δ::KANMX6, rad51Δ, KANMX6-pCLB2-3HA-SMC5* *dmc1Δ::KANMX6, rad51Δ KANMX6-pCLB2-3HA-SMC5*
Y5710		SK1	2n	*MAT α, HIS4::LEU2-(BamHI;+ori) , leu2::hisG, ura3Δ(sma-pst), ho::hisG* *MAT **a** his4-X::LEU2-(NgoMIV;+ori)--URA3 leu2::hisG ura3Δ(sma-pst) ho::hisG* *dmc1Δ::KANMX6, rad51Δ, KANMX6-pCLB2-3HA-SMC5* *dmc1Δ::KANMX6, rad51Δ KANMX6-pCLB2-3HA-SMC5*
Y5711		SK1	2n	*MAT α, HIS4::LEU2-(BamHI;+ori) , leu2::hisG, ura3Δ(sma-pst), ho::hisG* *MAT **a** his4-X::LEU2-(NgoMIV;+ori)--URA3 leu2::hisG ura3Δ(sma-pst) ho::hisG* *dmc1Δ::KANMX6, rad51Δ, KANMX6-pCLB2-3HA-NSE4* *dmc1Δ::KANMX6, rad51Δ KANMX6-pCLB2-3HA-NSE4*

Y5712		SK1	2n	*MAT α, HIS4::LEU2-(BamHI;+ori) , leu2::hisG, ura3Δ(sma-pst), ho::hisG* *MAT **a** his4-X::LEU2-(NgoMIV;+ori)--URA3 leu2::hisG ura3Δ(sma-pst) ho::hisG* *dmc1Δ::KANMX6, rad51Δ, KANMX6-pCLB2-3HA-NSE4* *dmc1Δ::KANMX6, rad51Δ KANMX6-pCLB2-3HA-NSE4*
Y5752	JKD202	SK1	2n	*MAT α, HIS4::LEU2-(BamHI;+ori) , leu2::hisG, ura3Δ(sma-pst), ho::hisG* *MAT **a** his4-X::LEU2-(NgoMIV;+ori)--URA3 leu2::hisG ura3Δ(sma-pst) ho::hisG* *msh5Δ::KANMX6* *msh5Δ::KANMX6*
Y5753	JKD203	SK1	2n	*MAT α, HIS4::LEU2-(BamHI;+ori) , leu2::hisG, ura3Δ(sma-pst), ho::hisG* *MAT **a** his4-X::LEU2-(NgoMIV;+ori)--URA3 leu2::hisG ura3Δ(sma-pst) ho::hisG* *msh5Δ::KANMX6* *msh5Δ::KANMX6*
Y5695		SK1	2n	*MAT α, HIS4::LEU2-(BamHI;+ori) , leu2::hisG, ura3Δ(sma-pst), ho::hisG* *MAT **a** his4-X::LEU2-(NgoMIV;+ori)--URA3 leu2::hisG ura3Δ(sma-pst) ho::hisG* *dmc1Δ::KANMX6, rad51Δ* *dmc1Δ::KANMX6, rad51Δ*
Y5696		SK1	2n	*MAT α, HIS4::LEU2-(BamHI;+ori) , leu2::hisG, ura3Δ(sma-pst), ho::hisG* *MAT **a** his4-X::LEU2-(NgoMIV;+ori)--URA3 leu2::hisG ura3Δ(sma-pst) ho::hisG* *dmc1Δ::KANMX6, rad51Δ* *dmc1Δ::KANMX6, rad51Δ*

Y5693		SK1	2n	*MAT α, HIS4::LEU2-(BamHI;+ori) , leu2::hisG, ura3Δ(sma-pst), ho::hisG* *MAT **a** his4-X::LEU2-(NgoMIV;+ori)--URA3 leu2::hisG ura3Δ(sma-pst) ho::hisG* *rad51Δ* *rad51Δ*
Y5694		SK1	2n	*MAT α, HIS4::LEU2-(BamHI;+ori) , leu2::hisG, ura3Δ(sma-pst), ho::hisG* *MAT **a** his4-X::LEU2-(NgoMIV;+ori)--URA3 leu2::hisG ura3Δ(sma-pst) ho::hisG* *rad51Δ* *rad51Δ*
Y5756	JKD210	SK1	2n	*MAT α, HIS4::LEU2-(BamHI;+ori) , leu2::hisG, ura3Δ(sma-pst), ho::hisG* *MAT **a** his4-X::LEU2-(NgoMIV;+ori)--URA3 leu2::hisG ura3Δ(sma-pst) ho::hisG* *msh5Δ::KANMX6, KANMX6-pCLB2-3HA-NSE4* *msh5Δ::KANMX6 KANMX6-pCLB2-3HA-NSE4*
Y5757	JKD211	SK1	2n	*MAT α, HIS4::LEU2-(BamHI;+ori) , leu2::hisG, ura3Δ(sma-pst), ho::hisG* *MAT **a** his4-X::LEU2-(NgoMIV;+ori)--URA3 leu2::hisG ura3Δ(sma-pst) ho::hisG* *msh5Δ::KANMX6, KANMX6-pCLB2-3HA-NSE4* *msh5Δ::KANMX6 KANMX6-pCLB2-3HA-NSE4*
Y5760	JKD212	SK1	2n	*MAT α, HIS4::LEU2-(BamHI;+ori) , leu2::hisG, ura3Δ(sma-pst), ho::hisG* *MAT **a** his4-X::LEU2-(NgoMIV;+ori)--URA3 leu2::hisG ura3Δ(sma-pst) ho::hisG* *dmc1Δ::KANMX6, rad51Δ, msh5Δ::KANMX6, KANMX6-pCLB2-3HA-NSE4* *dmc1Δ::KANMX6 rad51Δ msh5Δ::KANMX6 KANMX6-pCLB2-3HA-NSE4*

Y5761	JKD213	SK1	2n	*MAT α, HIS4::LEU2-(BamHI;+ori) , leu2::hisG, ura3Δ(sma-pst), ho::hisG* *MAT **a** his4-X::LEU2-(NgoMIV;+ori)--URA3 leu2::hisG ura3Δ(sma-pst) ho::hisG* *dmc1Δ::KANMX6, rad51Δ, msh5Δ::KANMX6, KANMX6-pCLB2-3HA-NSE4* *dmc1Δ::KANMX6 rad51Δ msh5Δ::KANMX6 KANMX6-pCLB2-3HA-NSE4*
Y5764	JKD214	SK1	2n	*MAT α, HIS4::LEU2-(BamHI;+ori) , leu2::hisG, ura3Δ(sma-pst), ho::hisG* *MAT **a** his4-X::LEU2-(NgoMIV;+ori)--URA3 leu2::hisG ura3Δ(sma-pst) ho::hisG* *dmc1Δ::KANMX6, msh5Δ::KANMX6, KANMX6-pCLB2-3HA-NSE4* *dmc1Δ::KANMX6 msh5Δ::KANMX6 KANMX6-pCLB2-3HA-NSE4*
Y5765	JKD215	SK1	2n	*MAT α, HIS4::LEU2-(BamHI;+ori) , leu2::hisG, ura3Δ(sma-pst), ho::hisG* *MAT **a** his4-X::LEU2-(NgoMIV;+ori)--URA3 leu2::hisG ura3Δ(sma-pst) ho::hisG* *dmc1Δ::KANMX6, msh5Δ::KANMX6, KANMX6-pCLB2-3HA-NSE4* *dmc1Δ::KANMX6 msh5Δ::KANMX6 KANMX6-pCLB2-3HA-NSE4*
Y5768	JKD224	SK1	2n	*MAT α, HIS4::LEU2-(BamHI;+ori) , leu2::hisG, ura3Δ(sma-pst), ho::hisG* *MAT **a** his4-X::LEU2-(NgoMIV;+ori)--URA3 leu2::hisG ura3Δ(sma-pst) ho::hisG* *msh5Δ::KANMX6, ndt80Δ::KANMX6* *msh5Δ::KANMX6 ndt80Δ::KANMX6*
Y5769	JKD225	SK1	2n	*MAT α, HIS4::LEU2-(BamHI;+ori) , leu2::hisG, ura3Δ(sma-pst), ho::hisG* *MAT **a** his4-X::LEU2-(NgoMIV;+ori)--URA3 leu2::hisG ura3Δ(sma-pst) ho::hisG* *msh5Δ::KANMX6, ndt80Δ::KANMX6* *msh5Δ::KANMX6 ndt80Δ::KANMX6*

Y5772	JKD226	SK1	2n	*MAT α, HIS4::LEU2-(BamHI;+ori) , leu2::hisG, ura3Δ(sma-pst), ho::hisG* *MAT **a** his4-X::LEU2-(NgoMIV;+ori)--URA3 leu2::hisG ura3Δ(sma-pst) ho::hisG* *msh5Δ::KANMX6, ndt80Δ::KANMX6, KANMX6-pCLB2-3HA-NSE4* *msh5Δ::KANMX6 ndt80Δ::KANMX6 KANMX6-pCLB2-3HA-NSE4*
Y5773	JKD227	SK1	2n	*MAT α, HIS4::LEU2-(BamHI;+ori) , leu2::hisG, ura3Δ(sma-pst), ho::hisG* *MAT **a** his4-X::LEU2-(NgoMIV;+ori)--URA3 leu2::hisG ura3Δ(sma-pst) ho::hisG* *msh5Δ::KANMX6, ndt80Δ::KANMX6, KANMX6-pCLB2-3HA-NSE4* *msh5Δ::KANMX6 ndt80Δ::KANMX6 KANMX6-pCLB2-3HA-NSE4*
Y650	ERY103	Y55	2n	*MAT α, his4:ATC, LEU2, ade1-1, trp5-1, cyhR, MET, lys2-c, CANS, ura3-1* *MAT **a** HIS4-HhaI leu2-r ADE1 TRP CYH met13-2 lys2-d CANS ura3-1* *FUS, RRP7, BIK1-939 (or BIK1-PvuII)* *FUS::HYG RRP7::NAT BIK1*
Y5536	PD84	XJ24-24a	2n	*MAT **a**, his4-ATC, leu2, ade6, TRP1, ARG4, TYR7, ura3, mal2, ho* *MAT α HIS4 LEU2 ADE6 trp1 arg4 tyr7 ura3 MAL2 ho*
Y5774	JKD194	XJ24-24a	2n	*MAT **a**, his4-ATC, leu2, ade6, TRP1, ARG4, TYR7, ura3, mal2, ho* *MAT α HIS4 LEU2 ADE6 trp1 arg4 tyr7 ura3 MAL2 ho*

Table 2.10

2.2. Methods

2.2.1. Bacterial methods

2.2.1.1. Growth of *E.coli*

Cells were grown at 37 °C in Luria Broth, with liquid culture being shaken at 180rpm.

2.2.1.2. Transformation of competent *E.coli* cells

Chemically competent DH5α strains are stored at -80 °C. To begin the transformation, an Eppendorf containing 100 µl of competent cells is thawed slowly on ice. Once the cells are thawed, plasmid DNA (1 µl of 1 ng/µl typically) is added to the *E.coli*. The mixture of cells and DNA is then left on ice for 30 minutes. This is followed by subsequent heat shock at 42 °C, for 45 seconds, and subsequent incubation on ice for 60 seconds. 300 µl of Luria Broth (LB) is added to the tube, and the cell suspension is incubated at 37 °C for 1 hour. The cell suspension is then spread onto LB-ampicillin plates, and left at 37 °C overnight. Colonies which grow should contain the transformed plasmid – this is verified via plasmid extraction and restriction enzyme digestion.

2.2.1.3. Plasmid extraction

QIAprep Spin Miniprep kits were used to isolate plasmids from bacterial cultures, following the manufacturer's protocol.

2.2.1.4. Storage of bacterial strains

Cells were grown as overnight culture in Luria Broth. They were subsequently spun down and re-suspended in 30% glycerol, and then placed at -80 °C for long term storage.

2.2.2. Yeast methods

2.2.2.1. Vegetative growth

Cells were initially patched to YEPEG plates and grown at 30 °C to ensure that mitochondria had been retained. Subsequently, they were streaked onto YPD plates and grown at 30 °C to isolate single colonies. If liquid cultures were required, a single colony would be inoculated into YPD liquid medium, and grown at 30 °C, shaking at 200 rpm

2.2.2.2. Mating haploid strains

Haploids are grown on YEPEG overnight if taken up from -80 °C stocks, or on YPD if they are taken directly from a spore post-dissection. A small and equal amount (less than a pinhead) from an a and α haploid strain are placed on a YPD plate and mixed thoroughly over a region. These can then be incubated at 30 °C for at least 6 hours, or potentially overnight. Once mating is complete, the mated strains are streaked onto YPD, and grown for 3 days at 30 °C on a YPD plate, until single diploid colonies can be visualised and isolated.

2.2.2.2.1. Pulling zygotes:

For some mutant strains, matings were sufficiently rare that it was uncommon to gain diploids via the methods mentioned above. In this instance, haploids are mated as above, but after 4 hours, zygotes are selected using a dissecting microscope, moved to a clear of region of YPD, and grow as a diploid colony.

2.2.2.3. Sporulation conditions

There are multiple reasons why sporulation might be required – for dissection to generate new strains; or in order to undertake genetic analysis. Each has slightly different requirements as outlined below.

2.2.2.3.1. Basic sporulation (used when constructing new SK1 strains):

A pure diploid colony might be grown up overnight prior to this; alternatively, cells which have been freshly mated can be used directly. Cells are placed in 5 ml of 1% KAc-COM at 30 °C overnight. Sporulation efficiency can be determined by visualising cells via a light microscope and counting the proportion of tetrads.

2.2.2.3.2. Sporulation for genetic analysis:

In order to be consistent with previous experiment, two different sporulation media were used – 1% KAc (plates); and KAc-COM (plates). Diploid strains were plated to sporulation media, and incubated at 23 °C for up to 4 days, in order to generate tetrads for genetic analysis.

2.2.2.4. Dissection of tetrads

Haploid strains were mated and sporulated as outlined in **2.2.2.2.** and **2.2.2.3.** Tetrads were then resuspended in 100 µl of dissection buffer and 5-10 µl of 10 mg/ml Zymolyase (20T). Tetrads were incubated at 37 °C for 30 minutes in a rotating incubator. 400 µl of dissection buffer is added to halt the reaction. Tetrads can either be dissected immediately, or stored at 4 °C for up to a month.

In order to undertake dissections, zymolyase digested tetrads were streaked in a single line down the centre of a flat YPD plate. A Nikon Eclipse 50i microscope and micromanipulator were used to visualise the tetrads upon the plate, and to separate individual ascospores to unique locations, typically in a line of 4. Plates were then incubated for 3 days at 30 °C, and then replica-plated onto selective media to select for prototrophy/drug resistance.

2.2.2.5. Genetic analysis

Genetic analysis allows us to identify half-conversion events during meiotic recombination. For our specific strains, dissected tetrads were replica plated to his- drop out media, and left to grow overnight. The growth was then scored, with half-conversions defined as those spores whereby one-half of the patch has *HIS*$^{+}$ phenotype, and the other half *his*$^{-}$ phenotype, as a result of an unrepaired DNA mismatch post meiosis that lead to the first post-mitotic division generating yeast cells with distinct phenotypes.

2.2.2.6. Lithium Acetate transformation of *S. cerevisiae*

Yeast cells are initially grown overnight in 5 ml YPD liquid at 30 °C. When the cells have reached stationary phase, 0.5 ml of saturated culture should be added to 4.5 ml of fresh YPD liquid. This should be grown at 30 °C for 3 hours (until an OD600 of 0.8 is achieved), to allow for two cell divisions. Cells are centrifuged, and washed 3× in dH_2O. The cell pellet is then resuspended in 1 ml 0.1 M lithium acetate, and divided into two Eppendorf tubes, before being pelleted again. To the pellet is then added: 240 µl 50% PEG 3,350; 36 µl 1 M lithium acetate; 50 µl of 2 mg/ml single stranded salmon sperm DNA; 50 µl of sample DNA for transformation (20 ng/µl), or for control cells 50 µl of dH_2O. The pellet is resuspended, and incubated at 30 °C for 30 minutes. The cells are then heat shocked at 42 °C for a background specific period of time (for SK1 strains, 20 minutes). 1 ml dH_2O is then added, and the solution is centrifuged gently (4,000 rpm) for 1 minute.

If selecting for auxotrophic markers, cells are resuspended in 500 µl dH_2O, and the solution is placed on 3× drop out plates, and spread evenly with sterile glass beads.

If selecting for toxin resistance, cells are initially resuspended in 500 µl YPD, and placed at 30 °C for 3 hours to allow them to recover before adding antibiotics. The cells are then pelleted, resuspended in 500 µl dH_2O, and plated on antibiotic containing YPD media.

All transformations should be incubated at 30 °C for 3 days, and colonies selected and verified by colony PCR to determine whether transformation is successful.

2.2.2.7. PCR based gene deletion in *S. cerevisiae*

PCR constructs to delete genes from the *S. cerevisiae* genome were generated by designing primers consisting of two portions – an upstream region with 45 base pairs of homology to the regions immediately outside the gene of interest; and a downstream region with base pair homology to the Longtine plasmid (LONGTINE, et al., 1998), allowing a PCR reaction to generate a DNA fragment with a selectable gene (either drug resistance or an auxotrophic marker) flanked by regions homologous to the *S. cerevisiae* genome. The fragments are then used in lithium acetate transformation of yeast cells, and transformation verified by junction PCR.

2.2.2.8. Storage of *S. cerevisiae* strains

For long-term storage, cells were re-suspended in 30% glycerol and frozen at -80 °C. For short-term storage, cells were kept on YPD plates at 4 °C.

2.2.3. Standard DNA methods

2.2.3.1. Polymerase Chain Reaction (DreamTaq™ polymerase)

PCR is used for a large variety of purposes – here mainly for generating DNA fragments for transformation, and for verifying these transformants.

2.2.3.1.1. General PCR

Components were added together in the following quantities.

Component	**Amount**
dH_2O	10.7 µl
10× DreamTaq™ buffer	2 µl
dNTPs (2 mM)	2 µl
Primer mix (10 µM Oligo 1, 10 µM Oligo 2)	2 µl
Sample DNA (50-250 ng)	1 µl
DreamTaq™ polymerase	0.3 µl

DreamTaq™ polymerase, including 10× DreamTaq™ buffer was purchased from ThermoFisher (product# EP0701), whilst PCR grade dNTPs were purchased from Sigma-Aldrich (product# DNTP-RO).

For a colony PCR (typically to undertake a junction PCR to verify transformation) a small amount of a fresh colony is resuspended in 0.02 M sodium hydroxide, and incubated at 95 °C for 5 minutes, cooled on ice, and centrifuged. 1 µl of this solution can be used in the place of sample DNA.

The PCR mixture is the loaded into a PCR machine (Eppendorf Mastercycler RP-Gradient S) and programmed to carry out the following cycle of commands.

Step	**Temperature (°C)**	**Time**	**No. of cycles**
Initial denaturation	95	1-3 min	1
Denaturation	95	30 s	25-40
Annealing	T_m	30 s	
Extension	72	Variable	
Final extension	72	5-15 min	1

The extension time is typically 1 minute/kb of amplification. Samples are then kept at 4 °C, and the size of fragments is distinguished by agarose gel electrophoresis.

2.2.3.2. Genomic DNA extraction (with Potassium acetate)

Cells were grown vegetatively overnight in 5 ml YPD. The cells were spun down, washed in dH_2O and resuspended in 500 µl of 1 M sorbitol, 15 µl DTT and 8 µl 100T Zymolyase. This was incubated at 37 °C for 1 hour. 200 µl of

10/1 TE buffer and 70 µl 10% SDS were added and incubated at 65 °C for 10 minutes. 320 µl of 5 M potassium acetate were added, the solution inverted, and left on ice for 30 minutes. Samples were centrifuged at full speed for 6 minutes. 650 µl of the centrifuged supernatant was removed, and added to a 2 ml Eppendorf containing 1 ml isopropanol, and 200 µl of 5 M ammonium acetate. Samples were centrifuged to obtain a DNA pellet, which were subsequently left to air-dry. The pellet was resuspended in 300 µl 10/1 TE buffer, and 8 µl of RNAse (10 mg/ml), and incubated at 37 °C for 30 minutes. Samples were stored at 4 °C for short term storage.

2.2.3.3 Plasmid design for Genscript synthesis

In order to ensure that fully codon optimised forms of protein tags were utilised, codon optimisation was performed on the tag of interest, utilising online software JCAT. This sequence was then sent to Genscript, which synthesised the gene into a pUC57 plasmid.

2.2.3.4. Restriction digests of DNA

Restriction digests were carried undertaken to incorporate a DNA fragment into a suitable vector. 1 µg of DNA is digested with 1 µl (10 enzymatic units) of restriction enzyme, in 5 µl of the appropriate 10× NEB buffer, made up to a final reaction volume of 50 µl. The enzymatic reaction was incubated for 2 hours at 37 °C, and in the case of plasmid DNA, 2 µl is typically visualised via agarose gel electrophoresis to determine whether the digestion has been successful.

2.2.3.5. Ligation of DNA fragments

To generate new plasmid constructs, cut DNA fragments were typically ligated into cut plasmids. Fragment DNA and linearised plasmid DNA were mixed in a 3:1 ratio. 10 enzymatic units of T4 DNA ligase (1 µl) were added, in addition to 1× T4 DNA ligase buffer, and incubated for 6 hours/overnight at 16 °C. Successful ligation was verified by agarose gel electrophoresis.

2.2.3.6. Agarose gel electrophoresis

Agarose gel electrophoresis was used to distinguish DNA fragments of different sizes and the presence of more complex three dimensional structures (such as linearised plasmid as opposed to circular super-coiled plasmid).

For standard separation of DNA fragments (see section **2.2.4.6.** for Southern specifics) a 1% agarose gel, in 1× TAE buffer was used. However, in order to effectively distinguish particularly small or large fragments the concentration of agarose was adjusted, with high percentages of agarose resolving smaller fragments more effectively.

DNA, in a solution containing 1× loading buffer (NEB), is loaded onto the gel. 250ng of DNA ladder (either 100bp or 1kb depending on fragment size) were loaded to determine the size of the fragment. Gels were run in 1× TAE buffer, with a voltage of ~4 V/cm between the electrodes (typically 60-100 V). Gels were stained for 30 minutes in 5 µM ethidium bromide, and imaged using a SYNGENE INGenius BIO Imager.

2.2.3.7. DNA quantification using Nanodrop

A Nanodrop was used to determine the concentrations of plasmid and PCR fragment DNA. 1 µl of solution was placed between the Nanodrop electrodes, and an OD260 reading was used to determine the concentration of DNA molecules. A_{260}/A_{280} and A_{260}/A_{230} readings were also obtained to determine the purity of the DNA obtained.

2.2.3.8. Gel extraction of DNA

PCR fragments were initially separated by agarose gel electrophoresis, stained with ethidium bromide, and a UV light box used to visualise individual bands of DNA on the agarose gel. The band was then excised from the gel using a scalpel. DNA was extracted from the agarose gel utilising a QIAgen QIAquick Gel Extraction Kit following the protocol included with the kit.

2.2.3.9. DNA probe manufacture for Southern hybridisation

DNA probes for radioactive hybridisation were constructed using a PCR reaction to generate a 400bp fragment that was homologous to the region of interest. This was then purified from the plasmid DNA using gel extraction methods. A second round of PCR followed by gel extraction was then performed to further purify the probe DNA.

2.2.4. Southern gel analysis of *HIS4LEU2* hotspot

This protocol is adapted from one shown in (HUNTER & KLECKNER, 2001).

2.2.4.1. Large scale meiotic time course

Strains were grown to stationary phase in YPD liquid, then inoculated to an OD600 of 0.01 in 250 ml pre-sporulation media - SPS and grown for 16 hours at 30 °C until an OD600 of 1.2-1.4 was achieved. Cells are washed and then resuspended in 1% KAc liquid (supplemented with amino acids as required) to begin the meiotic timecourse, and are incubated at 30 °C, being shaken at 300 rpm. Time points are taken as indicated, and for genomic DNA extractions, sodium azide is added to a final concentration of 0.1% to each sample. Samples are then centrifuged and the supernatant is discarded.

2.2.4.2. Psoralen cross-linking

Cells were re-suspended in psoralen solution (0.1 mg/ml Trioxalen [Sigma-Aldrich #T-6137], 50 mM Tris-HCl, 50 mM EDTA, 20% Ethanol). The suspension is placed onto a 60 mm culture dish and irradiated with 365 nm UV for 10 minutes. It is shaken several times during the course of this incubation. The solution is then removed from the culture dish (with 50/50 TE used to wash the dish to maximise the number of cells obtained) followed by pelleting the solution and discarding the supernatant.

2.2.4.3. Guanidine/Phenol chloroform DNA extraction

Cells are re-suspended in 0.5 ml Spheroblasting solution (Spheroblasting buffer, 1% β-mercaptoethanol, 0.5 mg/ml 100T zymolyase), and incubated at 37 °C for 15 minutes. Spheroblasts are harvested by centrifugation, then re-suspended in 2ml Guanidine solution (4.5 M Guanidine-HCl, 0.1 M EDTA, 0.15 M NaCl, 0.05% sodium lauryl sarkosyl), and incubated for 1 hour at 65 °C. An equal volume of Ethanol is added, and samples are put on ice for at least 30 minutes. Samples are then pelleted, and the supernatant discarded. The pellet is re-suspended in 0.6 ml RNase solution (50 µg/ml RNase A in 10/1 TE buffer) and incubated for 90 minutes at 37 °C. 25 µl of Proteinase K solution (20 mg/ml proteinase K, 20 mM $CaCl_2$, 10 mM Tris-HCl, 50% Glycerol) was added to each sample, and they are subsequently incubated for 90 minutes at 65 °C.

A phenol/chloroform extraction was then performed; a solution of phenol, chloroform and isoamyl alcohol in the ratio of 25:24:1 was added in an equal volume to the sample, they were mixed and then centrifuged, with the aqueous layer retained. This was repeated a second time. The DNA was then precipitated from the solution, by adding 2 volumes of ethanol and 35 µl 4 M sodium acetate, and leaving for 30 minutes. The samples are then centrifuged and washed in 70% ethanol. The DNA pellet was then allowed to air dry, before re-suspending it in 10/1 TE buffer.

2.2.4.4. Fluorometric determination of DNA quantification

198µl of Hoechst 33258 solution (100ng/ml Hoechst 33258, 1× TNE [10 mM Tris base, 200 mM NaCl, 1 mM EDTA]) was added to a 96 well plate. 2 µl of

sample DNA is added to each well, and then mixed thoroughly. In addition, a set of DNA standards of known concentration are also added to separate wells. A GloMax®-Multi Detection System 96 well plate reader was used to measure the UV fluorescence of the Hoechst stain, which was then used to calculate the concentration of DNA for each sample when plotted against the standard curve.

2.2.4.5. Preparation of DNA for gel analysis

2 µg of extracted total DNA were digested to completion with *XhoI* endonuclease. Typically, 2 µg in 80 µl final volume with 20-fold excess of restriction enzyme, 1× NEB4 buffer, digested for 2 hours at 37 °C. Digested DNA is then precipitated by the addition of 5 µl 3 M sodium acetate pH 5.2 and 190 µl ethanol, followed by centrifugation. The pellet was subsequently rinsed with 100 µl of 70% ethanol and then air dried. The pellet was then re-suspended in 15 µl 1× TE buffer, after which 5 µl of high salt loading buffer (100 µl 6× loading dye + 60 µl 10× NEB3; extra salt prevents sample jumping out of well) was added.

2.2.4.6. Gel analysis

In order to distinguish different molecular fragments from the meiotic recombination pathway, Southern analysis was undertaken.

2.2.4.6.1. One-dimensional gel analysis:

A large 0.6% SeaKem LE agarose gel in 1× TBE buffer was made. Samples were loaded, with no space left between filled wells. The gel is run in 2 L 1× TBE buffer at 70 V for a large gel (2 V/cm between the electrodes) for 24 hours at room temperature. After the gel has finished running, the gel was stained in 1L dH_2O with Ethidium Bromide (0.5 µg/ml final concentration) for 30 minutes. This was then imaged with a UV image analyser. The gel is then washed in 1 L dH_2O in preparation for alkaline blotting.

2.2.4.6.2. Two-dimensional gel analysis:

A large 0.4% SeaKem GOLD agarose gel in 1× TBE buffer was made. Samples were loaded, with a single space left between filled wells. The gel is run in 2 L 1× TBE buffer at 35 V for a large gel (1 V/cm between the electrodes) for 21 hours at room temperature. After the gel has finished running, the gel was stained in 1 L 1× TBE with Ethidium bromide (0.5 µg/ml final concentration) for 30 minutes. The gel is the viewed on a long wave UV box. Lanes were subsequently excised: typically, 1.5 cm from the wells down to the 2.2 kb band of *BstEII* digest λ marker. These excised lanes are rotated 90°, and set in 0.8% SeaKem LE agarose gel in 1× TBE with Ethidium Bromide (0.5 µg/ml final concentration). Once set, the gels were run in pre-chilled 1× TBE with Ethidium Bromide (0.5 µg/ml final concentration) at 4 °C for 6 hours at 140V (4 V/cm between the electrodes). The gel is then washed in 1 L dH_2O in preparation for alkaline blotting.

2.2.4.7. Southern blotting by alkaline transfer

The gel was initially inverted, and then soaked in 1L 0.25 M HCl for 20 minutes in order to depurinate the linear DNA and introduce ssDNA breaks to allow more efficient transfer of the DNA onto the membrane. The gel is then rinsed briefly with dH_2O. The gel is then soaked in 1L 0.4 M NaOH for 30 minutes in order to denature the dsDNA and generate ssDNA. The blot apparatus was concurrently set up, with a long wick of Whatman blotting paper soaked in 0.4 M NaOH, and two pieces of Whatman blotting paper the same size as the gel laid on top which were also soaked in 0.4 M NaOH. The prepared gel was then laid on top. A piece of ZetaProbe® GT nylon membrane (BioRad) the same size as the gel, soaked in dH_2O is laid on top, followed by two pieces of Whatman blotting paper soaked in dH_2O. The construction is sealed with Saran Wrap around the edges, and a stack of paper towels were laid flat on top of the construction, in direct contact with the topmost Whatman paper sheet. Blotting occurred for at least 6 hrs; generally overnight. The blot was subsequently neutralised, with the nylon membrane placed in sodium phosphate wash buffer. The blot was then either frozen, or proceeded directly to radioactive hybridisation.

2.2.4.8. Radioactive hybridisation of Southern blots

Hybridisation tubes, lids and hybridisation buffer are pre-warmed to 65 ºC. If the nylon membrane was frozen, it was thawed out in sodium phosphate wash buffer. The nylon membrane was inserted into a hybridisation tube, with the DNA containing face facing inwards. 20 ml of warmed hybridisation buffer was

added to each tube. In addition, 0.3 ml of denatured, sheared Salmon sperm DNA (10 mg/mL, Boehringer) was added to each tube. Blots were returned to the hybridisation oven and pre-hybridized overnight.

Stratagene Room Temp. Random Priming Kit for double-stranded probes was used to generate radioactive probes for this study. Dried reaction mix, 25 ng of probe DNA and ddH_2O are combined (to a total volume of 42 µl); in addition, for one-dimensional analysis 0.5 µl of 0.25 ng/µl *BstEII* λ digest is included. This solution was denatured at 95 ºC and quenched on ice. 3 µl magenta polymerase was added, followed by 5 µl 32P-dCTP; the solution was subsequently incubated at 37 ºC for 1 hr. The radioactive probe was then separated from unincorporated label using an Amersham Probe-Quant G-50 Micro Column. The probe was then denatured, and added to the hybridisation tube. Hybridisation occurred overnight.

The following day, the radioactive probe was removed from the bolt; the blot was then washed, firstly for 2× 10 minute incubations in 65 ºC low stringency wash buffer, followed by 4× 20 minute incubations in 65 ºC high stringency wash buffer. The blot was then removed from the hybridisation tube, excess wash buffer removed, and wrapped in Saran Wrap. The blot was subsequently exposed to a Fujifilm Phosphoimager plate for 6 hr – 4days.

2.2.4.9. Imaging and Quantification of Southern blots

A Fujifilm FLA 5100 fluorescent image analyser was used to image the Phosphoimager plate after sufficient exposure time. Imaging was undertaken at 100 µm resolution. Images were then imported to Aida, where a 2D

densitometry overlay was undertaken, to allow quantification of specific molecular species. This was initially achieved by selecting a region of interest (ROI) manually which encompassed the entirety of the DNA spot which was to be quantified. An identical-sized ROI was placed proximal to the DNA spot, but did not contain any signal above background. Aida then determines the pixel count for these regions of interest, and the value of the background ROI is subtracted from the ROI in which the DNA species resides to provide a signal level. This is then divided by the total signal for the lane/panel, to provide a proportion which is utilised in these graphs. In subsequent quantifications, ROIs are copied, so as to provide continuity between experiments, and manually centred on the DNA species of interest.

2.2.5. Cytological methods

2.2.5.1. DAPI to assess nuclear divisions

Cells were initially stored in 70% ethanol, and frozen at -20 °C until they were required. Samples were pelleted, resuspended in Vectashield® mounting medium with DAPI, and placed on a glass slide, from where they could be visualised using a DAPI filter.

2.2.5.2. Sporulation counts

Sporulation counts were undertaken on freshly sporulated cells, which were placed on a slide and visualised using a light microscope.

2.2.5.3. Spreads

Protocol is modified from that which is outlined in (NEWNHAM, et al., 2010). Meiotic cells are resuspended in 500µl (2% potassium acetate, 1 M sorbitol, 0.2 mg/ml 100T zymolyase, 0.01 M dithiothreitol) and incubated for 30 min at 30 °C. 2 ml of 4 °C (0.1 M MES, 1 mM EDTA, 0.5 mM MgCl2, 1 M sorbitol) is added to the solution and then gently pelleted, then gently resuspended in 50 µl of (0.1 M MES, 1 mM EDTA, 0.5 mM MgCl2) followed immediately by 50 µl 3% formaldehyde (Thermo scientific, prod # 28906), then 50 µl 1% aqueous lipsol. 50 µl of the cell is placed equally on to long coverslips, which have been ozonated, and are held at a shallow angle (30°). The direction of tilting is repeatedly inverted until the solution is dried. A further 100 µl 3% formaldehyde

is added, and dried in the same manner. Next, the coverslips are thoroughly washed in 0.4% photo-flo (KODAK).

To determine the quality of the spreading procedure, slides were stained with DAPI and antibodies (Newnham, Jordan et al. 2010) and imaged via standard fluorescence microscopy. This was performed using a Deltavision IX70 using an Olympus Plan Apo100× 1.4 numerical aperture objective lens and the softWoRx software. Emission and excitation filters for DAPI (DAPI-5060B, FF01-387/11–25 and FF409-Em02-25), FITC (FITC-3540B, FF506-Ex04-25 and FF506-Em02-25), Texas Red (TR-4040B, FF593-Ex03-25 and FF593-Em02-25), and Cy5 (Cy5-4040A, FF660-Ex03-25 and FF660-Em02-25) were used. Images were captured by a CoolSnap HQ CCD camera and deconvolved using the Constrained Iterative Deconvolution algorithm associated with softWoRx.

2.2.5.4. Image capture

Images were captured using the Deltavision IX70 system (Applied Precision) using the accompanying softWoRx software, and an Olympus Plan Apo 100× 1.4 numerical aperture objective lens. Emission and excitation filters for DAPI, FITC, Texas Red and Cy5 were obtained from Semrock. Images were captured by a 12-bit CoolSnap HQ CCD camera and deconvolved using the proprietary constrained iterative deconvolution algorithm. The softWoRx software was used to take Z-stack images (set at 0.2 µm) and to construct 2D-projections of such images.

2.2.6. Software/computational tools used

Image J - General image analysis and manipulation for Southern analysis (SCHNEIDER, et al., 2012)

Aida image analyser v.4.27 – for quantification of Southern analysis

DNASTAR Lasergene 11 Core suite – for sequence analysis/primer design

Reverse complement – to determine reverse complementarity for primers www.bioinformatics.org/sms/rev_comp.html

Vasserstats – statistics were carried out using this online tool http://vassarstats.net/

SGD – yeast genomic data/genetic sequence information http://www.yeastgenome.org/ (CHERRY, et al., 2012)

softWoRx Deltavision software – some of the microscopy (non-super resolution spreads) was undertaken using this software

Micro-Manager - some of the microscopy (super resolution spreads) was undertaken using this software (EDELSTEIN, et al., 2014)

https://micro-manager.org/

Chapter 3

The Smc5/6 complex affects early meiotic events in the absence of functional ZMM pathway repair

3.1. Introduction

In *S. cerevisiae,* there are two major meiotic recombination pathways that process induced DSBs to both crossovers and non-crossovers. The main crossover inducing pathway is the ZMM pathway, where the actions of the meiosis-specific MutSγ heterodimer and the MutLγ endonuclease generate predominantly crossover products that display interference (BORNER, et al., 2004; HOFFMANN, et al., 2005; PERRY, et al., 2005). A second crossover inducing pathway, dependent on the activity of the XPF-family of structure-specific endonuclease Mus81-Mms4 resolves double Holliday Junctions into equal proportions of crossovers or non-crossovers, and these events do not show genetic interference (DE LOS SANTOS, et al., 1993).

The Smc5/6 complex is required for the timely resolution of meiotic recombination intermediates, with Smc5/6 complex mutants accumulating a variety of joint molecule species (JMs) (COPSEY, et al., 2013; LILIENTHAL, et

al., 2013; XAVER, et al., 2013). These JMs require the specific action of the Mus81-Mms4 endonuclease pathway (COPSEY, et al., 2013; XAVER, et al., 2013), raising the possibility that the Smc5/6 complex promotes a mitotic fate on DSB repair events that do not undergo a ZMM, crossover-specific fate.

Previous work indicates that the early stages of the ZMM recombination pathway are predominantly unaffected in Smc5/6 complex mutants (COPSEY, et al., 2013). Synapsis occurs with normal efficacy, and whilst the number of Zip3 foci (denoting crossover sites determined by the ZMM pathway (AGARWAL & ROEDER, 2000) does increase (COPSEY, et al., 2013), there is no overall change in the designation of Zip3 foci, as determined by the coefficient of coincidence (CoC) (ZHANG, et al., 2014). Collectively, these observations suggest that although the number of Zip3 foci is increased their distribution along chromosomes is unaffected in Smc5/6 complex mutants.

It has been demonstrated through ChIP-Seq analysis that the Smc5/6 complex and the BLM helicase (Sgs1 in *S. cerevisiae*) localize to the same chromosomal interaction sites (XAVER, et al., 2013). The Smc5/6 complex has a number of overlapping molecular functions (XAVER, et al., 2013). In particular, Sgs1 has an activity that prevents the formation or encourages the dissociation of multi-chromatid joint molecules (mcJMs), aberrant recombination structures where more than two chromatids are connected (JESSOP & LICHTEN, 2008; OH, et al., 2007). In Smc5/6 complex mutants, these mcJMs also accumulate, suggesting that the Smc5/6 complex may have a role in preventing their

formation; however, Sgs1 and the Smc5/6 complex have a synergistic relationship, with the double mutant accumulating far more mcJMs than either single mutant alone (COPSEY, et al., 2013). Despite the similar accumulation of mcJMs in Sgs1 and Smc5/6 complex single mutants, a number of key differences indicate substantially different molecular roles for the two complexes. In the first instance, Sgs1 is considered an anti-crossover factor that promotes the dissociation of early meiotic recombination intermediates into NCOs during meiotic prophase. Hence there is no reduction in the number of crossovers in Sgs1 mutants, but rather an increase (DE MUYT, et al., 2012; JESSOP, et al., 2006; OH, et al., 2007). In contrast, in the absence of the Smc5/6 complex, the number of COs is reduced (COPSEY, et al., 2013), although this may be as a result of the later function of the Smc5/6 complex in JM resolution. In ZMM deficient mutants, knocking out Sgs1 can partially restore the number of COs observed (OH, et al., 2007), suggesting an anti-crossover function that specifically opposes the pro-crossover function of the ZMM pathway, to enable the orderly formation of dHJs. Whether this restoration of CO levels occurs has yet to be investigated, and will be addressed in this study.

A second manner in which Sgs1 and the Smc5/6 complex mechanistically differ is through their roles in the establishment and maintenance of IH:IS bias. The bias in meiotic recombination towards using the interhomolog DNA strand, established at an early stage of the repair pathway, is maintained in Sgs1 mutants: in an Sgs1 mutant alone, the amount of IS-dHJs is increased (an apparent contradiction); however when the transcription factor Ndt80 is deleted

to prevent pachytene exit (XU, et al., 1995), the bias towards interhomolog repair is restored (JESSOP & LICHTEN, 2008; OH, et al., 2007). This suggests that Sgs1 has a late function in dissolving IS-dHJs, and is not affecting the establishment of bias. In Smc5/6 complex mutants, both the levels of IH-dHJs and IS-dHJs are elevated, and the bias towards interhomolog repair is reduced; this reduction also occurs when pachytene exit is blocked (COPSEY, et al., 2013), suggesting an earlier role for the Smc5/6 complex in determining the recombination template for repair substrates.

In this chapter, I investigate the role of the Smc5/6 complex in the establishment and maintenance of meiotic interhomolog repair bias. Initially I will reproduce results obtained previously, with a view to determining a baseline level of bias in this experimental set up. I then move on to assess the effect of Smc5/6 complex mutants in combination with depleting Msh5, a meiosis specific MutS homolog (HOLLINGSWORTH, et al., 1995), and component of the ZMM pathway, in order to determine whether the absence of the Smc5/6 complex is able to restore CO-specific recombination intermediates designation in this context, in a manner similar to that which has been observed in Sgs1 in other studies. This will allow an insight into the complex relationship between the Smc5/6 complex and the ZMM meiotic repair pathway, to help further elucidate the role of Smc5/6 complex in meiosis.

3.2. Results

3.2.1. Meiotic recombination in wild type and pachytene blocked cells

3.2.1.1. *HIS4LEU2* assay system

The *HIS4LEU2* hotspot was developed as a method for detecting meiotic recombination intermediates (SCHWACHA & KLECKNER, 1995; SCHWACHA & KLECKNER, 1997) in *S. cerevisiae*. A stretch of DNA containing *LEU2* and a portion of *NSF1*, in addition 77 bp of bacterial DNA that includes the major DSB site (DSB I), was inserted adjacent to the *HIS4* locus. Nucleotide polymorphisms on parental strands generated *Xho*I cut sites at different molecular distances from the DSB site. Using Southern analysis one can distinguish between the two parental alleles (Figure 3.1), and detect a wide variety of joint molecules (JMs) composed of different combinations of parental DNA (Figure 3.2). Analysis of other artificial hotspots generated at the *HIS4* loci, containing an *arg4*- palindromic sequence to allow the characterisation of which parental strands were being incorporated into these joint molecules, showed that these JM intermediates contained heteroduplex DNA, and were thus dHJs and SEIs predicted by the DSB repair model (ALLERS & LICHTEN, 2001b). Almost every wild type cell entering meiosis generates a DSB at the modified *HIS4LEU2* locus, which is reported to yield either a crossover or non-crossover (STORLAZZI, et al., 1995). It should be noted that there is a second, minor DSB site (DSB II) that falls outside the region of *Xho*I digestion.

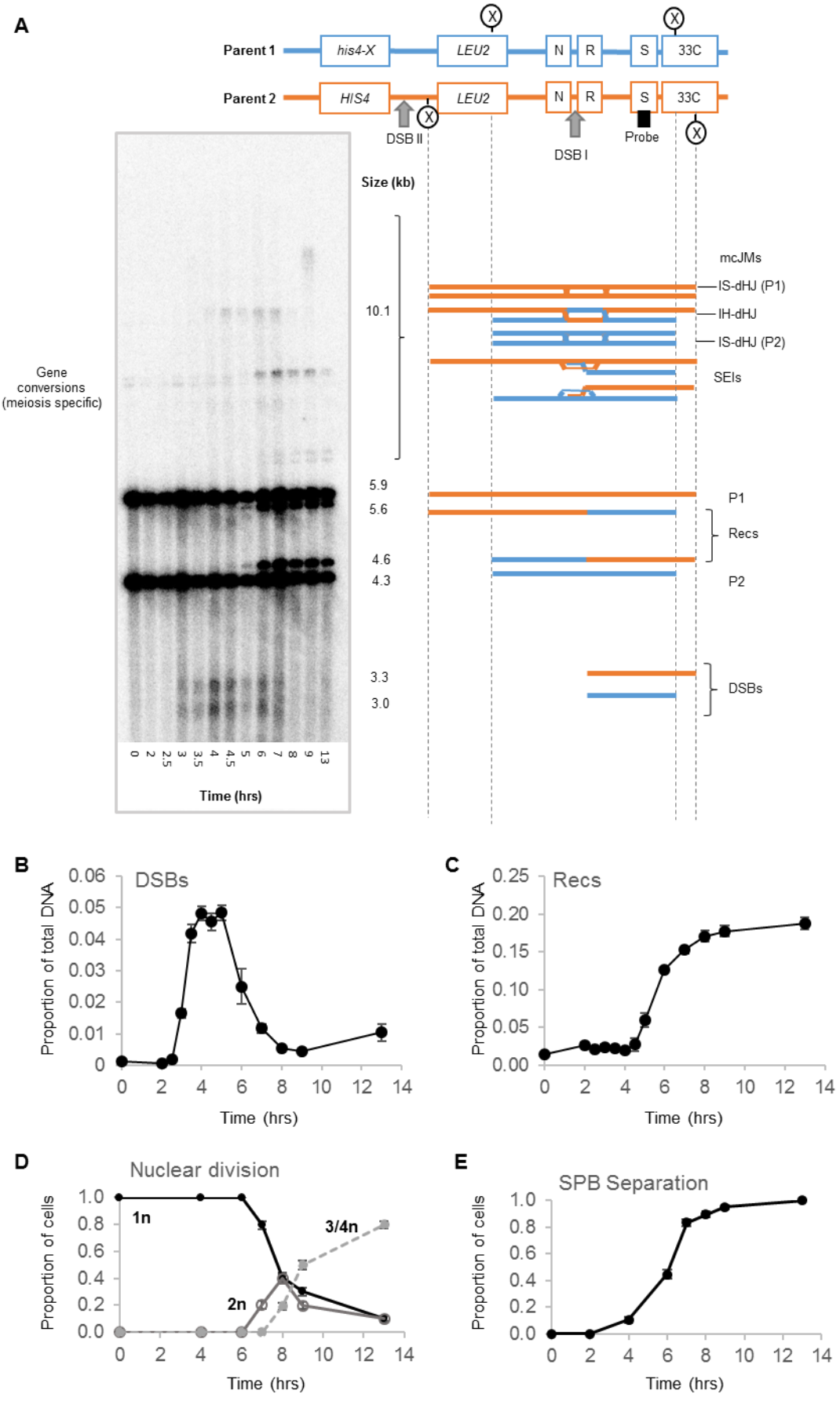
A
Parent 1
his4-X
LEU2
N
R
S
33C
Parent 2
HIS4
LEU2
N
R
S
33C
DSB II
DSB I
Probe
Size (kb)
Gene conversions (meiosis specific)
Time (hrs)
0
2
2.5
3
3.5
4
4.5
5
6
7
8
9
13
10.1
mcJMs
IS-dHJ (P1)
IH-dHJ
IS-dHJ (P2)
SEIs
5.9
5.6
P1
Recs
4.6
4.3
P2
3.3
3.0
DSBs
B
DSBs
Proportion of total DNA
Time (hrs)
C
Recs
Proportion of total DNA
Time (hrs)
D
Nuclear division
Proportion of cells
1n
2n
3/4n
Time (hrs)
E
SPB Separation
Proportion of cells
Time (hrs)

Figure 3.1 Molecular analysis of recombination intermediates in *S. cerevisiae*

(A) Physical map and Southern blot of the *HIS4LEU2* hotspot in wild type SK1 strain. The *HIS4LEU2* hotspot is an artificial hotspot with a high incidence of double strand break (DSB) formation during meiosis. It was generated by the insertion of recombinogenic DNA, consisting of the *LEU2* ORF and bacterial DNA, adjacent to *HIS4* (Xu and Kleckner, 1995). The two parental alleles P1 and P2 (historically referred to as "Mom" and "Dad") are distinguished by a polymorphic arrangement of *XhoI* restriction sites (represented by encircled X). ORFs are denoted by white boxes, with the Southern blotting probe (denoted with a black box) binding within the *STE50* ORF (S). The two major DSB sites are denoted with grey arrows. The different species detected after *XhoI* digestion, their molecular weights, and their migration is shown. It should be noted that the different joint molecule species (SEIs, dHJs and mcJMs) run over a range of ~7.5-20.5kb (denoted by large bracket), and are not distinguishable, and are hence analysed by two dimensional gel electrophoresis (**Figure 3.2**)

(B) Double strand break levels over a 13 hour meiotic timecourse, quantified as a proportion of total detectable DNA species in the lane. Time points were obtained at 30 minute interviews between 2 and 8 hours, where we would expect to see the greatest rate of change, and then hourly between 5 an 9 hours.

(C) Levels of recombinant molecules during a 13 hour meiotic timecourse. In the wild type recombinants represent crossovers between parental strands, and are quantified as a proportion of total detectable DNA species in the lane.

(B-C) Average of two independent diploids is given, and error bars represent S.E.M.

(D) Population kinetics of nuclear divisions, as determined by the number of distinct DAPI foci that can be visualized.

(E) Population kinetics of spindle pole body separation, as determined by the first instance when two Spindle pole bodies can be visualised.

(E-F) n=200 per time point. Error bars represent S.E.P.

Strains: JKD200, Y3912.

Experiment ID: E07_JK1_131021; E28_JK2_150921 respectively.

3.2.1.2. Linear recombination intermediates in *S. cerevisiae*

In order to validate that the meiotic timecourses which were being undertaken showed concordant results to the existing literature, I performed a one-dimensional analysis of recombination intermediates in wild type *HIS4LEU2* diploids (Figure 3.1). A one-dimensional analysis of repair products at the *HIS4LEU2* hotspot is used to reveal the levels of the earliest molecular intermediate of meiotic repair, Spo11-induced DSBs (KEENEY, et al., 1997), and the final products of meiotic repair – in this instance, crossovers between parental strands were quantified (SCHWACHA & KLECKNER, 1997). DSBs are initially detected at 3 hours (Figure 3.1A), peak between 4 and 5 hours, and become undetectable by 8-9 hours (Figure 3.1A&B). This is consistent with the range described in the literature (BORNER, et al., 2004; COPSEY, et al., 2013; HUNTER & KLECKNER, 2001; OH, et al., 2007). CO levels become detectable by 4.5-5hrs, which is consistent with COs being a product of DSBs, and plateau at 18.6% ± 0.7 of total DNA (Figure 3.1C), also consistent with what is observed in the literature (COPSEY, et al., 2013; HUNTER & KLECKNER, 2001).

The population kinetics of the meiotic timecourse are assessed by two methods. The number of DAPI stained foci per cell is counted as a function of time and used to indicate meiotic progression, with one DAPI body representing nuclei prior to anaphase I, two DAPI bodies representing MII nuclei prior to anaphase II, and 3/4 DAPI bodies indicating cells which have completed the meiotic nuclear divisions. In mutants that fail to segregate chromosomes, cell cycle progression is measured by spindle body separation, which is under the control of Cdc28/CDK1, and hence distinct from chromosome segregation

(SOURIRAJAN & LICHTEN, 2008). The number of cells with distinct spindle pole bodies, which separate during diplotene of meiotic prophase, may be determined, and used as a measure of cell cycle progression. In both instances, the results obtained in the wild type (Figure 3.1D, E) are similar to those from previously published data from the Hoffmann lab (COPSEY, et al., 2013). Taken together, these data suggest that the time courses are running synchronously, with a timely elevation of the earliest meiotic precursor DSBs. COs also begin to become detectable at the same time as spindle pole bodies separate (ALLERS & LICHTEN, 2001b). This is consistent with the co-ordination of entry into M-phase, promoted by CDK1, and resolution of joint molecules into COs, and mediated by Cdc5. Both Cdc5 and CDK1 are regulated by Ndt80 (SOURIRAJAN & LICHTEN, 2008).

3.2.1.3. Branched recombination intermediates in *S. cerevisiae*

In order to assess the progression of joint molecule intermediates that cannot be resolved in the first dimension, two-dimensional electrophoresis of wild type strains was undertaken (Figure 3.2). Two-dimensional gel electrophoresis was initially developed to visualise the progression of replication origins (BREWER & FANGMAN, 1987) and was later adapted to allow the visualisation of the different molecular species that occur as part of meiotic recombination (SCHWACHA & KLECKNER, 1995) (Figure 3.2A). After DSB breaks are formed, and resected to ssDNA by the action of the Exo1 exonuclease (TSUBOUCHI & OGAWA, 2000), the ssDNA forms a semi-stable interaction with a homologous DNA strand, the stable single-end invasion (HUNTER & KLECKNER, 2001). This event may either be dissolved by the action of Sgs1;

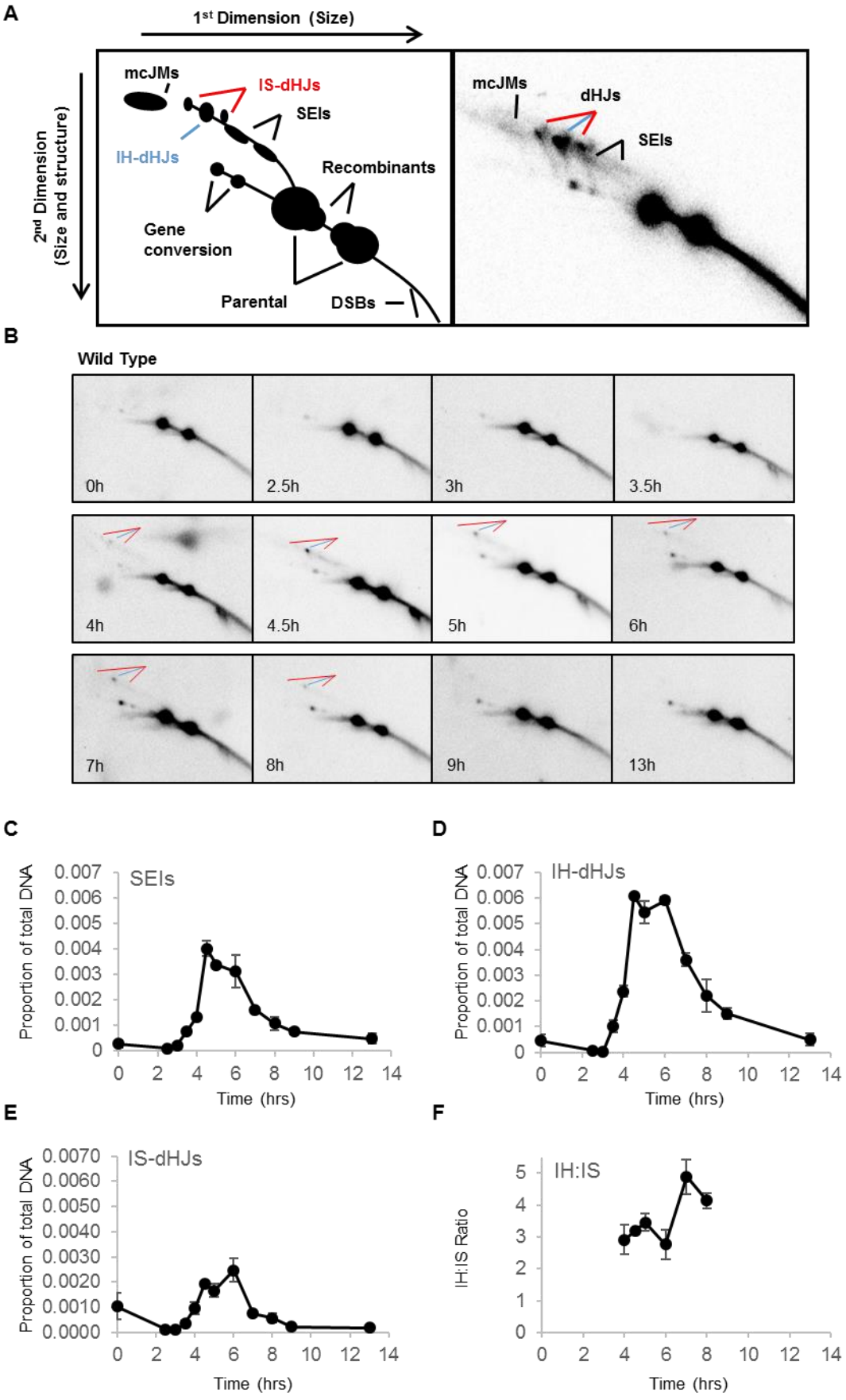
A
1st Dimension (Size)
2nd Dimension (Size and structure)
mcJMs
IS-dHJs
SEIs
IH-dHJs
Recombinants
Gene conversion
Parental
DSBs
mcJMs
dHJs
SEIs
B
Wild Type
0h
2.5h
3h
3.5h
4h
4.5h
5h
6h
7h
8h
9h
13h
C
SEIs
Proportion of total DNA
Time (hrs)
D
IH-dHJs
Proportion of total DNA
Time (hrs)
E
IS-dHJs
Proportion of total DNA
Time (hrs)
F
IH:IS
IH:IS Ratio
Time (hrs)

Figure 3.2 Analysis of branched recombinant molecules during meiosis

Quantification of DNA species at the *HIS4LEU2* hotspot from two dimensional gel electrophoresis, followed by Southern blotting.

(A) Left: A cartoon depicting the regions where we would expect different molecular species to migrate by 2D gel electrophoresis, with the 1st and 2nd dimensions labelled. Joint molecules suffer a greater degree of retardation compared to linear molecules in the 2nd dimension, as a result of the intercalation of ethidium bromide into the DNA strands. **Right:** Representative image of a 13hr time point in the *msh5Δ nse4-mn* strain, selected as it demonstrates a wide variety of JM intermediates. IS-dHJs are indicated in red, whilst IH-dHJs are indicated in blue. In SMC5/6 complex mutants, we see particularly deformed and smeary dHJ bands (Figure 3.5)

(B) A representative meiotic time course to visualise recombination intermediates at the *HIS4LEU2* in a wild type SK1 strain.

(C) Single end invasions (SEIs), quantified as a proportion of the total DNA for this panel.

(D) Interhomolog double Holliday Junctions (IH-dHJs), quantified as a proportion of the total DNA for this panel.

(E) Intersister double Holliday Junctions (IS-dHJs), with P1 and P2 IS-dHJs quantified as a proportion of the total DNA for this panel.

(F) IH:IS bias. The ratio of IH-dHJs to IS-dHJs molecules between 4-8 hours. Outside of this range, there are insufficient levels of each molecule to give a meaningful ratio

(C-F) The average of two independent diploids is given and error bars represent S.E.M.

Strains: Y200, Y3912.

Experiment ID: E07_JK1_131021; E28_JK2_150921 respectively

alternatively, the other side of the DSB (the “second end”) is subsequently captured and converted into a double Holliday junction (SCHWACHA & KLECKNER, 1995). SEIs are the first molecular precursor on the pathway to generate a crossover. By using psoralen-mediated interstrand UV cross-linking, these intermediates (SEIs, IS-dHJs and IH-dHJs) can be effectively quantified. In certain mutant backgrounds, aberrant multi-chromatid joint molecules (mcJMs) are also visualised; however, these do not accumulate to appreciable levels in the wild type, and so have not been shown here.

The first recombination events to be detected are SEIs (Figure 3.2C). This is concurrent with detection of DSBs in the 1D gel and suggests that these structures are formed very rapidly after the onset of DSB formation. In addition, this is also indicative of the fact that the two-dimensional analysis is more sensitive than one-dimensional analysis, and low levels of DSBs can be visualised at 2.5 hours using two-dimensional analysis. These appear with similar timing to the published literature, but to lower levels than would be expected from the published literature, with a peak at 0.40% ±0.03 of DNA in the panel (Figure 3.2B, t=4.5h, quantified in Figure 3.2C), compared to ~4% (HUNTER & KLECKNER, 2001) or ~1.5% (OH, et al., 2007). This suggests that the psoralen cross-linking, which allows the visualisation of short-lived branched intermediates, is not cross-linking JMs together as efficiently as has previously occurred in other laboratory settings – either as a result of alterations in reagents or differing equipment.

IH-dHJs and IS-dHJs (Figure 3.2D, E), also begin to accumulate from 3.5-4 hours, with a peak IH-dHJ level of 0.61% ±0.01 at t=4.5h, and a peak IS-dHJ level of 0.24% ±0.04. This was once again to lower levels than reported elsewhere in the literature (IH-dHJs were ~3% (HUNTER & KLECKNER, 2001) or ~1.1% (OH, et al., 2007) whilst IS-dHJs were ~0.8% (HUNTER & KLECKNER, 2001) or ~0.25% (OH, et al., 2007)). The ratio of IH-dHJs to IS-dHJs was calculated from the range of 4-8 hours (Figure 3.2F). Outside of this region, the levels of dHJs are low such that accurate determination of the ratio is compromised by the small denominator. The ratio of IH:IS dHJs I observed is similar to those observed in the literature over a similar time frame (average IH:IS bias is 3.6 between 4-8 hours, compared with 2.4 (SCHWACHA & KLECKNER, 1997) or ~4 (COPSEY, et al., 2013)).

Broadly, the data obtained in Figure 3.2 is similar to the published literature, particularly with regards to the timings with which different JM species are formed. In contrast levels of recombination intermediates are generally lower than those observed elsewhere (COPSEY, et al., 2013; HUNTER & KLECKNER, 2001; OH, et al., 2007) . It should be noted that there is a large degree of variation between absolute levels of different molecules in the published literature, and hence absolute quantification of DNA may not be identical between studies, but should be similar within studies.

3.2.1.4. JMs accumulate in pachytene arrested *ndt80*Δ cells

In order to more accurately assess the interhomolog repair bias of strains that fail to accumulate dHJs to wild type levels (such as *msh5*Δ strains), cells can be

blocked in pachytene by the deletion of the transcription factor Ndt80 (XU, et al., 1995), to prevent the resolution of JMs, and cause their accumulation. This can also be used to control for different resolution pathways acting with different efficiencies on specific JMs, e.g. Sgs1 acting to specifically dissolve IS-dHJs, but not IH-dHJs (OH, et al., 2008). The *ndt80*Δ system has been used frequently, and here also serves as another useful control for how well the meiotic timecourses in this study concur with those previously published (ALLERS & LICHTEN, 2001a).

DSBs occurred with similar timings and levels as those seen in wild type, with DSBs beginning to be detected at 2.5 hours, and peaking at 6.5% ±1.6 of total DNA at t=4.5hours (Figure 3.3C); this timing is similar to the levels observed in the literature (ALLERS & LICHTEN, 2001a), and whilst the absolute DSBs levels appear higher than the Lichten study, they observed that wild type and *ndt80*Δ strains accumulated DSBs to similar levels, which is consistent with what is observed here (Figure 3.3C). This agrees with the established model of *ndt80*Δ mutants being blocked at the exit of pachytene, but unperturbed at early meiotic stages when DSB formation occurs. Recombinants appear at lower levels (11.5% ±0.5 at t=13h) than I have observed in wild type (Figure 3.3D). This suggests that given sufficient time, some recombination intermediates can indeed be resolved in the absence of Ndt80, although whether this resolution occurs via the same repair pathways as are utilised in wild type is unclear.

All quantified JMs accumulate to higher levels in the absence of Ndt80 (Figure 3.3E, F): SEI levels peak at 0.98% ±0.23 at t=8h, IH-dHJs levels peak at 3.3%

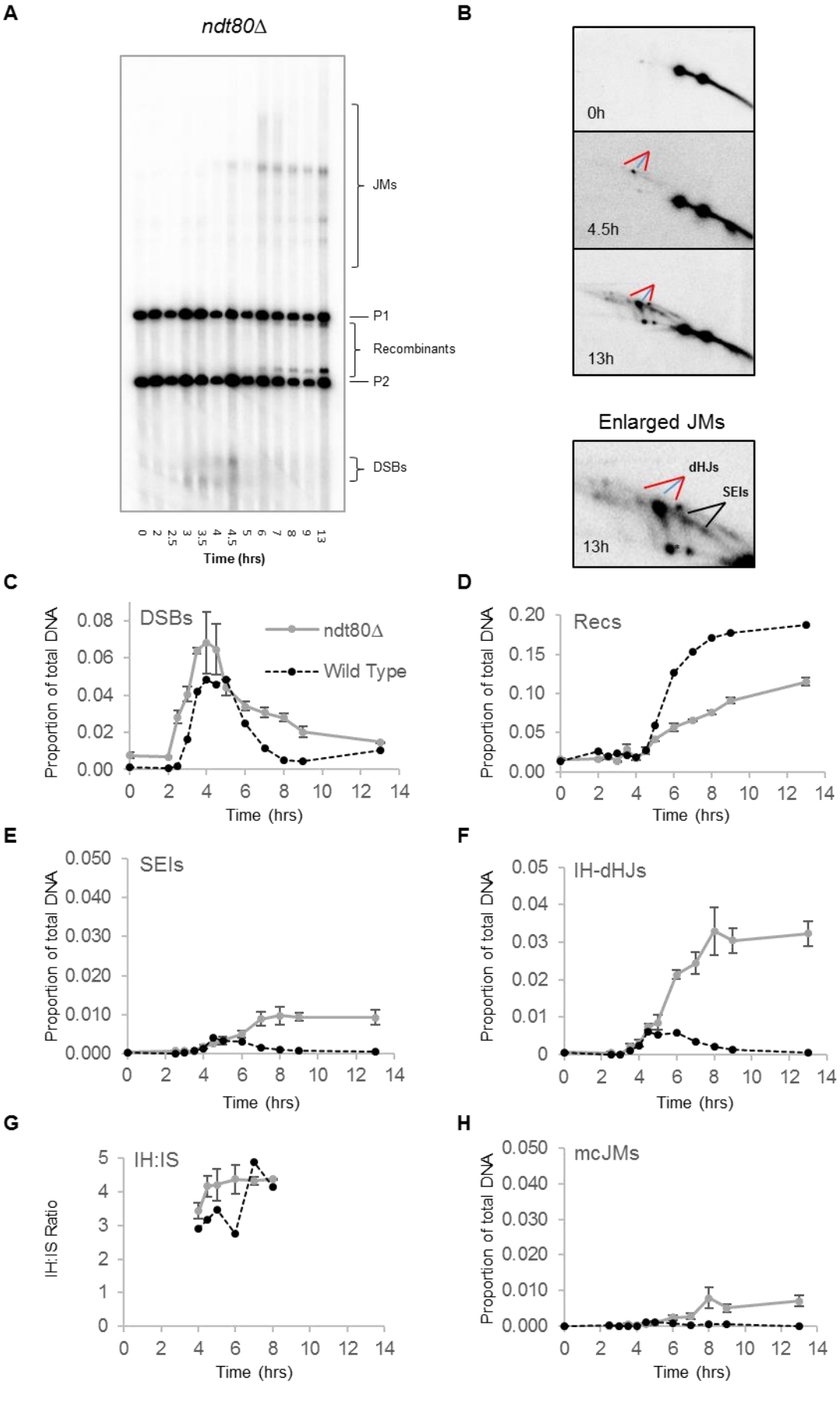
A
ndt80Δ
JMs
P1
Recombinants
P2
DSBs
0 2 2.5 3 3.5 4 4.5 5 6 7 8 9 13
Time (hrs)
B
0h
4.5h
13h
Enlarged JMs
dHJs
SEIs
13h
C
DSBs
ndt80Δ
Wild Type
Proportion of total DNA
0.00 0.02 0.04 0.06 0.08
0 2 4 6 8 10 12 14
Time (hrs)
D
Recs
Proportion of total DNA
0.00 0.05 0.10 0.15 0.20
0 2 4 6 8 10 12 14
Time (hrs)
E
SEIs
Proportion of total DNA
0.000 0.010 0.020 0.030 0.040 0.050
0 2 4 6 8 10 12 14
Time (hrs)
F
IH-dHJs
Proportion of total DNA
0 0.01 0.02 0.03 0.04 0.05
0 2 4 6 8 10 12 14
Time (hrs)
G
IH:IS
IH:IS Ratio
0 1 2 3 4 5
0 2 4 6 8 10 12 14
Time (hrs)
H
mcJMs
Proportion of total DNA
0.000 0.010 0.020 0.030 0.040 0.050
0 2 4 6 8 10 12 14
Time (hrs)

Figure 3.3 Accumulation of unresolved joint molecules *ndt80*Δ

(A) Representative 1D Southern blot of an *ndt80*Δ strain.
(B) Representative images of key time points (T=0,4.5,13) in *ndt80*Δ strain in 2D Southern analysis. Last panel is an enlarged image of the branched molecule region at 4.5 hrs, with different observed species indicated. Red line indicates IS-dHJs, blue line indicates IH-dHJs. Gene conversions are indicated by *
(C) Double strand break levels over a 13 hour meiotic timecourse, quantified as a proportion of total detectable DNA species in the lane
(D) Levels of recombinant molecules during a 13 hour meiotic timecourse, quantified as a proportion of total detectable DNA species in the lane
(E) Single end invasions (SEIs), quantified as a proportion of the total DNA for this panel.
(F) Interhomolog double Holliday Junctions (IH-dHJs), quantified as a proportion of the total DNA for this panel.
(G) IH:IS bias. The ratio of IH-dHJs to both IS-dHJs bands
(H) Multi-chromatid joint molecules (mcJMs), quantified as a proportion of the total DNA for this panel.
(C-H) The average of two independent diploids is given and error bars represent S.E.M. Wild type levels are illustrated with a dashed line.

Strains: JKD174, JKD175
Experiment ID: E26_JK2_150520, E07_JK1_130928 respectively

±0.6 at t=8h, and IS-dHJ levels peak at 0.83% ±0.11 at t=13h. These JMs also persist as opposed to being resolved as seen in wild type. The overall levels of JMs, as observed in the wild type scenario, are lower than those indicated in the literature (IH-dHJs peak at ~7.5% in OH, et al., 2007). In the absence of Ndt80, the IH:IS bias was slightly higher than observed in the wild type (averaging 4.1 over 4-8 hour time points, as opposed to 3.6 observed in wild type, Figure 3.3G). This is consistent with results obtained in the literature (COPSEY, et al., 2013). The elevation of IH:IS bias seen in *ndt80*Δ might be a result of the fact that joint molecule intermediates are no longer being resolved, and so might be considered more representative of the formation bias than is observed in wild type cells, which may resolve different dHJs at different speeds. However, unlike in wild type cells, a large molecular weight JM that accumulates in *ndt80*Δ (0.80% ±0.28 at t=8h represents the peak in *ndt80*Δ, Figure 3.3H): these represent mcJMs, whereby molecular connections are made between more than two chromatids. This molecular species is generally considered aberrant. (Figure 3.3H).

3.2.2. Meiotic repair is abrogated in Smc5/6 complex mutants

3.2.2.1. In the absence of the Smc5/6 complex, crossovers are reduced, and interhomolog bias is reduced.

In the absence of the Smc5/6 complex, JMs accumulate during meiosis, and are not effectively processed into crossovers (COPSEY, et al., 2013). Here, I intend to replicate previously reported results, in order to verify my experimental methods, and probe the nature of the abrogation of the recombination pathway

in Smc5/6 complex mutants. I will utilise a common laboratory technique to generate meiotic depletions of proteins within this complex which would be lethal if a full knockdown occurred – the *CLB2* promoter. *CLB2* is expressed throughout the mitotic cell cycle, but is strongly suppressed during the meiotic cell division (CHU, et al., 1998). This allows for essential genes to be knocked down and characterised only within the meiotic cell cycle, whilst not affecting the viability of the mitotic cells (COPSEY, et al., 2013). Hereafter they will be referred to as *meiotic null* or *mn* alleles.

In the mutant strains *smc5-mn* and *nse4-mn*, the DSBs appear with similar timing for all strains (Figure 3.4B) first becoming detectable at 2.5 hours in *nse4-mn* and 3 hours in *smc5-mn*. The DSB levels peak at similar levels (5.0% ±0.8 *nse4-mn*, 4.6% ±0.6 *smc5-mn*). DSBs are removed with similar timing becoming undetectable at 8 hours in wild type cells, whilst in *smc5-mn* and *nse4-mn* the DSBs become undetectable after 9 hours

In the *nse4-mn*, we see that the number of recombinant DNA molecules is severely reduced compared to wild type (10.4% ±0.4 for *nse4-mn* at t=13h) (Figure 3.4C). It was also observed that while spindle pole bodies still separated (Figure 3.4 D), in *nse4-mn* mutant's nuclei generally fail to separate their DNA effectively into distinct spores, and instead DNA remains diffuse outside of spores (Figure 3.4G), as previously observed (COPSEY, et al., 2013). Hence, as it is unclear whether the canonical crossover pathways are functional in the absence of the Smc5/6 complex, it may not be correct to call these recombinants crossovers. It should be noted that whilst there is a slight

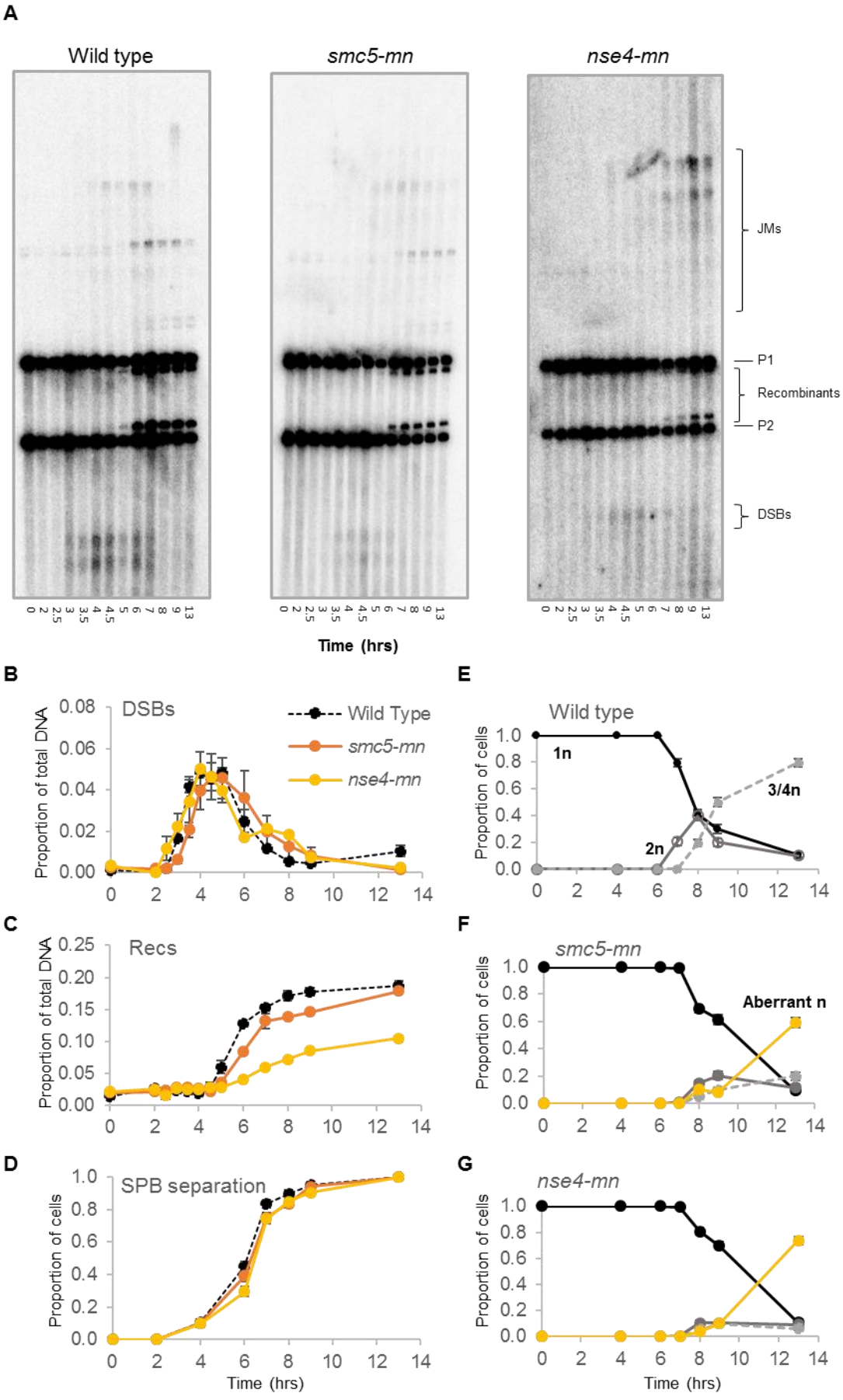
A
Wild type
smc5-mn
nse4-mn
JMs
P1
Recombinants
P2
DSBs
Time (hrs)
B
DSBs
Wild Type
smc5-mn
nse4-mn
Proportion of total DNA
C
Recs
Proportion of total DNA
D
SPB separation
Proportion of cells
Time (hrs)
E
Wild type
1n
2n
3/4n
Proportion of cells
F
smc5-mn
Aberrant n
Proportion of cells
G
nse4-mn
Proportion of cells
Time (hrs)

Figure 3.4 Crossovers are delayed and decreased in the SMC5/6 complex depleted cells

(A) Representative 1D Southern blots of Wild type, *nse4-mn* and *smc5-mn* strains. JMs are not distinguishable in 1D gels – see fig 3.5 for 2D quantification.
(B) Double strand break levels over a 13 hour meiotic timecourse, quantified as a proportion of total detectable DNA species in the lane.
(C) Levels of recombinant molecules during a 13 hour meiotic timecourse, quantified as a proportion of total detectable DNA species in the lane.
(B-C) Average of two independent diploids is given, and error bars represent S.E.M.
(D) Population kinetics of spindle pole body separation, as determined by the first instance when two Spindle pole bodies can be visualised. n=200 per time point. Error bars represent S.E.P.
(E-G) Population kinetics of nuclear divisions, as determined by the number of distinct DAPI foci that can be visualized. n=200 per time point. Error bars represent S.E.P. Aberrant nuclei appear stretched, and DNA does not fall within the nuclei following the meiotic cell divisions. These nuclei have previously been extensively documented in (COPSEY et. al, 2013)
(E) Wild type population kinetics of nuclear divisions
(F) *smc5-mn* population kinetics of nuclear divisions
(G) *nse4-mn* population kinetics of nuclear divisions

Strains: JKD196, JKD197, JKD198, JKD199
Experiment ID: E29_ JK2_151118

delay in the timing when recombinants appear in *smc5-mn* (first detected at 5 hours) compared to wild type, over the length of the time course, recombinants accumulated to near wild type levels (17.9% ±0.1), which is contrary to what has previously been observed (COPSEY, et al., 2013), whereby crossover levels mirrored *nse4-mn* as opposed to wild type crossover levels. Smc5 depleted cells also exhibited an intermediate phenotype with regards to cytological meiotic progression, with no observed delay in spindle pole body separation, but showed a large accumulation of nuclei with aberrant DAPI staining at later time points (Figure 3.4F). Overall, these data suggest there is no significant effect of the absence of the Smc5/6 complex on the formation of DSBs, but that there may be a delay with later processing events.

It has previously been reported that in both *smc5-mn* and *nse4-mn* mutants, the repair bias towards interhomologs is reduced relative to wild type, and that all JM species are elevated in the absence of the Smc5/6 complex (COPSEY, et al., 2013). The abolition of interhomolog repair bias suggests an early function for the Smc5/6 complex in meiotic recombination, whilst the accumulation of JMs suggests a later function in resolution of intermediates. JMs accumulate to higher levels in the *nse4-mn* strains (SEIs accumulate to 0.55% ±0.01, IH-dHJs accumulate to 1.1% ±0.04 and IS-dHJs accumulate to 1.9% ±0.2 at t=13) (Figure 3.5C-E), and these JMs also increase throughout meiosis as opposed to being resolved as we see in wild type. In *smc5-mn*, we see an intermediate phenotype between wild type and *nse4-mn* (SEIs accumulate to 0.82% ±0.08, IH-dHJs accumulate to 2.0% ±0.1 and IS-dHJs accumulate to 0.60% ±0.01, peaking at t=6), with JMs accumulating to higher levels than in wild type, and

persisting for longer. However, unlike in *nse4-mn*, the level of these intermediates does eventually begin to decrease by the latest time points. Aberrant mcJMs also accumulate in both mutants, unlike in wild type (1.0% ±0.02 in *nse4-mn* at t=13h, 0.37% ±0.04 in *smc5-mn* at t=6h). These persist in *nse4-mn*, and begin to decrease over the later time points in the *smc5-mn* strain (Figure 3.5G); the presence of these large molecular weight JMs is highly suggestive of severe issues in the meiotic recombination pathway in the mutant strains.

As has been previously reported, the IH:IS bias is reduced in the absence of the Smc5/6 complex (COPSEY, et al., 2013; LILIENTHAL, et al., 2013; XAVER, et al., 2013). The loss of bias was more severe in *nse4-mn* (1.0) compared to *smc5-mn* (2.0) over 4-8 hour time points (Figure 3.5F). Whilst the overall reduction in bias was previously observed, the difference between these mutant strains was not; however, the intermediate phenotype would seem consistent with other joint molecule data observed, whereby in this study *smc5-mn* showed an intermediate phenotype between wild type and *nse4-mn*. This failure to establish a distinct interhomolog bias in meiosis is in contrast with Sgs1 mutant alleles, which show elevations in meiotic JMs, but no loss of bias (OH, et al., 2007). This has been suggested to demonstrate the late function of Sgs1 in meiotic recombination. Conversely, the distinct loss of bias in Smc5/6 complex mutants would appear to suggest an early meiotic function, as it is unlikely that there is a differential sorting of intersister and interhomolog dHJs into different repair pathways with different repair kinetics. A further curious point that has been previously observed, but that remains unexplained, is the observation that

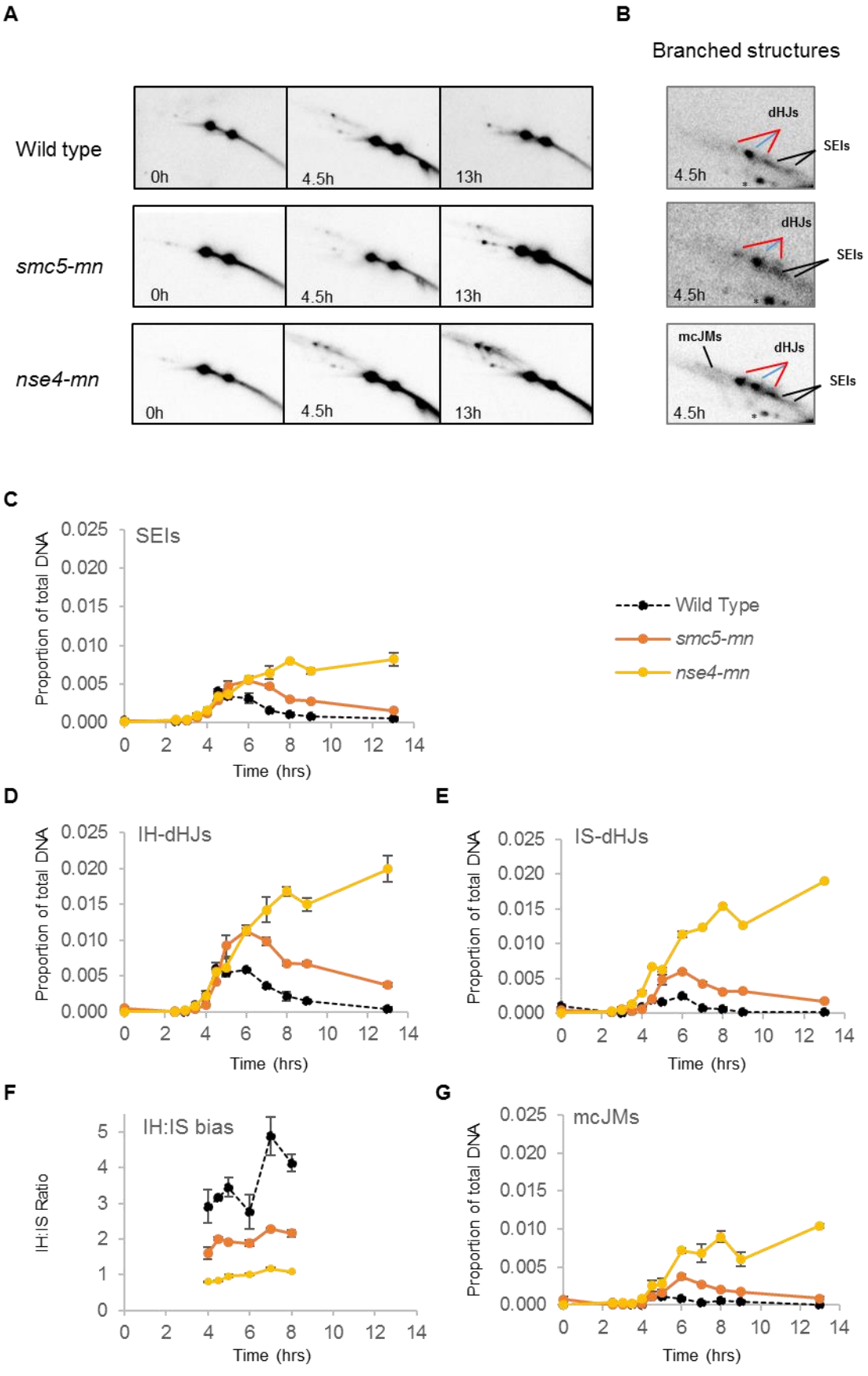
A
B
Branched structures
Wild type
smc5-mn
nse4-mn
0h
4.5h
13h
dHJs
SEIs
mcJMs
C
SEIs
Proportion of total DNA
Time (hrs)
Wild Type
smc5-mn
nse4-mn
D
IH-dHJs
E
IS-dHJs
F
IH:IS bias
IH:IS Ratio
G
mcJMs

Figure 3.5 Joint molecules accumulate, and interhomolog bias is reduced in Smc5/6 complex mutants

(A) Representative images of key time points (T=0,4.5,13) in WT, *nse4-mn* and *smc5-mn* strains.
(B) Enlarged images of the branched molecule region at 4.5 hrs in WT, *nse4-mn* and *smc5-mn* strains, with different observed species indicated. Red line indicates IS-dHJs, blue line indicates IH-dHJs. Gene conversions are indicated by *
(C) Single end invasions (SEIs), quantified as a proportion of the total DNA for this panel.
(D) Interhomolog double Holliday Junctions (IH-dHJs), quantified as a proportion of the total DNA for this panel.
(E) Intersister double Holliday Junctions (IS-dHJs), with P1 and P2 IS-dHJs quantified as a proportion of the total DNA for this panel.
(F) IH:IS bias. The ratio of IH-dHJs to both IS-dHJs bands between 4-8 hours. Error bars are present for all strains, although at some points (particularly for *nse4-mn*) are covered by the graph itself.
(G) Multi-chromatid joint molecules (MCJMs), quantified as a proportion of the total DNA for this panel.
(C-G) Average of two independent diploids is given and error bars represent S.E.M.

Strains: JKD196, JKD197, JKD198, JKD199
Experiment ID: E29_ JK2_151118

the dHJs observed in the absence of the Smc5/6 complex appear more smeared, in a “teardrop” shape (Figure3.5A). One might speculate that this is as a result of subtly different, novel dHJ arrangements that are only observed in the absence of the Smc5/6 complex. No quantification of the ”smeariness” of the foci has been undertaken in this study, but it be of interest in future work.

As *nse4-mn* appears to show a more severe phenotype as a result of the Smc5 protein being less efficiently depleted using the *CLB2* promoter system, as demonstrated using AID induced degradation (COPSEY, et al., 2013), I decided to focus on *nse4-mn* in future experiments.

3.2.3. Smc5/6 complex mutants allow progression of early meiotic recombination mediates in *msh5*Δ mutants

3.2.3.1. Smc5/6 complex mutants fail to alleviate low crossover levels in *msh5*Δ mutants

Msh5 is a meiosis specific component of the MutS heterodimer, and in addition to Msh4 forms a key part of the ZMM pathway (HOLLINGSWORTH, et al., 1995), upstream of the Mlh1/3 resolvase. In the absence of Msh5, crossovers are decreased (HOLLINGSWORTH, et al., 1995). There is however some discordance in the literature with regards to the overarching effects of Msh5, with very different phenotypes observed at different temperature ranges: at 23°C, a minor phenotype of SEIs existing for a prolonged period, and lower levels of dHJs than wild type, whilst at 33°C, a reduction in levels of SEIs is observed in addition to a much more severe in dHJs (BORNER, et al., 2004).

It has been observed that the crossover reduction phenotype observed in ZMM mutants (Mlh3 and Msh5) can be alleviated in conjunction with Sgs1 truncated alleles (OH, et al., 2007; JESSOP, et al., 2006). This has been suggestive of the fact that either Sgs1 activity is responsible for the CO defects in ZMM mutants, or that part of the role of ZMM family proteins is to protect nascent intermediates from the action of Sgs1. This is one of the key areas where the actions of Sgs1 and the Smc5/6 complex differ, as in *nse4-mn*, *msh5*Δ still exhibit a CO defect, which indicates that the Smc5/6 complex may well act in a different meiotic recombination pathway (Mus81-Mms4) (COPSEY, et al., 2013). This study also determined that there was a synergistic decrease in crossover levels in *mlh3 nse4-mn* double mutants. If the Mlh1-3 complex and Smc5/6 complex functioned in the same repair pathway, it would be suspected that the double mutant would have no decrease in crossover, hence when the converse is observed, it suggests that these complexes function in parallel repair pathways. However, this does not take account of the possibility that as Mlh1/3 dependant resolution of ZMM pathway intermediates occurs once DSBs have already been committed to a ZMM repair pathway fate. It could be the case that no such synergistic increase would be observed in mutants with an abrogated ZMM pathway; in this instance, we will be utilising *MutS* homolog Msh5. We would predict that if the ZMM pathway and Smc5/6 complex mediated repair function in parallel, we would observe a synergistic increase in crossover levels.

In the absence of Msh5, I observe that DSBs appear with similar timing to wild type, first becoming detectable at 2.5 hours. In *msh5*Δ, DSBs also accumulate

to similar peak levels as observed in wild type (5.3%± 2.6 at 4 hours). However, *msh5*Δ mutants have persistent DSBs for far longer than is observed in the wild type situation (Figure 3.6B), with DSBs not being entirely removed until the 13 hour time point. This is consistent with previously observed results (LAO, et al., 2013; OH, et al., 2007). This would suggest that either DSBs are not being processed to later intermediates in the absence of *msh5*Δ, or that more DSBs are being produced due to relaxation of DSB control. In the *nse4-mn msh5*Δ double mutant, DSBs are produced to wild type levels (6.4%± 0.2 at 3.5 hours), and removed in a more timely fashion than *msh5*Δ, (although slightly slower than in wild type). This would be suggestive of the fact that in *msh5*Δ, fewer DSBs are entering the meiotic recombination pathway, and that the Smc5/6 complex may have a role in preventing early recombination intermediates from entering the pathway. As has previously been observed (COPSEY, et al., 2013; OH, et al., 2007), *msh5*Δ strains produce fewer recombinants than wild type (accumulating recombinants to 9.1%± 0.2 at 13 hours). The *nse4-mn msh5*Δ double mutant exhibit similar timings for recombinants becoming detectable, at 6 hours, and these accumulate to similar overall levels as *msh5*Δ alone, to 8.4%± 0.4 of DNA at 13 hours (Figure 3.6C). This indicates that the Smc5/6 complex is functioning in a different manner to Sgs1, as the depletion of Sgs1 leads to the alleviation of the crossover accumulation defect observed in *msh5*Δ cells, which does not occur in Smc5/6 complex mutants.

There is a lack of clear consensus on nuclear separation kinetics in *msh5*Δ cells, with some studies reporting a modest delay in meiotic progression with fewer cells overall entering meiosis (NISHANT, et al., 2010), whilst others saw a

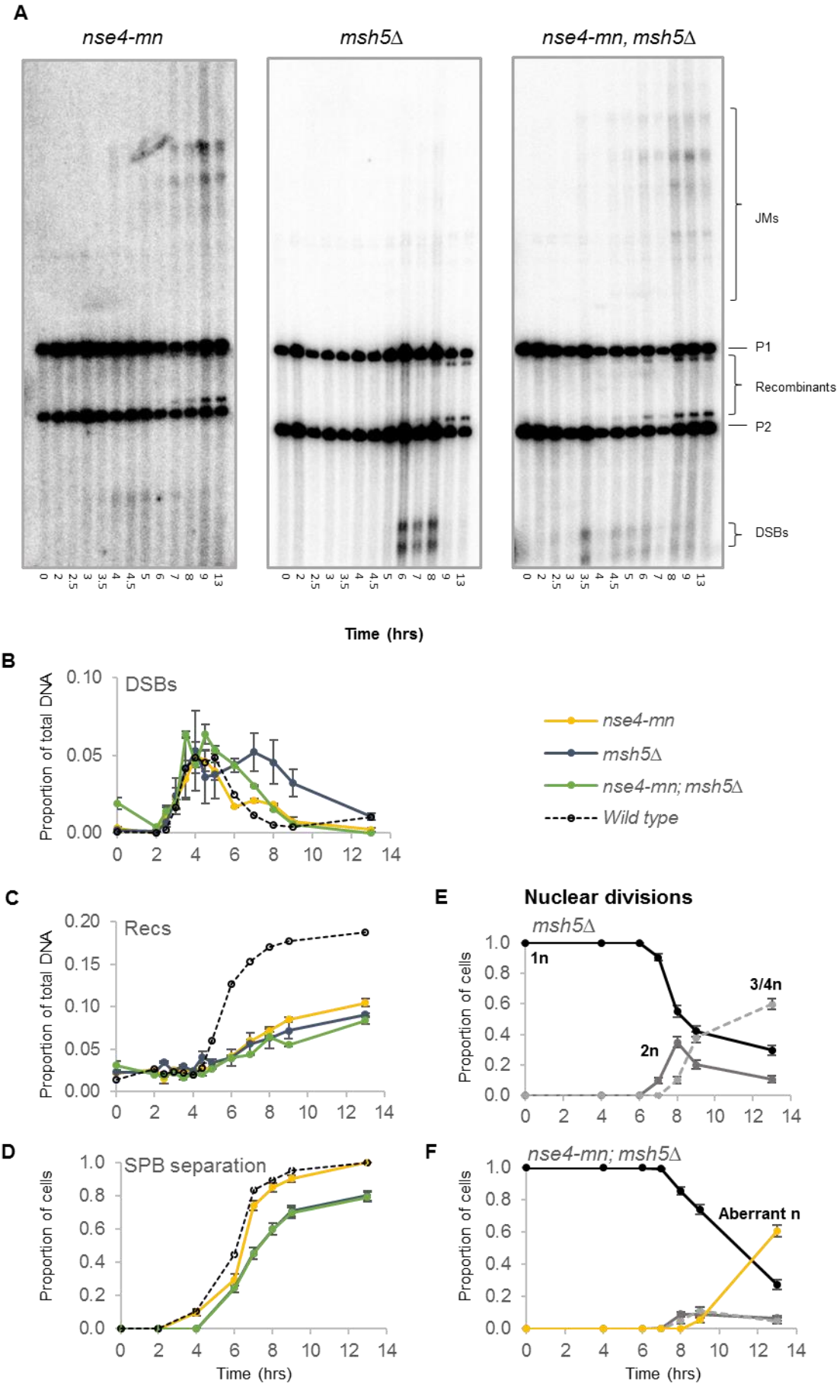
A
nse4-mn
msh5Δ
nse4-mn, msh5Δ
JMs
P1
Recombinants
P2
DSBs
Time (hrs)
B
DSBs
Proportion of total DNA
nse4-mn
msh5Δ
nse4-mn; msh5Δ
Wild type
C
Recs
Proportion of total DNA
D
SPB separation
Proportion of cells
Time (hrs)
E
Nuclear divisions
msh5Δ
Proportion of cells
1n
2n
3/4n
F
nse4-mn; msh5Δ
Proportion of cells
Aberrant n
Time (hrs)

Figure 3.6 *nse4-mn msh5*Δ mutants experience slight delays in meiotic progression, and *nse4-mn* like aberrant nuclei

(A) Representative 1D Southern blots of nse4-mn, msh5Δ and nse4-mn msh5Δ strains.
(B) Double strand break levels over a 13 hour meiotic timecourse, quantified as a proportion of total detectable DNA species in the lane.
(C) Levels of recombinant molecules during a 13 hour meiotic timecourse, quantified as a proportion of total detectable DNA species in the lane.
The average of two independent diploids is given, and error bars represent S.E.M. for graphs B-C
(D) Population kinetics of spindle pole body separation, as determined by the first instance when two Spindle pole bodies can be visualised. n=200 per time point. Error bars represent S.E.P.
(E) *msh5*Δ population kinetics of nuclear divisions
(F) *nse4-mn msh5*Δ population kinetics of nuclear divisions
Population kinetics of nuclear divisions, as determined by the number of distinct DAPI foci that can be visualized. n=200 per time point. Error bars represent S.E.P. for graphs E-F

Strains: JKD202, JKD203, JKD210, JKD211
Experimental ID: E34_ JK2_160218

delay, but no decrease in the total amount (OH, et al., 2007). Our data showed that spindle pole body separation was delayed in *msh5*Δ, whilst in *nse4-mn* there was a very minor delay. In addition, only 80%± 2.9 of *msh5*Δ completed spindle pole separation by 13 hours. I observed that the double mutant demonstrated spindle pole kinetics much more similar to *msh5*Δ than *nse4-mn* alone (Figure 3.6D), with 79%± 2.8 of cells completing spindle pole separation by 13 hours. This suggests that defects in the ZMM pathway are causing meiotic delays that are not relieved by the loss of the Smc5/6 complexes control of early meiotic events. Paradoxically, when DAPI counts were obtained for the strains, I initially observed that the phenotype of the double mutant was more similar to *nse4-mn* than *msh5*Δ, with the double mutant accumulating aberrant cells whereby DAPI staining was observed outside of spore walls (the cut phenotype). However, the number of mononuclear cells, and timing with which they are removed, appears similar between *msh5*Δ (Figure 3.6E) and *nse4-mn msh5*Δ strains (Figure 3.6F). This suggests that to some extent, the ZMM pathway is the dominant factor with regards to cell progression from mononucleate to dinucleate, whilst later meiotic fates, such as the generation of aberrant nuclei, are predominantly dependent on the absence of the Smc5/6 complex.

3.2.3.2. *msh5*Δ mutants accumulate JMs in the absence of the Smc5/6 complex

In order to determine the effect of the Smc5/6 complex on *msh5*Δ mutants, 2D gel electrophoresis was undertaken of *nse4-mn msh5*Δ double mutants to visualise the differences in recombination intermediates between strains. In the

published literature, *msh5*Δ had very similar levels of SEIs to wild type strains, that persist for a similar amount of time (OH, et al., 2007). I found that the peak of *msh5*Δ was slightly lower than in wild type, and that SEIs were significantly delayed with regards to their accumulation, with a peak level of 0.27%± 0.09 at 8 hours (Figure 3.7C). However, I found that in the double mutant, SEIs initially began to be detected at 3.5 hours, which is the same as observed in wild type, whilst the levels to which SEIs accumulate were similar to those seen in *nse4-mn* alone, peaking at 0.78%± 0.03. This suggests that in *msh5*Δ alone, DSBs accumulate for longer as they are not processed to SEIs in a timely fashion, and that the process which prevents SEIs forming requires the presence of the Smc5/6 complex.

A similar phenotype can be seen in relation to other JM species, with both IH-dHJs and IS-dHJs (Figure 3.7D, E) accumulating late, and to low levels, in the absence of *msh5*Δ (IH-dHJs peak at 0.27%± 0.08, and IS-dHJ peak at 0.10%± 0.03 at 8 hours), whilst the double mutant accumulates JMs to *nse4-mn* like levels (IH-dHJs peak at 2.3%± 0.01, and IS-dHJ peak at 1.3%± 0.01 at 13 hours). Furthermore, aberrant mcJMs do not accumulate to detectable levels in *msh5*Δ mutants, but do accumulate in *nse4-mn msh5*Δ (0.72%± 0.05) although with delayed timing compared to *nse4-mn* alone, only initially becoming detectable at 4.5 hours. (Figure 3.6G)

The most unexpected result observed was the alterations is IH:IS bias in the various mutant strains. In *msh5*Δ, the IH:IS bias was slightly lower than in the wild type strain (Figure 3.6F). As previously mentioned, *nse4-mn* exhibited

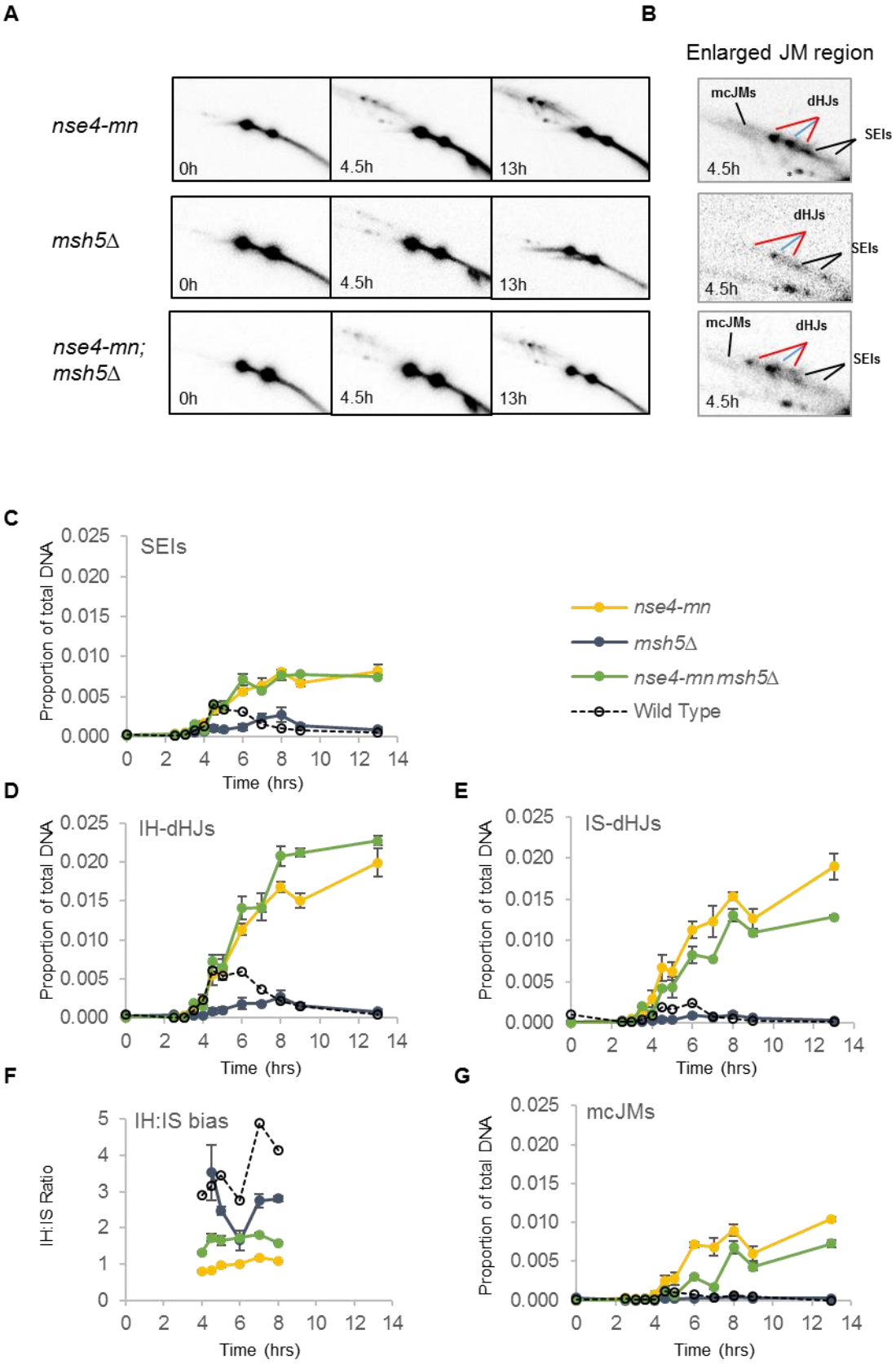
A
B
Enlarged JM region
nse4-mn
msh5Δ
nse4-mn; msh5Δ
0h
4.5h
13h
mcJMs
dHJs
SEIs
C
SEIs
Proportion of total DNA
Time (hrs)
nse4-mn
msh5Δ
nse4-mn msh5Δ
Wild Type
D
IH-dHJs
E
IS-dHJs
F
IH:IS bias
IH:IS Ratio
G
mcJMs

Figure 3.7 In the absence of *nse4*, joint molecules accumulate in *msh5*Δ mutants

(A) Representative images of key time points (T=0,4.5,13) in *nse4-mn, msh5*Δ and *nse4-mn msh5*Δ strains.
(B) Enlarged images of the branched molecule region at 4.5 hrs in *nse4-mn, msh5*Δ and *nse4-mn msh5*Δ strains, with different observed species indicated. Red line indicates IS-dHJs, blue line indicates IH-dHJs. Gene conversions are indicated by *
(C) Single end invasions (SEIs), quantified as a proportion of the total DNA for this panel.
(D) Interhomolog double Holliday Junctions (IH-dHJs), quantified as a proportion of the total DNA for this panel.
(E) Total Intersister double Holliday Junctions (IS-dHJs), quantified as a proportion of the total DNA for this panel.
(F) IH:IS bias. The ratio of IH-dHJs to both IS-dHJs bands between 4-8 hours.
(G) Multi-chromatid joint molecules (MCJMs), quantified as a proportion of the total DNA for this panel.
(C-G) The average of two independent diploids is given and error bars represent S.E.M. Wild type levels are illustrated with a dashed line.

Strains: JKD202, JKD203, JKD210, JKD211
Experiment ID: E34_ JK2_160218

lower levels of IH:IS bias as was previously reported (1:1). However, the double mutant displayed an intermediate IH:IS bias (1.6). This is curious, as we might assume that the phenotype of interhomolog bias loss in the absence of the Smc5/6 complex would not be alleviated by abrogating the ZMM pathway. A final point of note is that the dHJs that accumulate in the double mutant appear to have the same “smeared teardrop” shape via 2D Southern analysis as observed in *nse4-mn*, suggesting that the dHJs that accumulate in the double mutant have similar properties to those that accumulate in the absence of Nse4 alone.

In order to more precisely determine whether the loss of IH:IS bias observed in the absence of Nse4 is truly alleviated in *msh5*Δ mutants, timecourses were conducted in the absence of the Ndt80 transcription factor, to allow us to determine whether differences are as a result of altered turnover of recombination intermediates (which would be alleviated in the absence of Ndt80) or is a result of a true change in recombination bias as determined early in meiosis.

In the earliest JM recombination intermediates, SEIs, we observe that there is a significant reduction in the accumulation of SEIs in *ndt80*Δ *msh5*Δ double mutants, compared with *ndt80*Δ alone (0.39% ± 0.03 of total DNA for the double mutant at 13 hours) (Figure 3.8C). However, in the triple mutant *ndt80*Δ *msh5*Δ *nse4-mn* the level of SEI accumulation is similar to the *ndt80*Δ alone (0.98% ± 0.02 of total DNA at 13 hours). In the double mutant, we also observe very low levels of accumulation of dHJs, for both IH-dHJs (0.51% ± 0.02 at 13 hours)

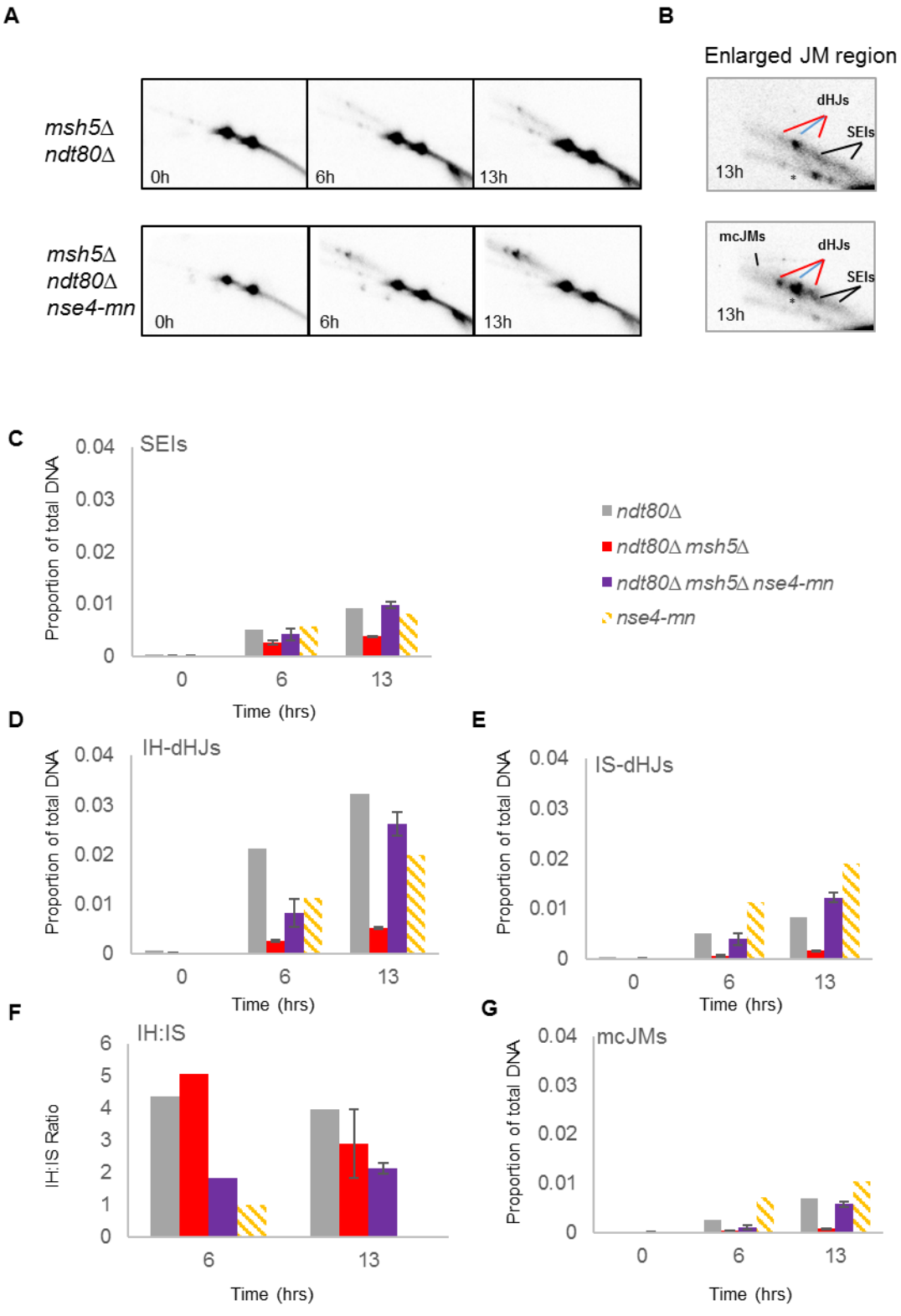
A
B
Enlarged JM region
msh5Δ
ndt80Δ
0h
6h
13h
dHJs
SEIs
13h
msh5Δ
ndt80Δ
nse4-mn
mcJMs
dHJs
SEIs
13h
C
SEIs
Proportion of total DNA
0.04
0.03
0.02
0.01
0
0
6
13
Time (hrs)
ndt80Δ
ndt80Δ msh5Δ
ndt80Δ msh5Δ nse4-mn
nse4-mn
D
IH-dHJs
Proportion of total DNA
Time (hrs)
E
IS-dHJs
Proportion of total DNA
Time (hrs)
F
IH:IS
IH:IS Ratio
6
5
4
3
2
1
0
Time (hrs)
G
mcJMs
Proportion of total DNA
Time (hrs)

Figure 3.8 In the pachytene arrested cells, absence of the Smc5/6 complex leads to *msh5*Δ mutants accumulating joint molecules, and a loss of interhomolog bias

(A) Representative images of key time points (T=0,6,13) in *msh5*Δ *ndt80*Δ and *msh5*Δ *ndt80*Δ *nse4-mn* strains.
(B) Enlarged images of the branched molecule region at 13 hrs in *msh5*Δ *ndt80*Δ *and msh5*Δ *ndt80*Δ *nse4-mn* strains, with different observed species indicated. Red line indicates IS-dHJs, blue line indicates IH-dHJs. Gene conversions are indicated by *
(C) Single end invasions (SEIs), quantified as a proportion of the total DNA for this panel. *nse4-mn* is modelled in to this and all subsequent graphs.
(D) Interhomolog double Holliday Junctions (IH-dHJs), quantified as a proportion of the total DNA for this panel.
(E) Total Intersister double Holliday Junctions (IS-dHJs), quantified as a proportion of the total DNA for this panel.
(F) IH:IS bias. The ratio of IH-dHJs to both IS-dHJs bands **(G)** Multi-chromatid joint molecules (mcJMs), quantified as a proportion of the total DNA for this panel.
(G) Multi-chromatid joint molecules (mcJMs), quantified as a proportion of the total DNA for this panel.
The average of two independent diploids is given and error bars represent S.E.M. in graphs C-G

Strains: JKD224, JKD225, JKD226, JKD227
Experimental ID: E36_JK2_160428

(Figure 3.8D) and IS-dHJs (0.17% ± 0.01 at 13 hours) (Figure 3.8E), more than an order of magnitude less than is observed in the *ndt80*Δ alone. In the triple mutant, we see a marked elevation in IH-dHJs (2.6% ± 0.2 at 13 hours) (Figure 3.8D) and IS-dHJs (1.2% ± 0.1 at 13 hours) compared to the double mutant (Figure 3.8E). This suggests that in the Smc5/6 complex depleted environment, the phenotype observed in *ndt80*Δ *msh5*Δ mutants whereby we observe lower levels of accumulated joint molecules is alleviated, which in turn suggests that the Smc5/6 complex might have a role in suppressing the accumulation of JMs in this mutant environment.

At the latest observed time point, we observe that the *ndt80*Δ *msh5*Δ double mutant has a IH:IS bias of 2.9 ± 0.1 (Figure 3.8F). This is slightly lower than the IH:IS bias observed at peak accumulations in *msh5*Δ alone. In the triple mutant *ndt80*Δ *msh5*Δ *nse4-mn,* the observed IH:IS bias at 13 hours is 2.1 ± 0.1 (Figure 3.8F). This is higher than is observed in the *msh5*Δ *nse4-mn* double mutant. Taken together, these results suggest that in this mutant context in the absence of *ndt80*Δ, the IH:IS bias is shifted towards the interhomolog JMs, and that resolution of JMs is indeed a major factor generating the differences in observed bias. However, there is still a difference (though reduced as an absolute proportion), which leaves open the possibility that there might be an early interplay between the Smc5/6 complex and the ZMM pathway which influences the establishment of IH:IS bias, although further experiments would obviously be required to be sure of this.

Finally, we observed that in the *ndt80*Δ *msh5*Δ double mutant, mcJMs did not accumulate significantly; however, in the triple mutant, there was a detectable population of mcJMs (0.56% ± 0.02 at 13 hours). It should also be noted that when blots were over-exposed (Figure 3.8B), in the double mutant we observe that IH-dHJs accumulate to a punctuate band, similar to what is observed in wild type strains; however, in the triple mutant, we see an *nse4-mn* like distorted band, suggesting that in the absence of ZMM proteins, Smc5/6 complex mutants still generate JMs that seem to run aberrantly by two-dimensional gel electrophoresis.

3.3. Discussion

In *S. cerevisiae*, meiotic recombination can occur via two different meiotic pathways – the crossover promoting ZMM repair pathway, and the Mus81-Mms4 repair pathway, which generates an equal proportion of crossovers and non-crossovers. The Smc5/6 complex has a profound effect on meiotic recombination outcomes, causing an accumulation of recombination intermediates, and reduction in the number of crossovers (COPSEY, et al., 2013; XAVER, et al., 2013). In addition, the Smc5/6 complex shows a reduction in interhomolog repair bias.

The Smc5/6 complex regulates Mus81-Mms4 in recruiting it to meiotic chromosomes, and modulating its JM resolution activity (COPSEY, et al., 2013). In the absence of the *MutL* resolvase a synergistic reduction in crossovers is observed in Smc5/6 complex mutants, suggesting that they function in distinct pathways (COPSEY, et al., 2013). However, *MutL* resolvase activity occurs at a late stage of recombination, whereas the Smc5/6 complex may have much earlier functions – in order to better determine its effect in the absence of the ZMM repair pathway, it would be important to look in mutant strains which do not allow DSBs to enter the ZMM pathway, in this case *msh5*Δ.

Here, I have undertaken work to reproduce data, to ensure that my data is representative, and to add to determine the reproducibility of data which has been previously obtained. I reproduced wild type meiotic cultures which generate meiotic recombination intermediates at the *HIS4LEU2* hotspot (SCHWACHA & KLECKNER, 1997). DSBs were generated and accumulated at

the onset of meiosis, and then levels reduced as they were processed to later intermediates; subsequently COs formed and were detected by 1D Southern analysis (HUNTER & KLECKNER, 2001). SEIs and dHJs accumulate and then disappear across the course of the timecourse, as quantified by 2D Southern analysis. There is a clear bias towards IH-dHJs, forming in a ratio of 3.6:1 over IS-dHJs (Figure 3.2F). A similar pattern of DSBs is seen when pachytene exit is blocked by the deletion of Ndt80, but SEIs, dHJs and mcJMs accumulate to higher levels, and do not get removed efficiently. COs, the final product of the recombination pathway, form at far lower levels as expected. As previously reported (COPSEY, et al., 2013; LILIENTHAL, et al., 2013; XAVER, et al., 2013), Smc5/6 complex mutants generate DSBs with normal timing, to normal levels, although the DSBs do appear to persist for longer. However, Smc5/6 complex mutants accumulate all quantified JMs to high levels, and these JMs persist throughout the time course (particularly in the more severe instance of *nse4-mn*). Another feature that is consistent with the previous literature is the loss of IH:IS bias in Smc5/6 complex mutants.

In the absence of the ZMM pathway component, meiosis specific Msh5, DSBs accumulate for longer than in wild type. SEIs appear later and to slightly lower levels than wild type, whilst dHJs and mcJMs accumulate only to very low levels as previously reported (OH, et al., 2007). In the absence of both Nse4 and Msh5 however, DSBs no longer accumulate to the same extent. Furthermore, JMs accumulate to *nse4-mn* like levels. This suggests that at an early point in meiotic recombination, DSBs are designated to enter the ZMM pathway, and if this pathway is abrogated, it leads to a persistence of DSBs, and fewer later

intermediates. This designation must depend upon the Smc5/6 complex, as when it is not present, DSBs are now able to enter other meiotic recombination pathways than the ZMM pathway, and progress to a later stage of meiotic recombination, where the second Smc5/6 complex mutant phenotype, an inability to efficiently resolve dHJs into linear products, leads to an accumulation of JMs, including aberrant mcJMs, and dHJ bands with the characteristic *nse4-mn* teardrop morphology.

A crucial finding of this study is the fact that crossover levels are not reduced in Smc5/6 complex mutants which lack *msh5* (Figure 3.6B). This is in contrast to mutants which lack the resolvase *mlh3*, which do observe a synergistic decrease (COPSEY, et al., 2013). This suggests that the Smc5/6 complex is modulating entry into both Mus81-Mms4 and ZMM repair pathways. The disparity between *mlh3* and *msh5* phenotypes is likely due to whether DSBs are permitted to enter the ZMM repair pathway – in the absence of *msh5*, DSBs will not enter the pathway, and might be resolved by other means, whilst in the absence of *mlh3*, DSBs may already be committed to the ZMM repair pathway, and so unable to be resolved by other recombination pathways in the absence of *mlh3*, indicating a fundamental difference in the stage at which commitment occurs in these two mutants. This suggests a more fundamental role for the Smc5/6 complex in modulating the repair of the majority of recombination intermediates, as opposed to a single pathway.

In addition, we initially observed that whilst there is a loss of IH:IS bias in the absence of Nse4*,* as previously reported, the bias is somewhat restored (1.0 vs

1.6) in the absence of *msh5*Δ. This might be indicative of meiotic recombination being pushed into a pathway that resolves IS-dHJs with better efficacy than IH-dHJs (thus leading to an apparent IH bias). This is borne out to some extent by the data that is obtained in the absence of the Ndt80 transcription factor, where IH:IS bias was elevated for both mutants compared to when Ndt80 was present, suggesting that some of the observed reduction is as result of altered rates of turnover of IH-dHJs relative to IS-dHJs. However, a smaller difference was still observed, which could indicate a true bias establishment interaction between the ZMM and Smc5/6 complex. However, further study is needed to clarify this fully.

These data clearly indicate an early role for the Smc5/6 complex in determining meiotic recombination pathway choice. One might imagine two possible mechanisms by which this might happen. Firstly, the Smc5/6 complex might act as a molecular chaperone, to associate with early recombination intermediates, and recruit additional factors to cause the DSB to enter the ZMM pathway. Alternatively, the Smc5/6 complex might have a protective role, preventing other molecular factors from associating with early intermediates. Given that it has been previously shown that Sgs1 and Mus81 collaborate to resolve JMs (JESSOP & LICHTEN, 2008), one might hypothesise that the Smc5/6 complex might act to protect early intermediates from this pathway, channelling them instead into the predominant, interfering crossover pathway.

Chapter 4

The Smc5/6 complex enables the accumulation of DSBs in recA homolog mutants

4.1. Introduction

4.1.1. RecA homologues in meiotic DSB repair

In *S. cerevisiae,* meiotic recombination is initiated by the formation of Spo11-dependent DSBs (KEENEY, et al., 1997). These DSBs are then processed by the action of the Exo1 exonuclease (TSUBOUCHI & OGAWA, 2000) to generate stretches of single stranded DNA (ssDNA) that are bound by two RecA orthologues, Rad51 and the meiosis-specific Dmc1 to form nucleoprotein filaments (BISHOP, 1994; SHINOHARA & SHINOHARA, 2004). The assembly of the nucleoprotein filaments is essential for the homology search by the ssDNA, and for the formation of semi-stable SEIs, that will eventually go on to form dHJs and crossovers

The Smc5/6 complex has been shown to be associated with early recombination events in a number of studies. The Smc5/6 complex co-localises with Rad51 foci on meiotic spreads (XAVER, et al., 2013) Although co-localization with Dmc1 was not assessed, Rad51 and Dmc1 co-localize at the

sites of DSBs (BISHOP, 1994), suggesting that the Smc5/6 complex is recruited to the sites of DSBs. Consistent with a role in DSB repair, Smc5/6 localizes with meiotic DSB sites by ChIP analysis in *S. cerevisiae* (COPSEY, et al., 2013). In *C. elegans*, it has been demonstrated that Smc5/6 complex component SMC-6 is enriched at meiotic chromosomes at early pachytene, when meiotic DSBs are generated (BICKEL, et al., 2010) although in yeast, the localization of Smc6 to meiotic DSBs appears to be independent of Spo11. In human spermatocytes, SMC6 foci co-localise with DMC1 foci on XY bodies (VERVER, et al., 2014); this has been suggested to indicate a role of the Smc5/6 complex in promoting intersister repair in the unsynapsed XY body. However, this particular model is complicated by the different results observed in mouse spermatogenesis, where Smc5/6 complex components appear to localise more generally to heterochromatin (GOMEZ, et al., 2013), suggesting that this particular mode of repair might be specific to human spermatogenesis. Together, these data indicate a crucial role for the Smc5/6 complex during the earliest stages of meiotic repair, although the exact mechanism by which the complex acts at this early stage has not been fully explored.

Rad51 and Dmc1 have redundant roles in *S. cerevisiae* meiosis (TSUBOUCHI & ROEDER, 2006); however, more recent studies have demonstrated that Dmc1 is the primary actor in the formation of joint molecule (JM) intermediates, whilst Rad51 functions primarily to enable the formation of nucleoprotein filaments (CLOUD, et al., 2012). This functional divergence of the two RecA orthologues may allow for the specialist formation of JMs in meiotic prophase,

with Rad51 potentially acting as a fail-safe should Dmc1 function be abrogated (CLOUD, et al., 2012).

The molecular structure of RecA homologues is informative for the dual functions of nucleoprotein filament formation, and D-loop formation for the two proteins. In *E. coli*, RecA possesses two DNA binding sites: a high affinity site that enables the formation of a protein-DNA filament, and a low affinity DNA binding site, that enables homology search and D-loop formation for invasion events (MULLER, et al., 1990). When orthologous sites are mutated in *S. cerevisiae*, a separation of molecular functions is observed, with only a mild reduction in spore viability when the low affinity site of Rad51 is mutated (*rad51-IIA*) compared to *rad51*Δ mutants, which do not produce viable spore. This is opposed to a total meiotic arrest for *dmc1-IIA* mutants, similar to what is observed in *dmc1*Δ mutants (CLOUD, et al., 2012).

In Chapter 3 (The Smc5/6 complex affects early meiotic events in the absence of functional ZMM pathway repair), we observe that depletion of the Smc5/6 complex rescues the formation of joint molecules in a *zmm* mutant. This suggests that in addition to its well characterised role in promoting JM resolution, the Smc5/6 complex also functions in the earliest stages of recombination, allowing the accumulation of DSBs in strains where meiotic repair is abrogated at early stages of meiotic recombination.

Here, I analyse the relationship between RecA orthologues and the Smc5/6 complex. First, I establish a baseline for the level of molecular intermediates observed in mutants lacking the orthologues rad51 and dmc1. I then assess the recombination phenotypes in the RecA mutants, when the Smc5/6 complex is depleted. This is particularly important due to the large variation observed within the published literature (SHINOHARA, et al., 1997; TSUBOUCHI & ROEDER, 2006). We reasoned that if the Smc5/6 complex has a role in controlling the entry of DSBs into the meiotic recombination machinery, then the absence of the functioning Smc5/6 complex should allow an increased proportion of DSBs to be turned over into later recombination intermediates. This would suggest an early meiotic role for the Smc5/6 complex in regulating the fate of DSBs at early stages of stages of the DSB repair reaction

4.2. Results

4.2.1. In the absence of Rad51, but not Dmc1, the Smc5/6 complex has a pronounced effect on the accumulation of JMs

In order to assess the earliest stage at which the Smc5/6 complex would have an effect on meiotic recombination, Smc5/6 complex mutants were combined with recA homologue mutants to determine whether there was any accumulation of recombination intermediates when the progression of the earliest recombination events (single-end invasions) into the later stages of meiotic repair was abrogated.

4.2.1.1. RecA homologues exhibit significantly different meiotic behaviour, suggesting distinct roles in meiotic DSB repair

In the absence of *recA* homologues Rad51 and Dmc1, meiotic progression is severely abrogated (BISHOP, et al., 1992). DSBs in strains lacking functional Dmc1 experiences hyper-resection of meiotic DSBs (BISHOP, 1994), whilst mutants lacking Rad51 show highly degraded DSBs with ssDNA regions (SHINOHARA, et al., 1992). This occurs as a result of the DNA strand is unprotected from the action of the exonuclease Exo1 (TSUBOUCHI & OGAWA, 2000). Fewer DSBs progress through the meiotic repair machinery, leading to a reduction in COs.

In *rad51*Δ, we observe hyper-resection of DSBs; DSBs at later time points become more smeared, and migrate further than DSBs at earlier time points suggesting a lower molecular weight (Figure 4.1A). These species are indicated

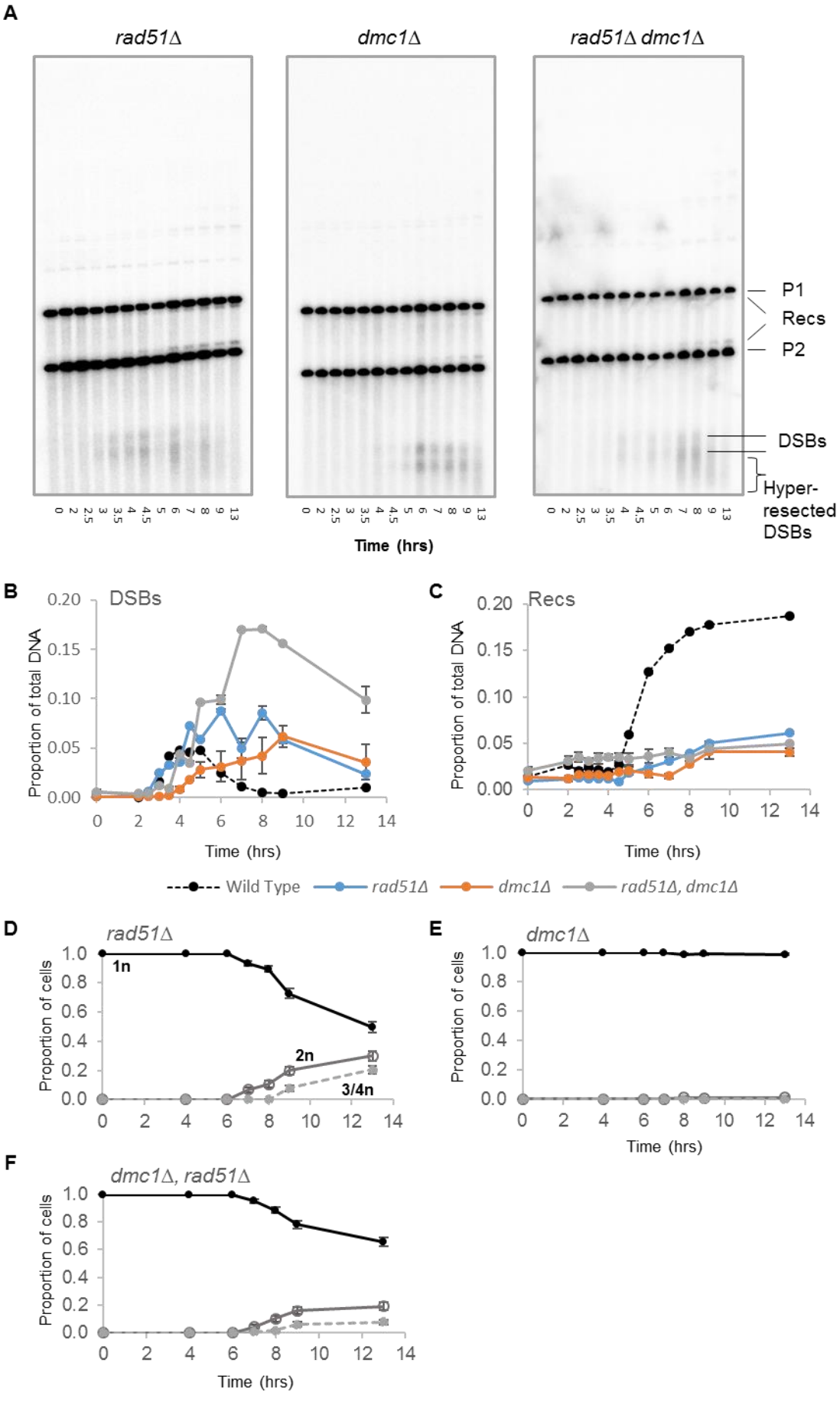
A
rad51Δ
dmc1Δ
rad51Δ dmc1Δ
P1
Recs
P2
DSBs
Hyper-resected DSBs
Time (hrs)
B
DSBs
Proportion of total DNA
Time (hrs)
C
Recs
Proportion of total DNA
Time (hrs)
Wild Type
rad51Δ
dmc1Δ
rad51Δ, dmc1Δ
D
rad51Δ
Proportion of cells
1n
2n
3/4n
E
dmc1Δ
Proportion of cells
Time (hrs)
F
dmc1Δ, rad51Δ
Proportion of cells
Time (hrs)

Figure 4.1 *recA* homologue mutants experience hyper-resected DSBs and reduced levels of crossovers

(A) Representative Southern blots of molecular recombination species in *rad51*Δ, *dmc1*Δ, and *rad51*Δ *dmc1*Δ strains. Linear molecular species, and hyper-resected DSBs are indicated.
(B) DSB levels over a 13 hour meiotic timecourse were quantified as the proportion of total detectable DNA species in the lane. Note that in *recA* orthologue mutants, DSBs are hyper-resected. This makes the DSBs appear less defined and to appear, at lower molecular weights at later time points, as resection progresses. Wild type levels have been modelled in (dashed line) for comparison.
(C) Levels of recombinant molecules (Recs) during a 13 hour meiotic timecourse, quantified as a proportion of total detectable DNA species in the lane.
The average of two independent diploids is given, and error bars represent S.E.M. for (B and C).
(D-F) Population kinetics of nuclear divisions in the mutants, as determined by the number of distinct DAPI foci that could be visualized. n=200 per time point. Error bars represent standard error of proportion (S.E.P.=√[p*(1-p)/n]) for graphs (D-F)

Strains: Y5693, Y5694, Y5597, JKD184, Y5695, Y5696
Experimental ID: E35_JK2_160218; E24_JK2_150603

in the region labelled “hyper-resected DSBs”. This smearing of the band is characteristic of hyper-resection of the unprotected DSB ends. Hyper-resection of DSBs is not observed in wild type, where DSBs persist as distinct, non-smeared bands until they are turned over by the meiotic repair machinery. DSBs appear at 3 hours and are not detectable at 6 hours in *rad51*Δ, with a broad peak (8.8%± 0.1 at t=6) (Figure 4.1B). A high proportion of DSBs persisting until later time points. Recombinants accumulate to lower levels than is observed in wild type, reaching 6.2% ±0.02 of total DNA at the latest time points (Figure 4.1C). This is consistent with previously published data (SHINOHARA, et al., 1997) (TSUBOUCHI & ROEDER, 2006). Half of *rad51*Δ diploid cells showed progression out of meiosis I; 49.7% of cells never displaying separated DAPI foci. In addition, 29.8% showed 2 distinct DAPI foci, and 20.4% showing 3 or four DAPI foci, suggesting that meiosis II had been completed (Figure 4.1D). This is a slower rate of progression than is observed in a wild type situation, and fewer cells in total complete meiosis; however, it is not as severe as the meiotic progression block observed in *dmc1*Δ strains.

For *dmc1*Δ strains, which lack the major enzymatic factor promoting the homology search stage of the single-end invasion of resected DSBs (CLOUD, et al., 2012), we observe some smearing of DSB bands at the latest time points in *dmc1*Δ mutant strains (Figure 4.1A), which would indicate hyper-resected DSBs. This qualitatively appears to be far less pronounced than is observed in *rad51*Δ, however, this may be as a result of a more rapid degradation of products, making smearing more difficult to detect in this setting. Two-dimensional analysis is a more sensitive tool for addressing this, and we do

observe extensive hyper-resection by this method (Figure 4.5G). We initially detect an accumulation of DSBs later than is observed in *rad51*Δ, only becoming detectable at 4 hours. These DSBs accumulate to a broad peak (6.1% ±1.1 at t=9), with many DSBs persisting until the latest time points (Figure 4.1B). Recombinants accumulate to lower levels compared with *rad51*Δ (4.1% ±0.4% at the latest time points) (Figure 4.1C).

In the *rad51*Δ *dmc1*Δ double mutant strain, DSBs are hyper-resected (Figure4.1A). DSBs appear at 3.5 hours, similar to the *dmc1*Δ and *rad51*Δ single mutant), and accumulate to far higher levels in the *rad51*Δ *dmc1*Δ double mutant compared to either single mutant (17.1% ±0.7 at t=8), before beginning to fall by the later time points (Figure 4.1B). Thus, deletion of Rad51 and Dmc1 has a more severe phenotype than either mutation alone, indicating a level of redundancy between the functions of these closely related proteins. This is consistent with the findings of (SHINOHARA, et al., 1997), but not with (TSUBOUCHI & ROEDER, 2006) where levels of DSBs in the double mutant appears to be similar to the levels detected in *rad51*Δ single mutant. The differences between the data obtained in SHINOHARA, et al., 1997 and our data compared to those of TSUBOUCHI & ROEDER, 2006 are unclear.

The levels of recombinants in the *rad51*Δ *dmc1*Δ double mutant appear to be intermediate between *rad51*Δ and *dmc1*Δ (4.9% ±0.02 at t=13) (Figure 4.1C). However, in all instances of recA mutants, the level of recombinants is substantially reduced when compared to wild type, in which recombinants accumulate to ~20% of total DNA at the latest time points The population

kinetics of nuclear division observed by DAPI counts in the double mutant appears to be intermediate between *rad51*Δ and *dmc1*Δ, with 66% of cells showing no nuclear divisions after 13 hours, 19% having undergone one division, and 8% completing meiosis II like divisions and having 3-4 DAPI foci (Figure 4.1F). This intermediate phenotype is in accordance with results in the published literature (SHINOHARA, et al., 1997).

The data which I have obtained here are consistent with some of the literature (BISHOP, 1994; BISHOP, et al., 1992), which observed hyper-resection in *dmc1*Δ mutants (although to more pronounced levels than I have observed), an increased accumulation of DSBs, and a reduction in the levels of COs. However, a wide variation in the accumulation of DSBs and recombinants have been reported, some of which differ markedly from my data (TSUBOUCHI & ROEDER, 2006) (LAO, et al., 2013), with some reporting far higher levels of DSBs than I have observed. Whilst it seems likely that this is a result of specific differences in experimental procedures between laboratories, I cannot eliminate the possibility that there is less synchronicity of cell cultures in my data (and the published data which it mirrors) than is observed in the more recent papers; however, a budding index measurement was always taken before a timecourse was initiated to control for this possibility, and hence minimises the likelihood that this is the explanation.

It should also be noted that the published literature detects a much higher degree of hyper-resection in *dmc1*Δ mutant strains compared to *rad51*Δ strains, whilst here we observed little hyper-resection in *dmc1*Δ strains. However, as

stated above, this could potentially be due to a lack of detection of rapidly turned over intermediates in this study in *dmc1*Δ strains, as opposed to a specifically different phenotype. In the absence of Dmc1, we also observe a failure of meiotic progression, with very few cells separating their nuclear DNA (99% of cells had one DAPI foci at t=13), and no cells exiting meiosis II by the last time point (Figure 4.1E). This is consistent with what is observed in the literature (BISHOP, 1994).

To summarise, we observe hyper-resection in both single and double mutants of RecA orthologues, Dmc1 and Rad51. DSBs accumulate in both single mutants, whilst the double mutant accumulates DSBs to higher levels. A severe reduction in the proportion of CO events is observed in both double and single mutants compared to wild type (Figure 4.1). Finally, we observe that in the absence of *dmc1,* meiotic progression is entirely blocked, whilst in *rad51* single mutant's progression is delayed compared to wild type. In the double mutant, we observe a more sever delay than is observed in *rad51* single mutants, but not a complete meiotic block. This implies that Rad51 is required to trigger the meiotic block observed in *dmc1* single mutants (SHINOHARA, et al., 1997).

4.2.1.2. The Smc5/6 complex is required for the accumulation of double strand breaks in *dmc1*Δ strains

To understand the role of Smc5/6 during early recombination steps, we used meiosis-specific depletion of Smc5 and Nse4 in combination with *dmc1* or *rad51*. Nse4 is depleted more extensively than Smc5 (COPSEY, et al., 2013) whereas PCLB2-SMC5 gives hypomorphic phenotypes. This appears to be as

result in differences in the efficacy of depletion of Smc5 using the PCLB2 system, as when the Smc5 protein is degraded using the Auxin induced degradation system (AID), a severe phenotype is observed which mimics PCLB2-NSE4 (COPSEY, et al., 2013).

In both the Smc5 and Nse4-depleted cells, steady-state levels of DSBs were decreased, which was especially notable in the more severe phenotype depletion of Nse4 (Figure 4.2B). A peak accumulation of 4.2% ±1.0 at t=6, followed by a decrease in the steady state levels of DSBs by t=13 (Figure 4.2B) was observed in *dmc1*Δ *smc5-mn* strains, whilst in *dmc1*Δ *nse4-mn* a peak accumulation of 1.8% ±0.2 at t=8 was observed, before levels became reduced at later time points. Depletion of either Smc5 or Nse4 did not appear to qualitatively affect hyper-resection of DSBs in the absence of Dmc1 (Figure 4.2A), although this is explored in greater detail utilising two-dimensional analysis (Figure 4.5G).

Recombinant formation, however, was not improved in the *dmc1*Δ *smc5-mn* and *dmc1*Δ *nse4-mn* mutants compared to *dmc1*Δ alone. This suggests that the altered DSB processing in the Smc5/6-depleted cells does not improve recombination outcomes in the absence of Dmc1. Recombinants accumulated to very similar levels in the mutants (*dmc1*Δ *smc5-mn* accumulate to 4.4% ±0.4, *dmc1*Δ *nse4-mn* to 4.9% ±0.2) (Figure 4.2C). This suggests that the Smc5/6 complex is required for the accumulation of DSBs in *dmc1* mutants, and indicates and early function in DSB assurance for the Smc5/6 complex.

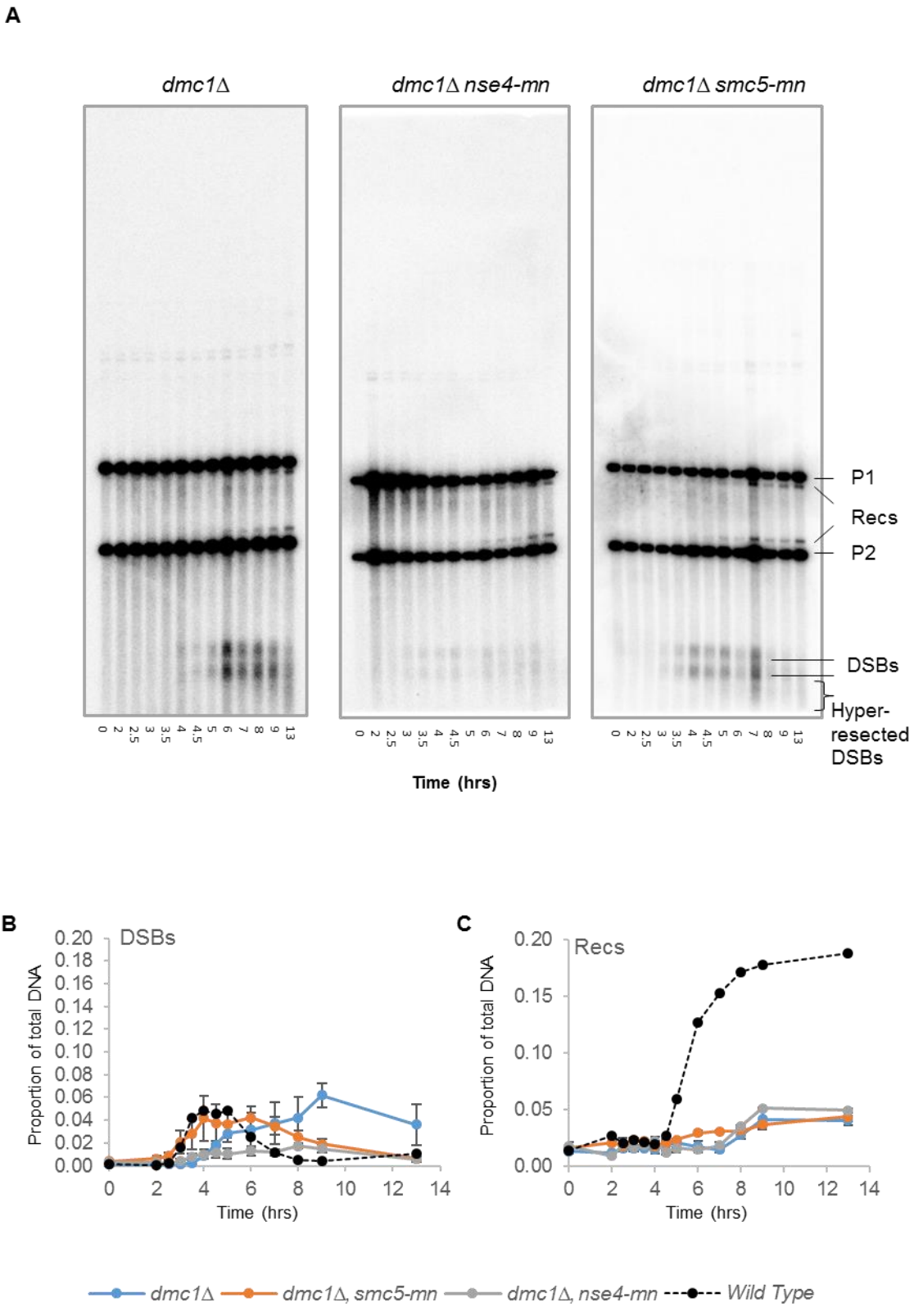
A
dmc1Δ
dmc1Δ nse4-mn
dmc1Δ smc5-mn
P1
Recs
P2
DSBs
Hyper-resected DSBs
Time (hrs)
B
DSBs
Proportion of total DNA
Time (hrs)
C
Recs
Proportion of total DNA
Time (hrs)
dmc1Δ
dmc1Δ, smc5-mn
dmc1Δ, nse4-mn
Wild Type

Figure 4.2 The accumulation of DSBs in *dmc1*Δ is reduced in the absence of the Smc5/6 complex, whilst level of crossovers is unaffected

(A) Representative 1D Southern blots of *dmc1*Δ , *dmc1*Δ *nse4-mn*, and *dmc1*Δ *smc5-mn* strains.
(B) Double strand break levels over a 13 hour meiotic timecourse, quantified as a proportion of total detectable DNA species in the lane. It should be noted that in recA homologue mutants, DSBs are hyper-resected, leading to DSBs appearing at lower molecular weights at later time points.
(C) Levels of recombinant molecules during a 13 hour meiotic timecourse, quantified as a proportion of total detectable DNA species in the lane.
The average of two independent diploids is given, and error bars represent S.E.M. for graphs B-C

Strains: JKD184, Y5597, Y5599, Y5601, JKD188, JKD192
Experimental ID: E30_JK2_151118

4.2.1.3. The Smc5/6 complex modulates DSB accumulation and crossover formation in *rad51* mutants

I next investigated the effect that the absence of the Smc5/6 complex had on the steady state levels of DSBs in the absence of the recA homologue Rad51, which is present in both meiotic and mitotic repair and the effect on the accumulation of recombinant DNA strands. The most striking initial observation is the increase in high molecular weight species observed at later time points in these mutants (Figure 4.3A). These will be investigated using two-dimensional analysis later in this study (Figure 4.6). However, this does suggest there are significant differences in later repair intermediates in *rad51*Δ mutants that lack the Smc5/6 complex. I observed lower peak accumulation of DSBs in both double mutants (*rad51*Δ *smc5-mn* peak at to 4.7% ±0.7 at t=7, *rad51*Δ *nse4-mn* to 5.6% ±0.1 at t=9) (Figure 4.3B). In addition, DSBs persisted far later in *rad51*Δ *nse4-mn* mutants, with 4.3% of the total DNA in the lane still being DSBs at the latest time point observed. This would seem to suggest that fewer DSBs are accumulating in the absence of the Smc5/6 complex in *rad51*Δ strains. Alternatively, it might suggest a defect in synapsis leading to the formation of late DSBs.

In the *rad51*Δ *nse4-mn* strain, we see a decrease in the proportion of recombinants compared to *rad51*Δ single mutant (4.7% ±0.3), whilst in *rad51*Δ *smc5-mn* strains, we see *rad51*Δ like levels of recombinants (6.6% ±0.3). These data indicate that in the absence of the Smc5/6 complex, the production of recombinants is abrogated in *rad51*Δ strains. This in turn suggests that in the absence of Rad51, recombinants are being generated via the canonical meiotic

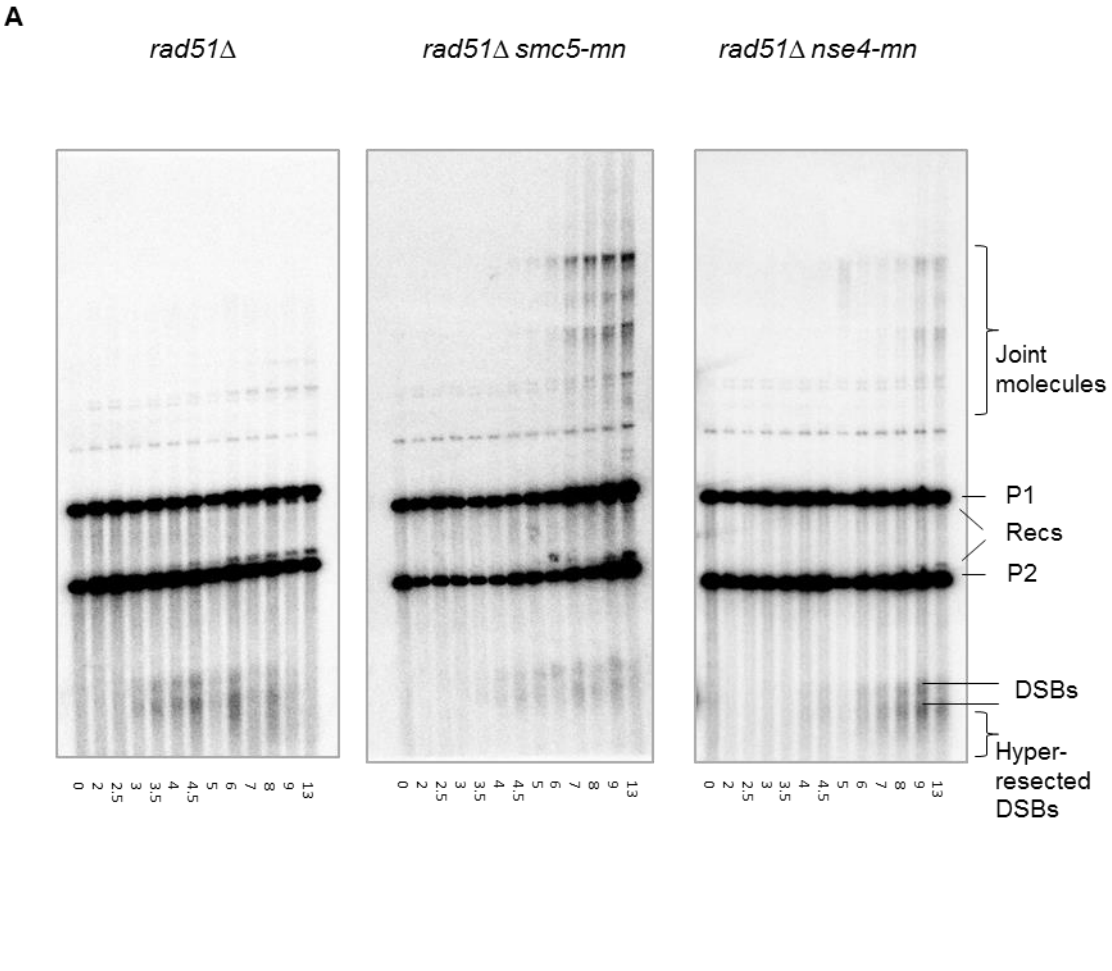
A
rad51Δ
rad51Δ smc5-mn
rad51Δ nse4-mn
Joint molecules
P1
Recs
P2
DSBs
Hyper-resected DSBs
0 2 2.5 3 3.5 4 4.5 5 6 7 8 9 13
Time (hrs)
B
DSBs
Proportion of total DNA
0.20
0.15
0.10
0.05
0.00
0 2 4 6 8 10 12 14
Time (hrs)
rad51Δ
rad51Δ nse4-mn
rad51Δ smc5-mn
Wild Type
C
Recs
Proportion of total DNA
0.20
0.15
0.10
0.05
0.00
0 2 4 6 8 10 12 14
Time (hrs)

Figure 4.3 The accumulation of DSBs in *rad51*Δ is mildly reduced in the absence of the Smc5/6 complex, and recombinants are reduced

(A) Representative 1D Southern blots of *rad51*Δ, *rad51*Δ *nse4-mn*, and *rad51*Δ *smc5-mn* strains.
(B) Double strand break levels over a 13 hour meiotic timecourse, quantified as a proportion of total detectable DNA species in the lane. It should be noted that in recA homologue mutants, DSBs are hyper-resected, leading to DSBs appearing at lower molecular weights at later time points.
(C) Levels of recombinant molecules during a 13 hour meiotic timecourse, quantified as a proportion of total detectable DNA species in the lane.
The average of two independent diploids is given, and error bars represent S.E.M. for graphs B-C

Strains: Y5693, Y5694, Y5705, Y5706, Y5707, Y5708
Experimental ID: E33_JK2_160109

repair machinery. Recombinant levels were not increased despite the rescue in joint molecule formation. This is consistent with the defect in joint molecule resolution in Smc5/6 complex depleted cells.

4.2.1.4. The Smc5/6 complex is required for the accumulation of DSBs in *dmc1*Δ *rad51*Δ

I next looked at the phenotypes observed when both *recA* homologues were deleted (*rad51*Δ and *dmc1*Δ) in conjunction with Smc5/6 complex mutants. In the double mutant, we see a *dmc1*Δ-like reduction in recombinant accumulation, but cells are still able to progress through meiosis I, although at a delayed rate. Given that in the absence of *dmc1*Δ alone, we observe that DSBs do not accumulate to high levels, we would predict that when both *recA* homologues are depleted, we would observe a similar phenotype, as Dmc1 contains the catalytic ability to mediate strand invasion, and so we might consider that it would be the necessary factor for DSB processing at this stage. The only caveat might be if in the absence of the Smc5/6 complex, Hed1-dependant repression of Rad51 mediated repair were alleviated, in which case we would expect DSBs to accumulate in the triple mutant background.

Prominent hyper-resection of DSBs was observed in the double and triple mutants (Figure 4.4A). In all mutant strains (*dmc1*Δ *rad51*Δ, *dmc1*Δ *rad51*Δ *smc5-mn*, *dmc1*Δ *rad51*Δ *nse4-mn*), DSBs become detectable with similar timing in all mutants (3.5 hours) (Figure 4.4B). In the absence of Nse4, DSBs accumulate to lower steady state levels compared to the *dmc1*Δ *rad51*Δ double mutant (DSB levels peak at 8.9% ±0.3 at t=8), whilst *dmc1*Δ *rad51*Δ *smc5-mn*

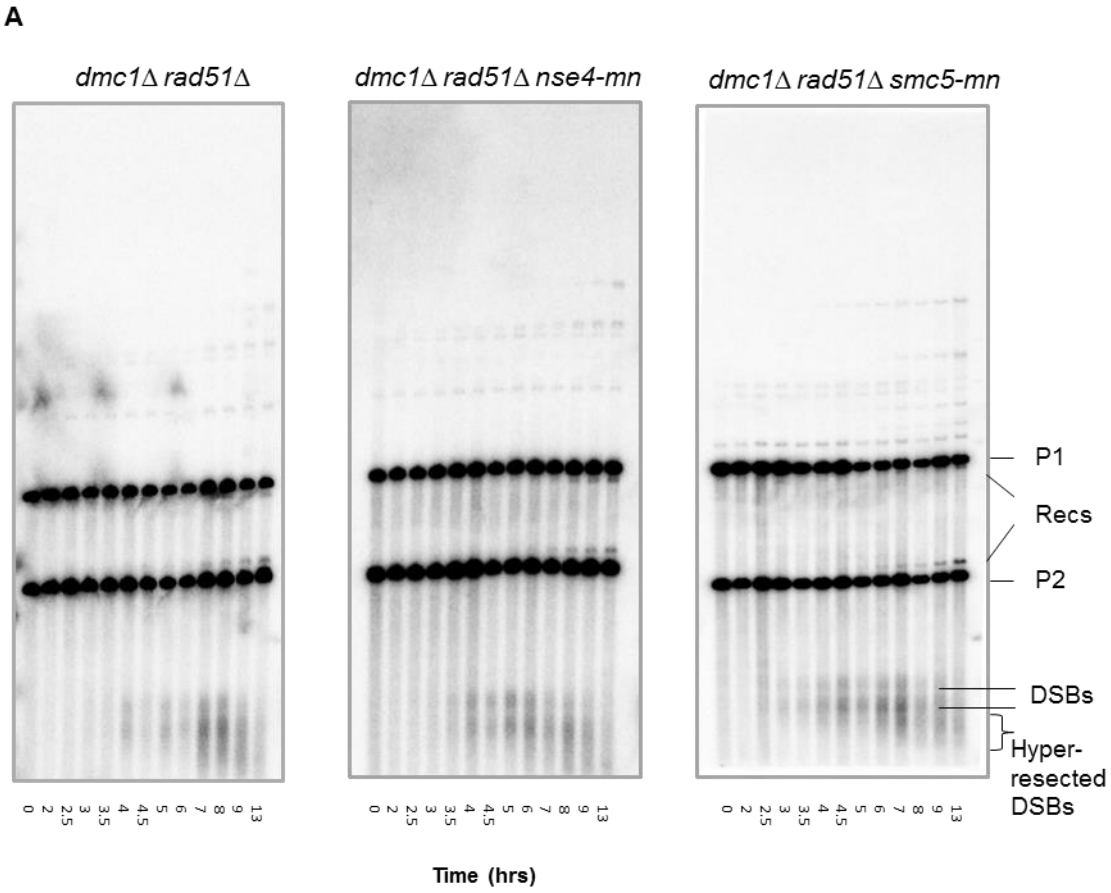
A
dmc1Δ rad51Δ
dmc1Δ rad51Δ nse4-mn
dmc1Δ rad51Δ smc5-mn
P1
Recs
P2
DSBs
Hyper-resected DSBs
Time (hrs)
B
DSBs
Proportion of total DNA
Time (hrs)
Wild Type
dmc1Δ rad51Δ
dmc1Δ rad51Δ smc5-mn
dmc1Δ rad51Δ nse4-mn
C
Recs
Proportion of total DNA
Time (hrs)

Figure 4.4 The accumulation of DSBs in *dmc1*Δ *rad51*Δ is reduced in the absence of the Smc5/6 complex, whilst level of recombinants is unaffected

(A) Representative 1D Southern blots of *dmc1*Δ *rad51*Δ; *dmc1*Δ *rad51*Δ *nse4-mn*, and *dmc1*Δ *rad51*Δ *smc5-mn* strains.
(B) Double strand break levels over a 13 hour meiotic timecourse, quantified as a proportion of total detectable DNA species in the lane. It should be noted that in *recA* homologue mutants, DSBs are hyper-resected, leading to DSBs appearing at lower molecular weights at later time points.
(C) Levels of recombinant molecules during a 13 hour meiotic timecourse, quantified as a proportion of total detectable DNA species in the lane.
The average of two independent diploids is given, and error bars represent S.E.M. for graphs B-C.

Strains: Y5709, Y5710, Y5711, Y5712
Experimental ID: E33_JK2_160109

display an intermediate phenotype between the *dmc1*Δ *rad51*Δ double mutant and the *dmc1*Δ *rad51*Δ *nse4-mn* triple mutant, (peak of 14.9% ±0.1 at t=8). All mutants showed some decrease in the level of DSBs at the latest time points, suggesting that even in the absence of recA homologues DSBs were being resected. Alternatively, we might consider that DSBs were not being generated with the same efficacy in the absence of the Smc5/6 complex, although this seems less likely given that the Smc5/6 complex has no known function in the formation of DSBs.

Levels of recombinants do not appear to be affected by the absence of the Smc5/6 complex in the *dmc1*Δ *rad51*Δ double mutant background. The mutants all accumulated to similar levels over the meiotic time course (*dmc1*Δ *rad51*Δ accumulate to 4.9% ±0.1, *dmc1*Δ *rad51*Δ *smc5-mn* accumulate to 4.3% ±0.2, *dmc1*Δ *rad51*Δ *nse4-mn* accumulate to 3.7% ±0.1). This suggests that the DSBs which are not failing to accumulate in the Smc5/6 complex mutants are not being resolved into crossovers by the meiotic repair machinery.

Taken together, these results suggest that the number of crossovers is not affected by the absence of the Smc5/6 complex in both *dmc1*Δ and *dmc1*Δ *rad51*Δ strains, whilst the number of crossovers is reduced in the absence of the Smc5/6 complex for *rad51*Δ. This suggests that in the absence of *dmc1*Δ, the formation of any recombinants (crossovers) does not require functional Smc5/6 complex proteins. However, when Dmc1 is present (and Rad51 is

absent) functional Smc5/6 complex proteins are required for the formation of at least some of the recombinants.

These effects occur in the context of all *nse4-mn* strains in these backgrounds accumulating significantly fewer DSBs than mutants with endogenous Nse4. This may imply that the absence of Nse4 is allowing DSBs to enter repair pathways which are not available in the presence of a fully functional Smc5/6 complex. In addition to the recombinants data, this would suggest that intermediates that enter these repair pathways are not leading to an increased number of crossovers. The fact that the degree to which hyper-resection was unaffected by the absence of the Smc5/6 complex suggests that the Smc5/6 complex is not having a direct impact on the formation of DSBs, or the polymerisation of recA homologues; however, it seems likely that it is affecting the entry of these processed DSBs into later stages of meiotic recombination.

To summarise: in all *recA* homologue mutants, we observe that the characteristic accumulation of DSBs phenotype is significantly reduced in *dmc1* and *rad51* strains when the Smc5/6 complex has been depleted. We observe that the degree to which hyper-resection occurs does not appear to be affected by the absence of the Smc5/6 complex. Finally, in strains where Dmc1 protein is present, the Smc5/6 complex reduces the proportion of crossovers observed. When Dmc1 protein is absent, the Smc5/6 complex does not have an effect on the proportion of crossovers.

4.2.1.5. In the absence of *dmc1*, the Smc5/6 complex has no effect on hyper-resection or the accumulation of JMs

In order to investigate the fate of the DSBs which are failing to accumulate in the absence of the Smc5/6 complex, I undertook two-dimensional analysis of *dmc1*Δ mutants with Nse4 depleted. The first crucial thing to note is the qualitative absence of branched intermediates as observed in the images directly (Figure 4.5B & C). Whilst quantitative analysis is undertaken, it is immediately clear that both strains lack punctate staining in the JM region of the blot (Figure 4.5C) and so it is unlikely that the 'lost' DSBs have been incorporated into specific JMs which will be observed here.

The earliest JM intermediates, SEIs, were quantified. Accumulation appeared to occur towards the latest time points (*dmc1*Δ had the highest accumulation at 13 hours, at 0.29% of quantified DNA, whilst *dmc1*Δ *nse4-mn* peaked at 13 hours, at 0.21% of quantified DNA), although to substantially lower levels than observed in wild type. IH-dHJs experienced a similarly substantial reduction and were essentially undetectable. IS-dHJs were quantified at low levels at 13 hours (*dmc1*Δ at 0.08%, *dmc1*Δ *nse4-mn* at 0.12% of quantified DNA). However, given that no punctuate staining was observed, it is arguable whether these results should be considered.

Finally, in order to better interpret the effect that the presence of the Smc5/6 complex might be having on hyper-resection, the DSB region was over-exposed and imaged (Figure 4.5G). I observed no substantial difference in the degree to which hyper-resection occurred (here, interpreted as the degree to which the

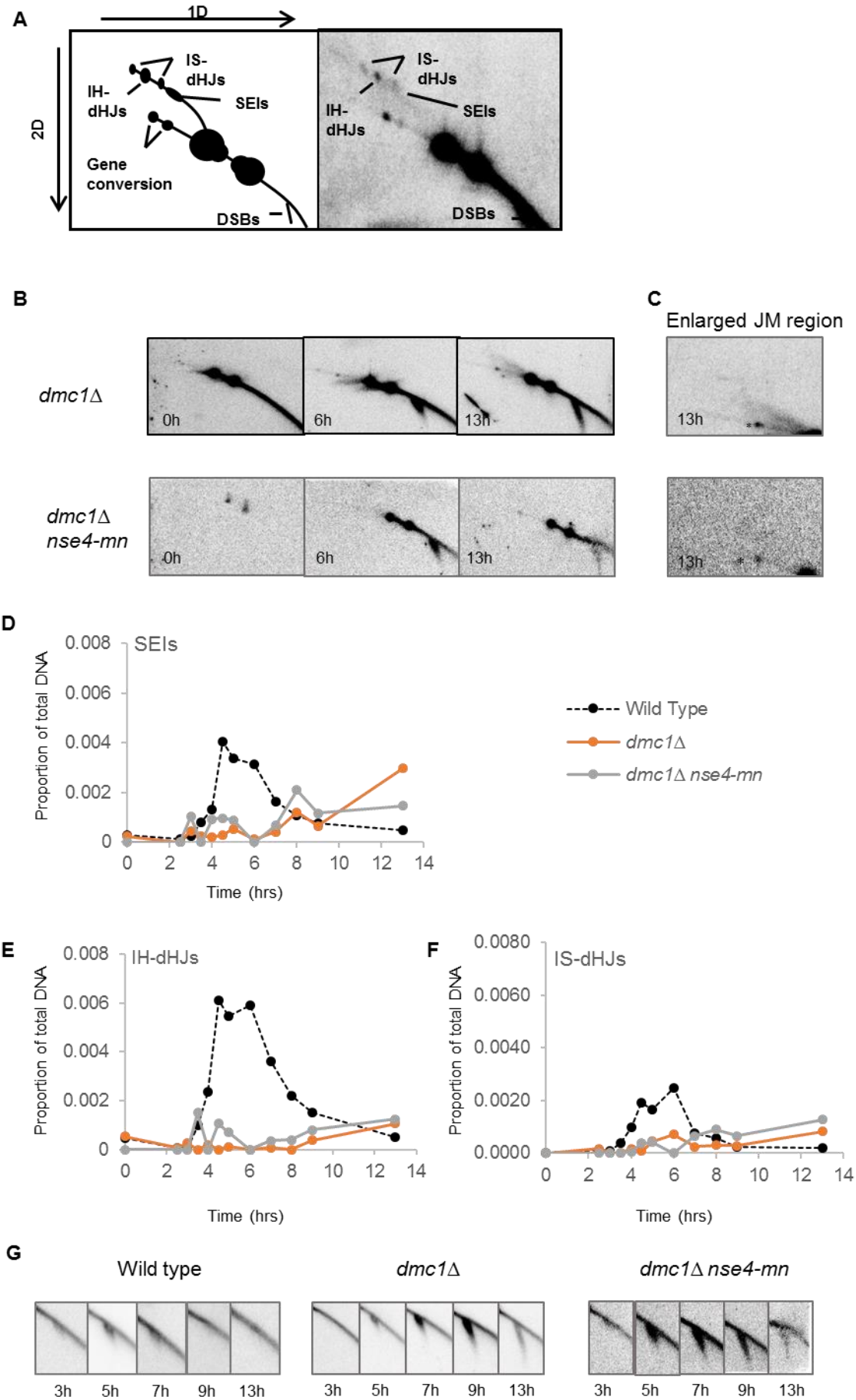
A
1D
2D
IS-dHJs
IH-dHJs
SEIs
Gene conversion
DSBs
B
C
Enlarged JM region
dmc1Δ
dmc1Δ nse4-mn
0h
6h
13h
D
SEIs
Proportion of total DNA
Time (hrs)
Wild Type
dmc1Δ
dmc1Δ nse4-mn
E
IH-dHJs
F
IS-dHJs
G
Wild type
dmc1Δ
dmc1Δ nse4-mn
3h
5h
7h
9h
13h

Figure 4.5 In the absence of *dmc1*, JMs do not accumulate to appreciable levels, and hyper-resection of DSBs occurs at later time points

(A) Diagrammatic illustration of retardation of JM species by two-dimensional electrophoresis. *ndt80*Δ (t=13) panel is shown beside the diagram for illustrative purposes.
(B) Representative images of key time points (t=0,6,13hr) in *dmc1*Δ and *dmc1*Δ *nse4-mn* strains. T=0 appears underexposed in the *dmc1 nse4-mn* strain.
(C) Enlarged images of the branched molecule region at 13 hrs in *rad51*Δ and *rad51*Δ *nse4-mn* strains strains, with different observed species indicated. Red line indicates IS-dHJs, blue line indicates IH-dHJs. Gene conversions are indicated by *
(D) Single end invasions (SEIs), quantified as a proportion of the total DNA for this panel.
(E) Interhomolog double Holliday Junctions (IH-dHJs), quantified as a proportion of the total DNA for this panel.
(F) Total Intersister double Holliday Junctions (IS-dHJs), quantified as a proportion of the total DNA for this panel.
It should be noted that here, only a single diploid was analyzed, and hence no standard error bars can be included. Wild type values have been modelled in, and are indicated with a dashed line.
(G) Images of the DSB region at 3,5,7,9 and 13 hour time points in Wild type, *dmc1*Δ and *dmc1*Δ *nse4-mn*, to qualitatively demonstrate the degree of hyper-resection in each mutant.

Strains: Y5597, Y5601
Experiment ID: E24_JK2_150603

DSB band is elongated in the vertical axis). These data suggest that the Smc5/6 complex has no detectable role in protecting DSBs from hyper-resection, and that 'lost' DSBs do not appear to be being incorporated into branched intermediates, and hence must be being processed via an alternative mechanism.

4.2.1.6. The absence of the Smc5/6 complex significantly affects JM accumulation in *rad51*Δ strains

In *rad51*Δ *nse4-mn* strains, we observe a reduction in the number of recombinants generated utilising one-dimensional analysis, and this reduction is unique to strains lacking Rad51. Furthermore, we observed a range of high molecular weight bands, by one-dimensional analysis (Figure 4.3A). In order to probe these large molecular weight intermediates, and account for the reduction in crossovers, I undertook two-dimensional analysis of *rad51*Δ in the *Nse4-mn* depleted background.

Immediately apparent from the two-dimensional analysis is the variation in JMs observed in the two mutants (Figure 4.6A & B). In *rad51*Δ alone, we observe a prominent band where IH-dHJs are detected. It should be noted however, that this band is substantially elongated in comparison to what is observed in wild type (Figure 4.6B). As the smear is predominantly in the second dimension (although to some extent also in the first dimension), this suggests that whilst these intermediates vary only a small amount with regards to size, there is a wide variety of secondary structures exhibited here. It is also apparent that in *rad51*Δ *nse4-mn*, the distribution of JM intermediates is substantially different,

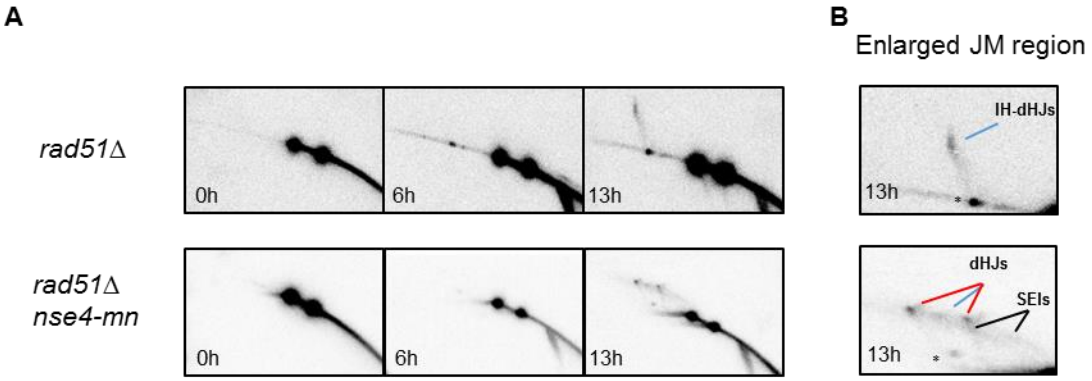
A
B
Enlarged JM region
rad51Δ
rad51Δ
nse4-mn
0h
6h
13h
IH-dHJs
dHJs
SEIs

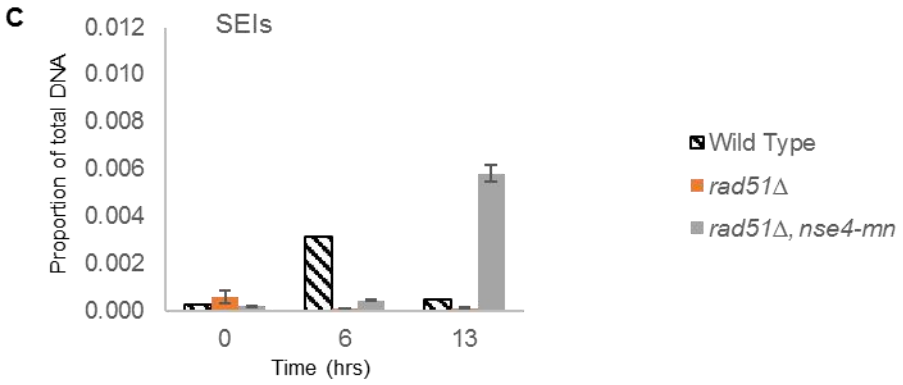
C
SEIs
Proportion of total DNA
0.012
0.010
0.008
0.006
0.004
0.002
0.000
0
6
13
Time (hrs)
Wild Type
rad51Δ
rad51Δ, nse4-mn

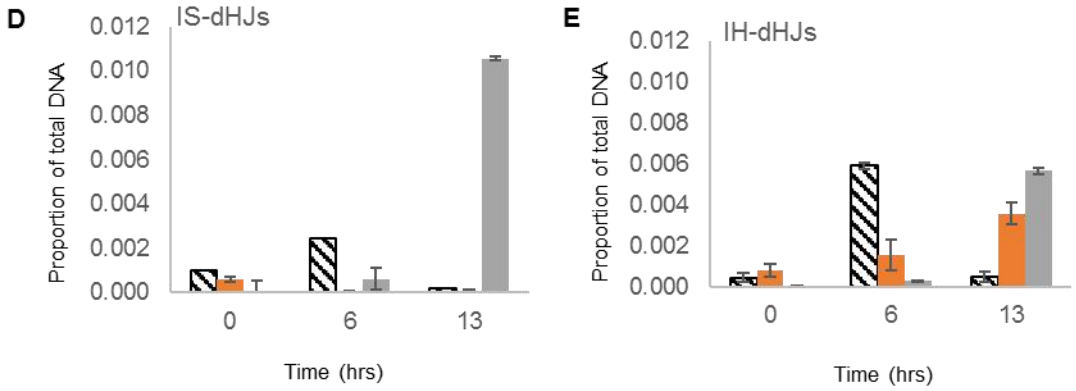
D
IS-dHJs
Proportion of total DNA
Time (hrs)
E
IH-dHJs
Proportion of total DNA
Time (hrs)

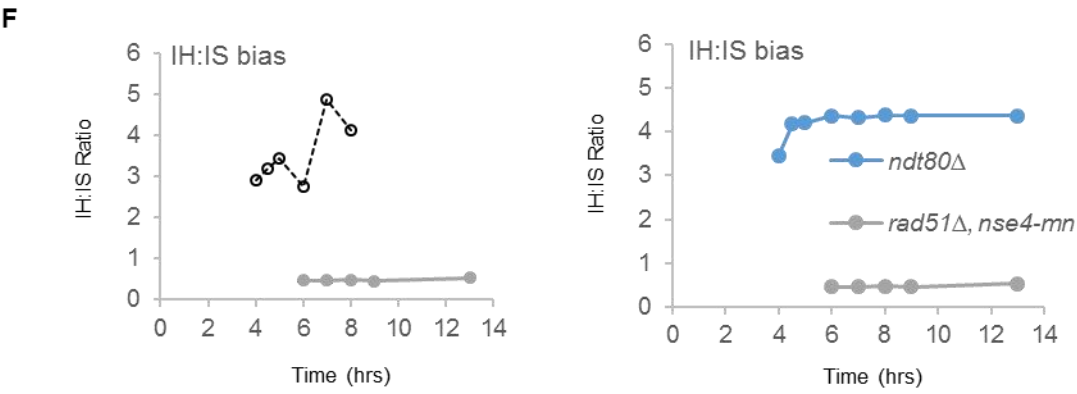
F
IH:IS bias
IH:IS Ratio
Time (hrs)
IH:IS bias
IH:IS Ratio
ndt80Δ
rad51Δ, nse4-mn
Time (hrs)

Figure 4.6 In the absence of *nse4*, joint molecules accumulate in *rad51*Δ mutants, and IH:IS bias is abolished

(A) Representative images of key time points (t=0,6,13hr) in *rad51*Δ and *rad51*Δ *nse4-mn* strains.
(B) Enlarged images of the branched molecule region at 13 hrs in *rad51*Δ and *rad51*Δ *nse4-mn* strains strains, with different observed species indicated. Red line indicates IS-dHJs, blue line indicates IH-dHJs. Gene conversions are indicated by *
(C) Single end invasions (SEIs), quantified as a proportion of the total DNA for this panel.
(D) Interhomolog double Holliday Junctions (IH-dHJs), quantified as a proportion of the total DNA for this panel.
(E) Total Intersister double Holliday Junctions (IS-dHJs), quantified as a proportion of the total DNA for this panel.
(F) IH:IS bias. The ratio of IH-dHJs to both IS-dHJs bands over a period where both intermediates are present to detectable amounts. As *rad51*Δ did not accumulate IS-dHJs to appreciable levels, it was not included in this graph. Error bars are present for *rad51*Δ *nse4-mn*, but are not distinguishable on this graph. More time points were available for *rad51*Δ *nse4-mn,* and are included here. The left hand panel compares *rad51*Δ wild type at peak accumulation, the right panel compares *rad51*Δ to *ndt80*Δ data.
The average of two independent diploids is given and error bars represent S.E.M. in graphs D-F Wild type levels are illustrated with a dashed line.

Strains: Y5693, Y5694, Y5707, Y5708
Experiment ID: E35_JK2_160218

and the elongated IH-dHJ band does not appear to be present to the same extent in this context.

In the absence of Rad51 alone, no appreciable quantity of SEIs is detected throughout the time points; in stark contrast, in *rad51*Δ *nse4-mn* strains, SEIs accumulate to high levels (0.58% ±0.04) at the latest time point observed (Figure 4.6C). IH-dHJs are detected in *rad51*Δ mutant strains from the 6-hour time point, and these accumulate to higher levels at the latest time point (0.36% ±0.05) (Figure 4.6E).

In *rad51*Δ *nse4-mn*, IH-dHJs do not become detectable until the latest time point, however at the latest time point they accumulate to higher levels than is observed in *rad51*Δ single mutant (0.57% ±0.02) (Figure 4.6D). IS-dHJs are not detectable in the *rad51*Δ mutant; however, in the absence of Nse4, they accumulate to high levels at the latest time points (1.1% ±0.01) (Figure 4.6E). The IH:IS bias in the absence of *rad51*Δ strain could not be calculated, due to the absence of detectable IS-dHJs, and so we might conclude that in the absence of Rad51, all JMs formed are IH-dHJs. In contrast, we see that at the latest time points in *rad51*Δ *nse4-mn*, there is a significant reduction in bias compared to what is observed in a wild-type situation, reduced to 0.54:1, suggesting a significant reduction, if not elimination, of bias towards interhomolog repair in these mutants.

These results indicate a significant role for the Smc5/6 complex in determining IH:IS bias. In the *rad51*Δ, we observe that all JM interactions appear to be

between homologous chromosomes, suggesting an important role in IH:IS bias. We also observe a far less punctuate IH-dHJ spot, suggesting that in the absence of Rad51 there is less fidelity in the HR process during meiotic DSB repair. When the Smc5/6 complex is also removed, we observe a dramatic shift in the accumulation of JMs, with accumulation shifting firmly in favour of intersister interactions. Given that no IS-dHJ interactions were detected in the absence of Rad51 alone, this suggests a profoundly important role for the Smc5/6 complex in the maintenance of interhomolog bias. Whether this effect on the ratio of IH:IS is as a result of an effect on the establishment of meiotic bias, or is a result of a role of the Smc5/6 complex in enabling the dissolution of early intersister intermediates will be addressed later in this chapter (see 4.3).

4.2.1.7. In the absence of components of the ZMM pathway, DSB accumulation is restored to Smc5/6 complex mutants

In *recA* homologue mutants, DSBs accumulate to far higher levels than in wild type (Figure 4.1) (SHINOHARA, et al., 1997). Here, we have demonstrated that the Smc5/6 complex is required for this accumulation phenotype. In order to ascertain whether the loss of DSB accumulation observed in the absence of the Smc5/6 complex was dependent on the functionality of the ZMM repair pathway, one-dimensional analysis was undertaken of a quadruple mutant, *dmc1*Δ *rad51*Δ *nse4-mn msh5*Δ, to determine whether DSB accumulation could be restored (Figure 4.7). We observe hyper-resection of DSBs in both the double and quadruple mutant (Figure 4.7A). It is immediately apparent that in *msh5*Δ strains, DSBs accumulate to similar levels to those observed in the *dmc1*Δ *rad51*Δ double mutant (peaking at 16.3% ±0.6 of total DNA at the 6-hour

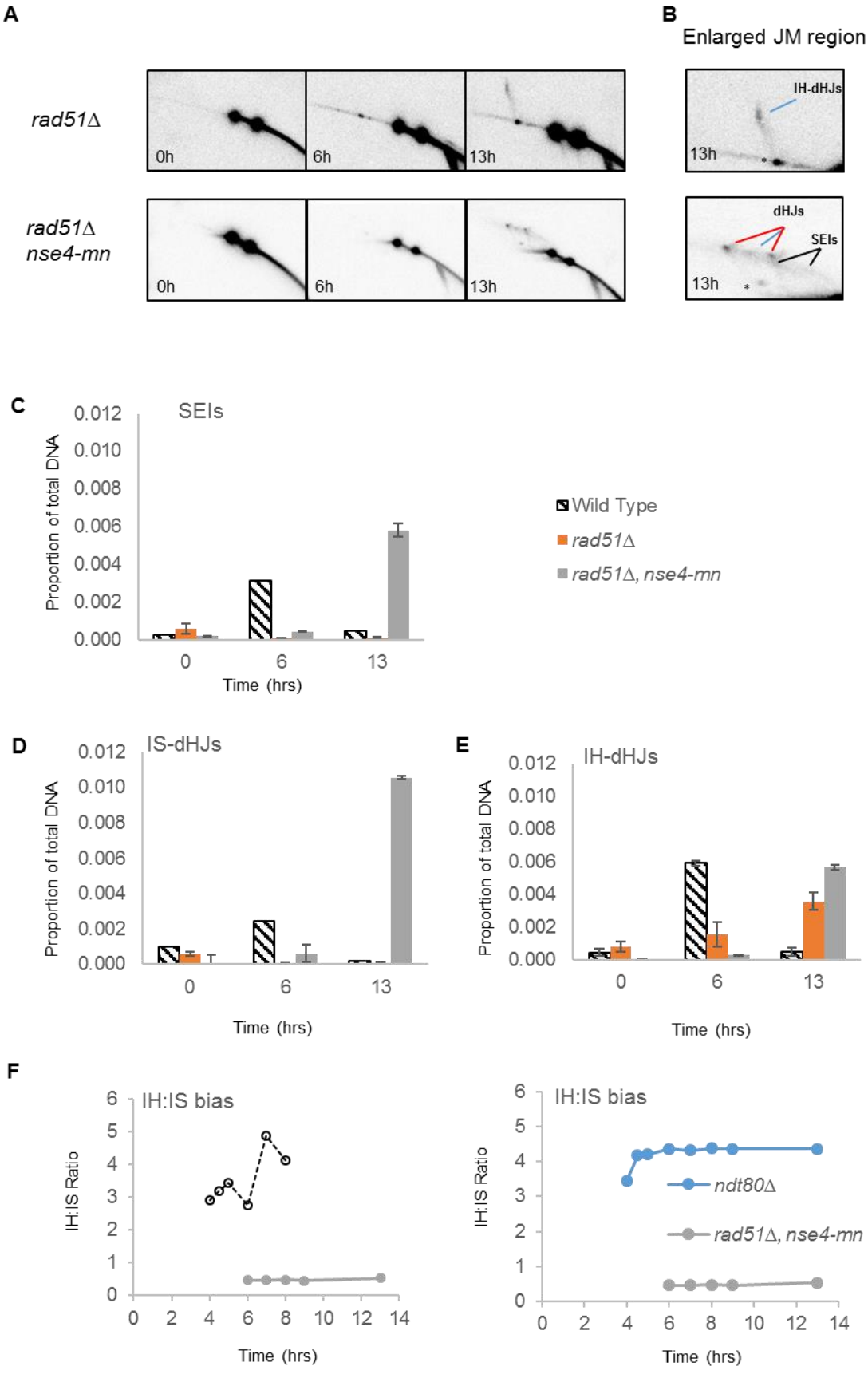
A
B
Enlarged JM region
rad51Δ
rad51Δ
nse4-mn
0h
6h
13h
IH-dHJs
dHJs
SEIs
C
SEIs
Proportion of total DNA
0.012
0.010
0.008
0.006
0.004
0.002
0.000
0
6
13
Time (hrs)
Wild Type
rad51Δ
rad51Δ, nse4-mn
D
IS-dHJs
E
IH-dHJs
F
IH:IS bias
IH:IS Ratio
0
1
2
3
4
5
6
0
2
4
6
8
10
12
14
ndt80Δ
rad51Δ, nse4-mn

Figure 4.7 In the absence of the Smc5/6 complex, DSBs in *recA* homologue mutants do not aberrantly enter the ZMM pathway

(A) Representative 1D Southern blots of *dmc1*Δ *rad51*Δ, and *dmc1*Δ *rad51*Δ *nse4-mn msh5*Δ strains.
(B) Double strand break levels over a 13 hour meiotic timecourse, quantified as a proportion of total detectable DNA species in the lane. It should be noted that in recA homologue mutants, DSBs are hyper-resected, leading to DSBs appearing at lower molecular weights at later time points.
(C) Levels of recombinant molecules during a 13 hour meiotic timecourse, quantified as a proportion of total detectable DNA species in the lane.
The average of two independent diploids is given, and error bars represent S.E.M. for graphs B-C

Strains: Y5695, Y5696, JKD214, JKD215
Experimental ID: E34_JK2_160218

time point in the quadruple mutant, compared to 17.1% ±0.2 in the double mutant) (Figure 4.7B). This is highly suggestive that in a *recA* mutant background in which the Smc5/6 complex is depleted, DSBs are able to enter the ZMM pathway, leading to a decrease in their accumulation.

The proportion of recombinants that accumulated by the latest time point was increased in the quadruple mutant, compared to the double mutant alone (*dmc1*Δ *rad51*Δ *nse4-mn msh5*Δ accumulated recombinants to 7.2% ±0.2 of total DNA, compared to *dmc1*Δ *rad51*Δ accumulating 4.9% ±0.2). This is somewhat unexpected, as we typically observe a reduction in recombinants in the absence of the Smc5/6 complex, and there is little reason to suggest that *msh5*Δ would affect this. However, given that the DSB accumulation data is suggesting an early 'protector' role for the Smc5/6 complex, we might interpret these data as suggesting the quadruple mutant exists in a highly de-regulated repair environment, and so many non-canonical repair outcomes may be occurring in this context.

4.3. Discussion

4.3.1. *RecA* homologue mutants accumulate DSBs, and have reduced levels of meiotic crossovers.

The *recA* homologues Dmc1 and Rad51 are required for the formation of nucleoprotein filaments around resected DSBs, and catalyse strand invasion events during meiotic recombination (BISHOP, 1994; SHINOHARA & SHINOHARA, 2004). In the absence of these proteins, DSBs accumulate, and in order to better understand the early phenotypes of the Smc5/6 complex, I studied mutants lacking both *recA* homologues and Smc5/6 complex components. Initially, I performed one-dimensional analysis of single and double mutants of the *recA* homologues Dmc1 and Rad51, in order to establish a baseline level for comparisons to Smc5/6 complex.

The results obtained demonstrate the different roles of the recA homologues during meiotic prophase. With regards to meiotic DSB repair, in *dmc1*Δ we see a low number of recombination events, and an accumulation of DSBs, suggesting an abrogation of meiotic repair (Figure 4.1B & C). We also observe a block to meiotic progression (Figure 4.1E). In *rad51*Δ mutant strains, we observe an accumulation of DSBs, and a larger proportion of recombinant DNA molecules than in *dmc1*Δ single mutant (Figure 4.1B & C). We also observe a delay in meiotic progression, but not a block as is observed in *dmc1*Δ (Figure 4.1D). In the double mutant, we see a higher level of accumulation of DSBs than in either single mutant, and also observe a level of recombinants which is similar to *dmc1*Δ single mutant (Figure 4.1B & C). We observe a delay in meiotic progression compared to *rad51*Δ single mutants, but not an absolute

meiotic progression block as is observed in *dmc1*Δ single mutants. All mutants appear to experience hyper-resection of DSBs. These phenotypes are in accordance with the literature (SHINOHARA, et al., 1997).

These data suggest a complex interplay with regards to the different roles of the two *recA* homologues. All mutants appear to have some role in protecting DSBs from hyper-resection (which has been proposed to be a result of the action of Exo1 on unprotected DSB ends (TSUBOUCHI & OGAWA, 2000). The presence of higher levels crossovers in the *rad51*Δ single mutants, compared to *dmc1*Δ and *dmc1*Δ *rad51*Δ strains, suggests that Dmc1 is sufficient to generate a small subset of crossovers, whilst Rad51 is not. This is likely as a result of Dmc1 being able to catalyse the formation of JMs in meiotic repair, a functionality that Rad51 does not possess (CLOUD, et al., 2012). We observe that DSBs accumulate to higher levels in the double mutant than either single mutant, suggesting that individually, each protein is able to remove a subset of DSBs from the accumulated pool.

Finally, a distinct phenotype of the three mutants is their effect on timely meiotic progression as measured by DAPI counts. In the absence of *rad51*, there is a delay in meiotic progression compared to wild type, whilst in the absence of *dmc1*, there appears to be a firmer block, with virtually no cells showing a segregation of DNA to mark the first meiotic division. The *dmc1*Δ *rad51*Δ mutant exhibits an intermediate phenotype, with a more significant delay than is observed in *rad51*Δ single mutant, but still allowing some cells to progress, unlike in *dmc1*Δ. This result is concordant with those in the existing literature

(SHINOHARA, et al., 1997). This suggests that in the absence of Dmc1, meiotic progression is inhibited, and that in order for the inhibition to occur effectively, Rad51 must be present. This surveillance mechanism seems likely to be important for ensuring a meiosis specific repair outcome, through the use of the meiosis specific recA homologues homology search activity.

4.3.2. The Smc5/6 complex acts as a 'protector' of meiotic DSBs

Here, I attempted to distinguish the early functions of the Smc5/6 complex during meiotic DSB repair. Firstly, I looked in the absence of *recA* homologues, to determine whether the Smc5/6 complex was required to act as barrier to entry for meiotic DSBs which should not be entering the meiotic repair machinery.

In all mutant contexts (*dmc1*Δ, *rad51*Δ, *dmc1*Δ *rad51*Δ) we observe that in the absence of *nse4* (the more severe phenotype) that the peak accumulation of DSBs is reduced. In the depletion of *smc5* (which generates a hypomorphic phenotype), we observe very mild phenotypes, but all show a reduced accumulation at later time points compared to when Smc5 is present. We also observe that hyper-resection does not appear to be affected by the presence or absence of the Smc5/6 complex. This is confirmed in *dmc1*Δ by two-dimensional analysis (Figure 4.5G), where no difference in the elongation of the DSB band is detected in the absence of *nse4.*

We observed that in the absence of the meiosis specific recA homolog *dmc1*, there was very little effect on the level of recombinants in the absence of

Smc5/6 complex components. However, in the absence of the mitotic homolog *rad51,* the Smc5/6 complex did appear to have a role in generating crossovers, as the levels of crossovers were reduced in the absence of *nse4.* Furthermore, we observed the appearance of high molecular weight species by one-dimensional analysis (Figure 4.3A), suggesting that JMs were being formed in *rad51*Δ strains. In the double mutant, we observed a *dmc1*Δ single mutant phenotype, suggesting that the Smc5/6 complex was only affecting recombinants generated by the initial activity of Dmc1.

This leads to a model where, in a wild type strain *recA* homologues are required to catalyse DSBs becoming SEIs. When *recA* homologues are absent, DSBs accumulate and are hyper-resected, and cannot transition to SEIs. However, in order for this accumulation to occur, the Smc5/6 complex must be present; in its absence, DSBs cannot accumulate. One might imagine two possible fates for these DSBs which might be explored in future work: either that they are unprotected and hence get degraded, leading to a loss of genetic material, or they are repaired non-stringently or ectopically utilising non-canonical repair mechanisms. As a secondary phenotype, in the absence of *rad51* (but with Dmc1 still present), a small subset of crossovers is generated, and these crossovers are lost in the *nse4* mutant strains.

4.3.3. The ‘lost’ DSBs do not enter the meiotic repair pathway in the absence of *dmc1*

In order to investigate whether the absence of the Smc5/6 complex was allowing accumulated DSBs to enter the meiotic repair pathway, two-

dimensional analysis was undertaken. We do not qualitatively observe any branched structures in *dmc1*Δ, in either the presence or absence of *nse4-mn*. Quantitative analysis shows only very low levels of SEIs and dHJs, and there seems to be very little difference between the accumulation in the presence of absence of *nse4-mn*.

These results suggest that in the absence of *dmc1*, there is no detectable accumulation of JM intermediates which normally lead to the generation of recombinants. This might indicate that formation of JMs is so severely abrogated as to make them undetectable to the method utilised here. Alternatively, it might indicate that there truly are no JMs generated in the absence of *dmc1*, and any repair products are being generated by alternative mechanisms to meiotic homologous recombination. This second hypothesis is supported by the *dmc1*Δ *nse4-mn* data; given the well characterised role of the Smc5/6 complex in promoting the resolution of branched intermediates, we would predict that if undetectable levels of branched molecules were leading to the formation of the low levels of recombinants observed in *dmc1*Δ strains, we would observe an accumulation of JMs and a reduction of recombinant products in the absence of the Smc5/6 complex. Given this is not the case, we must conclude that in the absence of *dmc1*, JMs are not formed, and recombinants are generated via different means.

These data also suggest that the lower level of accumulation of DSBs observed in *dmc1*Δ *nse4-mn* compared to *dmc1*Δ single mutant is not as a result of DSBs being accumulated in the meiotic DSB repair pathway. This would indicate that the role of the Smc5/6 complex in the accumulation of DSBs is not to control

their entry into the meiotic repair pathway, but instead to protect these DSBs from being removed by other mechanisms. This might potentially be as a result of rapid degradation (although this seems unlikely, given that we see no significant alteration in hyper-resection as detected by two-dimensional analysis). Alternatively, the Smc5/6 complex may be preventing DSBs from entering repair pathways that do not utilise homologous recombination (and hence do not form crossovers, or generate JMs.

4.3.4. The Smc5/6 complex is required for interhomolog bias in *rad51*Δ mutants

When only Dmc1 (and not Rad51) is present, we observe a reduction in the formation of recombinants in the *nse4-mn*. In order to probe this, two-dimensional analysis was undertaken. In *rad51* we observe that a smeared band of IH-dHJs is detected, and effectively no IS-dHJs. We also observe very few SEIs in this context. In the absence of *nse4*, we observe a dramatic shift in the JMs accumulated. We see similar numbers of IH-dHJs, but a large increase in the numbers of IS-dHJs and SEIs, particularly at later time points. This would seem to imply that in the absence of *rad51*, Dmc1 primarily catalyses the formation of IH-dHJs. However, in the absence of *nse4*, we observe that there is a shift in the bias of formation, and a large number of IS-dHJs is present. This could be interpreted in two ways. Firstly, the Smc5/6 complex is responsible for establishing IH:IS bias in the absence of *rad51*; this will be further analysed in Chapter 5. Secondly, it might be the case that the Smc5/6 complex is involved in the repression/ catalysing the dissolution of intersister interactions, and in its absence, these can now be seen in abundance.

Given the dramatic shift in repair outcomes, and the observation that the levels of IS-dHJs have increased, whilst levels of IH-dHJs remained similar, I would suggest that the shift in these repair outcomes is not as a result of an alteration in early repair designations in Smc5/6 complex mutants, but instead is a result of the accumulation of molecules which would normally be disassociated in the presence of the Smc5/6 complex. This would also fit with some of the similarities previously attributed between the Smc5/6 complex phenotype and the Sgs1 helicase, and might imply that whilst Sgs1 has been considered an anti-crossover factor, the Smc5/6 complex might fill the role of anti-noncrossover factor. This suggests a role for the Smc5/6 complex in the disassociation of intersister interactions which is likely distinct from its later role in the resolution of meiotic dHJs, which leads to the accumulation of both interhomolog and intersister JMs.

4.3.5. 'Loss' of DSBs in Smc5/6 complex mutants requires the activity of the ZMM repair pathway.

To attempt to account for the loss of accumulation of DSBs in the absence of the Smc5/6 complex, I deleted a component of the ZMM pathway to determine whether the loss of accumulation phenotype might be restored. In *recA* homologue double mutants, DSBs accumulate over time. This accumulation is lost in the absence of *nse4*, but restored when *msh5*Δ is added. This suggests that DSBs which are failing to accumulate in the absence of the Smc5/6 complex are to some extent being processed by the ZMM pathway (although the DSBs being processed by the ZMM pathway does not lead to an increase in recombinants). This suggests that in the absence of the Smc5/6 complex, DSBs

are transiently – as SEIs are not detected by southern analysis for *dmc1* mutants – entering the ZMM repair pathway, but not leading to an increased accumulation of recombinant DNA molecules.

Together, these data suggest that in the absence of the Smc5/6 complex, there is a shift in the proportions of JMs observed, such that there is an increase in the proportion of intersister JMs accumulating. This could be the result of a number of modes of action. Firstly, it could be as a result of a previously uncharacterised role in establishing repair bias at early meiotic stages. However, given that in the absence of *rad51*, rather than a shift in JM accumulation outcomes, we observe similar levels of IH-dHJs but a large increase in the proportion of IS-dHJs, this would seem unlikely.

A second model, which the data appears to favour, would be a role of the Smc5/6 complex in preventing the formation of IS-dHJs at an earlier stage, in a similar manner to the BLM helicase Sgs1. This would explain the situation observed in the absence of Rad51, where no IS-dHJs are observed when the Smc5/6 complex is present, and a large number of IS-dHJs is observed when the Smc5/6 complex is abrogated, whilst the level of IH-dHJs remains broadly the same. This would represent a novel role of the Smc5/6 complex in anti-establishment activity specifically of intersister interactions.

Chapter 5

The Smc5/6 complexes role in homologous recombination is independent of its function in cohesin regulation

5.1. Introduction

The cohesin complex belongs to the same protein family as the Smc5/6 complex, and both are involved in higher order chromosome organisation and dynamics (FREEMAN, et al., 2000) (OUTWIN, et al., 2009). Cohesin is required to hold sister chromosomes together after DNA replication has occurred during S-phase (MICHAELIS, et al., 1997), in addition to being an essential component of the lateral elements of the synaptonemal complex (SC) during meiotic prophase.

During meiotic cell divisions, chromosome arm localised-cohesin is removed at the onset of anaphase I (BUONOMO, et al., 2000); however, the action of Sgo1-PP2A at centromeres protects centromere localised cohesin from the action of Separase (KITAJIMA, et al., 2004). This allows for the dissociation of homologous chromosomes, which were held together by the action of

chiasmata and cohesin along the chromosome arms, whilst sister chromatids are still held together by the actions of centromeric cohesin. At the second meiotic division, this centromeric cohesin is removed, to allow the separation of sister chromatids into distinct daughter cells.

The cohesin complex has been shown to have a variety of roles in DNA damage repair. Cohesin mutants have been shown to be defective in repairing damaged DNA (SJOGREN & NASMYTH, 2001). Cohesin has been shown to accumulate around the sites of DSBs (STROM, et al., 2004). It has also been demonstrated in *S. pombe* that when the removal of cohesin is inhibited, by either inactivating Separase or utilising Separase resistant Scc1 alleles, DNA damage repair defects occur (NAGAO, et al., 2004).

In addition, the cohesin complex has been demonstrated to interact with meiotic DSBs and affect meiotic DSB repair in a variety of ways. In the absence of the meiosis specific kleisin subunit Rec8, a mild DSB hyper-resection phenotype is observed (KLEIN, et al., 1999), suggesting that cohesin has a protective role with regards to DSBs. Rec8 mutants also exhibit reduced recombinant formation, whilst appearing to maintain similar levels of DSBs to wild type cells (KLEIN, et al., 1999; BRAR, et al., 2009). Finally, it has been demonstrated that in *rec8* mutants, the interhomolog bias observed in wild type is lost, and interhomolog dHJs accumulate at the same rate as intersister dHJs (1:1 ratio).

The formation of chiasmata during meiosis is essential for the stable association of homologous chromosomes until anaphase I (together with sister chromatid cohesion), with the pairing itself mediated by the cohesin complex (BUONOMO, et al., 2000). Removal of meiotic cohesin has also been shown to be instrumental for resolution of chiasmata, which in turn allows accurate disjunction of paired homologous chromosomes. This was demonstrated using a Rec8 allele that is resistant to Separase-cleavage; this led to centromeric regions of homologous chromosomes separating at the metaphase I to anaphase I transition, but distal chromosome regions failing to dissociate (BUONOMO, et al., 2000).

There is a strong inter-relationship between the Smc5/6 complex and cohesin. They cohesin loading complex Scc2/4 is necessary for the chromosomal association of the Smc5/6 complex, through the action of cohesin itself (JEPPSSON, et al., 2014) and have a much higher correlation of localisations than would be expected from random dispersal along the chromosome (COPSEY, et al., 2013; JEPPSSON, et al., 2014) There also seems to be interplay between the two complexes, with Smc5/6 complex mutants experiencing aberrant cohesin organisation during meiosis. The Smc5/6 complex has been shown to be required for the timely removal of cohesin from chromosome arms, and in addition regulates centromere cohesion (COPSEY, et al., 2013).

Here, I intend to better characterise the role of the Smc5/6 complex during meiosis in *S. cerevisiae*, with particular focus on whether its well characterised JM resolution phenotypes require functional cohesin activity to accumulate, and hence whether mis-regulation of cohesin is the downstream effect that the Smc5/6 complex acts through. This might suggest functions in chromosome organisation that were previously uncharacterised. This will be achieved by combining *rec8*Δ mutations which have been previously characterised (KLEIN, et al., 1999) (BRAR, et al., 2009), with Smc5/6 complex depletions, to determine whether JMs accumulate in the double mutant background to higher levels than *rec8*Δ single mutants. Furthermore, given the differential effect observed on intersister and interhomolog JMs in the previous chapter, and the characterised loss of interhomolog bias experienced in *rec8* mutants, I will determine whether the Smc5/6 complexes effect on recombination bias occurs as a result of its role regulating cohesin

5.2. Results

5.2.1. In the absence of Rec8, progression of recombination intermediates is severely abrogated

In the absence of the meiosis specific kleisin subunit of cohesin, sister chromatid cohesion fails to form effectively, and severely disrupts chromosome architecture. However, a subset of cells still enters meiosis, and generate meiotic DSBs which are then processed via the meiotic recombination pathways. Given the previously characterised roles of the Smc5/6 complex in timely removal of meiotic cohesin from chromosome arms, it seemed pertinent to determine whether the effects of the Smc5/6 complex in meiotic recombination still persisted in the absence of meiotic cohesin, to determine whether the phenotypes observed in the absence of the Smc5/6 complex might be a result of its actions through moderating the cohesin complex.

Initially, I looked at the levels of DSBs and recombinants in two mutant strains, *rec8*Δ and *rec8*Δ *ndt80*Δ (Figure 5.1). As described previously, Ndt80 is a transcription factor that promotes exit from meiotic pachytene, and so in *rec8*Δ *ndt80*Δ mutants we would hope to distinguish early and late meiotic functions of the Smc5/6 complex. Furthermore, as it has previously been reported that *rec8*Δ accumulates JM intermediates to lower levels than observed in wild type, the *ndt80*Δ mutation potentially allows for an accurate determination of IH:IS bias that would not be able to be calculated effectively in *rec8*Δ single mutants.

In the absence of *rec8*Δ, I observe that DSBs achieve a lower peak level in both mutant strains (peaking at 2.8% ±0.5 of total DNA at the 4.5-hour time point for

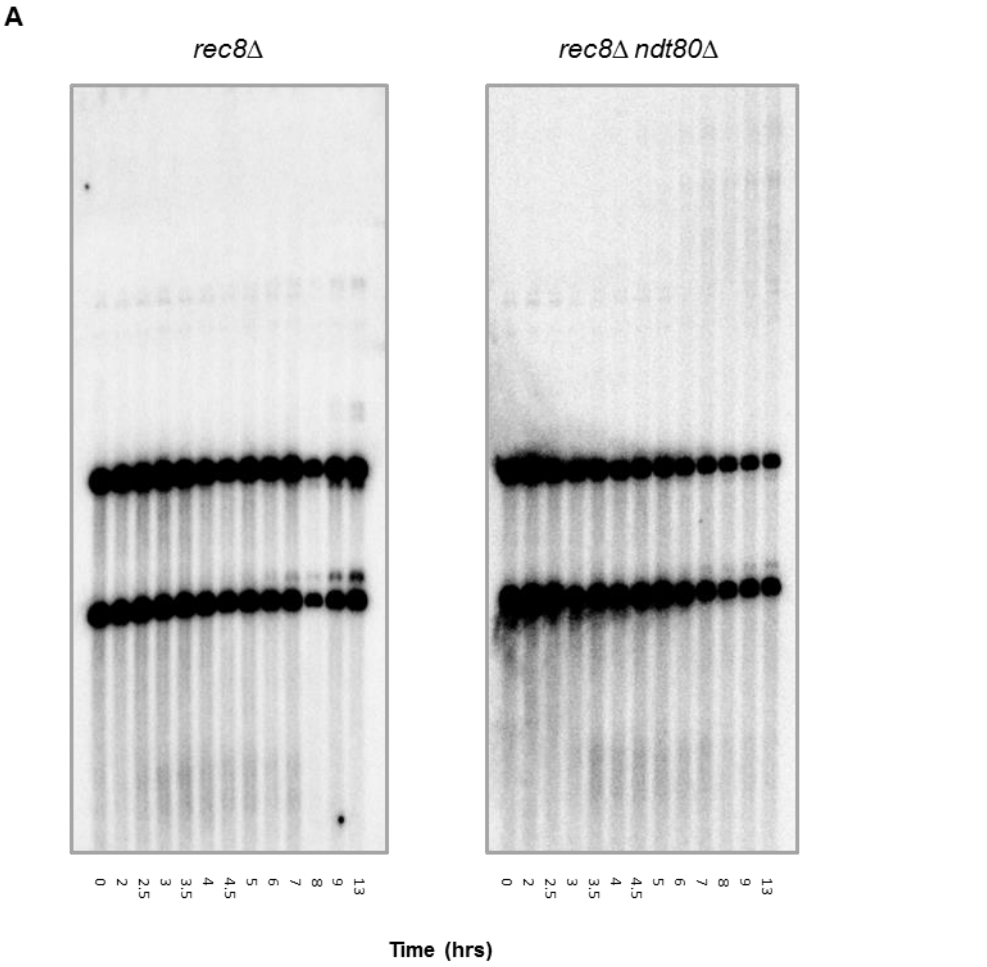
A
rec8Δ
rec8Δ ndt80Δ
0 2 2.5 3 3.5 4 4.5 5 6 7 8 9 13
0 2 2.5 3 3.5 4 4.5 5 6 7 8 9 13
Time (hrs)
B
DSBs
Proportion of total DNA
0.06
0.05
0.04
0.03
0.02
0.01
0
0 2 4 6 8 10 12 14
Time (hrs)
Wild type
rec8Δ
rec8Δ, ndt80Δ
C
Recs
Proportion of total DNA
0.20
0.15
0.10
0.05
0.00
0 2 4 6 8 10 12 14
Time (hrs)

Figure 5.1 In the absence of *rec8*, cells produce fewer DSBS and fewer crossovers

(A) Representative 1D Southern blots of *rec8*Δ, and *rec8*Δ *ndt80*Δ strains.
(B) Double strand break levels over a 13 hour meiotic timecourse, quantified as a proportion of total detectable DNA species in the lane.
(C) Levels of recombinant molecules during a 13 hour meiotic timecourse, quantified as a proportion of total detectable DNA species in the lane.
The average of two independent diploids is given, and error bars represent S.E.M. for graphs B-C

Strains: JKD176, JKD177, JKD110, JKD201
Experimental ID: E07_JK1_130928, E26_JK2_150520

*rec8*Δ, and 2.9% ±0.3 at 4 hours for *rec8*Δ *ndt80*Δ) (Figure 5.1B). DSBs appear to persist for longer in the absence of Rec8 than is observed in the wild type, with a broad peak that is only entirely removed by the latest time point in both mutant strains. The levels of recombinants are significantly lower than observed in the wild type situation, as expected (at the latest time point, crossovers accounted for 10.1% ±0.1 of total DNA for *rec8*Δ, and 6.4% ±0.1 for *rec8*Δ *ndt80*Δ) (Figure 5.5C). The *rec8*Δ data presented here is similar to the published literature with regards to the reduction in accumulated molecules observed compared to wild type (BRAR, et al., 2009), although it should be noted that they should not be directly compared numerically, due to variation in normalisation techniques.

Taken together, these data would indicate similar early kinetics of repair in both *rec8*Δ and *rec8*Δ *ndt80*Δ strains, as the levels of DSBs, and the profile of their accumulation are very similar. These DSBs accumulate to lower levels than in wild type strains, but the accumulation persists for longer, suggesting an abrogation of the repair pathway. The proportion of crossovers is lower in *rec8*Δ *ndt80*Δ strains than in *rec8*Δ single mutant, which supports the hypothesis that in the absence of Ndt80, there is a pachytene arrest, preventing the crossovers from being generated, and supports our use of these model systems to distinguish the early and late functions of the Smc5/6 complex in meiotic DSB repair.

In order to analyse the effects of the Smc5/6 complex on meiotic recombination in the absence of *Rec8*, a baseline for JM levels must be established (Figure

5.2). The earliest JM intermediates, SEIs, accumulate to lower peak levels in the absence of Rec8 than in wild type (peaking at 0.25% ±0.05 of total DNA at the 6-hour time point), and levels of SEIs persist for longer than in wild type, only being fully removed by the latest time point. In the *rec8*Δ *ndt80*Δ double mutant, SEIs accumulated to similar peak levels as *rec8*Δ alone, but the level of these intermediates did not decrease at later time points (peaking at 0.25% ±0.01 at 13 hours) (Figure 5.2C).

IH-dHJs follow a similar progression: in *rec8*Δ they accumulate later (first detectable at 5 hours), and accumulate to lower peak levels than observed in wild type (0.30% ±0.10 at the 6-hour time point). IH-dHJs also persist longer than in wild type, and are only entirely removed by the 13-hour time point. In the *rec8*Δ *ndt80*Δ double mutant, IH-dHJs accumulate to higher levels, and these IH-dHJs persist until the latest time points (peaking at 0.40% ±0.01 at the 9-hour time point) (Figure 5.2D). IS-dHJs followed a broadly similar profile of detection as IH-dHJs; however, the levels of IS-dHJs that accumulated were not significantly different to wild type in this instance (peaking at 0.21% ±0.06 at the 6-hour time point) (Figure 5.2E). This is reflected in the IH:IS bias, with both *rec8*Δ and *rec8*Δ *ndt80*Δ strains showing a reduction in interhomolog repair bias compared to wild type (at peak accumulation of intermediates, 6 hours, *rec8*Δ demonstrated an IH:IS bias of 1.3 ±0.2, whilst *rec8*Δ *ndt80*Δ demonstrated a bias of 1.7±0.1 at the 13-hour time point) (Figure 5.5F). This reduction in bias is less than has been reported elsewhere, although some of this variation may be as a result of differences in experimental design (KIM, et al., 2010). Finally, we observed that in both mutants, the DSB band appeared to be elongated and

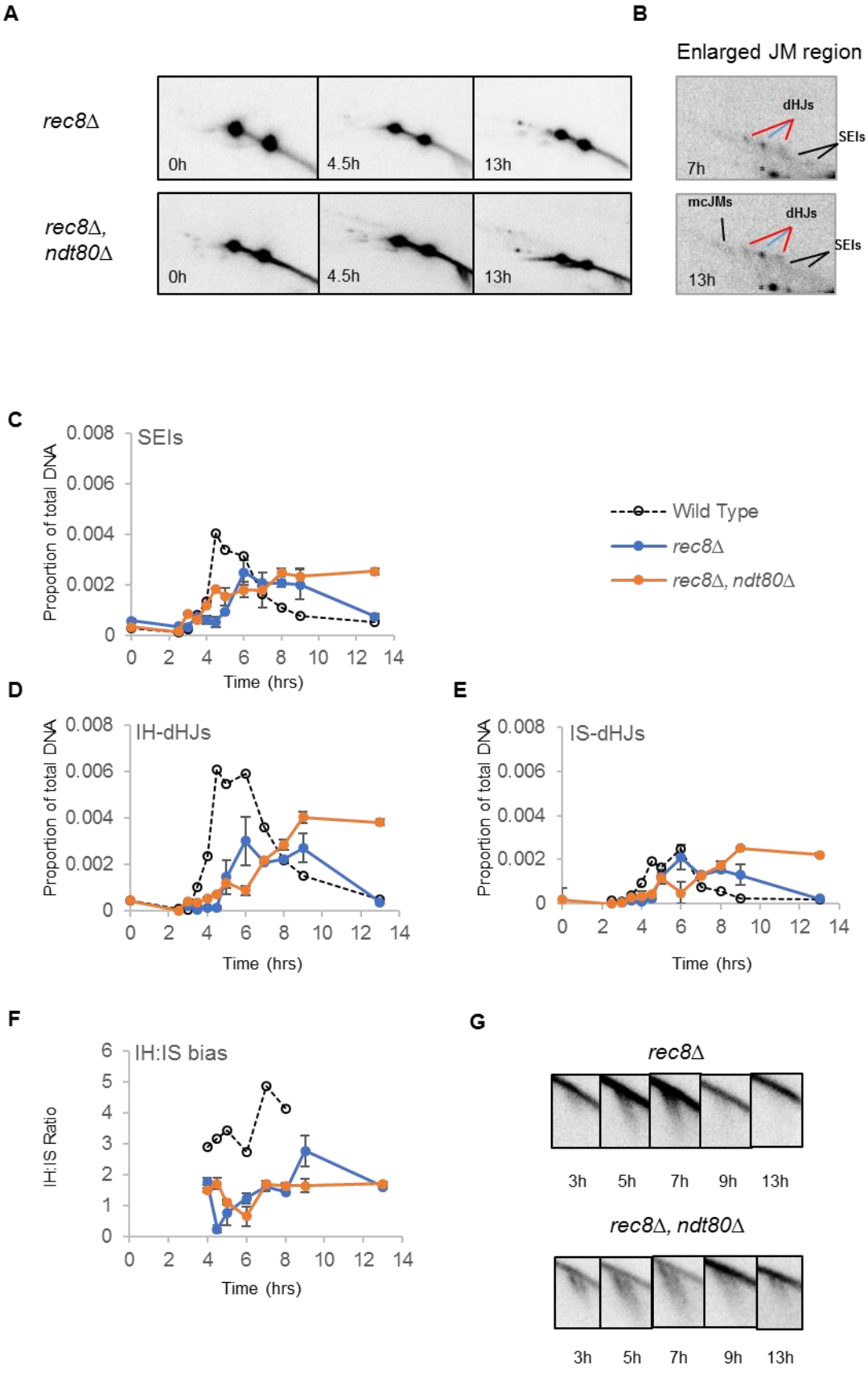
A
B
Enlarged JM region
rec8Δ
rec8Δ, ndt80Δ
0h
4.5h
13h
dHJs
SEIs
7h
mcJMs
13h
C
SEIs
Proportion of total DNA
Time (hrs)
Wild Type
rec8Δ
rec8Δ, ndt80Δ
D
IH-dHJs
E
IS-dHJs
F
IH:IS bias
IH:IS Ratio
G
rec8Δ
3h
5h
7h
9h
13h
rec8Δ, ndt80Δ

Figure 5.2 In the absence of *rec8*, fewer joint molecules are formed, and interhomolog bias is severely reduced

(A) Representative images of key time points (T=0,4.5,13) in *rec8*Δ and *rec8*Δ *ndt80*Δ strains.
(B) Enlarged images of the branched molecule region at 7 hrs in *rec8*Δ, and 13 hrs in *rec8*Δ *ndt80*Δ strains, with different observed species indicated. Red line indicates IS-dHJs, blue line indicates IH-dHJs. Gene conversions are indicated by *
(C) Single end invasions (SEIs), quantified as a proportion of the total DNA for this panel.
(D) Interhomolog double Holliday Junctions (IH-dHJs), quantified as a proportion of the total DNA for this panel.
(E) Total Intersister double Holliday Junctions (IS-dHJs), quantified as a proportion of the total DNA for this panel.
(F) IH:IS bias. The ratio of IH-dHJs to both IS-dHJs bands between 4-8 hours.
The average of two independent diploids is given and error bars represent S.E.M. in graphs C-F Wild type levels are illustrated with a dashed line.
(G) Images of the DSB region at 3,5,7,9 and 13 hour time points *rec8*Δ and *rec8*Δ *ndt80*Δ to qualitatively demonstrate the degree of hyper-resection in each mutant.

Strains: JKD176, JKD177, JKD110, JKD201
Experimental ID: E07_JK1_130928, E26_JK2_150520

smeared, suggesting that hyper-resection is occurring in the absence of *rec8* (Figure 5.2G). This may indicate that cohesin has a protective role with regards to meiotic DSBs.

These results demonstrate that in *rec8*Δ, a lower proportion of DNA is incorporated into the earliest recombination intermediates, SEIs, than is observed in wild type, and that there is a clear reduction in the amount of IH-dHJs formed. There seems to be little reduction in the proportion of IS-dHJs accumulated, and so there is reduction in the IH:IS bias in these mutant strains.

5.2.2. In a cohesin complex deficient background, absence of the Smc5/6 complex leads to a reduction in the levels of crossovers

In order to ascertain whether the Smc5/6 complex still affected meiotic recombination intermediates in the absence of functional meiotic cohesin, levels of DSBs and crossovers were analysed in double mutants. DSBs accumulated to broadly similar levels in the presence and absence of Smc5/6 complex mutants, although the peaks did tend to occur later than in *rec8*Δ single mutant (peaking at 3.3% ±0.7 of total DNA for *rec8*Δ nse4-mn, and 2.9% ±0.4 for *rec8*Δ *smc5-mn*, both at the 8-hour time point) (Figure 5.3B). Crossovers accumulated to lower levels by the latest time points (6.2% ±0.5 of total DNA for *rec8*Δ *nse4-mn*, and 6.4% ±0.3 for *rec8*Δ *smc5-mn*) (Figure 5.3C).

This is in line with what we would expect – the absence of Smc5/6 complex does not appear to affect the level of DSB accumulation when recA homologues are present (Figure 3.4B) (COPSEY, et al., 2013), and so we would not

A

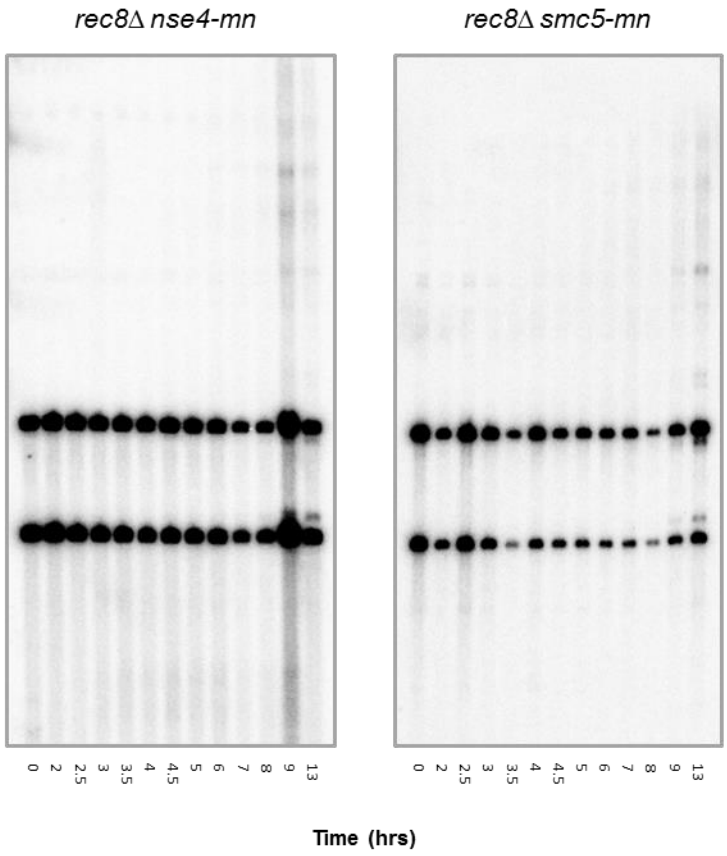
rec8Δ nse4-mn
rec8Δ smc5-mn
0 2 2.5 3 3.5 4 4.5 5 6 7 8 9 13
0 2 2.5 3 3.5 4 4.5 5 6 7 8 9 13
Time (hrs)

B

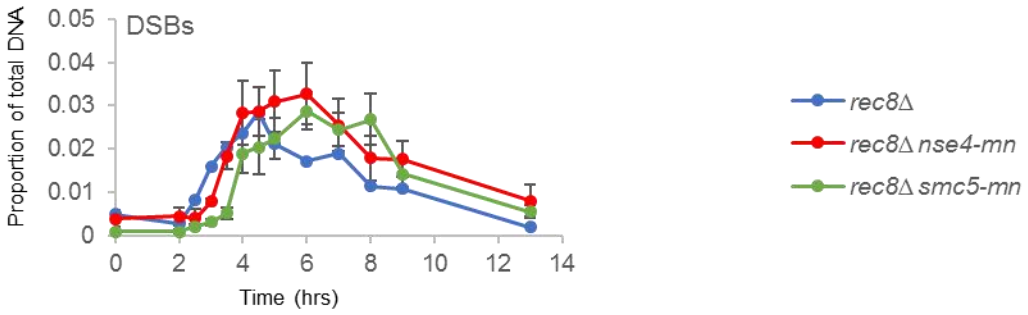
DSBs
Proportion of total DNA
0.05
0.04
0.03
0.02
0.01
0
0 2 4 6 8 10 12 14
Time (hrs)
rec8Δ
rec8Δ nse4-mn
rec8Δ smc5-mn

C

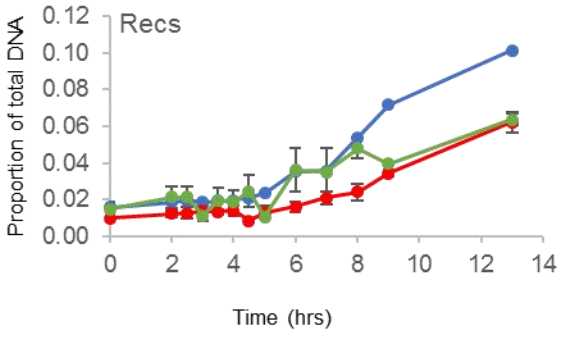
Recs
Proportion of total DNA
0.12
0.10
0.08
0.06
0.04
0.02
0.00
0 2 4 6 8 10 12 14
Time (hrs)

Figure 5.3 In the absence of the Smc5/6 complex, *rec8*Δ cells produce fewer crossovers and accumulate DSBs later into meiosis

(A) Representative 1D Southern blots of *rec8*Δ *nse4-mn*, and *rec8*Δ *smc5-mn* strains.
(B) Double strand break levels over a 13 hour meiotic timecourse, quantified as a proportion of total detectable DNA species in the lane.
(C) Levels of recombinant molecules during a 13 hour meiotic timecourse, quantified as a proportion of total detectable DNA species in the lane.
The average of two independent diploids is given, and error bars represent S.E.M. for graphs B-C

Strains: JKD112, JKD1113, JKD182, JKD178
Experimental ID: E07_JK1_130718, E26_JK2_150520

anticipate it affecting the level of accumulation here. A reduction in recombinants suggests an aberration to the repair process in the absence of the Smc5/6 complex, even in the absence of a functional meiotic cohesin complex.

5.2.3. In the absence of meiotic cohesin, Smc5/6 complex mutants cause accumulation of JMs

In order to determine whether the accumulation of specific JMs is affected by the absence of Smc5/6 complex components in conjunction with *rec8*Δ, two-dimensional electrophoresis was undertaken (Figure 5.4). It is immediately apparent that there is an increase in the proportion of all JMs at the latest time-points in the double mutants (Figure 5.4A & B). We observe that JMs appear to persist for longer and accumulate to higher levels than is observed in the *rec8*Δ single mutant. In *rec8*Δ *nse4-mn* and *rec8*Δ *smc5-mn* strains, it is observed that SEIs become detectable with similar timing as is observed in *rec8*Δ single mutant. However, in the double mutants, rather than accumulating to a peak and then being removed, the proportion of SEIs increases to the latest time point observed, with a greater accumulation in the *nse4-mn* (0.58% ±0.05 of total DNA for *rec8*Δ *nse4-mn*, and 0.32% ±0.05 for *rec8*Δ *smc5-mn*) (Figure 5.4C).

IH-dHJs and IS-dHJs followed a similar progression for the double mutants; becoming detectable at the same time as in *rec8*Δ single mutants, however, unlike in *rec8*Δ mutants where levels of these intermediates peaks and then falls, the dHJs in the double mutant continues to accumulate over the length of the timecourse. For IH-dHJs this accounted for 1.1% ±0.25 of total DNA for

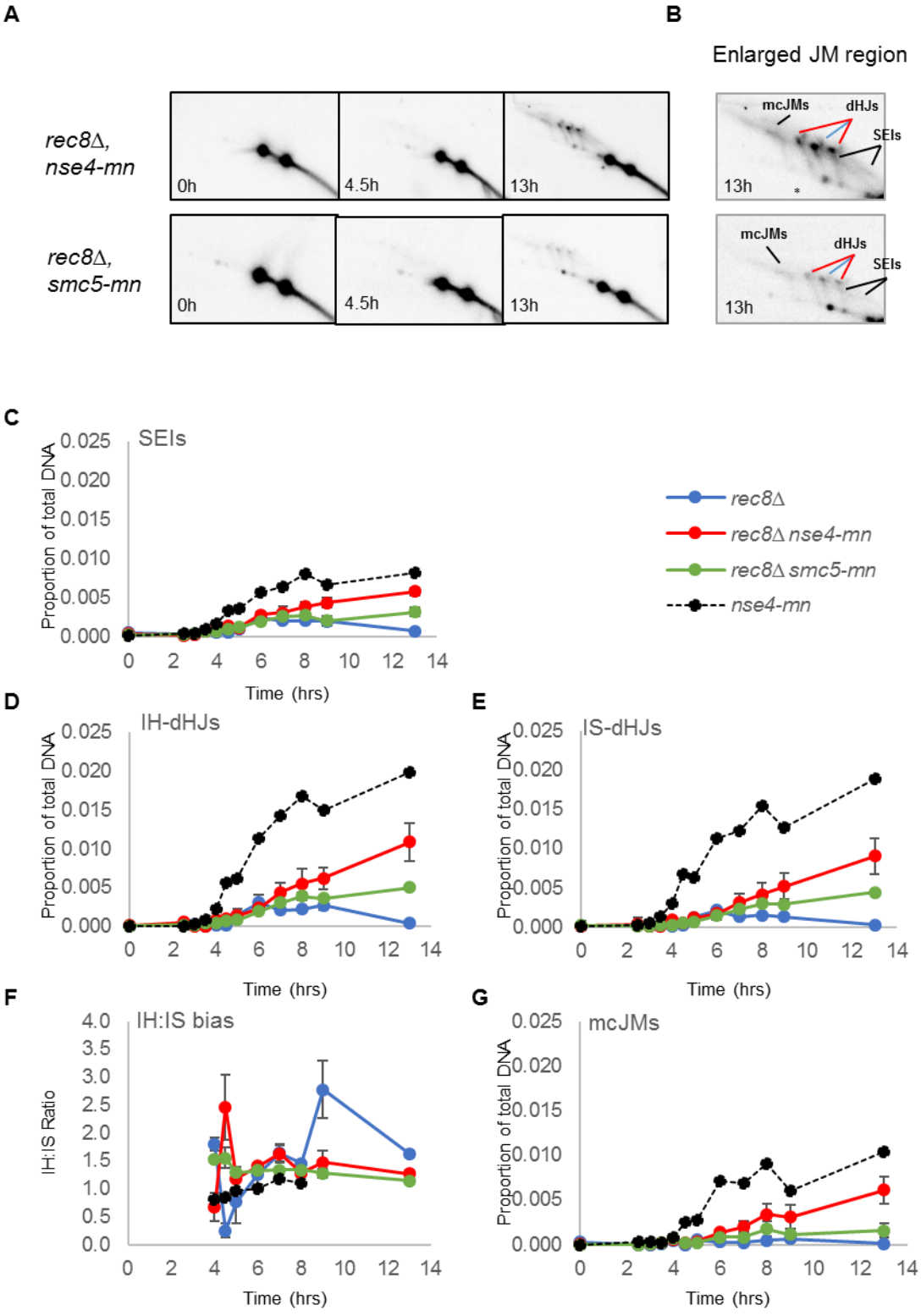
A
B
Enlarged JM region
rec8Δ, nse4-mn
rec8Δ, smc5-mn
0h
4.5h
13h
mcJMs
dHJs
SEIs
C
SEIs
Proportion of total DNA
Time (hrs)
rec8Δ
rec8Δ nse4-mn
rec8Δ smc5-mn
nse4-mn
D
IH-dHJs
E
IS-dHJs
F
IH:IS bias
IH:IS Ratio
G
mcJMs

Figure 5.4 In the absence of the Smc5/6 complex, *rec8*Δ accumulate joint molecules, and there is no apparent interhomolog bias

(A) Representative images of key time points (T=0,4.5,13) in *rec8*Δ *nse4-mn* and *rec8*Δ *smc5-mn* strains.
(B) Enlarged images of the branched molecule region at 13 hrs in *rec8*Δ *nse4-mn* and *rec8*Δ *smc5-mn* strains, with different observed species indicated. Red line indicates IS-dHJs, blue line indicates IH-dHJs. Gene conversions are indicated by *
(C) Single end invasions (SEIs), quantified as a proportion of the total DNA for this panel.
(D) Interhomolog double Holliday Junctions (IH-dHJs), quantified as a proportion of the total DNA for this panel.
(E) Total Intersister double Holliday Junctions (IS-dHJs), quantified as a proportion of the total DNA for this panel.
(F) IH:IS bias. The ratio of IH-dHJs to both IS-dHJs bands between 4-8 hours.
(G) Multi-chromatid joint molecules (mcJMs), quantified as a proportion of the total DNA for this panel.
The average of two independent diploids is given and error bars represent S.E.M. in graphs C-F

Strains: JKD112, JKD1113, JKD182, JKD178
Experimental ID: E07_JK1_130718, E26_JK2_150520

*rec8*Δ *nse4-mn* at the latest time point, and 0.50% ±0.03 for *rec8*Δ *smc5-mn* (Figure 5.4D). With regards to IS-dHJs this accounted for 0.90% ±0.23 of total DNA for *rec8*Δ *nse4-mn* at the latest time point, and 0.44% ±0.01 for *rec8*Δ *smc5-mn* (Figure 5.4E).

At peak dHJ accumulation in *rec8*Δ single mutants, no difference in IH:IS bias is observed (IH:IS bias of 1.41 ±0.04 for *rec8*Δ *nse4-mn* strains and 1.32 ±0.02 for *rec8*Δ *smc5-mn* at 6 hours) (Figure 5.4E). However, at later time points in the double mutants, where levels of dHJs are too low in the *rec8*Δ single mutant to determine an accurate bias, the IH:IS bias becomes lower in the double mutants (IH:IS bias of 1.26 ±0.05 for *rec8*Δ *nse4-mn* strains and 1.14 ±0.02 for *rec8*Δ *smc5-mn* at 13 hours). Hence, the extent to which this is a valid assessment of the establishment of IH:IS bias is open to debate, as we would anticipate a higher rate of turnover of joint molecules in the presence of a functional Smc5/6 complex than in its absence, which may distort the ratio. This will be addressed in the next section (5.2.4). Finally, whilst in the absence of *rec8* we see no appreciable levels of mcJMs, we do see accumulations of mcJMs in the double mutants, which show similar accumulation profiles to other JM species, with the highest levels of mcJMs observed at the latest time-points for *rec8*Δ *nse4-mn* mutants (0.61% ±0.15 of total DNA), whilst in *rec8*Δ *smc5-mn* mcJMs peak at 8 hours (0.17% ±0.08 of total DNA), before the proportion of mcJMs plateaus.

These data indicate a role in JM resolution for the Smc5/6 complex in a context of abnormal chromosome architecture, and suggests that the Smc5/6

complexes functions in meiotic recombination are independent of its previously characterised roles in cohesin organisation, as these effects persist in the absence of the Smc5/6 complex. SEIs and double Holliday junctions show similar initial accumulation rates in *rec8*Δ, regardless of the presence of a functional Smc5/6 complex. This suggests that the Smc5/6 complex is unlikely to have a significant role in the formation of these branched intermediates in this context, instead indicating a predominant role in the resolution and turnover of these intermediates, which appears to be at least partially blocked in the absence of the Smc5/6 complex, leading to the high levels of accumulation at later time points.

5.2.4. In *rec8* strains which do not exit pachytene, the Smc5/6 complex generates an interhomolog bias.

In order to accurately determine whether the Smc5/6 complex has a role in generating IH:IS bias in the absence of *rec8*, I compared the levels of JMs observed in an *rec8*Δ *ndt80*Δ mutant background, in the presence or absence of *nse4* meiotic depletion. We observe that DSBs accumulate to very similar levels in the double and triple mutants (peaking at 2.9% ±0.22 in *rec8*Δ *ndt80*Δ, and 2.5% ±0.27 in *rec8*Δ *ndt80*Δ *nse4-mn*, both at the 4-hour time point) and share similar shaped accumulation profiles, with DSBs persisting late into the time course (Figure 5.5C). Crossovers accumulate to higher levels in the double mutant compared to the triple mutant (6.4% ±0.13 in *rec8*Δ *ndt80*Δ, and 4.0% ±0.07 in *rec8*Δ *ndt80*Δ *nse4-mn*) (Figure 5.5D), which is consistent with the data obtained in *rec8*Δ mutants which may exit pachytene.

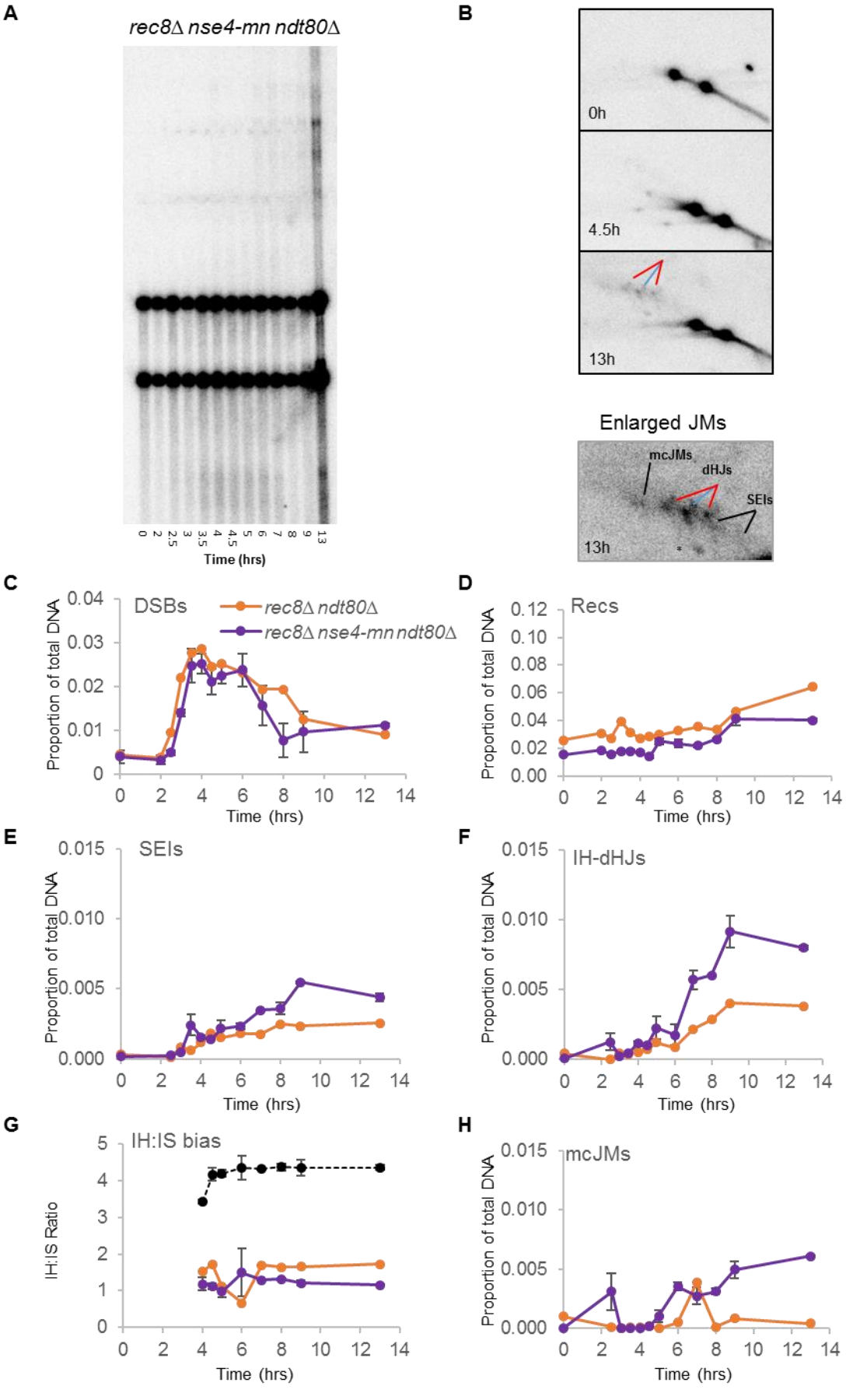
A
rec8Δ nse4-mn ndt80Δ
0 2 2.5 3 3.5 4 4.5 5 6 7 8 9 13
Time (hrs)
B
0h
4.5h
13h
Enlarged JMs
mcJMs
dHJs
SEIs
13h
C
DSBs
rec8Δ ndt80Δ
rec8Δ nse4-mn ndt80Δ
Proportion of total DNA
Time (hrs)
D
Recs
Proportion of total DNA
Time (hrs)
E
SEIs
Proportion of total DNA
Time (hrs)
F
IH-dHJs
Proportion of total DNA
Time (hrs)
G
IH:IS bias
IH:IS Ratio
Time (hrs)
H
mcJMs
Proportion of total DNA
Time (hrs)

Figure 5.5 In the absence of the Smc5/6 complex, there is a reduction in interhomolog bias in *rec8*Δ *ndt80*Δ mutant strains

(A) Representative 1D Southern blot of an *rec8*Δ *ndt80*Δ *nse4-mn* strain.
(B) Representative images of key time points (T=0,4.5,13) in *rec8*Δ *ndt80*Δ *nse4-mn* strain in 2D Southern analysis. Last panel is an enlarged image of the branched molecule region at 13 hrs, with different observed species indicated. Red line indicates IS-dHJs, blue line indicates IH-dHJs. Gene conversions are indicated by *
(C) Double strand break levels over a 13 hour meiotic timecourse, quantified as a proportion of total detectable DNA species in the lane
(D) Levels of recombinant molecules during a 13 hour meiotic timecourse, quantified as a proportion of total detectable DNA species in the lane
(E) Single end invasions (SEIs), quantified as a proportion of the total DNA for this panel.
(F) Interhomolog double Holliday Junctions (IH-dHJs), quantified as a proportion of the total DNA for this panel.
(G) IH:IS bias. The ratio of IH-dHJs to both IS-dHJs bands. *ndt80* Δ is modelled in as the dashed black line.
(H) Multi-chromatid joint molecules (mcJMs), quantified as a proportion of the total DNA for this panel.
The average of two independent diploids is given and error bars represent S.E.M. Wild type levels are illustrated with a dashed line in graphs C-H

Strains: JKD111, JKD180
Experiment ID: E26_JK2_150520

In two dimensional analyses, we observe that the triple mutant, with *nse4-mn*, accumulates JMs to higher levels than those observed in the double mutant. At the latest time point, SEIs account for 0.25% ±0.03 of total DNA in *rec8*Δ *ndt80*Δ, and 0.44% ±0.01 in *rec8*Δ *ndt80*Δ *nse4-mn* (Figure 5.5E). IH-dHJs followed a similar pattern of accumulation, and at 13-hours the levels appeared to have plateaued, to 0.38% ±0.02 of total DNA in *rec8*Δ *ndt80*Δ, and 0.80% ±0.01 in *rec8*Δ *ndt80*Δ *nse4-mn* (Figure 5.5F). IS-dHJs exhibited a similar profile of accumulation and then plateauing of levels of the JM species (0.22% ±0.01 of total DNA in *rec8*Δ *ndt80*Δ, and 0.70% ±0.01 in *rec8*Δ *ndt80*Δ *nse4-mn*) (data not shown).

We observe a reduction of IH:IS bias in pachytene blocked *rec8*Δ which lack *nse4* compared with those with functional Smc5/6 complex (IH:IS bias of 1.72 ±0.02 for *rec8*Δ *ndt80*Δ strains and 1.15 ±0.06 for *rec8*Δ *ndt80*Δ *nse4-mn* at 13 hours) (Figure 5.5F). This suggests that there is a shift in the bias of the formation of dHJs in the absence of Smc5/6, and that this is independent of the role of the cohesin complex in determining bias. In addition, as this is observed in pachytene exit blocked cells, the reduction of bias is not an artefact of different levels of turnover for IS-dHJs as opposed to IH-dHJs, and is a result of an earlier meiotic function of the Smc5/6 complex. Finally, we observe that mcJMs accumulate and persist in the triple mutant, whilst when the Smc5/6 complex is present, there is no persistence of mcJMs (Figure 5.5G).

These data support much of what was observed when Ndt80 was present, showing that the absence of a functional Smc5/6 complex does not appear to

have an effect on the accumulation of DSBs, nor on the initial rate of accumulation of SEIs and dHJs. Instead, mutants with *nse4-mn* genotype appear to accumulate JMs to higher levels, particularly at the latest time points. This suggests that there is still some turnover of JM intermediates in the absence of *ndt80* (which is also implied by the presence of recombinants in the one-dimensional analysis), and that this limited turnover is reduced in the absence of *nse4*.

5.3. Discussion

Here, I attempted to determine whether the functions of the Smc5/6 complex, with regards to both the accumulation of JMs and the effect that the complex has on interhomolog bias, were dependent on the cohesin complex, which has been shown to be regulated by the Smc5/6 complex in some instances.

5.3.1. In *rec8* strains, there is a reduction in the accumulation of IH-dHJs and crossovers.

In *rec8*Δ strains, we observe that levels of DSBs are reduced, and that crossovers do not accumulate to wild type levels (Figure 5.1). There is a further reduction in levels of recombinant DNA when pachytene exit is blocked, suggesting that many of the crossovers formed in *rec8*Δ strains are formed via canonical meiotic repair pathways. IH-dHJs accumulate to lower levels in *rec8*Δ strains than in wild type, whilst the levels of IS-dHJs remains relatively similar. This leads to a shift in IH:IS bias away from interhomolog repair. These data are broadly similar to the published literature (KLEIN, et al., 1999; BRAR, et al., 2009), however I observe a reduction in the level of DSBs compared to wild type, unlike the published literature. Furthermore, whilst I do observe a shift in IH:IS bias in the absence of *rec8*, it is less severe than the 1:1 ratio previously observed (KIM, et al., 2010).

There appears to be significant delays in the earliest detection of all meiotic repair intermediates, suggesting that the significant structural aberrations expected in the absence of meiotic cohesin is inhibiting the timely meiotic progression of intermediates. Given that DSBs appeared to accumulate with

similar timing to wild type in the *rec8*Δ strains, this would suggest that the delay occurred in the formation of JMs as opposed to the initiation of meiotic recombination with DSBs.

In addition, the shift in IH:IS bias appears to be a result of a decrease in the accumulation of IH-dHJs; even when pachytene exit was blocked, IH-dHJs failed to accumulate to the same peak levels as is observed in wild type. This would suggest that the meiotic cohesin complex is necessary for the preferential formation of interhomolog interactions in meiosis. Given that Rec8 is a crucial part of the lateral element of the synaptonemal complex, this is not entirely surprising.

5.3.2. Smc5/6 complex mutants maintain their JM accumulation phenotype, and have reduced levels of crossovers, in the absence of *rec8*

We observed that accumulation of meiotic DSBs was not affected by the presence of the Smc5/6 complex in *rec8* deficient strain backgrounds. In addition, *rec8*Δ strains accumulated less crossovers in *nse4-mn* mutant backgrounds. This was indicative of early meiotic events being unaffected in this context, whilst the later stages of the repair pathway are being affected by the absence of the Smc5/6 complex. We observed that JMs accumulated to higher levels in the absence of the Smc5/6 complex. In the more severe *nse4-mn* background, we observed an accumulation of all categorised intermediates, whilst in the hypomorphic *smc5-mn* strain, we observe a similar level of accumulation of JMs as seen in the *rec8*Δ single mutant, but that these levels persist across observed time points. Together these data suggest that the JM

accumulation phenotype observed in Smc5/6 complex mutants, or to be more descriptive a JM resolution defect, is not dependent on the presence of the cohesin complex.

This suggests that the Smc5/6 complex has two distinct roles throughout meiotic prophase. Firstly, it has a role in facilitating meiotic recombination, both at the earliest stages (discussed in Chapter 4), and in enabling the resolution of JMs. Independently, the Smc5/6 complex has a role in regulating meiotic cohesin. It should be noted that whilst this study has demonstrated that the accumulation of JMs in Smc5/6 complex mutants is not dependent on the complexes role regulating cohesin, the converse has not been shown to be true, and it may yet be shown to be the case that the extended retention of cohesin on chromosome arms (COPSEY, et al., 2013) may be a response to the accumulation of aberrant JMs; this would be an area of interest for future work.

5.3.3. Smc5/6 complex mutants experience a reduction in interhomolog bias, and this is not dependent on the presence of *rec8*

When pachytene exit is blocked, in the absence of *rec8*, a reduction in bias towards interhomolog repair is observed, compared to wild type. In the absence of the *nse4*, we observe a pronounced reduction in the IH:IS. This would suggest that in a context where cohesin is not present, the Smc5/6 complex is having an important role in determining the ratio of interhomolog to intersister molecules. This is particularly noteworthy, as whilst a reduction in IH:IS bias had been observed previously (COPSEY, et al., 2013), the nature of this alteration in bias had not been fully explored. We can now categorically state

that the Smc5/6 complexes role in IH:IS bias is independent of the activity of the cohesin complex, and consequently is independent of the previously characterised role of the Smc5/6 complex in modulating cohesin localisation.

Taken together, the two-dimensional gel analysis data suggest that in the absence of the Smc5/6 complex, there is a shift in the proportions of JMs observed, such that there is an increase in all detected JMs, and that there is a greater increase in the number of intersister JMs accumulating in the absence of the Smc5/6 complex. This is concordant (although to a far lesser degree) to the shift in bias observed in the absence of the Smc5/6 complex in the absence of *rad51* (Chapter 4). This could be the result of a number of modes of action.

Firstly, we might assume a differential rate of turnover of different intermediates, with the turnover of IS-dHJs more strongly inhibited by the absence of the Smc5/6 complex than IH-dHJs, leading to an apparent shift in the bias of intermediates being caused by differential levels of resolution. However, if this were the case, we might expect that in the absence of the transcription factor Ndt80, which should block pachytene exit and hence all resolution of dHJs, we would see an alleviation of this shift. This is not the case, and hence we should discount this model.

A second model which the data appears to favour, would be a role of the Smc5/6 complex in preventing the formation of IS-dHJs at an earlier stage, and thus having a role in lessening intersister bias as opposed to generating interhomolog bias. It would explain the data observed in *rec8*Δ cells, which

might be considered a no-bias context with regards to repair – as this model would assume that the Smc5/6 complex would not be affecting bias specifically, but instead the levels of IS-dHJs in particular. This would be in addition to its previously characterised role in enabling the resolution of all dHJs (and in the absence of *rec8,* we see an accumulation of both IH-dHJs and IS-dHJs in the absence of *nse4*). This reinforce the model suggested in the previous chapter regarding the role of the Smc5/6 complex as anti-establishment factor, specifically of intersister interactions.

Chapter 6

DSB formation adjacent to the *HIS4* locus shows a disparity between alleles in response to environmental factors

6.1. Introduction

6.1.1. Historic evidence of DSB disparity

Much of the work of the previous chapters focused on a bias in the formation of repair intermediates at meiosis, between intersister and interhomolog interactions. However, little has been studied on the potential implications on the uneven formation of DSBs on homologous chromosomes with different alleles. The potential for this disparity has been shown in previous studies looking at gene conversions at the *HIS4* DSB hotspot (DETLOFF, et al., 1991; ALANI, et al., 1994), although it is not observed in all studies (HOFFMANN, et al., 2005). A disparity of repair outcomes (and hence DSB formation) has also been observed at the *URA3-ARG4* DSB hot spot (JESSOP, et al., 2005), suggesting that this might be a phenomenon prevalent at several genomic locations.

The underlying premise of these studies involves the process of mis-match repair in generating gene-conversions (BISHOP, et al., 1987; HOLLIDAY, 1964). Following the formation of a meiotic DSB, and resection, the ssDNA invades the template strand, and associates in a manner dependant on complementary base-pairing. If there is a base mis-match in this pairing, then the mismatch is liable to be repaired, resulting in the conversion of one allele to that of the template. In this scenario, we would expect that if there was a disparity in DSB break formation between strands, then we would observe a disparity in the frequency of conversion events, such that the allele which is less frequently broken is more commonly found in conversion events.

This is somewhat complicated by situations where mis-matched heteroduplex DNA is not repaired, and hence mismatches in heteroduplex DNA can persist passed the end of meiosis. This leads to different alleles being replicated during the round of DNA replication following meiosis, which leads to the daughter offspring possessing distinct genotypes and phenotypes (Figure 6.1C), generating post meiotic segregation (PMS) events.

An additional layer of complexity is that different base pair mismatches appear to be repaired with different efficiency by the meiotic repair machinery (WHITE, et al., 1985). Particularly, C/C mismatches appear resistant to repair, and in the *his4-ATC* system used in many of the studies, C/C mismatches are generated (DETLOFF, et al., 1991). Hence, biases in DSB formation might be potentially masked.

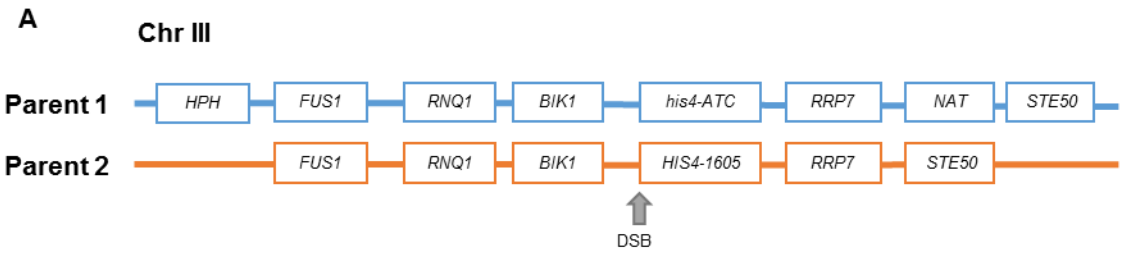
A
Chr III
Parent 1
HPH
FUS1
RNQ1
BIK1
his4-ATC
RRP7
NAT
STE50
Parent 2
FUS1
RNQ1
BIK1
HIS4-1605
RRP7
STE50
DSB

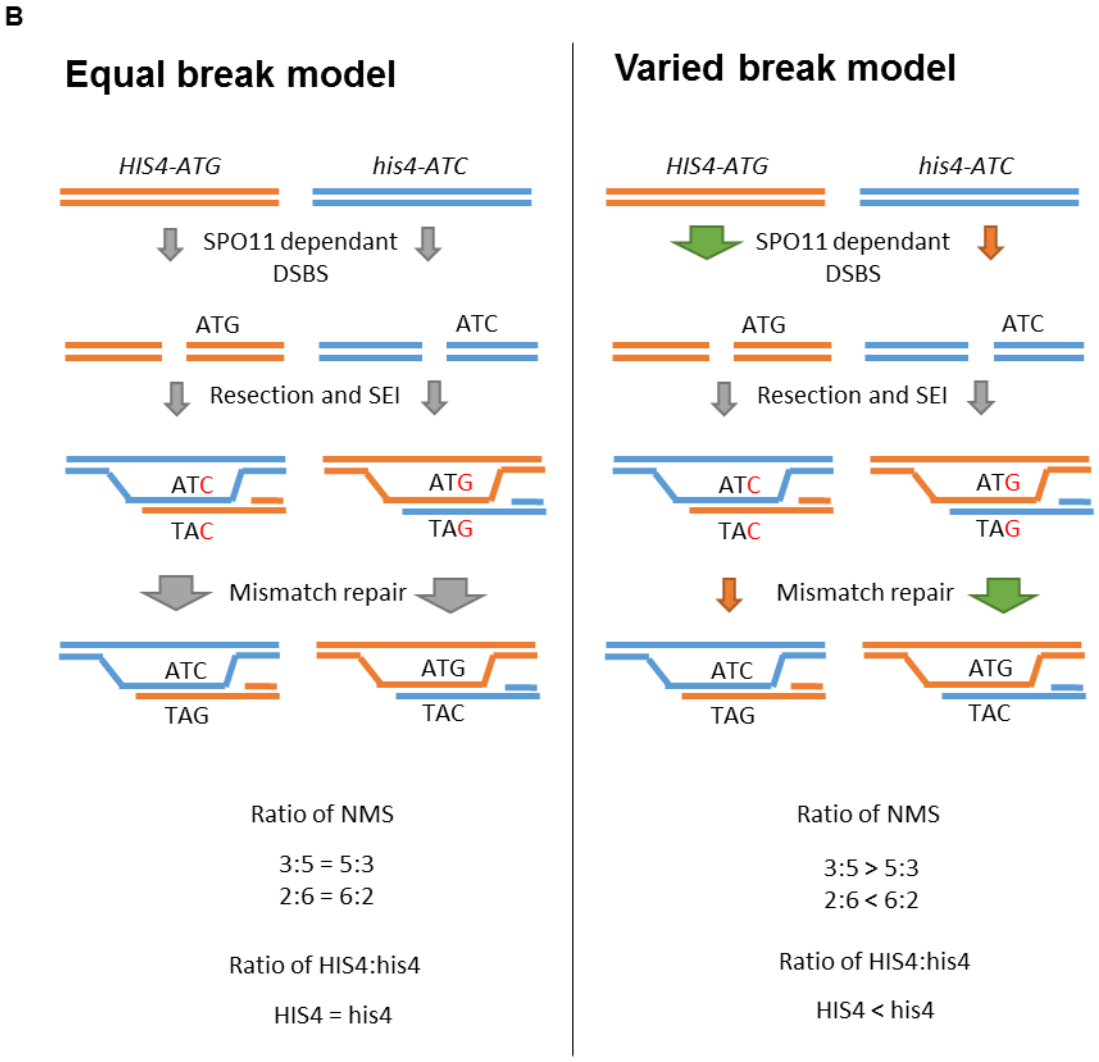
B
Equal break model
HIS4-ATG
his4-ATC
SPO11 dependant DSBS
ATG
ATC
Resection and SEI
ATC
TAC
ATG
TAG
Mismatch repair
ATC
TAG
ATG
TAC
Ratio of NMS
3:5 = 5:3
2:6 = 6:2
Ratio of HIS4:his4
HIS4 = his4
Varied break model
HIS4-ATG
his4-ATC
SPO11 dependant DSBS
ATG
ATC
Resection and SEI
ATC
TAC
ATG
TAG
Mismatch repair
ATC
TAG
ATG
TAC
Ratio of NMS
3:5 > 5:3
2:6 < 6:2
Ratio of HIS4:his4
HIS4 < his4

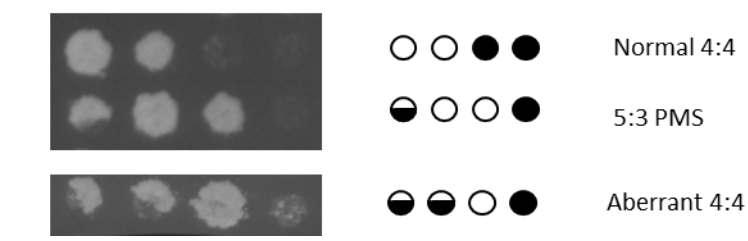
C
Normal 4:4
5:3 PMS
Aberrant 4:4

Figure 6.1 Experimental approach to investigate gene conversion events during meiosis

(A) Physical map of the region of Chr III surrounding the HIS4 recombination hotspot in Y55 strain. The haploid strains have a variety of auxotrophic markers on other chromosomes to allow assessment of recombination outcomes, however on chromosome III they possess a variety of drug resistance markers inserted around the HIS4 marker (NAT and HPH). In addition, the HIS4 alleles have been engineered such that in Parent 2 there is a functional HIS4 allele, with a silent point mutation at 1605 (See Figure 6.3) and in Parent 1 the start codon has been mutated from ATG to ATC, making the allele non-functional. There are allelic difference between the copies of BIK1, but these are not analyzed in this study.
(B) Diagrammatic representation of two models to be investigated; the equal break model and the varied break model. In the equal break model, DSBs are generated to the same degree on each parental chromosome, and repaired with similar efficacy, leading to similar ratios of HIS4:his4- events. In the unequal break model, different rates of breakage and repair lead to different levels of NMS events. The predicted numerical outcomes are displayed at the bottom of the diagram
(C) Representative images, and diagrammatic representations, of different non-Mendelian segregants observed by genetic analysis.

In three historic papers, very different patterns of gene conversion events are observed at the *HIS4* DSB hotspot on chromosome III (Figure 6.1C). In the data produced in the Borts lab, an equal proportion of *HIS4*$^{+}$:*his4*$^{-}$ events are observed (HOFFMANN, et al., 2005). In the data produced in the Petes lab, a strong bias is observed towards repair using the *HIS4* allele as a template for full 6:2 conversions, (DETLOFF, et al., 1991), whilst half conversion events appear evenly distributed between repair outcomes. A third study appeared to show a high proportion of gene conversions, but with an opposite bias to the that observed in the Petes lab (ALANI, et al., 1994).

This has led to the possibility of two models, one involving a disparity in the formation of DSBs, and one involving no disparity in breaks (Figure 6.1B). The Borts lab data would suggest an even level of breaks being formed, and efficient mismatch repair leading to a high prevalence of full conversion events compared half conversion events. As all intermediates are generated and acted upon without bias, no bias in *HIS4* repair outcomes is observed. The Petes lab data would suggest a disparity in the levels of DSBs, with the *his4-ATC* allele undergoing the greatest proportion of DSB initiation. This would be assumed to lead to a bias of both full conversions and half conversions to *HIS4* repair outcomes; however, as the C/C mismatch is resistant to repair, this leads to an accumulation of 3:5 PMS events, which leads to an apparent loss of bias.

Given the differences in the published literature, particularly with regards to the data obtained at the *HIS4* DSB hotspot, here I shall attempt to determine what factors are leading to differences in repair outcomes. Strain-backgrounds,

media conditions, and the length of post-mating mitotic growth in diploids were all potential areas where we expected that we might observe differences in repair outcomes. I observe that the main difference between the data in the literature are as a result of strain background differences, and likely how these strain backgrounds respond to various experimental conditions. The data obtained here suggest that in general, there is no disparity in the frequency of breaks between *HIS4* alleles, although in specific circumstances, it is possible to generate a disparity.

6.2. Results

6.2.1. Comparison to historic data

Initially, I compared the historic data to model, bias free outcomes to determine whether the biases observed were significant. In the data produced in the Borts lab, an equal proportion of *HIS4*$^{+}$:*his4*$^{-}$ events are observed (116:136, with 7:1 and 8:0 ratios counted twice, as they would represent two DSB repair events, G-test from an equal distribution, p= 0.37) (Figure 6.2A & B), with full conversions making up a larger proportion of events that half conversion events (HOFFMANN, et al., 2005). In the data produced in the Petes lab, a strong bias is observed towards repair using the *HIS4* allele as a template (92:46, p= 0.0094), suggesting that the *his4-ATC* allele is on the chromosome that is undergoing the greatest proportion of DSB initiation (DETLOFF, et al., 1991). Only full conversion events show a bias (46:18, p=0.011), whilst half conversion events appear evenly distributed between *HIS4*$^{+}$:*his4*$^{-}$. It should also be noted that this data shows a higher overall rate of conversion events than is observed in the other studies here (Borts lab showed 1488:243 mendelian to non-mendelian events, compared to 122:134 for Petes lab data, p= 2.7×10^{-39}). A final point of note is that while neither study observed aberrant 4:4 PMS events (Figure 6.1C) in wild type cells, ~4% of the outcomes observed in Detloff et al. 1991 fell within this class. Finally, a third study appeared to show a high proportion of gene conversions, but with an opposite bias to the bias observed in the Petes lab (ALANI, et al., 1994). However, it should be noted that due to the smaller sample size than the other studies, there was no statistically significant difference from an equal

A

Publication	HIS⁺:*his*⁻ ratio										
	8:0	7:1	6:2	5:3	4:4	3:5	2:6	1:7	0:8	Aberrant 4:4	Total spores
Hoffmann et al. 2005	1	1	96	14	1488	15	111	2	3	0	1731
Detloff et al. 1991	9	3	46	22	122	21	18	3	2	10	256
Alani et al. 1994	2	0	6	2	78	0	14	0	0	0	102

B

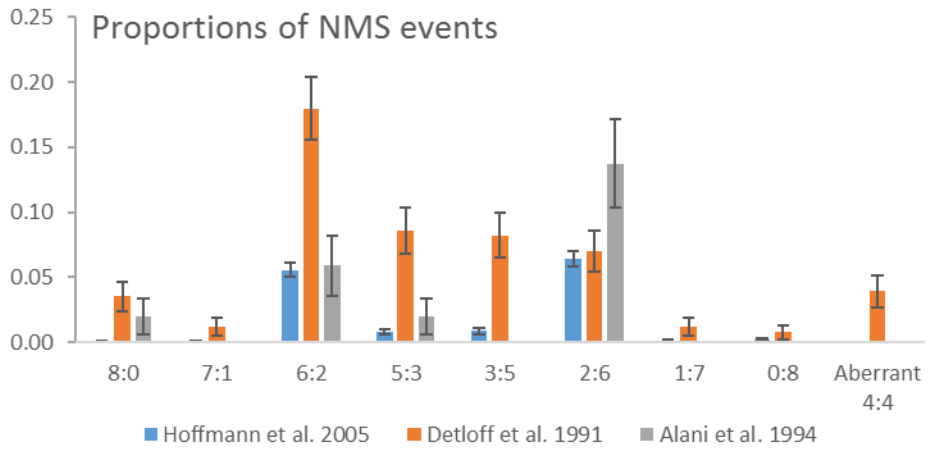

C

Strain	HIS⁺:*his*⁻ ratio										
	8:0	7:1	6:2	5:3	4:4	3:5	2:6	1:7	0:8	Aberrant 4:4	Total spores
WT (*HIS4-1605*)	0	0	21	1	287	6	19	0	1	0	335

D

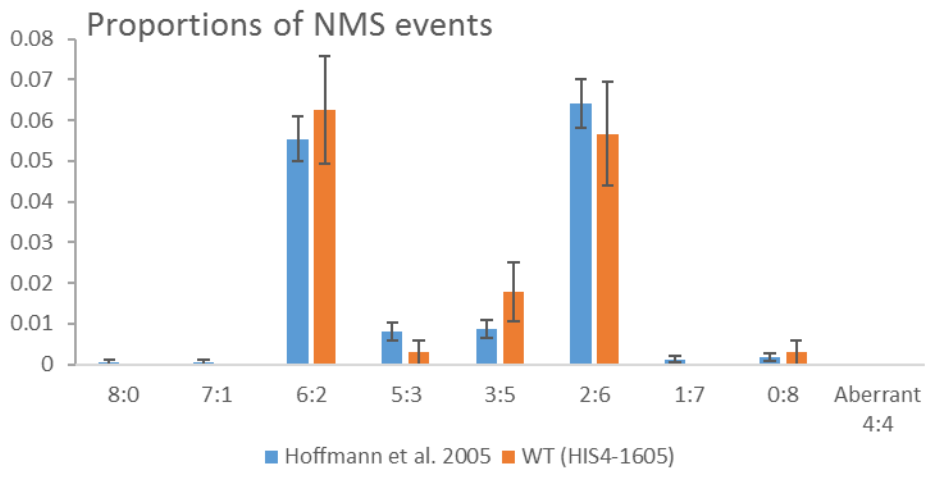

Figure 6.2 Comparisons between modern and historical data

(A) Table of published data from a variety of strains used to investigate recombination and non-Mendelian segregants at the HIS4 locus, utilizing a functional allele, and a non-functional his4-ATC allele. Total number of each species observed, and total number of spores analyzed is displayed.
(B) Graphical representation of the proportion of each NMS species from the 3 strains
(C) Table of NMS data collected in this study, utilizing the same strains and growth conditions as in (HOFFMANN et al., 2005)
(D) Graphical comparison between the data collected in this study, and the data previously obtained in (HOFFMANN et al., 2005), showing the proportion of each NMS species.

distribution of HIS4^{+}:*his4*$^{-}$ events (G-test p= 0.36), and so this study shall focus on the Petes lab and Borts lab data.

There are significant differences between the materials and methods used in these studies which may account for the difference. The strain used by the Petes lab is derived from XJ24-24a, which is less well characterised than many yeast strains. Furthermore, some of its derivatives have unusual patterns of recombination (STRATHERN, et al., 1979), generating exotic chromosome structures. The strain used in the Borts lab was a Y55 derivative, which has been well characterised in meiotic recombination studies (BORTS, et al., 1984; MALKOVA, et al., 2004). Other significant differences were media conditions – with the Borts lab using amino acid supplemented media (ABDULLAH & BORTS, 2001), whilst the Petes lab did not use supplemented media for their study. Allelic difference existed, with a point mutation having been undertaken in the HIS4 allele of the Borts lab strain. Finally, the length of time between mating and sporulation differed significantly between studies, with the Borts lab allowing a 4-hour mating period, before immediately placing cells into sporulation media, whilst the Petes lab made diploid strains which were frozen for storage, and grown for many generations in rich media before sporulation was undertaken.

In the first instance, I attempted to repeat the data obtained in the Borts lab (Figure 6.2C & D). The data that were obtained showed no bias in *HIS4*$^{+}$:*his4*$^{-}$ repair products (22:27, p= 0.610, and were not significantly different from the historic data obtained in the Borts lab, either with regards to the ratio of *HIS4*

events (p= 0.61), or with regards to the relative levels of full conversions when compared to half conversion (p= 0.56). I do observe a bias in PMS events, although the sample size is not adequate to determine whether this is significant. Together, these data suggest that I am able to recreate historic data from the Borts lab, and hence, I will attempt to determine what factors, if any, affect DSB bias in this model system.

6.2.2. Introduced allelic differences do not affect the repair outcomes

The strain utilised in the Borts lab possessed a silent mutation in the *HIS4* at base pair 1605 (*HIS4-1605*, Figure 6.3A), in order to remove a *HhaI* cut site. In order to control for the potential that this site is altering the recombination landscape in an unforeseen manner (for example generating a site of ectopic recombination). We observe no significant differences in *HIS4* bias in the gene conversion events observed in the presence and absence of the *HIS4-1605* allele (17:31 in HIS4 allele, 22:27 in *HIS4-1605*, p= 0.34) indicating that the silent mutation is not having a significant effect on meiotic repair at this locus (Figure 6.3B & C). Allelic variations do not account for the differences observed between the two historic data sets.

6.2.3. Sporulation media composition affects *HIS4* DSB bias

The historic data was obtained in different media conditions, with the Borts lab using amino acid complemented media, and the Petes lab supplementing with adenine but no other amino acids. Given that the gene proximal to the DSB site is an auxotrophic marker, it seemed that this might be a potential source of

A

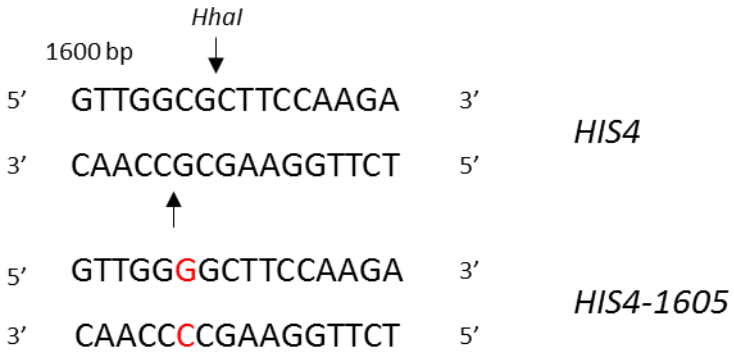

B

Strain	HIS⁺:*his*⁻ ratio										
	8:0	7:1	6:2	5:3	4:4	3:5	2:6	1:7	0:8	Aberrant 4:4	Total spores
WT (HIS4-1605)	0	0	21	1	287	6	19	0	1	0	335
WT (HIS4⁺)	0	0	16	1	294	5	24	1	0	0	341

C

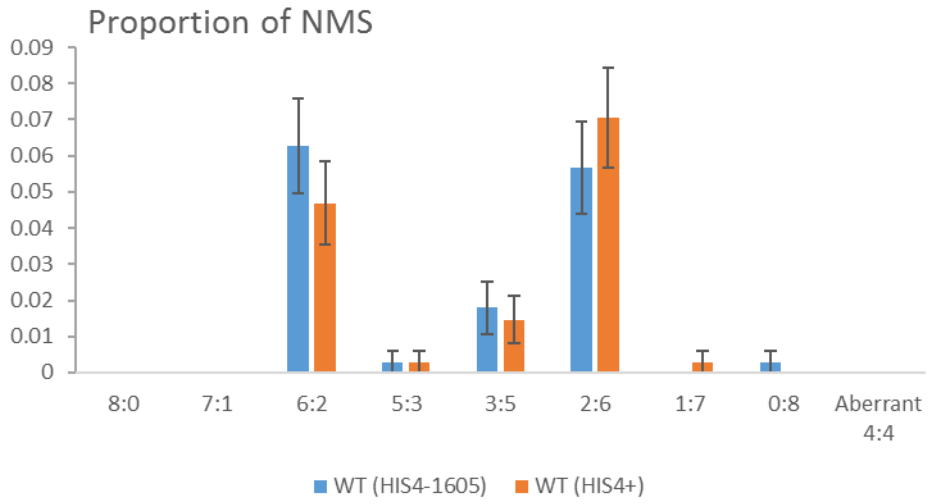

Figure 6.3 The presence of the *Hha*I cut site does not significantly affect the proportion of different NMS species observed

(A) DNA sequence around the *Hha*I cut site in each HIS4 allele. Arrows indicate the *Hha*I cut-site, and the site mutated in HIS4-1605 is shown in red.

(B) Table of results showing the absolute number of each NMS event observed in both mutants

(C) Graphical comparison between the HIS4-1605 and HIS4 wild type strains.

variation. It had been shown that recombination at the *HIS4* DSB site is altered by the metabolic state, particularly with regards to Nitrogen (ABDULLAH & BORTS, 2001), and given the variety of transcription factors involved in HIS4 activation (TICE-BALDWIN, et al., 1989; DEVLIN, et al., 1991), it would seem plausible that the upstream DNA, where the DSB hotspot is located, might potentially be in a more open confirmation, and hence more susceptible to induced breaks, resulting in a bias in the formation of DSBs.

There is no significant difference between *HIS4*$^{+}$ bias in each strain (30:71 in COM media, p= 0.068). However, it does seem as though there is a shift in repair outcomes, to favour *his4-* repair, in a 2:1 ratio (Figure 6.4B). When only full conversion events are considered, there is a significant difference between the media conditions (21:22 in 1% KAc, 27:62 in COM media, p=0.039). This shift is in the opposite direction to what was observed in the Petes lab study, but in the same direction as is observed in (ALANI, et al., 1994).

The most significant difference in methodology between the Petes lab approach and the Kolodner lab is the length of time the diploid cell is grown prior to sporulation (as an approximation for the number of mitoses undertaken). As previously stated, the Petes lab had a long post-mating period before sporulation was induced, whereas the Kolodner lab used the same short mating protocol as the Borts lab. This seemed like a potential cause for differences in DSB formation. Although an area which has not been extensively studied, one could envisage a scenario where diploid yeast that have recently mated might be in a substantially different epigenetic state to cells which have undergone

A

Strain	HIS⁺:*his*⁻ ratio										
	8:0	7:1	6:2	5:3	4:4	3:5	2:6	1:7	0:8	Aberrant 4:4	Total spores
Short mating, 1% KAc	0	0	21	1	287	6	19	0	1	0	335
Long mating 1% KAc	1	0	8	2	235	3	9	0	0	1	259
Short mating COM media	1	0	25	3	597	9	60	0	1	1	697

B

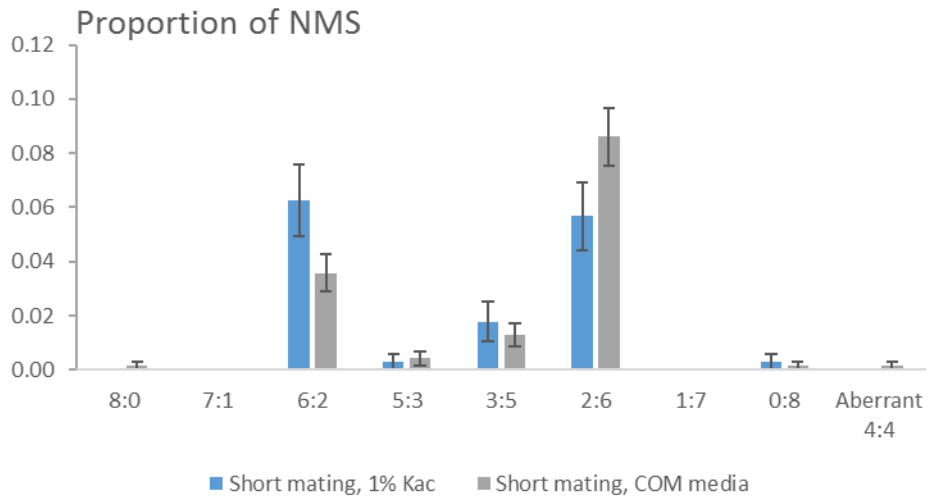

C

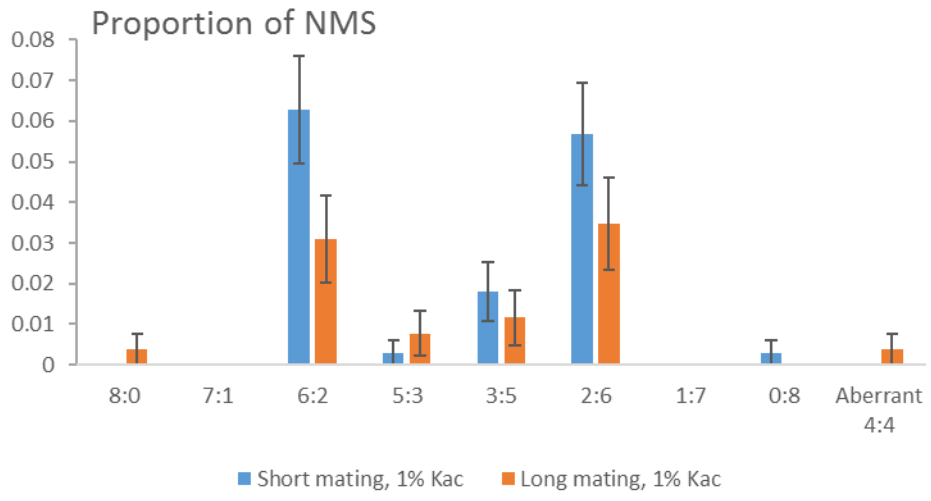

Figure 6.4 The sporulation media significantly alters the bias of HIS repair, whilst The number of mitotic cycles after mating does not

(A) Table of results showing the absolute number of each NMS event observed in 3 conditions: short mating, 1% KAc media; long-mating, 1% KAc media; short-mating, complete media

(B) Graphical comparison between the proportion of NMS events observed in the presence and absence of complete media for short-mating strains.

(C) Graphical comparison between the proportion of NMS events observed in short-mating strains, and strains that have been mated for a longer period.

several diploid cell divisions. Here, we refer to long-mating to describe cells which have undergone several rounds of mitosis (72 hours) as a diploid before being sporulated, whilst short-mating indicates cells which should have had no mitotic cell-divisions after mating and prior to sporulation (4 hours for mating).

However, the data obtained here suggests that in Y55 strain background, the length of mating does not appear to affect DSB break bias (22:27 for short mating, compared to 12:12 for short mating, p= 0.68) (Figure 6.4C). It remains possible that this phenomenon is specifically present in the XJ24-24a background. There is however a reduction in the overall proportion of NMS events in the “long mated” Y55 strain (287:48 for short-mated strains mendelian to non-mendelian events compared to 235:24 in long mated strains, p= 0.025), which suggests that the length of time cells spend in the diploid state prior to meiosis is having an effect on repair outcomes (but not on DSB bias in this instance).

In order to probe whether the different conditions were having more wide reaching effects across the genome, in addition to their effect on the HIS4 DSB site specifically, I analysed the rates of non-mendelian segregation (NMS) at other loci within the same chromosome. I also investigated the genetic distance between the loci, which would give an approximation of the relative rates of recombination in different conditions. I observed no significant differences in the proportion of NMS events observed at a number of sites (Figure 6.5A). In addition, I observed no significant differences in genetic distances between markers on chromosomes III (Figure 6.5B). This suggests that alterations in

A

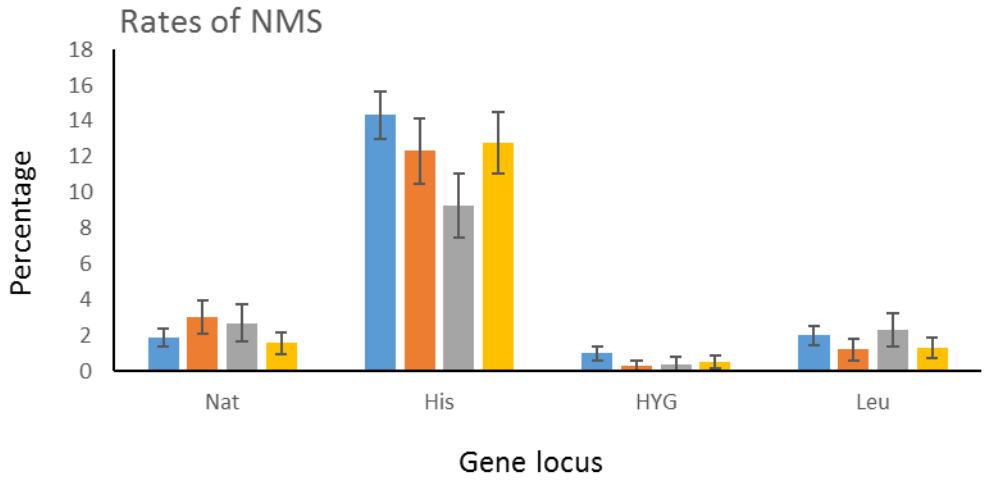

B

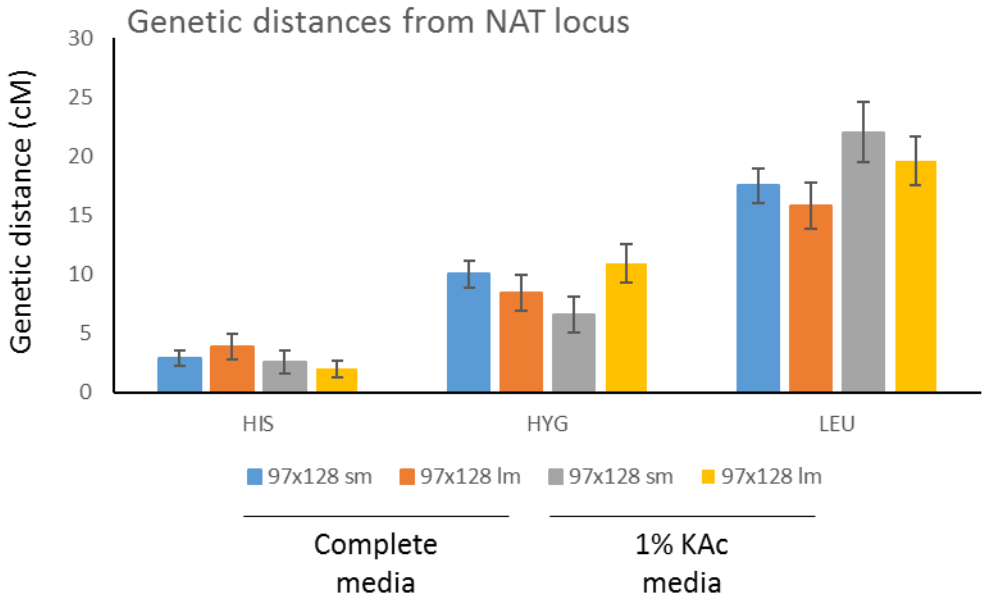

Figure 6.5 The total number of NMS events at non-HIS4 gene loci, and the observed genetic distances, does not differ significantly in a variety of sporulation conditions

(A) Comparison between the proportion of all NMS events observed at a specific loci in four strain conditions: short mating, 1% KAc media; long-mating, 1% KAc media; short-mating, complete media; long-mating, complete media.

(B) Comparison between the genetic distances from the NAT containing locus on chromosome III (in centimorgans) , and other observed loci, in a variety of sporulation conditions.

media conditions and the presence or absence of diploid growth do not appear to affect the global formation and repair of crossovers in a Y55 strain background.

6.2.4. *HIS4* DSB bias is affected by sporulation conditions in XJ24-24a strains

Given that we were unable to recreate the bias observed in the Petes lab XJ24-24a strain background, I decided to investigate whether the factors which we observed to have an effect on gene conversion and apparent *HIS4* DSB formation bias might affect the XJ24-24a strains in a similar manner. In the first instance, I attempted to recreate the data obtained in the original paper (Figure 6.6).

Firstly, I saw a significantly lower proportion of NMS events than was observed in DETLOFF et al. 1991 (270:100 mendelian to non-mendelian events compared to 122:134 in the historic study, $p= 1.3x10^{-6}$) (Figure 6.6B). This may be as a result of different media conditions or unforeseen technical changes to the protocol. However, with regards to bias in *HIS4*$^{+}$*:his4*$^{-}$ NMS events, we observe that there is a bias away from a 1:1 ratio in the new XJ24-24a data (75:33, p= 0.0029), and that there is no significant difference in the bias of intermediates between the historic data and the new data (p= 0.45). Whilst the reduction in the proportion of NMS events creates uncertainty when comparisons are drawn with the historic data, the bias appears to be sufficiently similar that meaningful assessments can be made.

A

Strain	HIS⁺:*his*⁻ ratio										
	8:0	7:1	6:2	5:3	4:4	3:5	2:6	1:7	0:8	Aberrant 4:4	Total spores
Detloff et al. 1991	9	3	46	22	122	21	18	3	2	10	256
XJ24-24a, 1% KAc	7	2	44	14	270	12	19	0	1	1	370
XJ24-24a, COM media	1	0	18	4	171	8	16	0	1	0	219

B

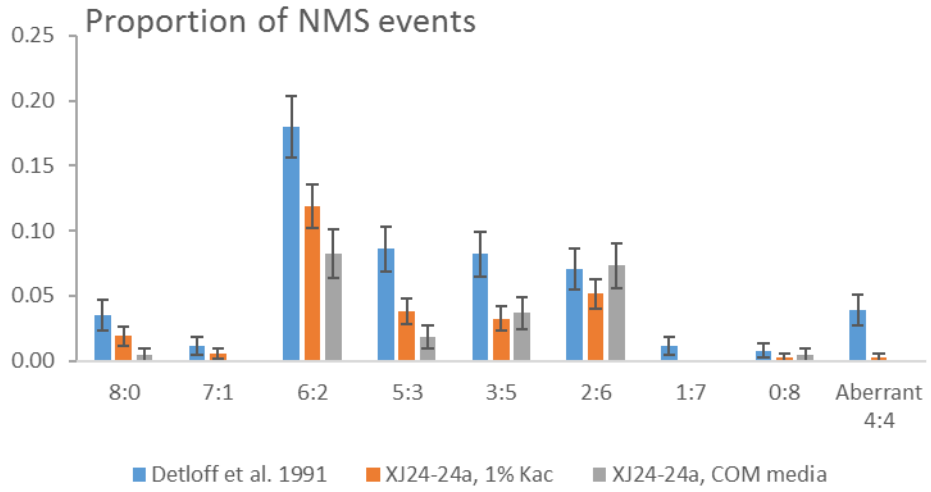

Figure 6.6 In the historic XJ24-24a, a bias towards HIS4 repair products is observed regardless of media conditions

(A) Table of results showing the absolute number of each NMS event observed in (DETLOFF et al., 1991) and 2 experimental conditions: 1% KAc media, and complete media.

(B) Graphical comparison between the proportion of NMS events observed in the three strain backgrounds

I altered the amino acid content of the media, to see whether bias is altered in response to the presence of different nutrients. In the presence of amino acids (COM-media), we observe that the bias between *HIS4*$^{+}$*:his4*$^{-}$ NMS events is lost (24:26, p= 0.81 compared to a predicted 1:1 ratio), and the difference between complete media and 1%KAc is significant (p= 0.0090). Overall, this suggests that the bias in repair outcomes towards *HIS4+* repair outcomes is lost in the presence of amino acid containing sporulation media in XJ24-24a. It should be noted that this is different to the shift observed in Y55 strains (Figure 6.4B), where no bias was observed in amino acid free media, and a bias towards *his-* repair outcomes is observed in amino acid containing media. However, the overall direction of the shift (from favouring *HIS4+* outcomes to favouring *his4-* outcomes) is consistent between strains.

In order to verify whether this “bias shift” is directly comparable in strains that have undergone the same mating procedures, I employed the long mating methodology on Y55 strains, in the presence of complete media. This showed no significant change in bias or levels of repair intermediates when compared with long mated Y55 strains in 1% KAc sporulation media (28:45, p= 0.32), or when compared to a hypothetical 1:1 bias (p= 0.16) (Figure 6.7B). In comparison to XJ24-24a strains, we observe that regardless of media conditions, the proportion of NMS events are lower in Y55 strains (235:40 mendelian to non-mendelian events compared to 270:100 in 1% KAc media, p= 1.0×10^{-8}; 604:71 compared to 171:48 in complete sporulation media, p= 3.8×10^{-5}) (Figure 6.7C). Overall this suggests that any changes in *HIS4* DSB bias that are observed are dependent on the strain background, and the length of diploid

A

Strain	HIS⁺:*his*⁻ ratio										
	8:0	7:1	6:2	5:3	4:4	3:5	2:6	1:7	0:8	Aberrant 4:4	Total spores
Y55, 1% KAc	1	0	8	2	235	3	9	0	0	1	259
Y55, COM media	0	1	22	4	604	5	38	0	1	0	675
XJ24-24a, 1% KAc	7	2	44	14	270	12	19	0	1	1	370
XJ24-24a, COM media	1	0	18	4	171	8	16	0	1	0	219

B

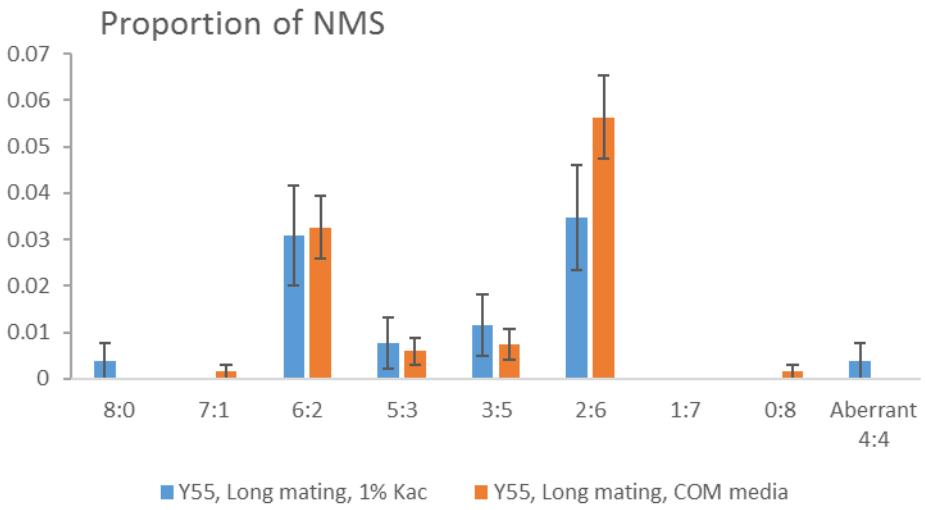

C

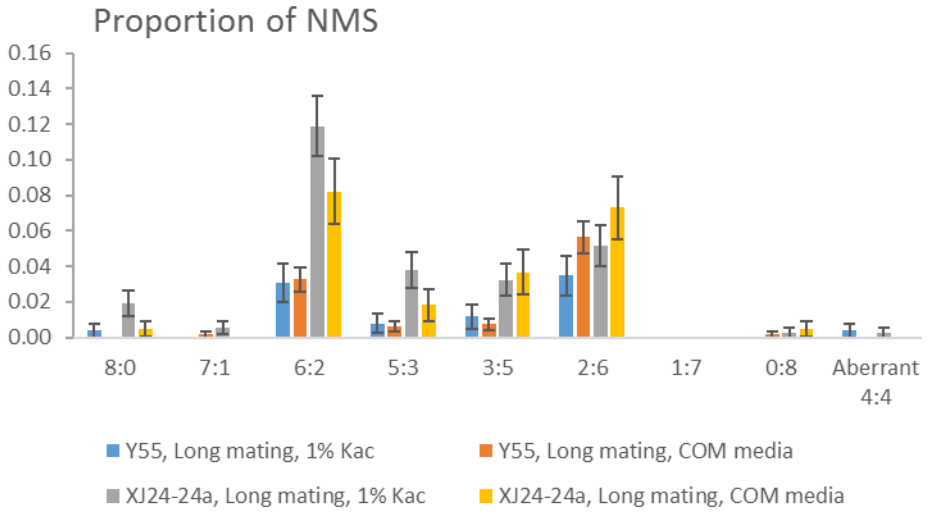

Figure 6.7 The Y55 and XJ24-24a strains have significantly different HIS4 repair biases regardless of media conditions

(A) Table of results showing the absolute number of each NMS event observed in 4 experimental conditions: Y55 background strains, and XJ24-24a in 1% KAc media, and complete media.
(B) Graphical comparison between the proportion of NMS events observed in the long-mating Y55 strains in 1% KAc media, and complete media.
(C) Graphical comparison between the proportion of NMS events observed in four strains in part (A)

growth that has been undertaken, but that it is difficult to predict the effect that might occur on a strain overall.

6.2.5. The freeze-thaw cycle affects DSB formation bias

It has been shown previously that the manner in which yeast cells are frozen for long-term storage has an effect on survival rates of *S. cerevisiae* (MAZUR & SCHMIDT, 1968; PARK, et al., 1997). Given the different methodologies used in the historic studies, it seemed pertinent to investigate whether introducing a freeze thaw cycle to diploid yeast cultures affected the gene conversion outcomes at the *HIS4* locus.

In the XJ24-24a strains, one diploid was mated, streaked, and grown for 72 hours before sporulation. This was compared to the previously characterised diploid, which had been frozen, re-streaked and grown for 72 hours before sporulation. The frequency of NMS events was not significantly different between strains (270:100 mendelian to non-mendelian events compared to 205:85 in the freshly mated strain, p= 0.52) (Figure 6.8B). The bias of gene conversion towards *HIS4+* outcomes does appear reduced in the freshly mated strains, and is no longer significantly different from a 1:1 distribution (54:40, p= 0.31). It is also significantly different from the strain which has undergone a freeze thaw cycle (p= 0.044). These data suggest that introducing a freeze thaw cycle to diploid *S. cerevisiae* may affect *HIS4* DSB formation bias; it seems possible that this might be a consistent source of difference between the historic studies.

A

Strain	HIS⁺:*his*⁻ ratio										
	8:0	**7:1**	**6:2**	**5:3**	**4:4**	**3:5**	**2:6**	**1:7**	**0:8**	**Aberrant 4:4**	**Total spores**
XJ24-24a, frozen pre-sporulation	7	2	44	14	270	12	19	0	1	1	370
XJ24-24a, directly sporulated	3	0	39	9	205	10	28	0	0	1	295

B

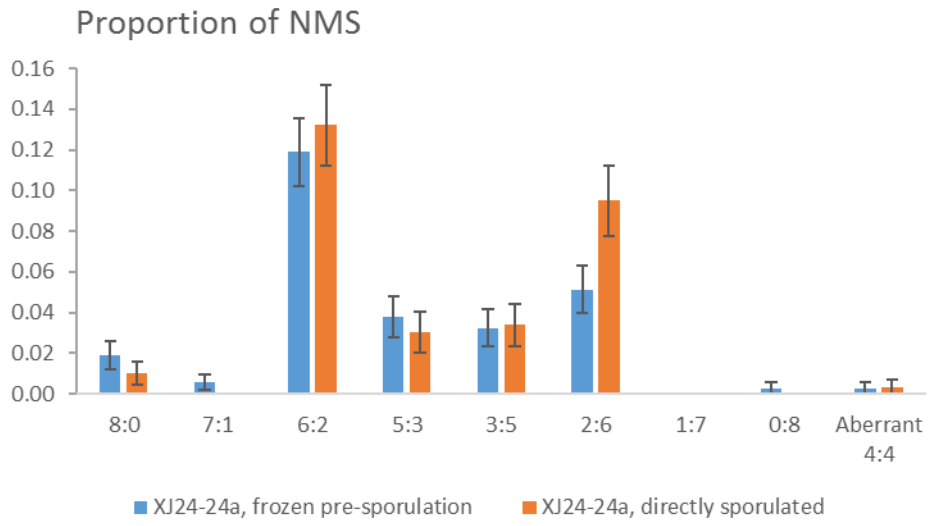

Figure 6.8 The action of freezing a strain prior to sporulation does not affect its HIS4 repair bias

(A) Table of results showing the absolute number of each NMS event observed in two XJ24-24a strains, which differ due to being frozen before being sporulated.
(B) Graphical comparison between the proportion of NMS events observed in the frozen and non-frozen XJ24-24a .

6.3. Discussion

6.3.1. Recreating historic conditions

Initially, I attempted to recreate the data from two historic strain backgrounds, Y55 from the Borts lab, and XJ24-24a from the Petes lab. I was able to recreate the historic data with regards to both the level of NMS events observed, and the bias between *HIS4*+ and *his4*- gene conversion events for the Y55 strain (Figure 6.2D) (HOFFMANN, et al., 2005). In the XJ24-24a strain, I observed a similar bias towards *HIS4*+ repair outcomes as was observed in the original literature (DETLOFF, et al., 1991), however, I was unable to achieve the same level of NMS events; my data exhibited significantly lower levels (Figure 6.5B). This was most likely as a result of unforeseen differences in media. However, as the *HIS4* bias of both of these samples was similar to historic data, we were able to use the new data sets for comparisons with different strain conditions.

6.3.2. A variety of factors affect *HIS4* bias in the strains analysed

As there were a number of technical differences between the methodologies used in the historic study, each variable was analysed in the strains if possible, in order to determine whether this might be affecting the gene conversion data. We observed that allelic differences did not in this instance affect gene conversion outcomes (Figure 6.3), and that the length of mating in the Y55 background did not have an effect on bias, although the number of NMS events detected was significantly reduced in strains which had a long diploid growth phase (Figure 6.4).

The composition of sporulation media did have a pronounced effect on *HIS4* bias, with Y55 which had undergone short mating experiencing a shift from no bias to *his4-* bias in the presence of amino acids (Figure 6.4), and XJ24-24a experiencing a shift from *HIS4+* bias to no bias (Figure 6.6). It should be noted that Y55 strains which had undergone long mating did not experience a shift in bias (Figure 6.7). In addition, whether or not a diploid had experienced a freeze thaw cycle also appeared to have an effect on bias, with the *HIS4+* bias observed in XJ24-24a being eliminated in strains which have been freshly mated.

6.3.3. Varied break model

These data seem to support a varied break model of DSB formation at the *HIS4* locus (Figure 6.1). We observe that bias in the formation of DSB breaks appears to change dependant on a variety of external factors, leading to a bias in the formation of breaks in some instances, and no bias in other settings. I observe that in the Y55 strain that whilst I observe no bias in gene conversions overall (Figure 6.1 & 6.2), there appears to be more 3:5 PMS events. Whilst the number of events is not sufficient to show statistical significance, it would follow the logic of C/C mismatches being repaired with reduced efficacy as has previously been shown (DETLOFF, et al., 1991). Whether this is an active process of determining break bias, or whether it is a passive effect of changes to the epigenetic nature of the chromosome in different situations was not determined, and would be an interesting area of further study.

6.3.4. Potential evolutionary consequences

This leads to the question of what impact this might have on the evolutionary fitness of a particular allele. In this interest, there is clearly an evolutionary conflict. A cell undergoing meiosis must form DSBs in order to generate the chiasmata necessary. However, an allele which does not allow the formation of meiotic DSBs proximal to it is less likely to be the subject of mis-match repair and gene conversion. This would lead us to assume that alleles which repress DSB formation will be selected for, even at the expense of the fitness of the organism overall.

In this instance, however, we observe alleles which, dependant on the media conditions will affect the fitness of the host organism. We observe that in the presence of complete media, which contains the amino acid histidine, we observe a general shift in gene conversion outcomes away from *HIS4+* and towards *his4-*, suggesting a greater proportion of DSB events are occurring on the *HIS4* allele when histidine is present in the media. We might speculate that in a histidine rich environment, the removal of an element of a synthesis pathway, which would require cellular resources to utilise, would be advantageous for the organism in the short term, such that it might more effectively utilise its limited resources. However, at this stage this is purely speculative, but certainly worthy of further investigation.

Chapter 7

Discussion

7.1 The Smc5/6 complex and the ZMM repair pathway

During meiotic recombination in *S. cerevisiae* there are two predominant repair pathways for joint molecule intermediates: repair utilising the ZMM repair pathway, and the Mlh1/3 resolvase to generate crossovers, or repair utilising the Mus81-Mms4 endonuclease to generate an equal proportion of crossovers and non-crossovers. It has previously been suggested that the Smc5/6 complex, which causes severe aberrations to meiotic repair, modulates entry into the Mus81-Mms4 repair pathway, as there is no reduction in crossover accumulation in *mms4 nse4-mn* double mutants compared to *mms4* single mutants (COPSEY, et al., 2013), whereas it appeared that the Smc5/6 complex acted in parallel with the ZMM repair pathway, as there is a synergistic decrease in the level observed in the double mutant lacking both the resolvase and Smc5/6 complex components (*mlh3 nse4-mn*) as opposed to the single *mlh3* mutant alone (COPSEY, et al., 2013). Furthermore, the accumulation of Zip3 foci in the absence of the Smc5/6 complex does not appear to be abrogated (ZHANG, et al., 2014), and given that Zip3 is a component of the ZMM repair pathway, this would suggest that the Smc5/6 complex is not necessarily affecting ZMM pathway repair.

Here, I have shown that when the ZMM pathway is abrogated at an earlier stage (by the deletion of *Mut*S homologue *msh5*), we observe that there is no additional reduction in the level of crossovers compared with *msh5* single mutants. This has two important implications. Firstly, it suggests that once a DSB has been committed to repair by the ZMM pathway, it cannot be resolved by other means. Recombination intermediates are therefore trapped in this repair pathway, which accounts disparity in crossovers accumulation phenotypes observed in the *mlh3 nse4-mn* and *msh5 nse4-mn* double mutants. Secondly, it implies a more general role for the Smc5/6 complex with regards to modulating early recombination events than the Mus81-Mms4 specific role previously proposed. Given that the Smc5/6 complex is recruited to DSBs, this is not necessarily unexpected.

We also observe a clear distinction between the roles of the Smc5/6 complex and the BLM helicase; whilst in *sgs1 msh5* mutants, the removal of sgs1 causes an increased proportion of crossover events (OH, et al., 2007), as a result of anti-crossover functionality of the BLM helicase, no such effect on crossovers is observed in the absence of the Smc5/6 complex. This is another crucial delineation in the roles of the BLM helicase and the Smc5/6 complex, and suggests more specialised roles for the two complexes at the earliest stages of meiotic DNA repair.

The most pertinent area which is left unresolved by the study is whether in mutants which lack both *msh5* and *mms4* in an Smc5/6 complex deficient

background experience a decrease in crossovers – if this was observed to be the case, it might suggest a role for the Smc5/6 complex in determining pathway choice. A further interesting area of future study with regards to the interaction of the Smc5/6 complex and ZMM pathway repair is whether crossovers would be increased in a *msh5 nse4-mn sgs1* triple mutant, by alleviating the anti-crossover role of the BLM helicase, studying this mutant might help to further delineate the roles of the Smc5/6 complex and the BLM helicase in meiosis.

7.2 The Smc5/6 complex is required for the accumulation of DSBs

Given the role of the Smc5/6 complex in the control of early meiotic recombination events, we investigated the effect of the Smc5/6 complex in mutants which accumulate DSBs, the *recA* homologue mutants *rad51* and *dmc1*, which form a nucleo-protein filament with ssDNA generated at the site of meiotic DSBs, and promote strand invasion events (BISHOP, 1994). In the absence of Smc5/6 complex components, *recA* homologue mutants no longer accumulate DSBs, suggesting that they are being repaired in some manner. However, levels of crossovers do not increase, and in *dmc1 nse4-mn* double mutants there is no increase in the level of JMs detected, so it is to be assumed that these DSBs are not being repaired by the canonical meiotic repair machinery. This implies a role for the Smc5/6 complex in modulating the repair of resected DSBs, in keeping with the early function predicted by the early experiments of this study. This would suggest that the Smc5/6 complex has at

least two distinct functions in meiotic DSB repair. Firstly, it acts as a gatekeeper of meiotic DSBs, ensuring that repair occurs via canonical mechanisms. Secondly, its well documented role in enabling the resolution of joint molecules (and hence the accumulation of joint molecules in mutants which lack components of the protein complex).

7.3 The Smc5/6 complex is necessary for the establishment of interhomolog repair bias

In the absence of *rad51*, where all strand invasion events are assumed to be catalysed by the action of Dmc1, we observed that the Smc5/6 complex had a profound effect on interhomolog bias. In the presence of Dmc1 alone, we observed that all detectable joint molecules appeared to persist as interhomolog interactions (although the shape of these intermediates in particular seemed to vary significantly from what is observed in a wild type, as the band appeared smeared in the second dimension of gel electrophoresis). However, in the absence of the Smc5/6 complex, we observed that this bias was reversed, with the greater proportion of repair intermediates being intersister interactions. Such a dramatic shift in repair bias suggests that a fundamental role in determining interhomolog bias in *S. cerevisiae*.

This lead to the conclusion that the Smc5/6 complex is affecting either the establishment of interhomolog bias in a similar manner to that which is observed for the cohesin complex (Figure 1.6), or the later maintenance of this

bias, which has previously been characterised to be controlled by the Red1-Hop1-Mek1 kinase pathway. In order to differentiate the two potential roles, I observed bias observed in the Smc5/6 complex in the absence of the cohesin complex – a further reduction in the IH:IS repair bias is observed, which is emblematic of a defect in the establishment of interhomolog bias, as opposed to the maintenance of bias.

Together, these data suggest a crucial role for the Smc5/6 complex that is independent of its role in the resolution of recombination intermediates. The Smc5/6 complex is required for the accumulation of DSBs in repair deficient background, and is required for the establishment of interhomolog bias at the earliest stages of meiotic DSB repair. Specifically, in a situation where Dmc1 alone is promoting the formation of nascent interactions between ssDNA and the repair template, it would appear that the Smc5/6 complex is necessary to distinguish intersister and interhomolog interactions, and promote the formation of interhomolog interactions. It has been considered that at the formation of ssDNA – repair template interactions, there is the possibility for either the interaction with the sister chromatid or the homologous chromosome to go on to form a stable SEI and joint molecule precursors to repair, and that these interactions require the presence of the cohesin complex in order to be distinguished (KIM, et al., 2010; HONG, et al., 2013). This study suggests that the Smc5/6 complex also has an important role at this stage, and is necessary for promoting the stabilisation of interhomolog interactions. In the absence of stabilisation by the Smc5/6 complex, not only is there a reduction in interhomolog repair bias, but in addition there is a loss of the ability to prevent

the turnover of programmed DSBs by alternative mechanisms to the canonical meiotic repair pathways, suggesting that the Smc5/6 complex has a fundamental role in determining DSB repair fate at the onset of meiotic repair.

This study has not addressed whether, given the role of the Smc5/6 complex in the establishment of interhomolog bias, the Smc5/6 complex has any role in the maintenance of interhomolog bias. By combining the Smc5/6 complex mutations with the *mek1(as)* allele, which experiences a severe reduction in interhomolog bias, we might gain important insights into the role of the Smc5/6 complex at the earliest stages of meiosis.

7.4 The Smc5/6 complexes roles on joint molecule resolution and control of cohesin are independent

The Smc5/6 complex has been shown to have a number of crucial roles in the control of the cohesin complex. In meiosis, in the absence of the Smc5/6 complex, cohesin localisation is temporally mis-regulated along the chromosomes (COPSEY, et al., 2013). Here, I investigated whether the mis-regulation of cohesin might be the cause of the accumulation of joint molecules in the absence of the Smc5/6 complex, given the role of the cohesin complex in DSB repair.

I observed that in mutants lacking both complexes, joint molecules still accumulated, suggesting that the Smc5/6 complexes role in modulating meiotic cohesin was not the factor which caused the accumulation of joint molecules. Instead, this suggests a more direct role of the Smc5/6 complex in the resolution of repair intermediates, which might be as a specific function of its ability to bind to DNA, potentially holding joint molecules in a resolution competent state. This would concur with the observation of distortions in the shape of the double Holliday junction band in Smc5/6 complex mutants, where an elongation in the second-dimension ("teardrop shaped") is detected, suggesting a distortion of the shape of the joint molecule intermediate compared to wild type. Alternatively, it may be the case that the Smc5/6 complex acts as a recruiter of other factors, to enable the efficient resolution of joint molecule repair intermediates; in its absence, there would be a reduction in the ability to recruit repair factors, and thus joint molecules might be accumulated.

It was originally intended that a super-resolution microscopy analysis, utilising PALM technology to determine the role of the Smc5/6 complex in the localisation of meiotic cohesin might form a part of this body of work. Unfortunately, due to technical difficulties with the procedures and equipment, this was not possible. However, better understanding the interaction between these two SMC complexes is likely crucial to fully understanding the functions of the Smc5/6 complex, and future work might contain additional cytological studies to determine the exact manner in which cohesin localisation is

abrogated in meiosis; and a single molecule localisation approach is likely to reveal the nuanced information required to answer these complex questions.

7.5 In *S. cerevisiae*, DSBs may be formed in a biased manner in response to environmental factors

There has been a conflict in the historic literature as to whether there is a bias in the formation of DSBs between distinct alleles at the *HIS4* gene locus (HOFFMANN, et al., 2005; ALANI, et al., 1990; DETLOFF, et al., 1991). The investigations in this study strain specific variations with regards to the formation of DSBs at different alleles, which is presumably what has led to the large discrepancy in the results reported in the published literature. However, a general trend was observed, where the amino acid complement of sporulation media appeared to affect the presence of a bias at the *HIS4* locus, supporting a model of varied DSB breaks (Figure 6.1) in certain environmental contexts. It also seemed that some of the strain specific differences could be identified as variable responses to the action of flash-freezing and defrosting, which occurs upon long-term storage of yeast cultures.

Given that these disparities are occurring at a heavily genetically engineered locus in a laboratory strain, it is difficult to know whether these observations represent an interesting potential phenomenon that might be broadly applicable to the selection of alleles in a general population, or whether this variability is a quirk of having introduced mutations and genetic alterations at nearby locations.

However, the presence of a variable level of break disparity appear logically consistent with the presence of unique alleles in a population; if a bias in the formation of DSBs was universally present, we would expect any allele which is universally more resistant to the formation of proximal DSBs to increase in frequency in the population, as it is used as a template for gene conversions more frequently. Assuming this increase in frequency had a greater impact that genetic drift, we would anticipate this allele would be selected, and become the prevalent allele in the population, thus rendering any appearances of DSB disparity transient.

In this instance on the other hand, it would appear that in a number of environmental scenarios, there is no selective pressure on alleles from DSB disparity, and so (assuming minimal genetic drift and a lack of other selective pressures) the alleles might co-exist in a relatively stable manner. However, when environmental factors change, the introduction of variable levels of DSBs on different alleles could potentially lead to the accelerated selection of different alleles which improve the fitness of the population as a whole. Alternatively, it may simply be a function of the structure of DNA surrounding different alleles, and any effects that it might have on the selection of alleles may be entirely incidental.

In the future, it would be useful to expand on the study size, particularly with regards to observing low frequency PMS events, to be able to draw solid conclusions from this data. It would also be interesting to probe this locus using

molecular tools to directly visualise the levels of DSBs generated by each strand, and thus directly quantify any bias between observed in the levels of DSBs between different alleles. Finally, given that it appeared that in the XJ24-24a strain background, the freeze thaw cycle appeared to affect the propensity of the strain to undertake variable levels of DSBs on each allele, it would be interesting to pursue this further; firstly to determine whether this also occurs in the Y55 strain background, and secondly to determine whether the differences observed are a function of heat shock proteins, reviewed in (PARSELL & LINDQUIST, 1993), and hence a response to cellular stress.

Bibliography

ABDULLAH, M. & BORTS, R., 2001. Meiotic recombination frequencies are affected by nutritional states in Saccharomyces cerevisiae. *Proc Natl Acad Sci USA,* Volume 98(25), pp. 14524–1452.

AGARWAL, S. & ROEDER, G., 2000. Zip3 provides a link between recombination enzymes and synaptonemal complex proteins. *Cell,* Volume 102(2), pp. 245-55.

ALANI, E., PADMORE, R. & KLECKNER, N., 1990. Analysis of wild-type and rad50 mutants of yeast suggests an intimate relationship between meiotic chromosome synapsis and recombination. *Cell,* Volume 61, pp. 419–436.

ALANI, E., REENAN, R. & KOLODNER, R., 1994. Interaction between mismatch repair and genetic recombination in Saccharomyces cerevisiae. *Genetics,* Volume 137(1), pp. 19-39.

ALEXANDRU, G., UHLMANN, F., MECHTLER, K., POUPART, M. A. & NASMYTH, K., 2001. Phosphorylation of the cohesin subunit Scc1 by Polo/Cdc5 kinase regulates sister chromatid separation in yeast. *Cell,* Volume 105(4), pp. 459-72.

ALLERS, T. & LICHTEN, M., 2001a. Differential timing and control of noncrossover and crossover recombination during meiosis. *Cell,* Volume 106, pp. 47-57.

ALLERS, T. & LICHTEN, M., 2001b. Intermediates of yeast meiotic recombination contain heteroduplex DNA. *Mol Cell,* Volume 8(1), pp. 225-231.

AMPATZIDOU, E., IRMISCH, A., O'CONNELL, M. & MURRAY, J., 2006. Smc5/6 is required for repair at collapsed replication forks. *Mol Cell Biol,* Volume 26(24), pp. 9387-401.

ANDREWS, E. A., PALECEK, J., SERGEANT, J., TAYLOR, E., LEHMANN, A. R. & WATTS, F. Z., 2005. Nse2, a component of the Smc5-6 complex, is a SUMO ligase required for the response to DNA damage. *Mol Cell Biol,* Volume 25(1), pp. 185-96.

ARUMUGAM, P., GRUBER, S., TANAKA, K., HAERING, C. H., MECHTLER, K. & NASMYTH, K., 2003. ATP hydrolysis is required for cohesin's association with chromosomes. *Curr Biol,* Volume 13, pp. 1941-53.

BICKEL, J., CHEN, L., HAYWARD, J., YEAP, S. L., ALKERS, A. E. & CHAN, R. C., 2010. Structural Maintenance of Chromosomes (SMC) Proteins Promote Homolog-Independent Recombination Repair in Meiosis Crucial for Germ Cell Genomic Stability. *PLoS Genetics,* p. e1001028.

BIRKENBIHL, R. & SUBRAMANI, S., 1992. Cloning and characterization of rad21 an essential gene of Schizosaccharomyces pombe involved in DNA double-strand-break repair. *Nucleic Acids Res,* Volume 20, pp. 6605–6611.

BISHOP, D. K., 1994. RecA homologs Dmc1 and Rad51 interact to form multiple nuclear complexes prior to meiotic chromosome synapsis. *Cell,* pp. 1081-92.

BISHOP, D. K., PARK, D., XU, L. & KLECKNER, N. 1992. DMC1: a meiosis-specific yeast homolog of E. coli recA required for recombination, synaptonemal complex formation, and cell cycle progression. *Cell,* Volume 69, pp. 439-56.

BISHOP, D. K., NIKOLSKI, Y., OSHIRO, J., CHON, J., SHINOHARA, M. & CHEN, X., 1999. High copy number suppression of the meiotic arrest caused by a dmc1 mutation: REC114 imposes an early recombination block and RAD54 promotes a DMC1-independent DSB repair pathway. *Genes Cells,* Volume 4, pp. 425–444.

BISHOP, D. K., WILLIAMSON, M., FOGEL, S. & KOLODNER, R., 1987. The role of heteroduplex correction in gene conversion in Saccharomyces cerevisiae. *Nature,* Volume 328, pp. 362 - 364.

BODDY, M. N., LOPEZ-GIRONA, A., SHANAHAN, P., INTERTHAL, H., HEYER, W. D. & RUSSELL, P., 2000. Damage tolerance protein Mus81 associates with the FHA1 domain of checkpoint kinase Cds1. *Mol Cell Biol,* Volume 20(23), pp. 8758-66.

BODDY, M. N., SHANAHAN, P., MCDONALD, W.H., LOPEZ-GIRONA, A., NOGUCHI, E., YATES, (III), JR. & RUSSELL, P., 2003. Replication checkpoint kinase Cds1 regulates recombinational repair protein Rad60. *Mol Cell Biol,* Volume 23(16), pp. 5939-46.

BORNER, G. V., KLECKNER, N. & HUNTER, N., 2004. Crossover/noncrossover differentiation, synaptonemal complex formation, and regulatory surveillance at the leptotene/zygotene transition of meiosis. *Cell,* Volume 117(1), pp. 29-45.

BORTS, R. H., LICHTEN, M., HEARN, M., DAVIDOW, L.S. & HABER, J.E., 1984. Physical monitoring of meiotic recombination in Saccharomyces cerevisiae. *Cold Spring Harb Symp Quant Biol,* Volume 49, pp. 67-76.

BRAR, G. A., HOCHWAGEN, A., EE, L. S. & AMON, A., 2009. The Multiple Roles of Cohesin in Meiotic Chromosome Morphogenesis and Pairing. *Molecular Biology of the Cell,* Volume 20, pp. 1030-47.

BREWER, B. J. & FANGMAN, W. L., 1987. The localization of replication origins on ARS plasmids in S. cerevisiae. *Cell,* Volume 51, pp. 463-71.

BRITO, I., YU, H.-G. & AMON, A., 2010. Condensins promote coorientation of sister chromatids during meiosis I in budding yeast. *Genetics,* Volume 185, pp. 55-64.

BROWN, M. S., GRUBB, J., ZHANG, A., RUST, M. J. & BISHOP, D. K., 2015. Small Rad51 and Dmc1 Complexes Often Co-occupy Both Ends of a Meiotic DNA Double Strand Break. *PLoS Genetics,* p. e1005653.

BUONOMO, S. B., CLYNE, R. K., FUCHS, J., LOIDL, J., UHLMANN, F. & NASMYTH, K., 2000. Disjunction of homologous chromosomes in meiosis I depends on proteolytic cleavage of the meiotic cohesin Rec8 by separin. *Cell,* Volume 103, pp. 387-398.

CARBALLO, J., JOHNSON, A., SEDGWICK, S. & CHA, R., 2008. Phosphorylation of the axial element protein Hop1 by Mec1/Tel1 ensures meiotic interhomolog recombination. *Cell,* Volume 132, pp. 758-770.

CHAVEZ, A., GEORGE, V., AGRAWL, V. & JOHNSON, F., 2010. Sumoylation and the structural maintenance of chromosomes (Smc) 5/6 complex slow senescence through recombination intermediate resolution. *J Biol Chem,* Volume 285(16), pp. 11922-30.

CHERRY, J. M, HONG, E.L., AMUNDSEN, C., BALAKRISHNAN, R., BINKLEY, G., CHAN, E. T., CHRISTIE, K. R., COSTANZO, M. C., DWIGHT, S. S., ENGEL, S. R., FISK, D. G., HIRSCHMAN, J. E., HITZ, B. C., KARRA, K., KRIEGER, C. J., MIYASATO, S. R., NASH, R. S., PARK, J., SKRYZPEK, M. S., SIMINSON, M., WENG, S. & WONG, E. D., 2012. Saccharomyces Genome Database: the genomics resource of budding yeast. *Nucleic Acids Res 40,* Volume 40(Database issue), pp. D700-5.

CHUA, P. & ROEDER, G., 1998. Zip2, a meiosis-specific protein required for the initiation of chromosome synapsis. *Cell,* Volume 93(3), pp. 349-59.

CHUONG, H. & DAWSON, D., 2010. Meiotic Cohesin Promotes Pairing of Nonhomologous Centromeres in Early Meiotic Prophase. *Mol Biol Cell,* Volume 21, pp. 1799-1809.

CHU, S., DERISI, J., EISEN, M., MULHOLLAND, J., BOTSTEIN, D., BROWN, P. O. & HERSKOWITZ, I., 1998. The transcriptional program of sporulation in budding yeast. *Science,* Volume 282(5389), pp. 699-705.

CIOSK, R., SHIRAYAMA, M., SHEVCHENKO, A., TANAKA, T., TOTH, A., SHEVCHENKO, A. & NASMYTH, K., 2000. Mol Cell. 2000 Feb;5(2):243-54. Cohesin's binding to chromosomes depends on a separate complex consisting of Scc2 and Scc4 proteins. *Mol Cell,* pp. 243-54.

CLOUD, V., CHAN, Y., L., GRUBB, J., BUDKE, B. & BISHOP, D., K., 2012. Rad51 is an accessory factor for Dmc1-mediated joint molecule formation during meiosis. *Science,* Volume 337, pp. 1222-5.

CLYNE, R. K., KATIS, V. L., JESSOP, L., BENJAMIN, K. R., HERSKOWITZ, I., LICHTEN, M. & NASMYTH, K., 2003. Polo-like kinase Cdc5 promotes chiasmata formation and cosegregation of sister centromeres at meiosis I. *Nat Cell Biol,* Volume 5(5), pp. 480-5.

COBBE, N. & HECK, M., 2004. The evolution of SMC proteins: phylogenetic analysis and structural implications. *Molecular biology and evolution,* Volume 21(2), pp. 332-347.

COHEN-FIX, O., PETERS, J., KIRSCHNER, M. & KOSHLAND, D., 1996. Anaphase initiation in Saccharomyces cerevisiae is controlled by the APC-dependent degradation of the anaphase inhibitor Pds1p. *Genes Dev,* Volume 10(24), pp. 3081-3093.

COPSEY, A., TANG, S., JORDAN, P. W., BLITZBLAU, H. G., NEWCOMBE, S., CHAN, A. C., NEWNHAM, L., LI, Z., GRAY, S., HERBERT, A. D., ARUMUGAM, R., HOCHWAGEN, A., HUNTER, N. & HOFFMANN, E., 2013. Smc5/6 coordinates formation and resolution of joint molecules with chromosome morphology to ensure meiotic divisions. *PLoS Genetics,* p. e1004071.

COST, G. & COZZARELLI, N., 2006. Smc5p promotes faithful chromosome transmission and DNA repair in Saccharomyces cerevisiae. *Genetics,* Volume 172(4), pp. 2185-200.

DE LOS SANTOS, T. HUNTER, N., LEE, C., LARKIN, B., LOIDL, J. & HOLLINGSWORTH, N. M.,., 2003. The Mus81/Mms4 endonuclease acts independently of double-Holliday junction resolution to promote a distinct subset of crossovers during meiosis in budding yeast. *Genetics,* Volume 164, pp. 81-94.

DE MUYT, A., JESSOP, L., KOLAR, E., SOURIRAJAN, A., CHEN, J. H., DAYANI, Y. & LICHTEN, M., 2012. BLM Helicase Ortholog Sgs1 Is a Central Regulator of Meiotic Recombination Intermediate Metabolism. *Mol Cell,* Volume 36, pp. 43-53.

DE PICCOLI, G., CORTES-LEDESMA, IRA, TORRES-ROSELL, UHLE, FARMER, HWANG, MACHIN, CESCHIA, MCALEENAN, CORDON-PRECADIO, CLEMENTE-BLANCO, VILELLA-MITJANA, ULLAL, JARMUZ, LEITAO, BRESSAN, DOTIWALA, PAPUSHA, ZHAO, MYUNG, HABER, J. E., AGUILERA, A. & ARAGON, L., 2006. Smc5-Smc6 mediate DNA double-strand-break repair by promoting sister-chromatid recombination. *Nat Cell Biol,* Volume 8(9), pp. 1032-4.

DETLOFF, P., SIEBER, J. & PETES, T., 1991. Repair of specific base pair mismatches formed during meiotic recombination in the yeast Saccharomyces cerevisiae. *Mol Cell Biol,* Volume 11(2), pp. 737-45.

DEVLIN, C., TICE-BALDWIN, K., SHORE, D. & ARNDT, K., 1991. RAP1 is required for BAS1/BAS2- and GCN4-dependent transcription of the yeast HIS4 gene. *Mol Cell Biol,* Volume 11(7), pp. 3642-51.

DIRICK, L., GOETSCH, L., AMMERER, G. & BYERS, B., 1998. Regulation of meiotic S phase by Ime2 and a Clb5,6-associated kinase in Saccharomyces cerevisiae. *Science,* Volume 281, pp. 1854-1857.

DONG, H. & ROEDER, G., 2000. Organization of the yeast Zip1 protein within the central region of the synaptonemal complex. *J Cell Biol,* Volume 148, pp. 417–426.

DUAN, X., YANG, Y., CHEN, Y. H., ARENZ, J., RANGI, G. K., ZHAO, X. & YE, H., 2009. Architecture of the Smc5/6 Complex of Saccharomyces cerevisiae Reveals a Unique Interaction between the Nse5-6 Subcomplex and the Hinge Regions of Smc5 and Smc6. *J Biol Chem,* Volume 284(13), pp. 8507-15.

EDELSTEIN, A. D., TSUCHIDA, M. A., AMODAJ, N., PINKARD, H., VALE, R. D. & STUURMANN, N., 2014. Advanced methods of microscope control using μManager software. *J Biol Methods ,* Volume 1(2):e10, p. 10.14440/jbm.2014.36.

FARMER, S., SAN-SEGUNDO, P. & ARAGON, L., 2011. The Smc5-Smc6 complex is required to remove chromosome junctions in meiosis. *PLoS One,* Volume 6(6), p. e20948.

FORMOSA, T. & ALBERTS, B., 1986. DNA-synthesis dependent on genetic-recombination – characterization of a reaction catalyzed by purified bacteriophage-T4 proteins. *Cell,* Volume 47, pp. 793-806.

FOUSTERI, M. & LEHMANN, A., 2000. A novel SMC protein complex in Schizosaccharomyces pombe contains the Rad18 DNA repair protein. *EMBO J,* Volume 19(7), pp. 1691–1702.

FREEMAN, L., ARAGON-ALCAIDE, L. & STRUNNIKOV, A., 2000. The condensin complex governs chromosome condensation and mitotic transmission of rDNA. *The Journal of cell biology,* Volume 149, pp. 811-24.

FRICKE, W. & BRILL, S., 2005. Slx1–Slx4 is a second structure-specific endonuclease functionally redundant with Sgs1-Top3. *Genes Dev ,* Volume 17, pp. 1768–1778.

GLIGORIS, T. G., SCHEINOST, J. C., BURMANN, F., PETELA, N., CHAN, K. L., ULUOCAK, P., BECKOUET, F., GRUBER, S., NASMYTH, K. & LOWE, J., 2014. Closing the cohesin ring: structure and function of its Smc3-kleisin interface. *Science,* Volume 346(6212), pp. 963–967.

GOLDFARB, T. & LICHTEN, M., 2010. Frequent and Efficient Use of the Sister Chromatid for DNA Double-Strand Break Repair during Budding Yeast Meiosis. *Plos Biology,* p. e1000520.

GOMEZ, R., JORDAN, P. W., VIERA, A., ALSHEIMER, M., FUKUDA, T., JESSBERGER, R., LLANO, E., PENDAS, A. M., HANDEL, M. A. & SUJA, J. A., 2013. Dynamic localization of SMC5/6 complex proteins during mammalian meiosis and mitosis suggests functions in distinct chromosome processes. *J Cell Sci,* Volume 126, pp. 4239–4252.

GRUBER, S., ARUMUGAM, P., KATOU, Y., KUGLITSCH, D., HELMHART, W., SHIRAHIGE, K. & NASMYTH, K., 2006. Evidence that Loading of Cohesin Onto Chromosomes Involves Opening of Its SMC Hinge. *Cell,* 127(3), pp. 523–537.

GRUBER, S., HAERING, C. H. & NASMYTH, K., 2003. Chromosomal cohesin forms a ring.. *Cell,* Volume 112, pp. 765-77.

GUACCI, V., KOSHLAND, D. & STRUNNIKOV, A., 1997. A direct link between sister chromatid cohesion and chromosome condensation revealed through the analysis of MCD1 in S-cerevisiae. *Cell,* Volume 91, pp. 47-57.

HAERING, C. H., FARCAS, A. M., ARUMUGAM, P., METSON, J. & NASMYTH, K., 2008. The cohesin ring concatenates sister DNA molecules. *Nature,* Volume 454, pp. 297-301.

HAERING, C. H., LOWE, J., HOCHWAGEN, A. & NASMYTH, K., 2002. Molecular architecture of SMC proteins and the yeast cohesin complex. *Mol Cell,* pp. 773-88.

HARVEY, S., SHEEDY, D., CUDDIHY, A. & O'CONNELL, M., 2004. Coordination of DNA damage responses via the Smc5/Smc6 complex. *Mol Cell Biol,* Volume 24(2), pp. 662-74.

HENDERSON, K. & KEENEY, S., 2004. Tying synaptonemal complex initiation to the formation and programmed repair of DNA double-strand breaks. *Proceedings of the National Academy of Sciences, USA,* Volume 101(13), pp. 4519-4524.

HIRANO, T., KOBAYASHI, M. & HIRANO, R., 1997. Condensins, chromosome condensation protein complexes containing XCAP-C, XCAP-E and a Xenopus homolog of the Drosophila Barren protein. *Cell,* Volume 89(4), pp. 511-21.

HOFFMANN, E. R., ERIKSSON, E., HERBERT, B. J. & BORTS, R. H., 2005. MLH1 and MSH2 promote the symmetry of double-strand break repair events at the HIS4 hotspot in Saccharomyces cerevisiae. *Genetics,* Volume 169, pp. 1291-1303.

HOLLIDAY, R., 1964. A mechanism for gene conversion in fungi. *Genet Res,* Volume 5(2), pp. 282-304.

HOLLINGSWORTH, N. & BRILL, S., 2004. The Mus81 solution to resolution: generating meiotic crossovers without Holliday junctions. *Genes Dev,* Volume 18(2), pp. 117–125..

HOLLINGSWORTH, N. M., PONTE, L. & HALSEY, C., 1995. MSH5, a novel MutS homolog, facilitates meiotic reciprocal recombination between homologs in Saccharomyces cerevisiae but not mismatch repair. *Genes Dev, 9(14): 1728-1739.,* Volume 9(14), pp. 1728-1739.

HONG, S., SUNG, Y., YU, M., LEE, M., KLECKNER, N. & KIM, K. P., 2013. The Logic and Mechanism of Homologous Recombination Partner Choice. *Mol cell,* Volume 51(4), pp. 440–453.

HUNTER, N. & KLECKNER, N., 2001. The single-end invasion: an asymmetric intermediate at the double-strand break to double-holliday junction transition of meiotic recombination. *Cell,* Volume 106(1), pp. 59-70.

JEPPSSON, K., CARLBORG, K. K., NAKATOA, R., BERTA, D. G., LILIENTHAL, I., KANNO, T., LINDGVIST, A., BRINK, M. C., DANTUMA, N. P., KATOU, Y., SHIRAHIGE, K. & SJOGREN, C., 2014. The chromosomal association of the Smc5/6 complex depends on cohesion and predicts the level of sister chromatid entanglement. *PLoS Genetics,* p. e1004680.

JESSOP, L., ALLERS, T. & LICHTEN, M., 2005. Infrequent Co-conversion of Markers Flanking a Meiotic Recombination Initiation Site in Saccharomyces cerevisiae. *Genetics,* Volume 169(3), pp. 1353–1367.

JESSOP, L. & LICHTEN, M., 2008. Mus81/Mms4 endonuclease and Sgs1 helicase collaborate to ensure proper recombination intermediate metabolism during meiosis. *Mol cell,* Volume 31(3), pp. 313-323.

JESSOP, L., ROCKMILL, B., ROEDER, G. S. & LICHTEN, M., 2006. Meiotic chromosome synapsis-promoting proteins antagonize the anti-crossover activity of sgs1. *PLoS Genetics,* Volume 2.

KADYK, L. & HARTWELL, L., 1992. Sister chromatids are preferred over homologs as substrates for recombinational repair in Saccharomyces cerevisiae. *Genetics,* Volume 132, pp. 387–402.

KASSIR, Y., GRANOT, D. & SIMCHEN, G., 1988. IME1, a positive regulator gene of meiosis in S. cerevisiae. *Cell,* Volume 52(6), pp. 853-62.

KATIS, V. L., LIPP, J. J., IMRE, R., BOGDANOVA, A., OKAZ, E., HABERMANN, B., MECHTLER, K., NASMYTH, K. & ZACHARIE, W., 2010. Rec8 phosphorylation by casein kinase 1 and Cdc7-Dbf4 kinase regulates cohesin cleavage by separase during meiosis. *Dev Cell,* Volume 18(3), pp. 397-409.

KAUR, H., DE MUYT, A. & LICHTEN, M., 2015. Top3-Rmi1 DNA single-strand decatenase is integral to the formation and resolution of meiotic recombination intermediates. *Mol Cell,* Volume 57(4), pp. 583–94.

KEENEY, S., GIROUX, C. N. & & KLECKNER, N., 1997. Meiosis-specific DNA double-strand breaks are catalyzed by Spo11, a member of a widely conserved protein family.. *Cell,* pp. 88375-84.

KIM, K. et al., 2010. Sister cohesion and structural axis components mediate homolog bias of meiotic recombination. *Cell,* Volume 143(6), pp. 924–937.

KITAJIMA, T. S., SAKUNO, T., ISHIGURO, K., IEMURA, S., NATSUME, T., KAWASHIMA, S. A. & WATANABE, Y., 2006. Shugoshin collaborates with protein phosphatase 2A to protect cohesin. *Nature,* Volume 441(7089), pp. 46-52.

KITAJIMA, T. S., KAWASHIMA, S. A. & WATANABE, Y., 2004. The conserved kinetochore protein shugoshin protects centromeric cohesion during meiosis. *Nature,* Volume 427, pp. 510-7.

KLEIN, F., MAHR, P., GALOVA, M., BUONOMO, S. B., MICHAELIS, C., NARIZ, K. & NASMYTH, K., 1999. A central role for cohesins in sister chromatid cohesion, formation of axial elements, and recombination during yeast meiosis. *Cell,* Volume 98, pp. 91-103.

LAO, J. P., OH, S. D., SHINOHARA, M., SHINOHARA, A. & HUNTER, N., 2008. Rad52 promotes post-invasion steps of meiotic double-strand-break repair. *Mol Cell,* Volume 29(4), pp. 517–524.

LAO, J. P., CLOUD, V., HUANG, C.-C., GRUBB, J., THACKER, D., LEE, C.-Y., DRESSER, M. E., HUNTER, N. & BISHOP, D. K., 2013. Meiotic Crossover Control by Concerted Action of Rad51-Dmc1 in Homolog Template Bias and Robust Homeostatic Regulation. *PLoS Genetics,* p. e1003978.

LEE, J. & HIRANO, T., 2011. RAD21L, a novel cohesin subunit implicated in linking homologous chromosomes in mammalian meiosis. *Journal of Cell Biology,* Volume 192(2), pp. 263-276.

LEHMANN, A. R., WALICKA, M., GRIFFITHS, D. J., MURRAY, J. M., WATTS, F. Z., MCCREADY, S. & CARR, A. M., 1995. The rad18 gene of Schizosaccharomyces pombe defines a new subgroup of the SMC superfamily involved in DNA repair. *Mol Cell Biol,* Volume 15(12), pp. 7067-80.

LILIENTHAL, I., KANNO, T. & SJOGREN, C., 2013. Inhibition of the Smc5/6 Complex during Meiosis Perturbs Joint Molecule Formation and Resolution without Significantly Changing Crossover or Non-crossover Levels. *PLoS Genetics,* Volume 9(11).

LIM, H., GOH, P. & SURANO, U., 1998. Cdc20 is essential for the cyclosome-mediated proteolysis of both Pds1 and Clb2 during M phase in budding yeast. *Curr Biol,* Volume 8(4), pp. 231-4.

LIU, J., WU, T.-C. & LICHTEN, M., 1995. The location and structure of double-strand DNA breaks induced during yeast meiosis: evidence for a covalently linked DNA-protein intermediate. *EMBO J,* Volume 14, pp. 4599–4608.

LLANO, E., GOMEZ, R., GUTIERREZ-CABALLERO, C., HERRAN, Y., SANCHEZ-MARTIN, M., VAZQUEZ-QUINONES, L., HERNANDEZ, T., DE ALAVA, E., CUADRADO, A., BARBERO, J. L., SUJA, J. A. & PENDAS, A. M., 2008. Shugoshin-2 is essential for the completion of meiosis but not for mitotic cell division in mice. *Genes Dev,* Volume 22(17), pp. 2400-13.

LONGTINE, M. S., MCKENZIE, A., DEMARINI, D. J., SHAH, N. G., WACH, A., BRACHAT, A., PHILIPPSEN, P. & PRINGLE, J. R., 1998. Additional Modules for Versatile and Economical PCR-based Gene Deletion and Modification in Saccharomyces cerevisiae. *Yeast,* Volume 14, pp. 953–961.

LOSADA, A., HIRANO, M. & HIRANO, T., 2002. Cohesin release is required for sister chromatid resolution, but not for condensin-mediated compaction, at the onset of mitosis. *Genes Dev,* Volume 16(23), pp. 3004-16.

LOWE, J., CORDELL, S. & VAN DEN ENT, F., 2001. Crystal structure of the SMC head domain: an ABC ATPase with 900 residues antiparallel coiled-coil inserted. *J Mol Biol,* Volume 306(1), pp. 25-35.

MALKOVA, A., SWANSON, J., GERMAN, M., MCCUSKER, J. H., HOUSWORTH, E. A., STAHL, F. W. & HABER, J. E., 2004. Gene conversion and crossing over along the 405-kb left arm of Saccharomyces cerevisiae chromosome VII. *Genetics,* Volume 168(1), pp. 49-63.

MARTINI, E., DIAZ, R., HUNTER, N. & KEENEY, S., 2006. Crossover homeostasis in yeast meiosis. *Cell,* Volume 126(2), pp. 285-95.

MASCARENHAS, J., SOPPA, J., STRUNNIKOV, A. & GRAUMANN, P., 2002. Cell cycle-dependent localization of two novel prokaryotic chromosome segregation and condensation proteins in Bacillus subtilis that interact with SMC protein. *EMBO J,* Volume 21(12), pp. 3108–18.

MATOS, J., BLANCO, M. G., MASLEN, S., SKEHEL, J. M. & WEST, S. C., 2011. Regulatory control of the resolution of DNA recombination intermediates during meiosis and mitosis. *Cell,* Volume 147, pp. 158–172.

MAZINA, O. M., MAZIN, A. V., NAKAGAWA, T., KOLODNER, R. D. & KOWALCZYHOWSKI, S. C., 2004. Saccharomyces cerevisiae Mer3 helicase stimulates 3'-5' heteroduplex extension by Rad51; implications for crossover control in meiotic recombination. *Cell,* Volume 117(1), pp. 47-56.

MAZUR, P. & SCHMIDT, J., 1968. Interactions of cooling velocity, temperature, and warming velocity on the survival of frozen and thawed yeast. *Cryobiology,* Volume 5(1), pp. 1-17.

MCMAHILL, M., SHAM, C. & BISHOP, D., 2007. Synthesis-Dependent Strand Annealing in Meiosis. *PLoS Biology,* p. e0050299.

MELBY, T. E., CIAMPAGLIO, C., BRISCOE, G. & ERICKSON, H. P., 1998. The symmetrical structure of structural maintenance of chromosomes (SMC) and MukB proteins: Long, antiparallel coiled coils, folded at a flexible hinge. *J Cell Biol,* Volume 142, pp. 1595-1604.

MENOLFI, D., DELAMARRE, A., LENGRONNE, A., PASERO, P. & BRANZEI, D., 2015. Essential Roles of the Smc5/6 Complex in Replication through Natural Pausing Sites and Endogenous DNA Damage Tolerance. *Mol Cell,* Volume 60, pp. 835–846.

MICHAELIS, C., CIOSK, R. & NASMYTH, K., 1997. Cohesins: chromosomal proteins that prevent premature separation of sister chromatids. *Cell,* Volume 91, pp. 35-45.

MIYABE, I., MORISHITA, T., SHINAGAWA, H. & CARR, A., 2009. Schizosaccharomyces pombe Cds1Chk2 regulates homologous recombination at stalled replication forks through the phosphorylation of recombination protein Rad60. *J Cell Sci,* Volume 122(20), pp. 3638-43.

MULLER, B., KOLEER, T. & STASIAK, A., 1990. Characterization of the DNA binding activity of stable RecA-DNA complexes. Interaction between the two DNA binding sites within RecA helical filaments. *J Mol Biol,* Volume 212, pp. 97-112.

MURRAY, J. & CARR, A., 2008. Smc5/6: a link between DNA repair and unidirectional replication?. *Nat Rev Mol Cell Biol,* Volume 9(2), pp. 177-82.

NAGAO, K., ADACHI, Y. & YANAGIDA, M., 2004. Separase-mediated cleavage of cohesin at interphase is required for DNA repair. *Nature,* Volume 430, pp. 1044-1048.

NAIRZ, K. & KLEIN, F., 1997. mre11S--a yeast mutation that blocks double-strand-break processing and permits nonhomologous synapsis in meiosis. *Genes Dav,* Volume 11(17), pp. 2272-90.

NEALE, M., PAN, J. & KEENEY, S., 2005. Endonucleolytic processing of covalent protein-linked DNA double-strand breaks. *Nature,* Volume 436(7053), pp. 1053-7.

NEWNHAM, L., JORDAN, P., ROCKMILL, B., ROEDER, G. S. & HOFFMANN, E., 2010. The synaptonemal complex protein, Zip1, promotes the segregation of nonexchange chromosomes at meiosis I. *Proc Natl Acad Sci USA,* Volume 107(2), pp. 781-5.

NIMONKAR, A., SICA, R. & KOWALCZYKOWSKI, S., 2009. Rad52 promotes second-end DNA capture in double-stranded break repair to form complement-stabilized joint molecules. *Proc Natl Acad Sci USA,* Volume 106(9), pp. 3077-82.

NISHANT, K. T., PLYS, A. & ALANI, E., 2008. A mutation in the putative MLH3 endonuclease domain confers a defect in both mismatch repair and meiosis in Saccharomyces cerevisiae. *Genetics ,* Volume 179, pp. 747-755.

NISHANT, K. T., CHEN, C., SHINOHARA, M., SHINOHARA, A., ALANI, E., 2010. Genetic Analysis of Baker's Yeast Msh4-Msh5 Reveals a Threshold Crossover Level for Meiotic Viability. *PLoS Genetics,* Volume 6(8).

NIU, H., WAN, L., BUSYGINA, V., KWON, Y., ALLEN, J. A., LI, X., KUNZ, R. C., KUBOTA, K., WANG, B., SUNG, P., SHOKAT, K. M., GYGI, S. P., HOLLINGSWORTH, N. M., 2009. Regulation of meiotic recombination via Mek1-mediated Rad54 phosphorylation. *Mol Cell,* Volume 36, pp. 393–404.

NOVAK, J., ROSS-MACDONALD, P. & ROEDER, G., 2001. The budding yeast Msh4 protein functions in chromosome synapsis and the regulation of crossover distribution. *Genetics,* Volume 58(3), pp. 1013-25.

OCAMPO-HAFALLA, M., MUNOZ, S., SAMORA, C. & UHLMANN, F., 2016. Evidence for cohesin sliding along budding yeast chromosomes. *Open Biol,* Volume 6, p. 150178.

OH, S. D., LAO, J. P., HWANG, P. Y. H., TAYLOR, A. F., SMITH, G. R. & HUNTER, N., 2007. BLM ortholog, Sgs1, prevents aberrant crossing-over by suppressing formation of multichromatid joint molecules. *Cell,* Volume 130(20), pp. 259-272.

OH, S. D., LAO, J. P., TAYLOR, A. F., SMITH, G. R. & HUNTER, N., 2008. RecQ helicase, Sgs1, and XPF family endonuclease, Mus81-Mms4, resolve aberrant joint molecules during meiotic recombination. *Mol Cell,* Volume 31(3), pp. 324-336.

ONO, T., LOSADA, A., HIRANO, M., MYERS, M. P., NEUWALD, A. F. & HIRANO, T., 2003. Differential contributions of condensin I and condensin II to mitotic chromosome architecture in vertebrate cells. *Cell,* Volume 115(1), pp. 109-21.

OUTWIN, E. A., IRMISCH, A., MURRAY, J. M. & O'CONNELL, M. J., 2009. Smc5-Smc6-dependent removal of cohesin from mitotic chromosomes. *Mol Cell Biol,* pp. 4363-75.

PADMORE, R., CAO, L. & KLECKNER, N., 1991. Temporal comparison of recombination and synaptonemal complex formation during meiosis in S. cerevisiae. *Cell,* Volume 66(6), pp. 1239-56.

PAK, J. & SEGALL, J., 2002. Regulation of the premiddle and middle phases of expression of the NDT80 gene during sporulation of Saccharomyces cerevisiae. *Mol Cell Biol,* Volume 22(18), pp. 6417-29.

PALECEK, J., VIDOT, S., FENG, M., DOHERTY, A. J. & LEHMANN, A. R., 2006. The Smc5-Smc6 DNA repair complex. bridging of the Smc5-Smc6 heads by the KLEISIN, Nse4, and non-Kleisin subunits. *J Biol Chem,* Volume 281(48), pp. 36952-9.

PAQUES, F. & HABER, J., 1999. Multiple pathways of recombination induced by double-strand breaks in Saccharomyces cerevisiae. *Microbiol Mol Biol Rev,* Volume 63, pp. 349-404.

PARELHO, V., HADJUR, S., SPIVAKOV, M., LELEU, M., SAUER, S., GREGSON, H. C., JARMUZ, A., CANZONETTA, C., WEBSTER, Z., NESTEROVA, T., COBB, B. S., YOKOMORI, K., DILLON, N., ARAGON, L., FISHER, A. G. & MERKENSCHLAGER, M., 2008. Cohesins functionally associate with CTCF on mammalian chromosome arms. *Cell,* Volume 132(3), pp. 422-33.

PARK, J., GRANT, C., ATTFIELD, P. & DAWES, I., 1997. The freeze-thaw stress response of the yeast Saccharomyces cerevisiae is growth phase specific and is controlled by nutritional state via the RAS-cyclic AMP signal transduction pathway. *Appl Environ Microbiol,* Volume 63(10), pp. 3818–3824.

PARSELL, D. & LINDQUIST, S., 1993. The function of heat-shock proteins in stress tolerance: degradation and reactivation of damaged proteins. *Annu Rev Genet,* Volume 27, pp. 437-96.

PEBERNARD, S., MCDONALD, W. H., PAVLOVA, Y., YATES, J. R., (III). & BODDY, M. N., 2004. Nse1, Nse2, and a novel subunit of the Smc5-Smc6 complex, Nse3, play a crucial role in meiosis. *Mol Biol Cel ,* Volume 15(11), pp. 4866-76.

PEBERNARD, S., WOHLSCHLEGEL, J., MCDONALD, W. H., YATES, J. R., (III). & BODDY, M. N., 2006. The Nse5-Nse6 dimer mediates DNA repair roles of the Smc5-Smc6 complex. *Mol Cell Biol,* Volume 26(5), pp. 1617-30.

PERRY, J., KLECKNER, N. & BORNER, G. V., 2005. Bioinformatic analyses implicate the collaborating meiotic crossover/chiasma proteins Zip2, Zip3, and Spo22/Zip4 in ubiquitin labeling. *Proc Natl Acad Sci USA,* Volume 102, pp. 17594-9.

RABITSCH, K. P., GREGAN, J., SCHLEIFFER, A., JAVERZAT, J. P., EISENHABER, F. & NASMYTH, K., 2004. Two fission yeast homologs of Drosophila Mei-S332 are required for chromosome segregation during meiosis I and II. *Curr Biol,* Volume 14(4), pp. 287-301.

RAMESH, M., MALIK, S. & LOGSDON, J. J., 2005. A phylogenomic inventory of meiotic genes; evidence for sex in Giardia and an early eukaryotic origin of meiosis. *Curr Biol,* Volume 15(2), pp. 185-91.

RENSHAW, M. J., WARD, J. J., KANEMAKI, M., NATSUME, K., NEDELEC, F. J. & TANAKA, T. U., 2010. Condensins promote chromosome recoiling during early anaphase to complete sister chromatid separation. *Dev Cell,* Volume 19, pp. 232–244.

RIEDEL, C. G., KATIS, V. L., KATOU, Y., MORI, S., ITOH, T., HELMHART, W., GALOVA, M., PETRONCZKI, M., GREGAN, J., CETIN, B., MUDRAK, I., OGRIS, E., MECHTLER, K., PELLETIER, L., BUCHHOLZ, F., SHIRAHIGE, K. & NASMYTH, K., 2006. Protein phosphatase 2A protects centromeric sister chromatid cohesion during meiosis I. *Nature,* Volume 441(7089), pp. 53-61.

ROWLAND, B. D., ROIG, M. B., NISHINO, T., KURZE, A., ULUOCAK, P., MISHRA, A., BECKOUET, F., UNDERWOOD, P., METSON, J., IMRE, R., MECHTLER, K., KATIS, V. L. & NASMYTH, K., 2009. Building sister chromatid cohesion: smc3 acetylation counteracts an antiestablishment activity. *Mol Cell,* pp. 763-74.

RUDRA, S. & SKIBBENS, R., 2013. Cohesin codes - interpreting chromatin architecture and the many facets of cohesin function. *J Cell Sci,* Volume 126(1), pp. 31-41.

SANTUCCI-DARMANIN, S., NEYTON, S., LESPINASSE, F., SAUNIERES, A., GAUDRAY, P. & PAQUIS-FLUCKLINGER, V., 2002. The DNA mismatch-repair MLH3 protein interacts with MSH4 in meiotic cells, supporting a role for this MutL homolog in mammalian meiotic recombination. *Hum Mol Genet,* Volume 11, pp. 1697–1706.

SCHNEIDER, C., RASBAND, W. & ELICEIRI, K., 2012. NIH Image to ImageJ: 25 years of image analysis. *Nature Methods,* Volume 9, pp. 671–675.

SCHWACHA, A. & KLECKNER, N., 1995. Identification of Double Holliday Junctions as Intermediates in Meiotic Recombination. *Cell,* Volume 83(5), pp. 783-791.

SCHWACHA, A. & KLECKNER, N., 1997. Interhomolog bias during meiotic recombination: meiotic functions promote a highly differentiated interhomolog-only pathway. *Cell,* Volume 90(6), pp. 1123-1135.

SERGEANT, J., TAYLOR, E., PALECEK, J., FOUSTERI, M., ANDREWS, E. A., SWEENEY, S., SHINAGAWA, H., WATTS, F. Z. & LEHMANN, A. R., 2005. Composition and Architecture of the Schizosaccharomyces pombe Rad18 (Smc5-6) Complex. *Mol Cell Biol,* Volume 25(1), pp. 172-184.

SERRENTINO, M.-E., CHAPLAIS, E., SOMMERMEYER, V. & BORDE, V., 2013. Differential Association of the Conserved SUMO Ligase Zip3 with Meiotic Double-Strand Break Sites Reveals Regional Variations in the Outcome of Meiotic Recombination. *PLoS Genet,* Volume 9(4), p. e1003416.

SHINOHARA, A., GASIOR, S., OGAWA, T., KLECKNER, N. & BISHOP, D. K., 1997. Saccharomyces cerevisiae recA homologues RAD51 and DMC1 have both distinct and overlapping roles in meiotic recombination. *Genes cells,* Volume 2(10), pp. 615-29.

SHINOHARA, A., OGAWA, H. & OGAWA, T., 1992. Rad51 protein involved in repair and recombination in S. cerevisiae is a RecA-like protein. *Cell,* Volume 69(3), pp. 457-470.

SHINOHARA, A. & SHINOHARA, M., 2004. Roles of RecA homologues Rad51 and Dmc1 during meiotic recombination. *Cytogenet Genome Res,* Volume 107, pp. 201-7.

SJOGREN, C. & NASMYTH, K., 2001. Sister chromatid cohesion is required for postreplicative double-strand break repair in Saccharomyces cerevisiae. *Curr Biol,* Volume 11(12), pp. 991-5.

SJOGREN, C. & STROM, L., 2010. S-phase and DNA damage activated establishment of sister chromatid cohesion–importance for DNA repair. *Exp Cell Res,* Volume 316, pp. 1445–1453.

SMITH, A. & . ROEDER, G., 1997. The yeast Red1 protein localizes to the cores of meiotic chromosomes. *J. Cell Biol,* Volume 136, pp. 957-967.

SMITH, H. E., DRISCOLL, S. E., SIA, R. A., YUAN, H. E., MITCHELL, A. P., 1993. Genetic evidence for transcriptional activation by the yeast IME1 gene product. *Genetics,* Volume 133(4), pp. 775-84.

SNOWDEN, T., ACHARYA, S., BUTZ, C., BERARDINA, M. & FISHEL, R., 2004. hMSH4-hMSH5 recognizes Holliday Junctions and forms a meiosis-specific sliding clamp that embraces homologous chromosomes. *Mol. Cell,* Volume 15(3), pp. 437-51.

SOURIRAJAN, A. & LICHTEN, M., 2008. Polo-like kinase Cdc5 drives exit from pachytene during budding yeast meiosis. *Genes Dev,* Volume 22(19), pp. 2627–2632.

STORLAZZI, A., XU, L., CAO, L. & KLECKNER, N., 1995. Crossover and noncrossover recombination during meiosis: timing and pathway relationships. *Proc Natl Acad Sci USA,* Volume 92(18), pp. 8512-8516.

STRATHERN, J., NEWLON, C., HERSKOWITZ, I. & HICKS, J., 1979. Isolation of a circular derivative of yeast chromosome III: implications for the mechanism of mating type interconversion. *Cell,* Volume 18(2), pp. 309-19.

STROM, L., LINDROOS, H., SHIRAHIGE, K. & SJORGEN, C., 2004. Postreplicative recruitment of cohesin to double-strand breaks is required for DNA repair. *Mol Cell,* Volume 16(6), pp. 1003-15.

SUMARA, I., VORLAUFER, E., STUKENBER, P. T., KELM, O., REDEMANN, N., NIGG, E. A. & PETERS, J. M., 2002. The dissociation of cohesin from chromosomes in prophase is regulated by Polo-like kinase. *Mol Cell,* Volume 9(3), pp. 515-25.

SYM, M., ENGEBRECHT, J. & ROEDER, G., 1993. Zip1 is a synaptonemal complex protein required for meiotic chromosome synapsis. *Cell,* Volume 72, pp. 365-378.

TICE-BALDWIN, K., FINK, G. & ARNDT, K., 1989. BAS1 has a Myb motif and activates HIS4 transcription only in combination with BAS2. *Science,* Volume 246(4932), pp. 931-5.

TORRES-ROSELL, J., MACHIN, F., FARMER, S., JARMUZ, A., EYDMANN, T., DALGAARD, J. Z. & ARAGON, L., 2005. SMC5 and SMC6 genes are required for the segregation of repetitive chromosome regions. *Nat Cell Biol,* Volume 7(4), pp. 412-9.

TOTH, A., CIOSK, R., UHLMANN, F., GALOVA, M., SCHLEIFFER, A. & NASMYTH, K. 1999. Yeast cohesin complex requires a conserved protein, Eco1p(Ctf7), to establish cohesion between sister chromatids during DNA replication. *Genes Dev,* Volume 3(3), pp. 320-33.

TSUBOUCHI, H. & OGAWA, H., 2000. Exo1 Roles for Repair of DNA Double-Strand Breaks and Meiotic Crossing Over in Saccharomyces cerevisiae. *Mol Cell,* Volume 11(7), pp. 2221–2233.

TSUBOUCHI, H. & ROEDER, G. S., 2006. Budding yeast Hed1 down-regulates the mitotic recombination machinery when meiotic recombination is impaired. *Genes Dev,* pp. 1766-75.

TSUBOUCHI, T., MACQUEEN, A. & ROEDER, G., 2008. Initiation of meiotic chromosome synapsis at centromeres in budding yeast. *Genes Dev,* Volume 22(22), pp. 3217–3226.

UHLMANN, F., LOTTSPIECH, F. & NASMYTH, K., 1999. Sister-chromatid separation at anaphase onset is promoted by cleavage of the cohesin subunit Scc1. *Nature,* Volume 400(6739), pp. 37-42.

VERKADE, H. M., BUGG, S. J., LINDSAY, H. D., CARR, A. M. & O'CONNELL, M. J., 1999. Rad18 is required for DNA repair and checkpoint responses in fission yeast. *Mol Biol Cell,* Volume 10(9), pp. 2905-18.

VERVER, D. E., LANGEDIJK, N. S. M., JORDAN, P. W., REPPING, S. & HAMER, G., 2014. The SMC5/6 Complex Is Involved in Crucial Processes During Human Spermatogenesis. *Biology of Reproduction,* Volume 91 (1).

VISINTIN, R., STEGMEIER, F. & AMON, A., 2003. The Role of the Polo Kinase Cdc5 in Controlling Cdc14 Localization. *Mol Biol Cell,* Volume 14(11), pp. 4486–4498.

WAIZENEGGER, I., HAUF, S., MEINKE, A. & PETERS, J., 2000. Two distinct pathways remove mammalian cohesin from chromosome arms in prophase and from centromeres in anaphase. *Cell,* Volume 103(3), pp. 399-410.

WAN, L., DE LOS SANTOS, T., ZHANG, C., SHOKAT, K. & HOLLINGSWORTH, N. M., 2004. Mek1 kinase activity functions downstream of RED1 in the regulation of meiotic double strand break repair in budding yeast. *Mol Biol Cell,* Volume 15, pp. 11-23.

WATANABE, Y. & NURSE, P., 1999. Cohesin Rec8 is required for reductional chromosome segregation at meiosis. *Nature,* Volume 400, pp. 461-4.

WENDT, K. & PETERS, J., 2009. How cohesin and CTCF cooperate in regulating gene expression. *Chromosome Research,* Volume 17(2), pp. 201-214.

WHITE, J., LUSNAK, K. & FOGEL, S., 1985. Mismatch-specific post-meiotic segregation frequency in yeast suggests a heteroduplex recombination intermediate. *Nature,* Volume 315(6017), pp. 350-2.

XAVER, M., HUANG, L. Z., CHEN, D. & KLEIN, F., 2013. Smc5/6-Mms21 Prevents and Eliminates Inappropriate Recombination Intermediates in Meiosis. *Plos Genetics,* Volume 9(12).

XU, L., AJIMURA, M., PADMORE, R., KLEIN, C. & KLECKNER, N., 1995. NDT80, a meiosis-specific gene required for exit from pachytene in Saccharomyces cerevisiae. *Mol Cell Biol,* Volume 15(12), pp. 6572-6581.

XU, L., WEINER, B. & KLECKNER, N., 1997. Meiotic cells monitor the status of the interhomolog recombination complex. *Genes Dev.,* Volume 11, pp. 106-118.

YU, H.-G. & KOSHLAND, D., 2003. Meiotic condensin is required for proper chromosome compaction, SC assembly, and resolution of recombination-dependent chromosome linkages. *J Cell Biol 163: 937–947,* Volume 163, pp. 937-947.

YU, H. & KOSHLAND, D., 2005. Chromosome morphogenesis: condensin-dependent cohesin removal during meiosis. *Cell,* Volume 123(3), pp. 397-407.

ZAKHEREYVICH, K., TANG, S., MA, Y. & HUNTER, N., 2012. Delineation of joint molecule resolution pathways in meiosis identifies a crossover-specific resolvase. *Cell,* Volume 149, pp. 334-347.

ZHANG, J. et al., 2008. Acetylation of Smc3 by Eco1 is required for S phase sister chromatid cohesion in both human and yeast. *Mol Cell,* Volume 31, pp. 143-51.

ZHANG, L. et al., 2014. Topoisomerase II mediates meiotic crossover interference. *Nature,* Volume 511(7511), pp. 551-556.

ZHU, Z., CHUNG, W. H., SHIM, E. Y., LEE, S. E. & IRA. G., 2008. Sgs1 helicase and two nucleases Dna2 and Exo1 resect DNA double-strand break ends. *Cell,* Volume 134, p. 981–994.